Basic Concepts:

A Little Electronic Structure
The X-Ray-Based Experiments
X-Ray Sources, Synchrotron Radiation, Free Electron Lasers

Core-Level Photoemission

Intensities and Quantitative Analysis, the 3-Step Model-Valence levels
Varying Surface and Bulk Sensitivity
Chemical Shifts
Multiplet Splittings
Electron Screening and Satellite Structure
Magnetic and Non-Magnetic Dichroism
Resonant Photoemission
Photoelectron Diffraction and Holography

Valence-Level Photoemission

Band-Mapping in the Ultraviolet Photoemission Limit
Densities of States in the X-Ray Photoemission Limit

Some New Directions

Photoemission with Hard X-Rays (throughout lectures)
Photoemission with Standing Wave Excitation
Photoemission with: Higher Pressures→multi-Torr→Atmosphere?
Spatial Resolution-Photoelectron Microscopy
Temporal Resolution

X-ray photoemission: some key elements

From UHV to multi-Torr
The Real World!

Photon

Up to 5-10 keV→deeper

Angle-resolved XPS (ARXPS)

•Standing wave/Total reflection
•Resonance
•Variable polarization

θ_{inc}

θ Three angles

ϕ

β

Sample

$\vec{K}, \vec{S}$

e-

Analyzer Slit

Irradiated Area

Angle∝ $\vec{K}$

No. e-

Energy

Imaging Detector

Kinetic Energy

Core-levels I(

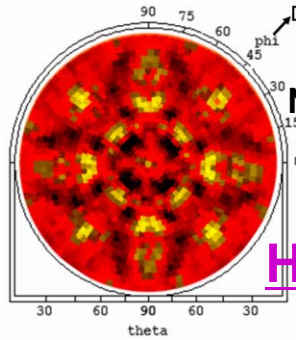

HXPD

Photoe- diffraction

Valence-levels

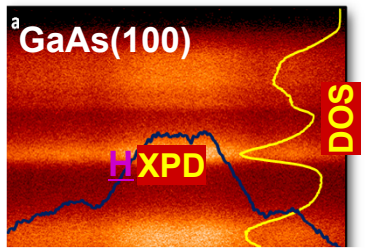

Binding Energy

Emission angle

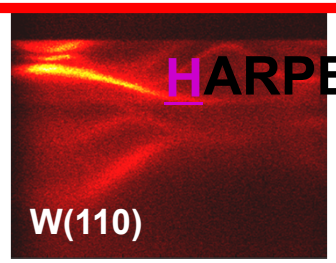

Binding Energy

Emission angle→$\vec{k}_x$

ATOMIC (CORE) PHOTOELECTRON INTENSITIES: THE "FOUR-STEP" MODEL

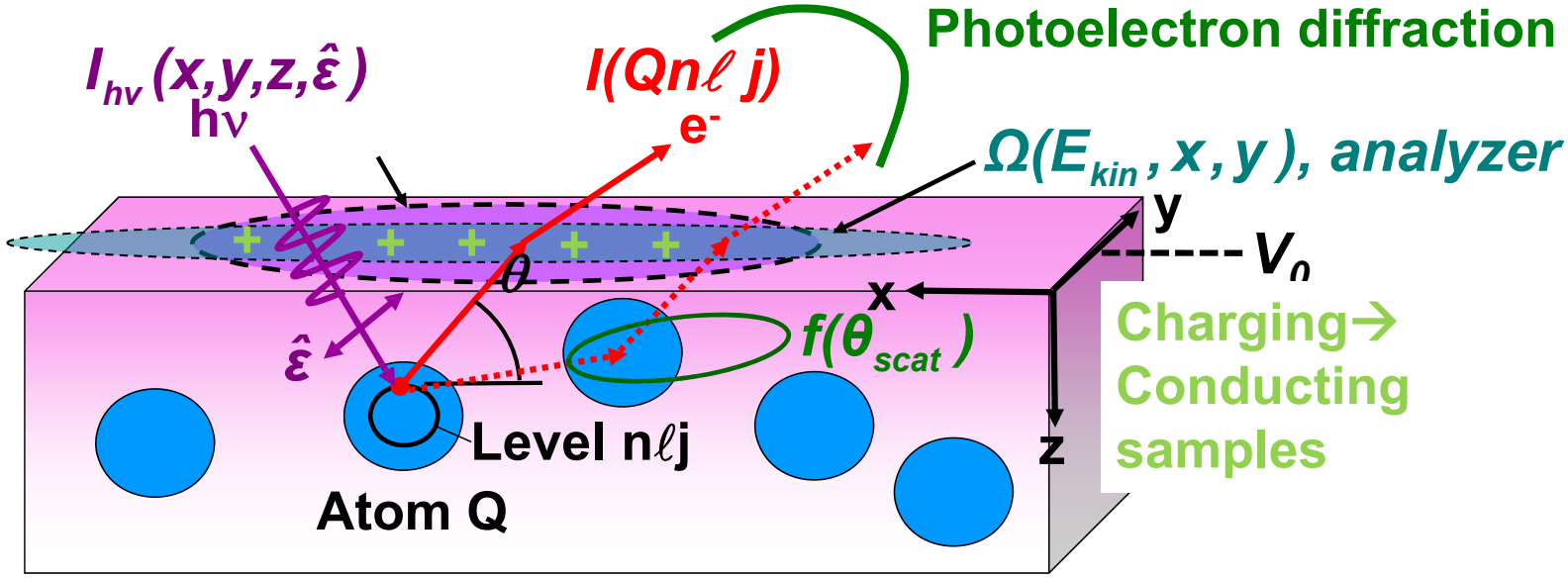

$I(Qn\ell\, j)$ = → Non-dipole effects* and resonant interchannel#

$$C\int_0^{\infty} I_{hv}(x,y,z,\hat{\varepsilon})\rho_Q(x,y,z)\frac{d\sigma_{Qn\ell j}(hv,\hat{\varepsilon})}{d\Omega}\exp\left[-\frac{z}{\Lambda_e(E_{kin})\sin\theta}\right]\Omega(E_{kin},x,y)\,dxdydz$$

$I_{hv}(x,y,z,\hat{\varepsilon})$ = x-ray flux, $\hat{\varepsilon}$ = polarization

$\rho_Q(x,y,z)$ = density of atoms Q → quantitative analysis

$\frac{d\sigma_{Qn\ell j}(hv,\hat{\varepsilon})}{d\Omega}$ = energy-dependent differential photoelectric cross section for subshell $Qn\ell\, j$

$\Lambda_e(E_{kin})$ = energy-dependent inelastic attenuation length + elastic scattering: $f(\theta_{scatt})$

→ Effective Attenuation Length (EAD) → Mean Emission Depth (MED)

$\Omega(E_{kin}, x, y)$ = energy-dependent analyzer acceptance solid angle = transmission function

V_0 = inner potential

VALENCE-BAND PHOTOELECTRON INTENSITIES IN THE DENSITY-OF-STATES LIMIT

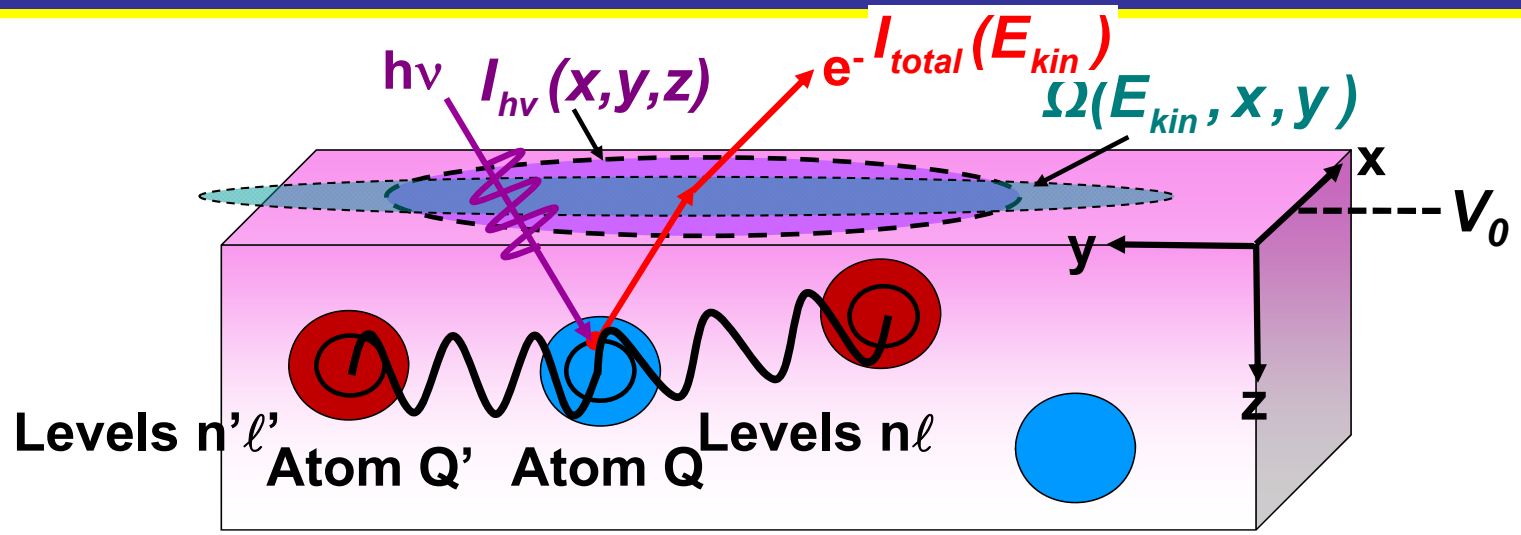

For a given subshell:

$$I(E_{kin},Qn\ell) =$$

$$C' \int_0^{\infty} I_{hv}(x,y,z)\,\rho_{Qn\ell}(E_b,x,y,z)\,\frac{d\sigma_{Qn\ell}(hv)}{d\Omega}\,exp\left[-\frac{z}{\Lambda_e(E_{kin})\sin\theta}\right]\Omega(E_{kin},x,y)\,dxdydz$$

$I_{hv}(x,y,z)$ = x-ray flux

$\rho_{Qn\ell}(E_b,x,y,z)$ = density of states, projected onto $Qn\ell$ character

$\frac{d\sigma_{Qn\ell}(hv)}{d\Omega}$ = energy-dependent differential photoelectric cross section for subshell $Qn\ell$

$\Lambda_e(E_{kin})$ = energy-dependent inelastic attenuation length

→ Mean Emission Depth

$\Omega(E_{kin},x,y)$ = energy-dependent spectrometer acceptance solid angle

For the total VB intensity:

$$I_{total}(E_{kin}) = \sum_{Qn\ell} I(E_{kin},Qn\ell)$$

1. Hydrogen

Symmetry: $D_{\infty h}$

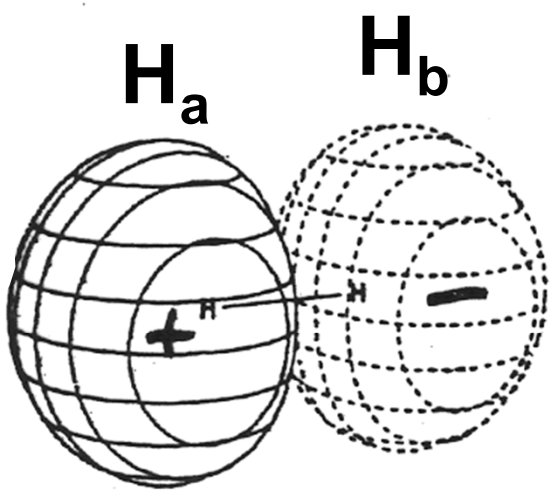

Anti-Bonding

$$\varphi_{anti}^{MO} \cong \varphi_{1sa} - \varphi_{1sa}$$

ε *positive (unoccupied)*

$1\sigma_u$ ε= 0.2656 a.u. = +7.21 eV

ε *negative (occupied)*

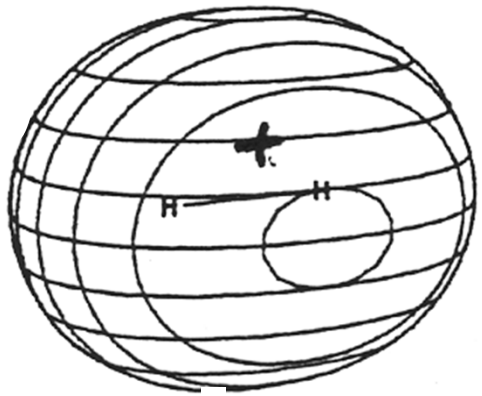

Bonding

$$\varphi_{bonding}^{MO} \cong \varphi_{1sa} + \varphi_{1sa}$$

$1\sigma_g$ ε=-0.5944 a.u. = -16.16 eV

(Compare – 13.61 for H atom 1s)

The electrons in carbon monoxide

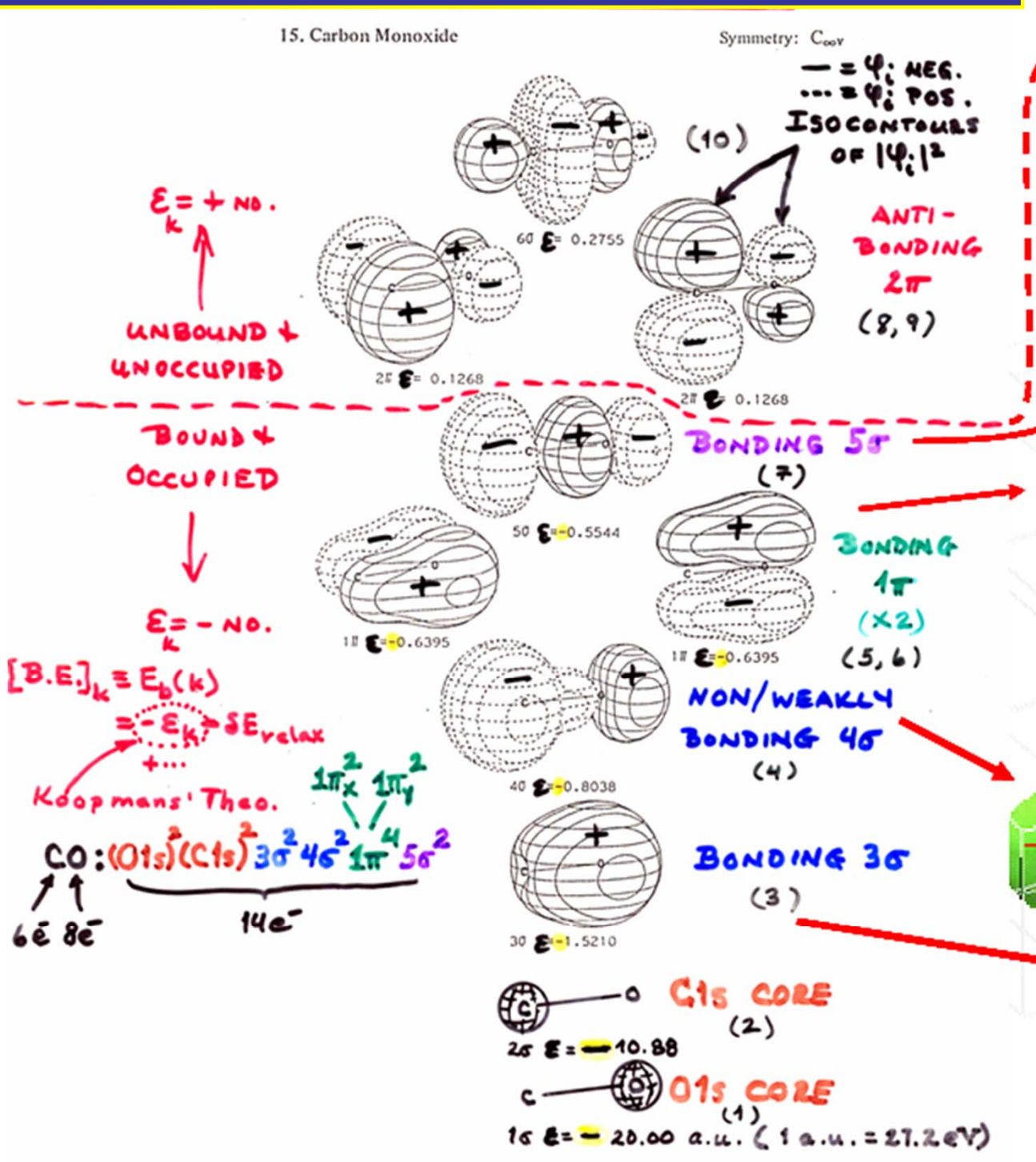

Atomic orbital makeup

$$\varphi_j^{MO}(\vec{r}) = \sum_{\substack{\text{Atoms } A \\ \text{Orbitals } i}} c_{Ai,j}\varphi_{Ai}^{AO}(\vec{r})$$

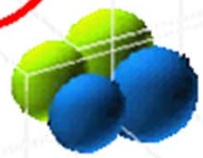

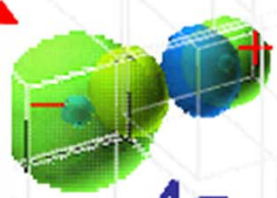

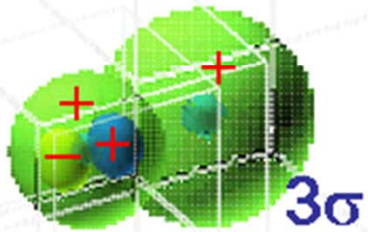

Photoelectron emission: basic matrix elements and selection rules

- ATOMIC-LIKE (LOCALIZED) STATES ⇒ CORE:

$$\varphi_i(\vec{r}) = \varphi_{n_i l_i m_i}(r,\theta,\phi) = R_{n_i l_i}(r) Y_{l_i m_i}(\theta,\phi)$$

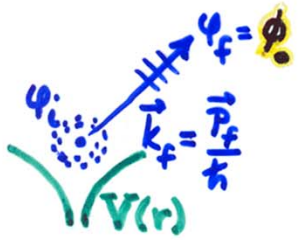

$$\varphi_f(\vec{r},\vec{k}_f) = \varphi_{E_f}(\vec{r},\vec{k}_f)$$

$$= 4\pi \sum_{l_f,m_f} i^{l_f} e^{-i\delta_{l_f}} Y^*_{l_f m_f}(\theta_{k_f},\phi_{k_f}) Y_{l_f m_f}(\theta,\phi) R_{E_f,l_f}(r)$$

(δ_{l_f}: PHASE SHIFT OF l_f WAVE IN V(r))

DIPOLE APPROX.: INT. $\propto |\langle\varphi_f|\hat{\varepsilon}\cdot\vec{r}|\varphi_i\rangle|^2 = |\hat{\varepsilon}\langle\varphi_f|\vec{r}|\varphi_i\rangle|^2 \Rightarrow$

$\Delta l = l_f - l_i = \pm 1$ TWO CHANNELS

$\Delta m = m_f - m_i = 0, \pm 1$ LINEAR POLARIZ.

$\Delta m = \pm 1$, CIRCULAR POLARIZATION

EQUIVALENT WITHIN CONSTANT FACTOR ($\vec{p} \leftrightarrow \vec{\nabla}V(r)$)

- BLOCH-FUNCTION (DELOCALIZED) STATES ⇒ VALENCE:

$$\varphi_i(\vec{r}) = u_{\vec{k}_i}(\vec{r}) e^{i\vec{k}_i\cdot\vec{r}}$$

$$\varphi_f(\vec{r}) = u_{\vec{k}_f}(\vec{r}) e^{i\vec{k}_f\cdot\vec{r}}\ ;\ E_f = \frac{p_f^2}{2m} = \frac{\hbar^2 k_f^2}{2m}$$ (USUALLY NEGLIG.)

$$|\langle\varphi_f|\hat{\varepsilon}\cdot\vec{p}|\varphi_i\rangle|^2 = |\hat{\varepsilon}\cdot\langle\varphi_f|\vec{p}|\varphi_i\rangle|^2 \Rightarrow \Delta\vec{k} = \vec{k}_f - \vec{k}_i - \vec{k}_{h\nu} + \vec{k}_{PHONON}$$

$$= \vec{g}_{BULK}\ (\text{OR } \vec{g}_{SURF})$$

"DIRECT" TRANSITIONS

BUT LATTICE VIBRATIONS ⇒ SUM OVER $\vec{k}_{PHONON}$

⇒ FRACTION DIRECT ≈ DEBYE-WALLER FACTOR

$$\approx \exp[-g^2\overline{u^2}]$$

"Basic Concepts of XPS" Chapter 3

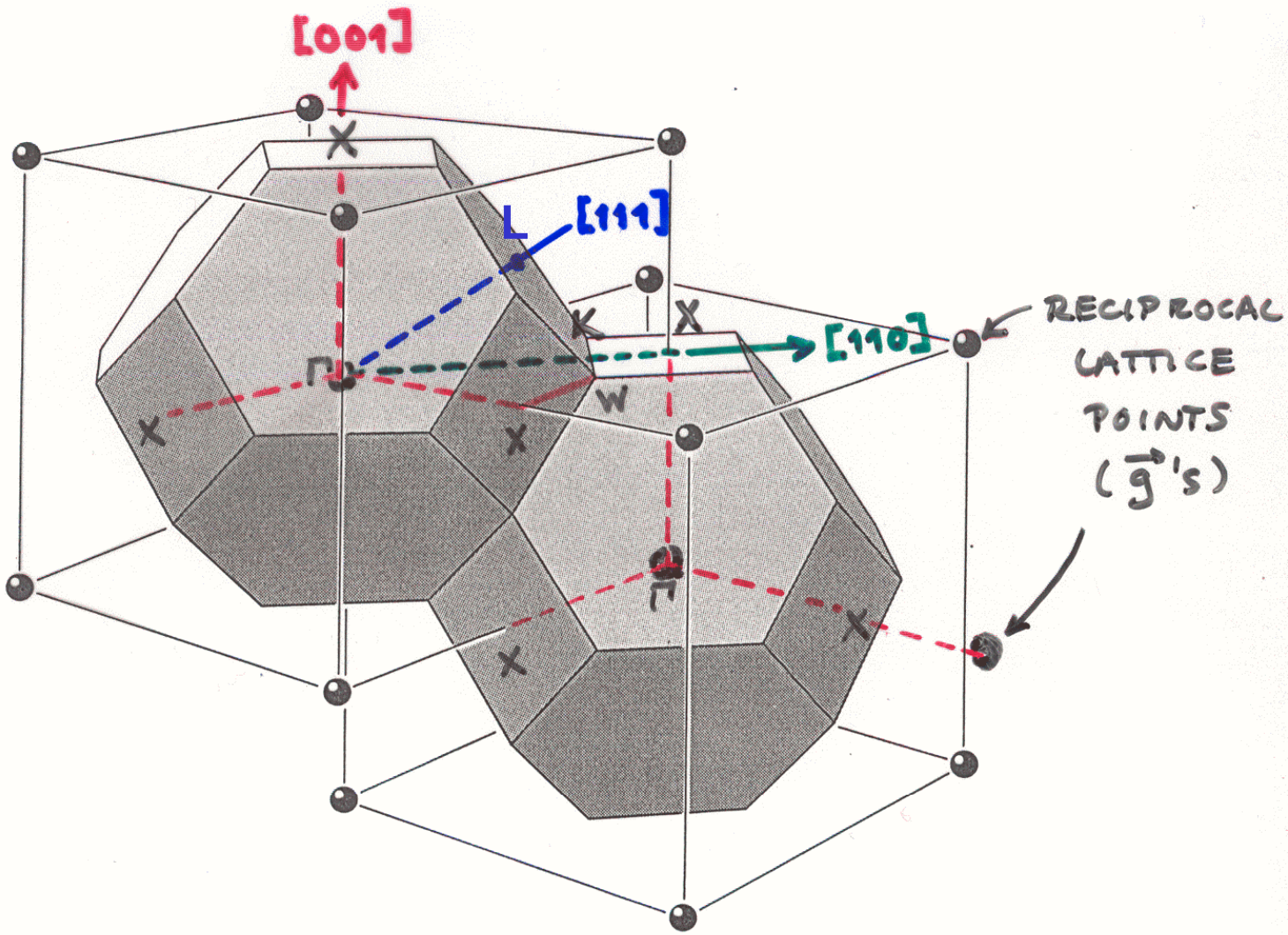

Figure 28 Brillouin zones of the face-centered cubic lattice. The cells are in reciprocal space, and the reciprocal lattice is body-centered, as drawn.

— STACKING OF fcc BRILLOUIN ZONES —

The electronic structure of a transition metal—fcc Cu

Vacuum level

ϕ_{Cu} = 4.4 eV = work function

$V_{0,Cu}$ =13.0eV

- 8.6 eV

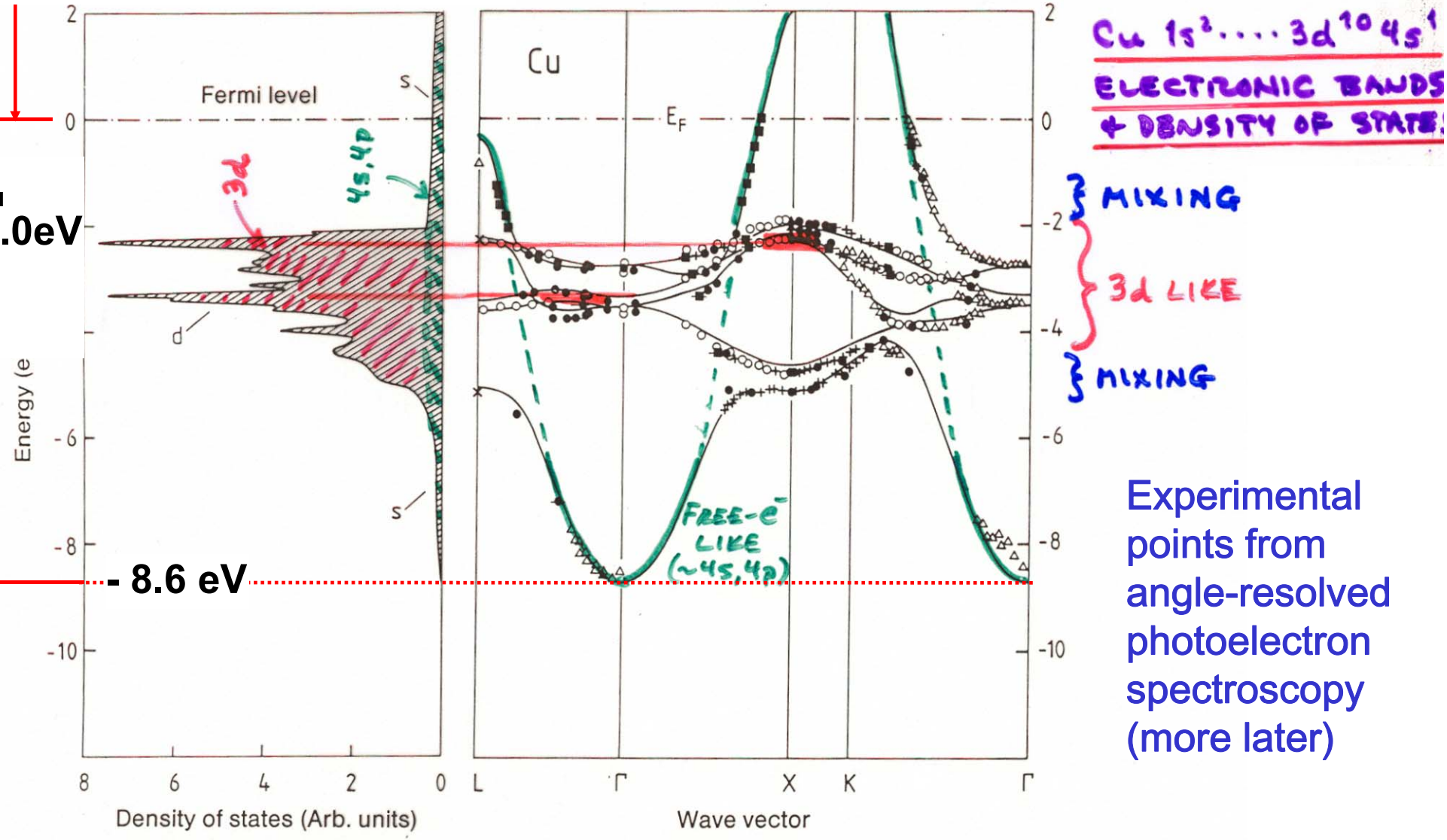

Experimental points from angle-resolved photoelectron spectroscopy (more later)

Fig. 7.12. Bandstructure $E(k)$ for copper along directions of high crystal symmetry (*right*). The experimental data were measured by various authors and were presented collectively by Courths and Hüfner [7.4]. The full lines showing the calculated energy bands and the density of states (*left*) are from [7.5]. The experimental data agree very well, not only among themselves, but also with the calculation

And the d orbitals are not equivalent in different bonding environments:

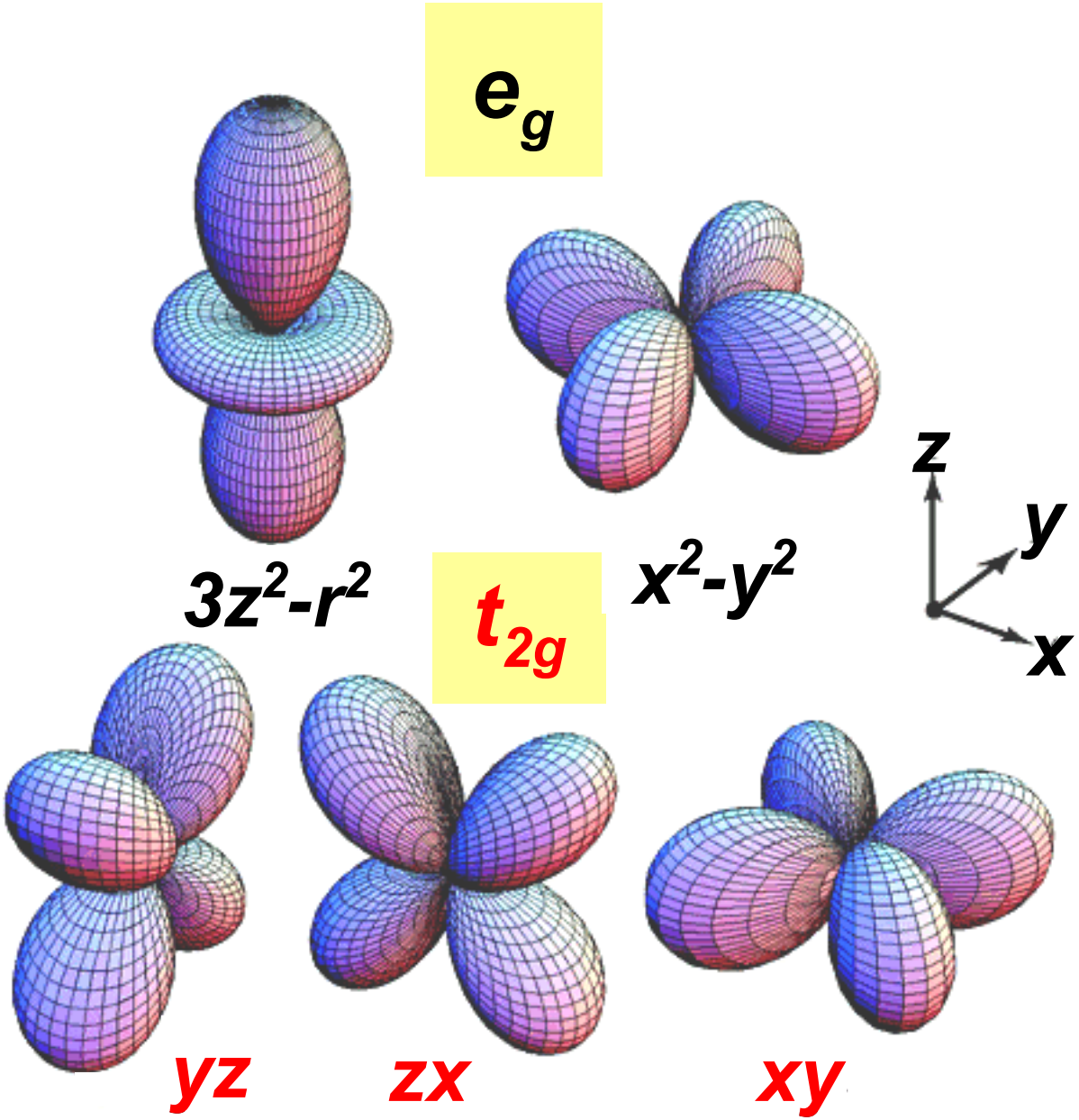

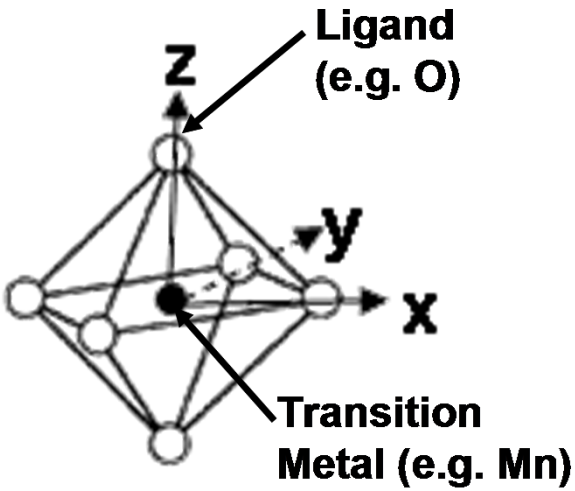

e_g and t_{2g} not equivalent in octahedral (cubic) environment

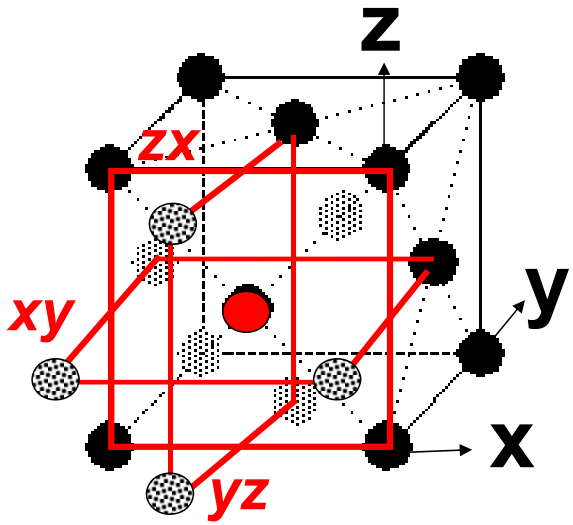

Face-centered cubic—12 nearest neighbors

Copper densities of states-total and by orbital type:

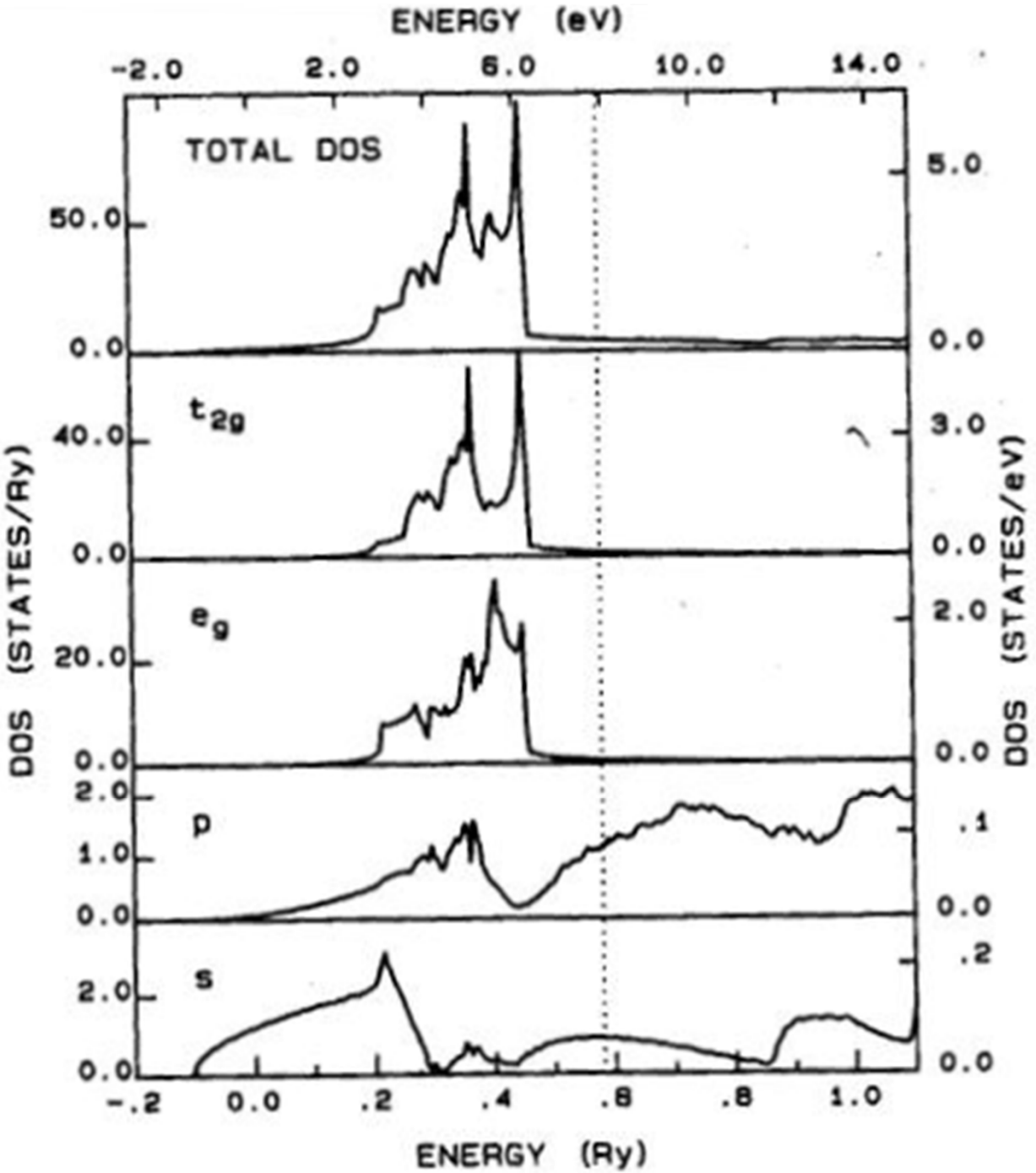

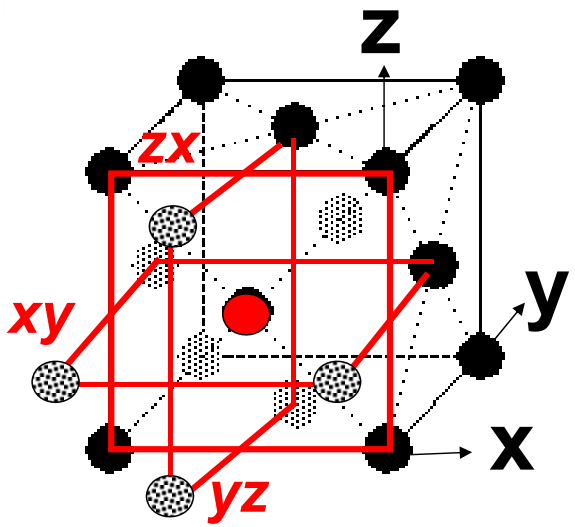

The electronic structures of the 3d transition metals— ≈ "rigid-band model"

$3s^2 3p^6$ filled + 3d,4s CB

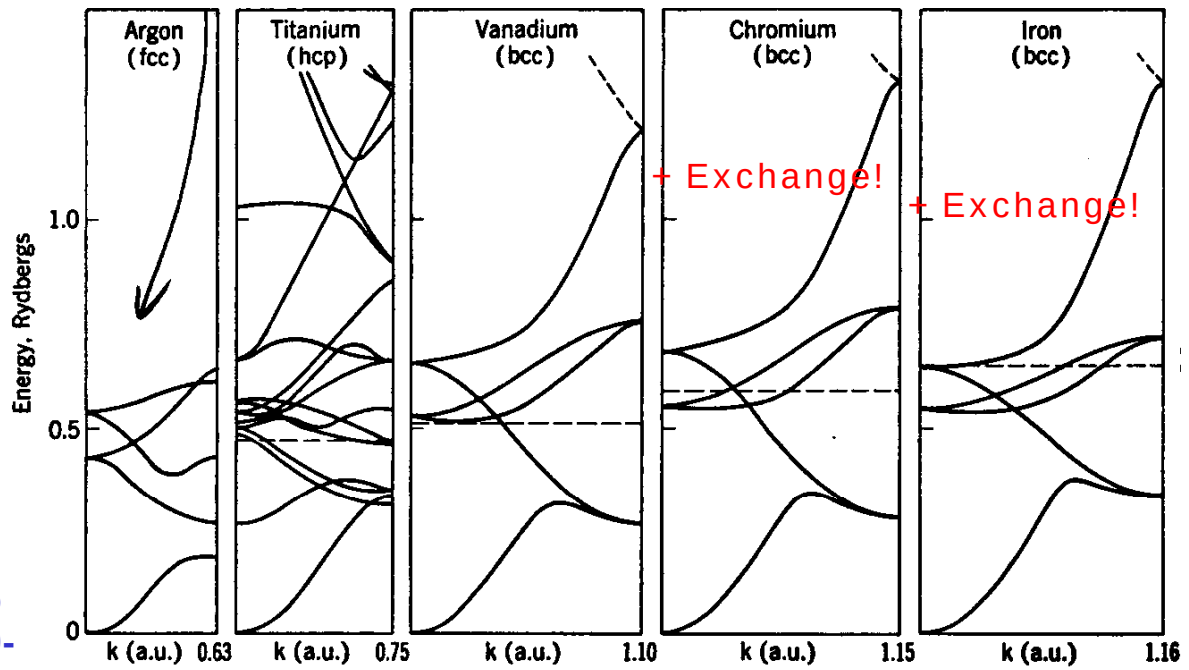

+ Flat "core-like" Ar 3s, 3p bands at ~-1.0-1.5 Rydbergs

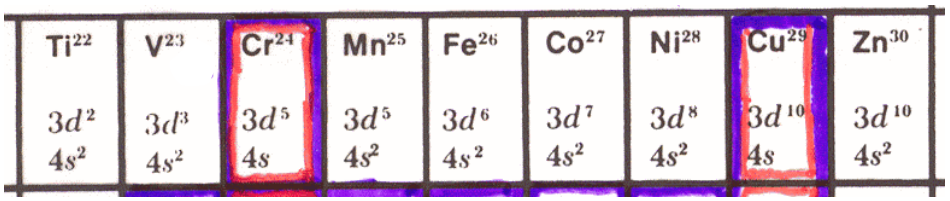

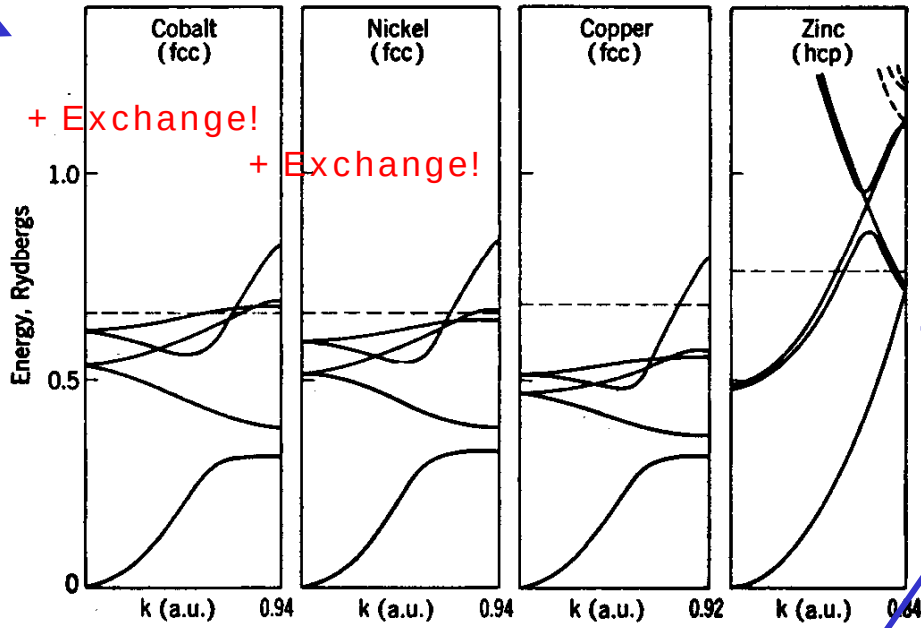

+ Flat "core-like" Zn 3d bands at ~-0.8 Rydberg

FIG. 10-20. Energy bands of 3d transition elements, along a single direction, from Mattheiss.

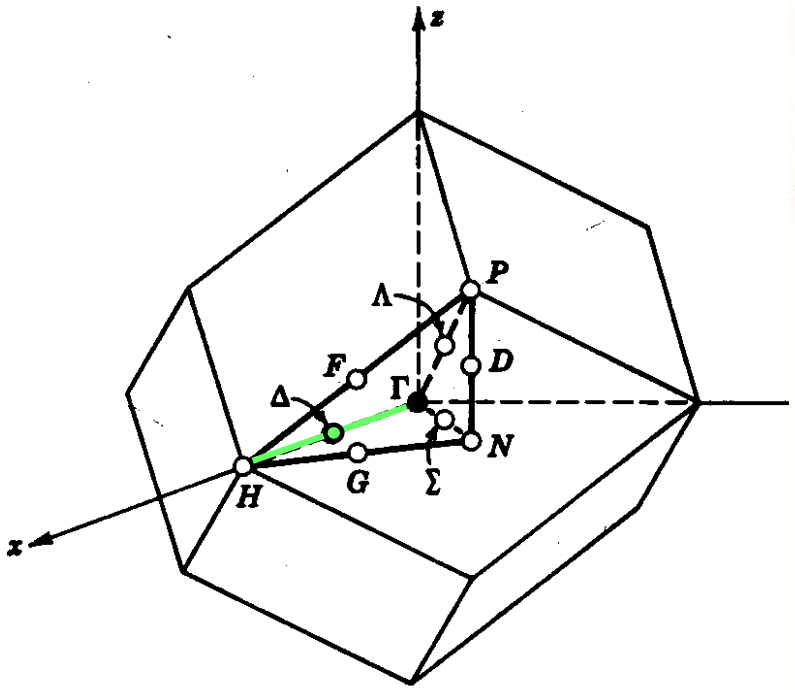

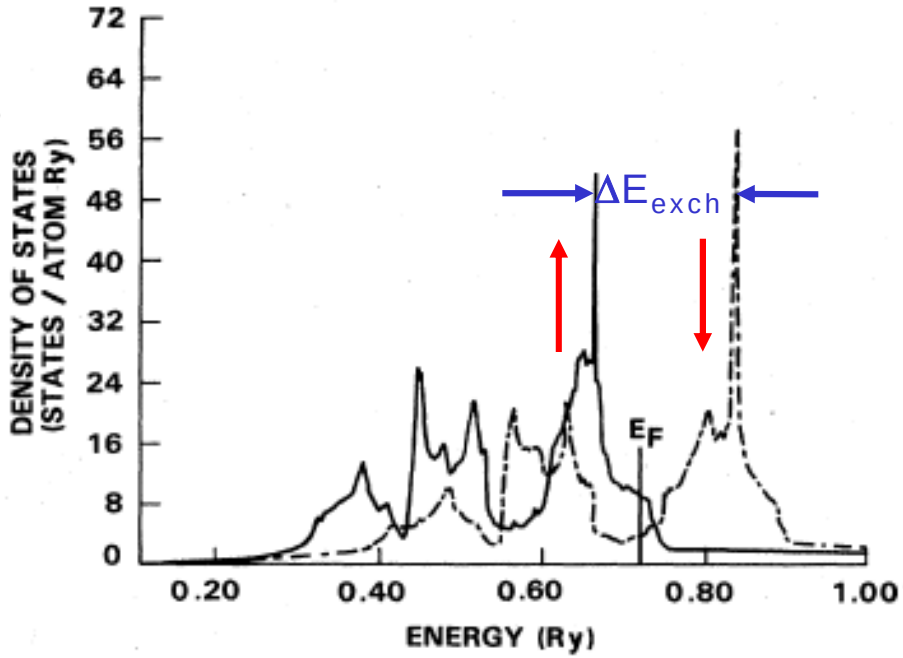

FIG. 4. Density of states at the equilibrium lattice constant of Fe for majority- (solid line) and minority- (broken line) spin states.

Hathaway et al., Phys. Rev. B 31, 7603 ('85)

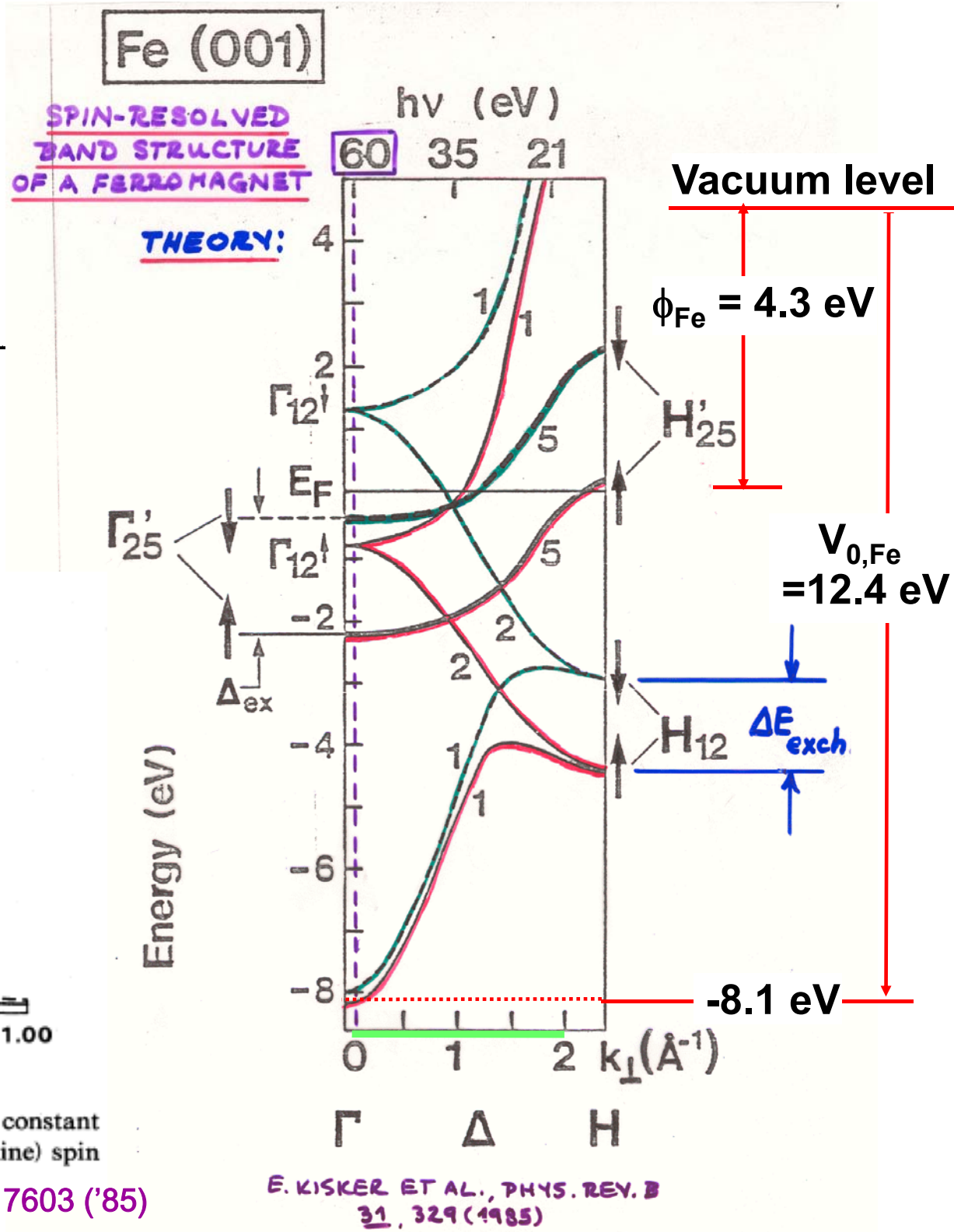

Fe: ANGLE AND SPIN-RESOLVED SPECTRA AT Γ POINT

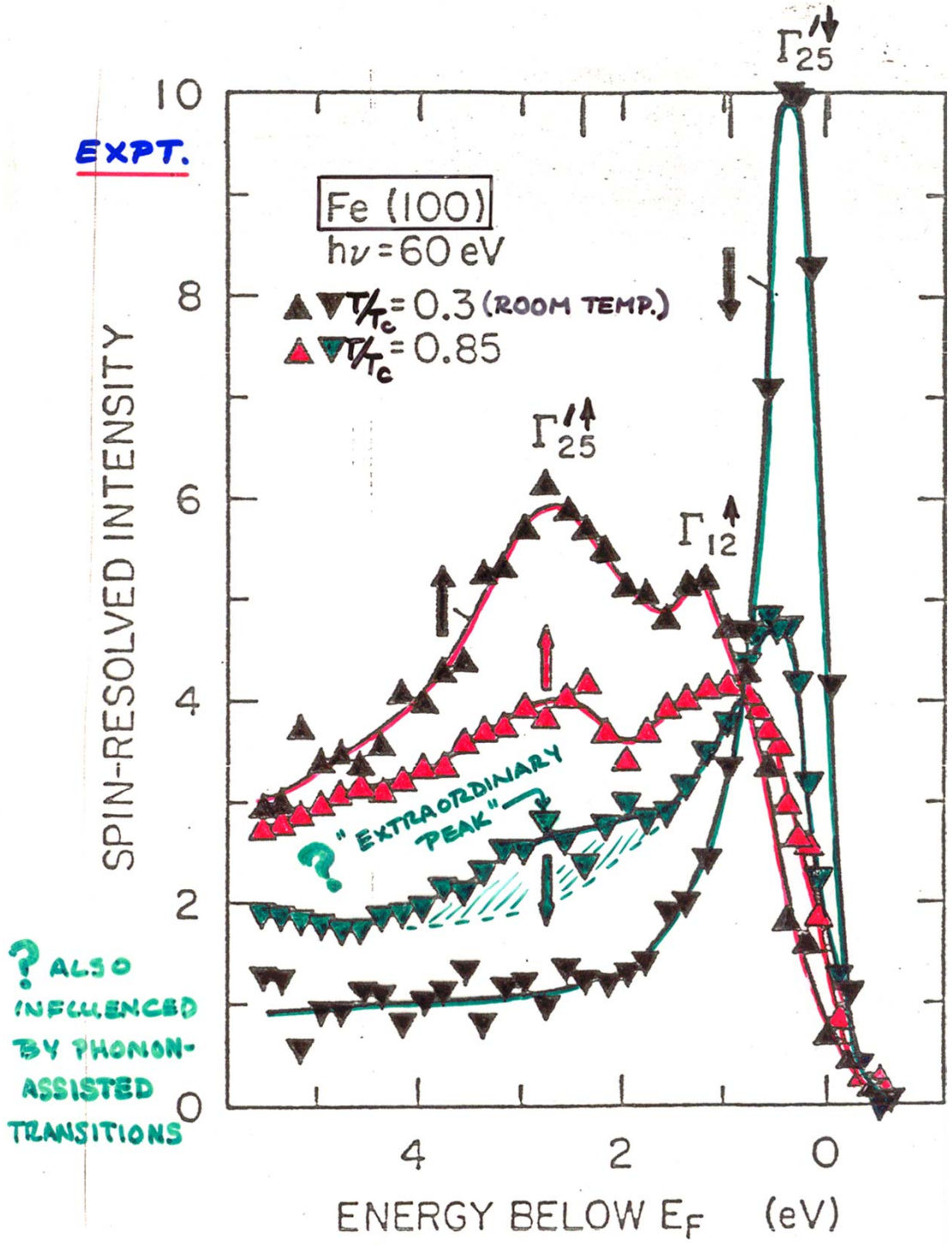

E. KISKER ET AL., PHYS. REV. B 31, 329 (1985)

$SrTiO_3$ and $La_{0.67}Sr_{0.33}MnO_3$ band structures and DOS

$SrTiO_3$-insulator

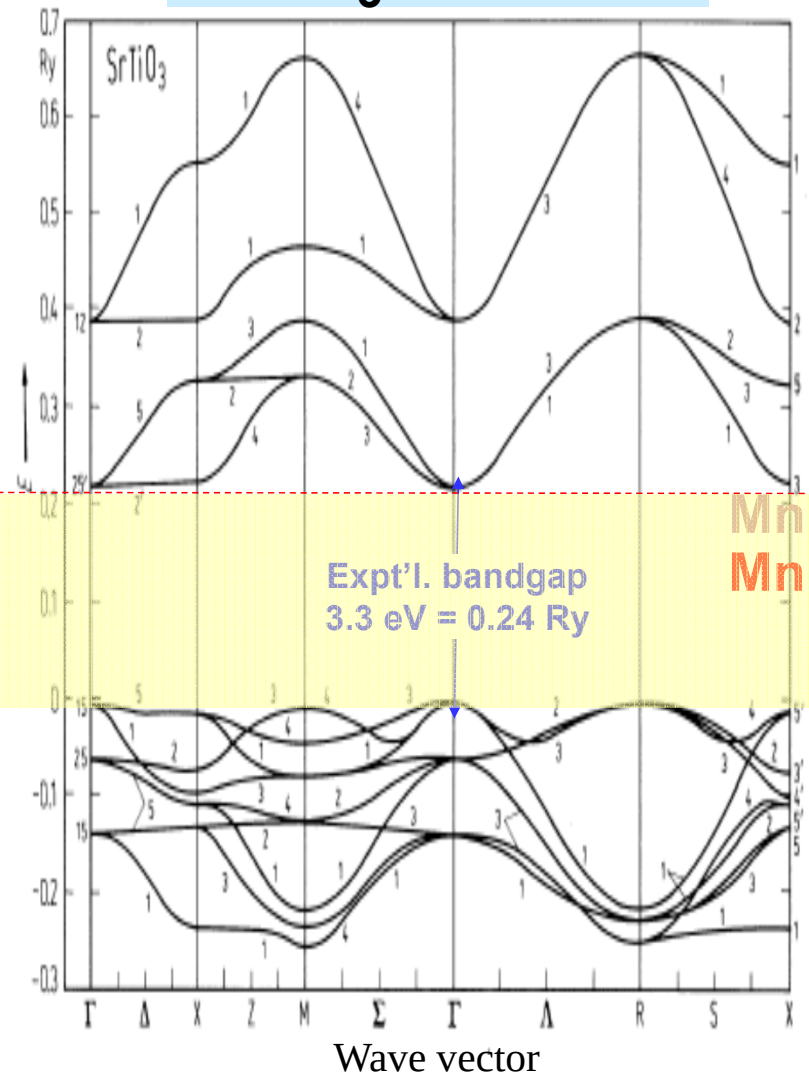

Mattheiss, PRB 6, 4718 (1972)

$La_{0.67}Sr_{0.33}MnO_3$-Half-Metallic Ferromagnetic metal

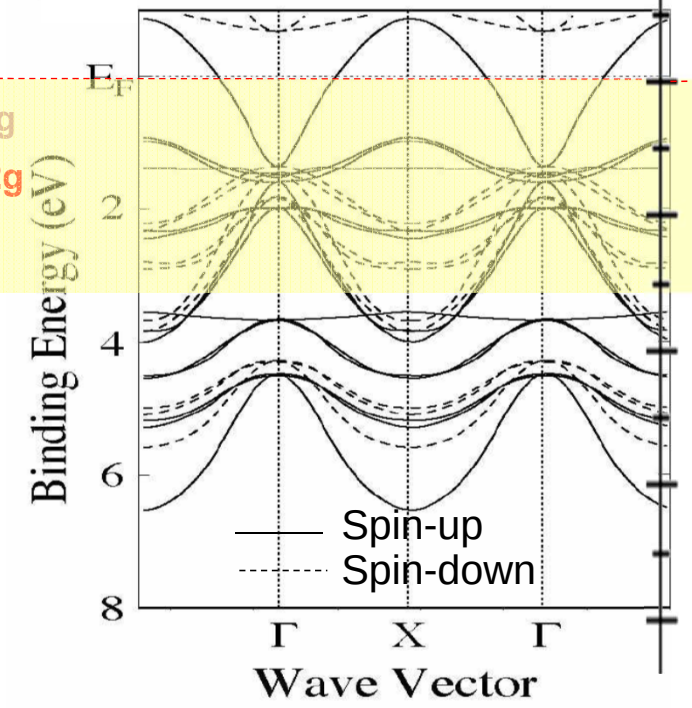

Chikamatsu et al., PRB 73, 195105 (2006)

Zheng, Binggeli, J. Phys. Cond. Matt. 21, 115602 (2009)

Projected DOSs

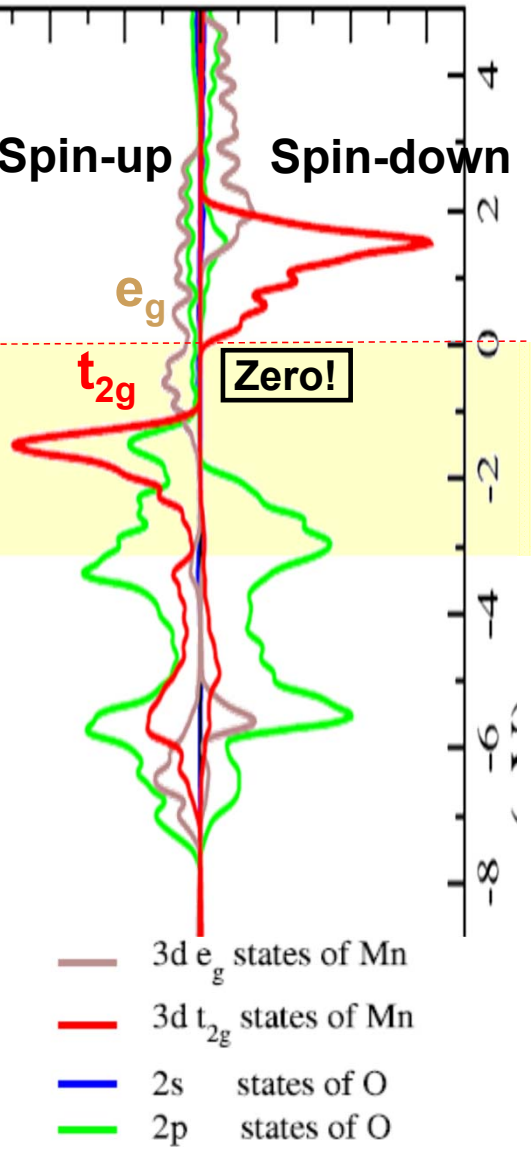

VALENCE-BAND PHOTOELECTRON INTENSITIES IN THE DENSITY-OF-STATES LIMIT

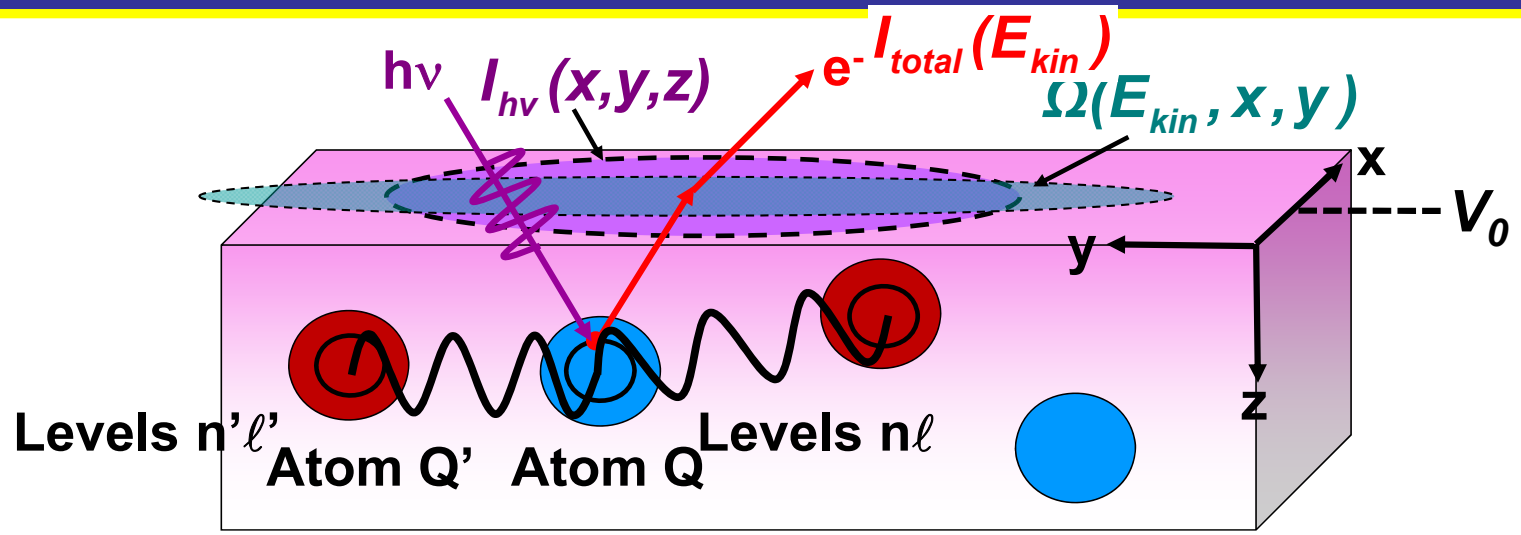

For a given subshell:

$$I(E_{kin},Qn\ell) =$$

$$C' \int_0^{\infty} I_{hv}(x,y,z)\,\rho_{Qn\ell}(E_b,x,y,z)\,\frac{d\sigma_{Qn\ell}(hv)}{d\Omega}\,exp\left[-\frac{z}{\Lambda_e(E_{kin})\sin\theta}\right]\Omega(E_{kin},x,y)\,dxdydz$$

$I_{hv}(x,y,z)$ = x-ray flux

$\rho_{Qn\ell}(E_b,x,y,z)$ = density of states, projected onto $Qn\ell$ character

$\frac{d\sigma_{Qn\ell}(hv)}{d\Omega}$ = energy-dependent differential photoelectric cross section for subshell $Qn\ell$

$\Lambda_e(E_{kin})$ = energy-dependent inelastic attenuation length

→ Mean Emission Depth

$\Omega(E_{kin},x,y)$ = energy-dependent spectrometer acceptance solid angle

For the total VB intensity:

$$I_{total}(E_{kin}) = \sum_{Qn\ell} I(E_{kin},Qn\ell)$$

Gold Valence Spectrum

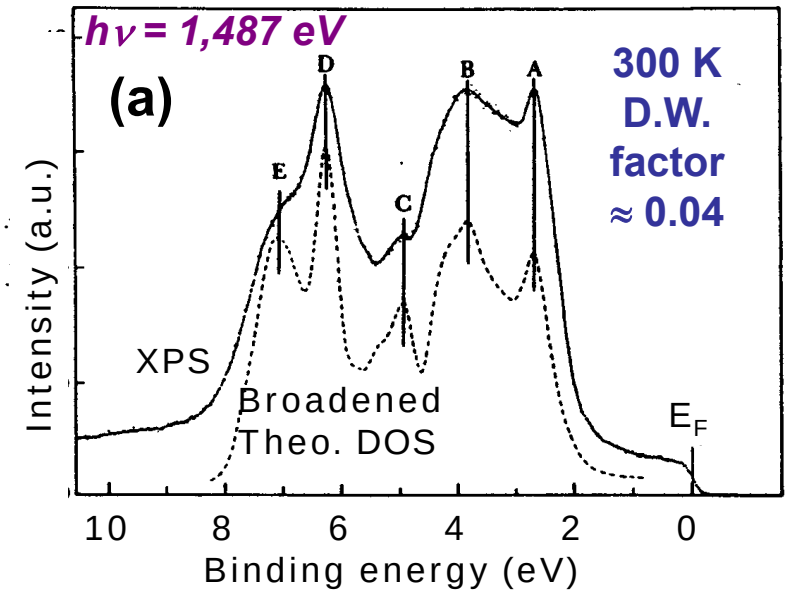

Valence spectra in the XPS Limit

Gold Valence Spectrum

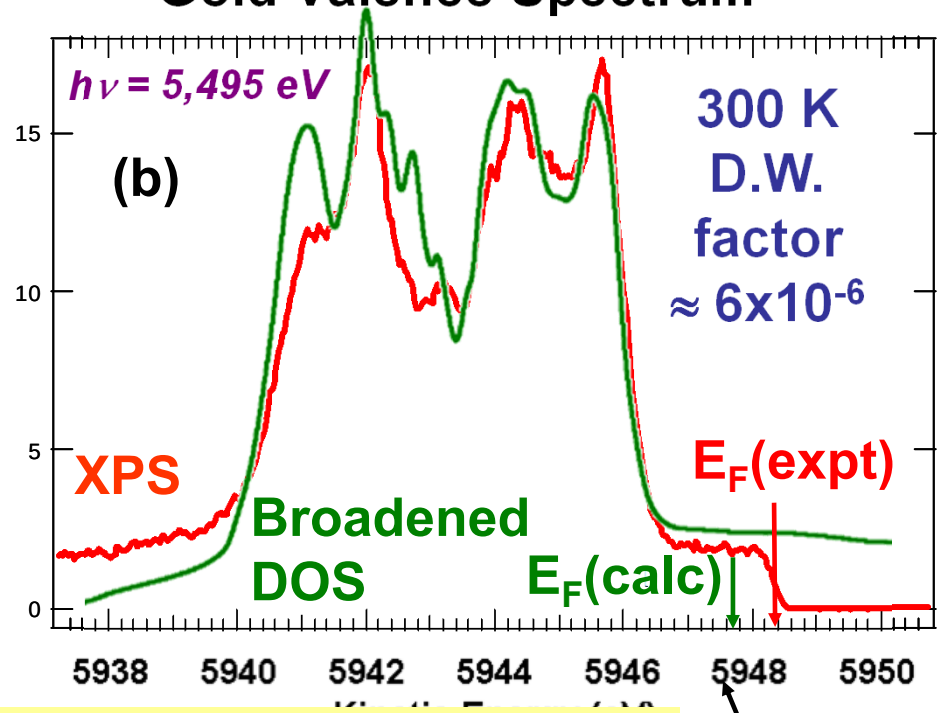

Silver Valence Spectrum

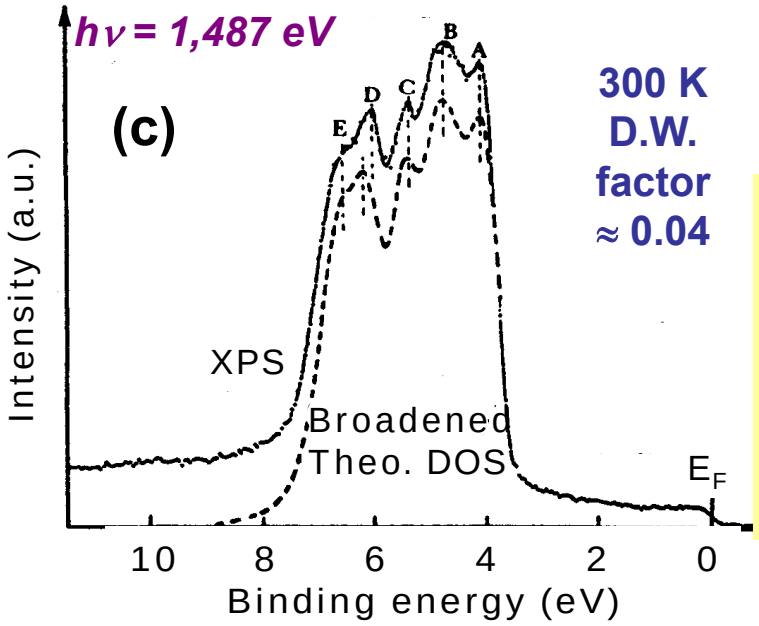

Au subshell photoelectric cross section ratios:
Au6s/Au5d = 0.012 at 1.5 keV
Au6s/Au5d = 0.028 at 6 keV
→6s weak but more imp. at 6 keV x 2.5x

Screening/ self-energy correction

In the XPS Limit— Comparison to theoretical DOSs

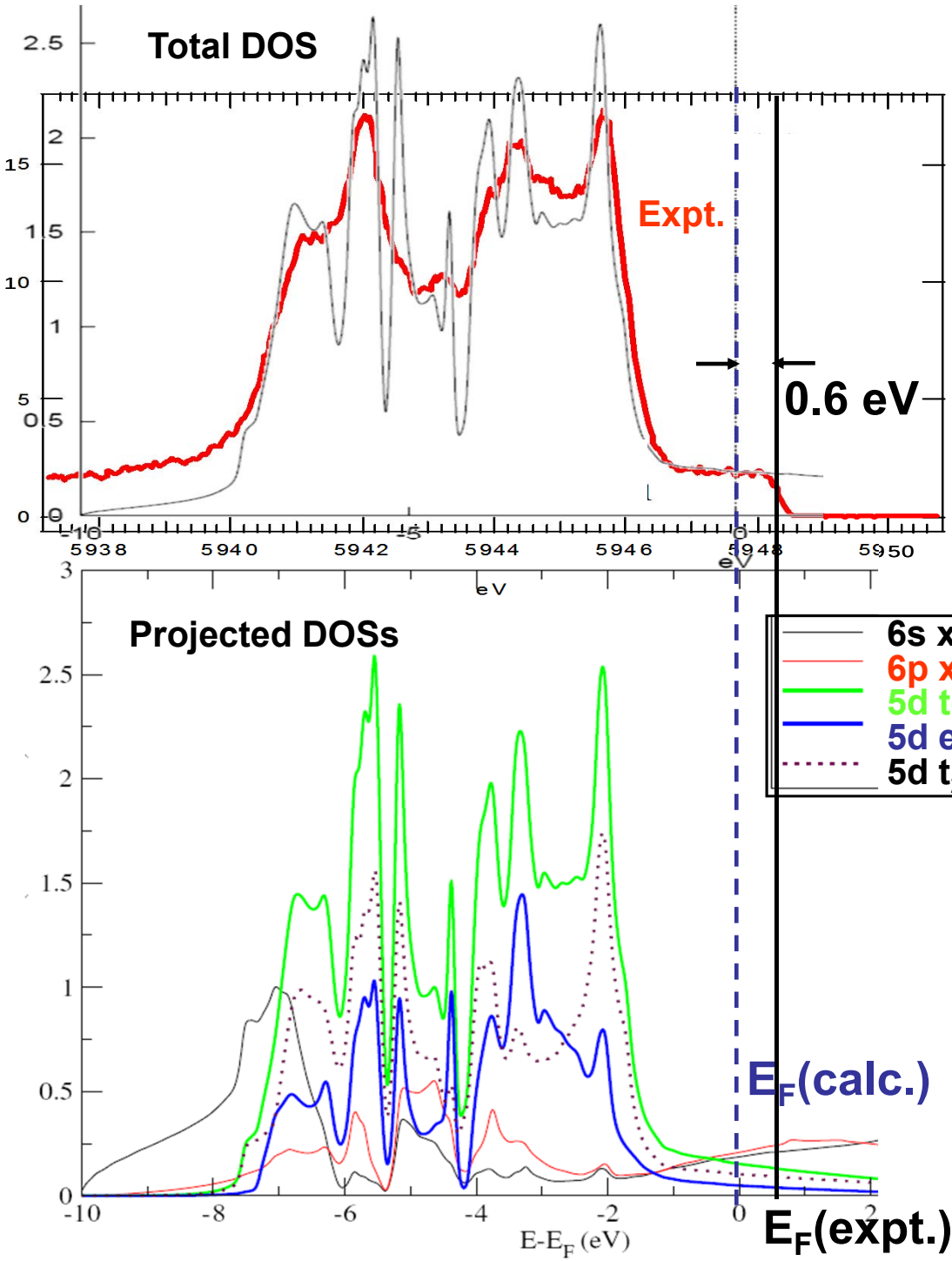

Takata et al., SPring8 @ 5.495 keV

Au subshell photoelectric cross section ratios: Au6s/Au5d = 0.012 at 1.5 keV and 0.028 at 6 keV→6s more imp. at 6 keV x 2.5x

Z. Yin
W.E. Pickett

Hard x-ray photoemission from Cr and $Cr_{0.80}Al_{0.20}$

hν = 5956 eV

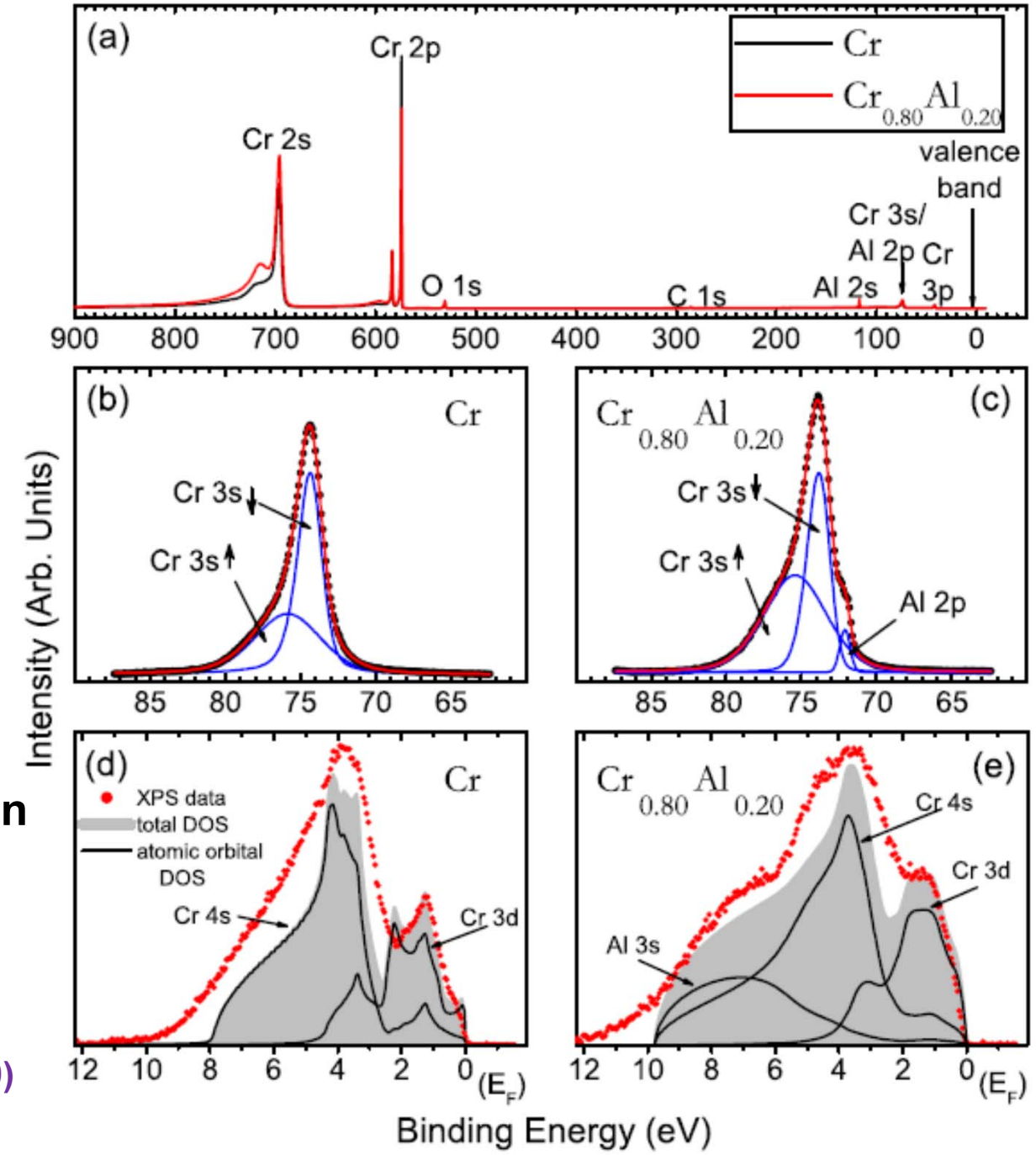

Experiment vs cross-section weighted projected densities of states

Gray et al., PRL 105, 236404 (2010)

Basic Concepts:

A Little Electronic Structure
The X-Ray-Based Experiments
X-Ray Sources, Synchrotron Radiation, Free Electron Lasers

Core-Level Photoemission

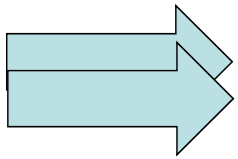

Intensities and Quantitative Analysis, the 3-Step Model
Varying Surface and Bulk Sensitivity
Chemical Shifts
Multiplet Splittings
Electron Screening and Satellite Structure
Magnetic and Non-Magnetic Dichroism
Resonant Photoemission
Photoelectron Diffraction and Holography

Valence-Level Photoemission

Band-Mapping in the Ultraviolet Photoemission Limit
Densities of States in the X-Ray Photoemission Limit

Some New Directions

Photoemission with Hard X-Rays (throughout lectures)
Photoemission with Standing Wave Excitation
Photoemission with: Higher Pressures→multi-Torr→Atmosphere?
Spatial Resolution-Photoelectron Microscopy
Temporal Resolution

Enhancing surface sensitivity at grazing exit angles

$$I(z) = I_0 e^{-\frac{z}{\Lambda_e \sin\Theta}}$$

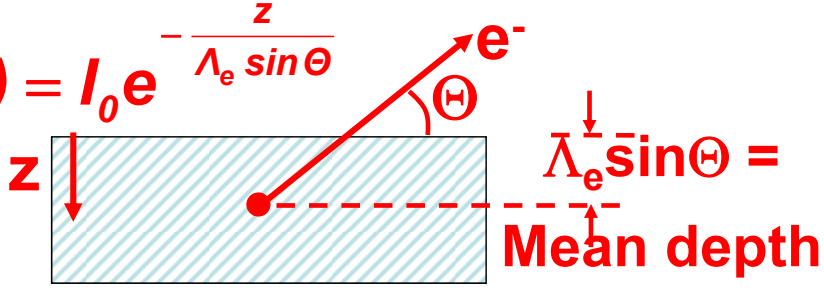

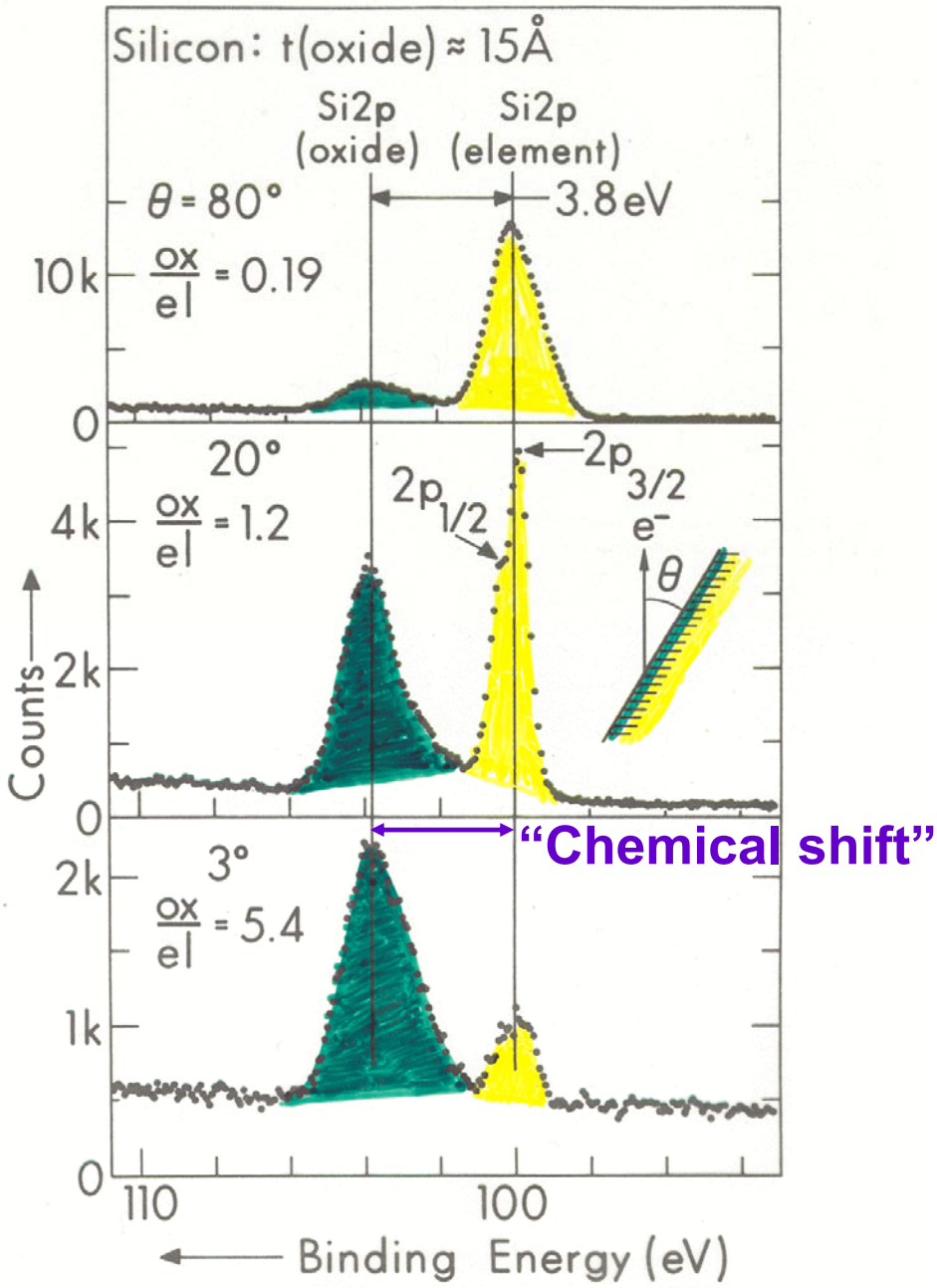

CSF, Prog. in Surf. Sci. 16, 275 (1984)

Chemical shifts:
Looking into the silicon dioxide layer with photoelectron spectroscopy

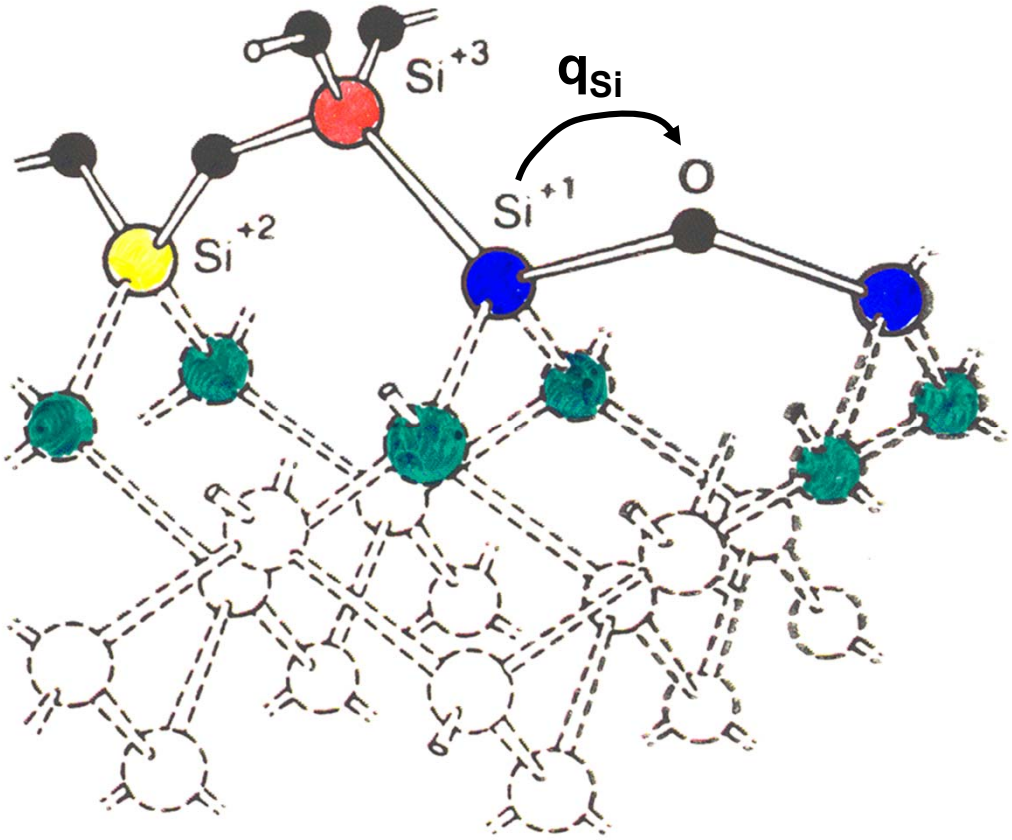

Charge transfer, e⁻- e⁻ coulomb integral:

$$Shift \approx q_{Si} K_{Si2p,Si3p} =$$

$$q_{Si} \int \varphi^*_{2p}(\vec{r}_1)\varphi^*_{3p}(\vec{r}_2)\frac{e^2}{r_{12}}\varphi_{2p}(\vec{r}_1)\varphi_{3p}(\vec{r}_2)dV_1dV_2$$

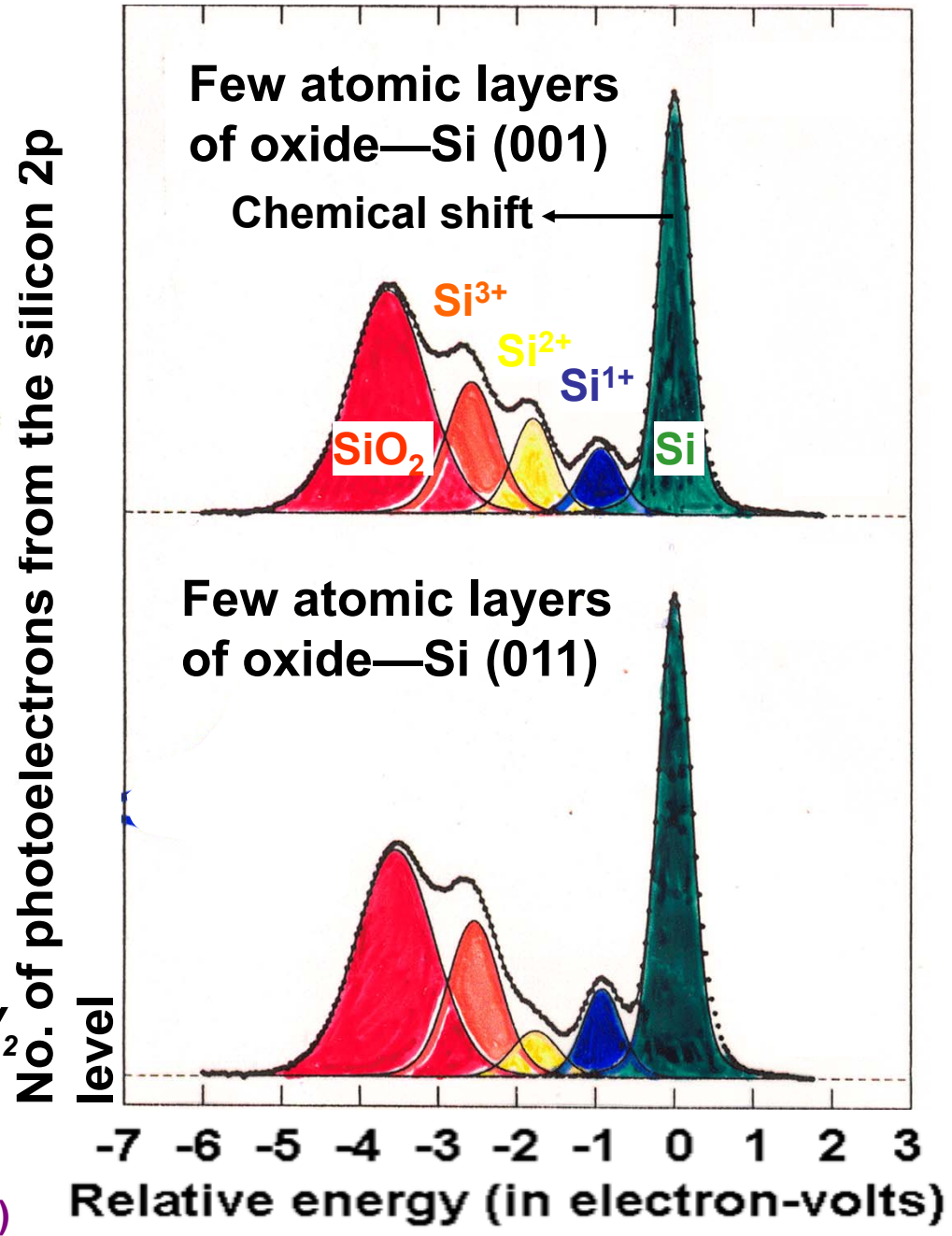

Himpsel et al., Phys. Rev. B 38, 6086 ('88)

W(110)/O—W $4f_{7/2}$ Chemical Shifts

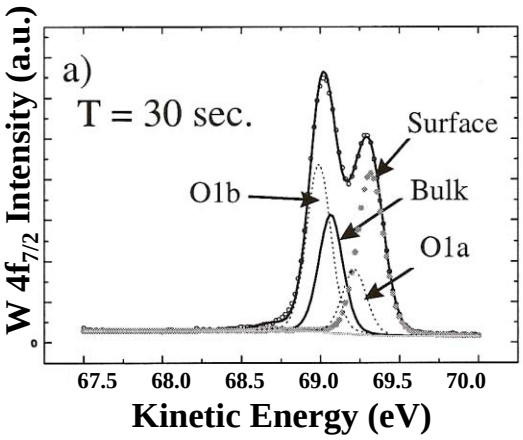

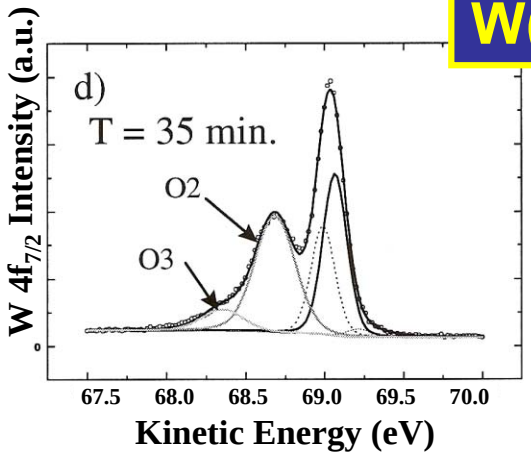

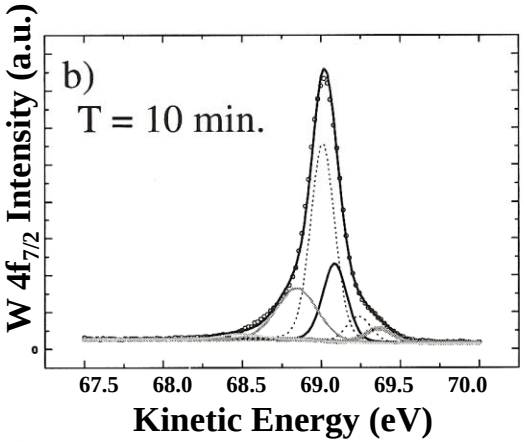

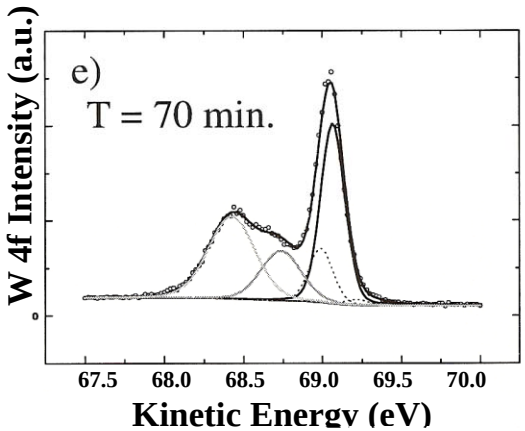

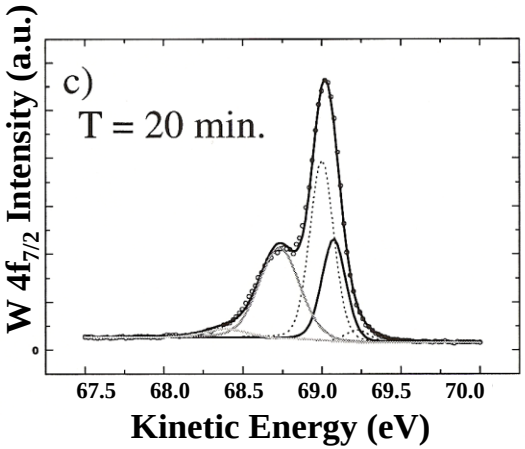

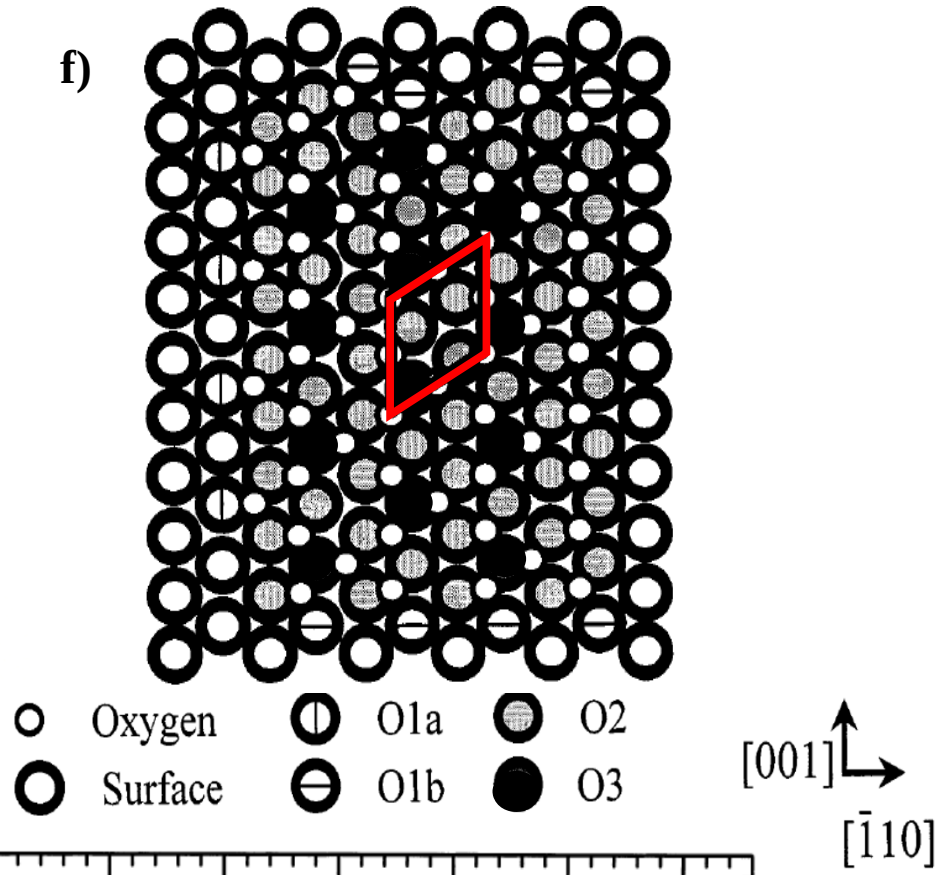

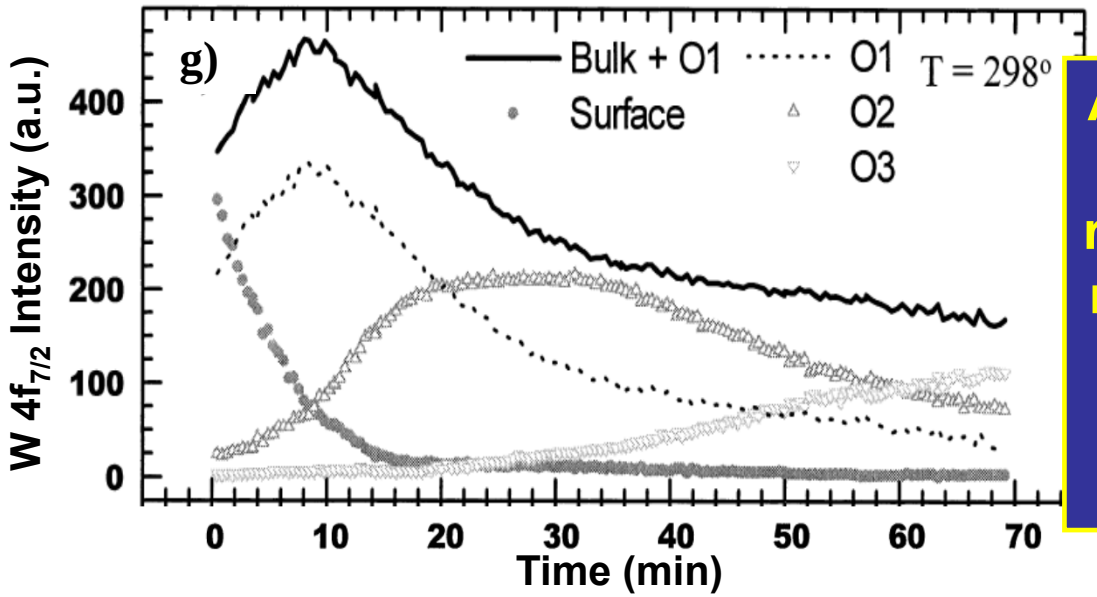

Ynzunza et al.,
Surf. Sci. 459 (2000) 69

An early time-resolved reaction study (more later)

Core and valence photoemission

$La_{0.6}Sr_{0.4}MnO_3$

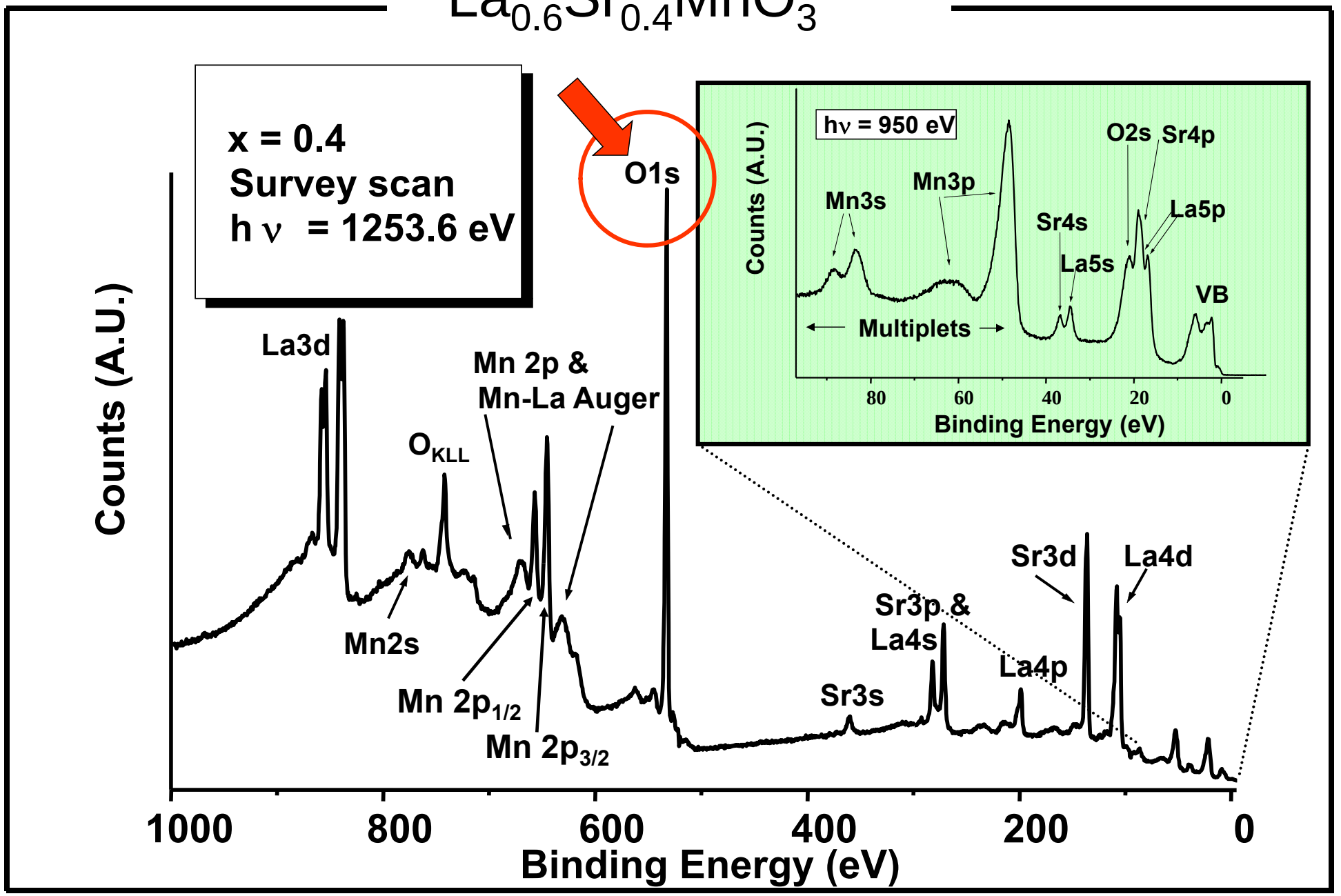

N. Mannella et al., Phys. Rev. Lett. 92, 166401 (2004)

Temperature dependence of Mn3s and O1s spectra: $La_{0.7}Sr_{0.3}MnO_3$

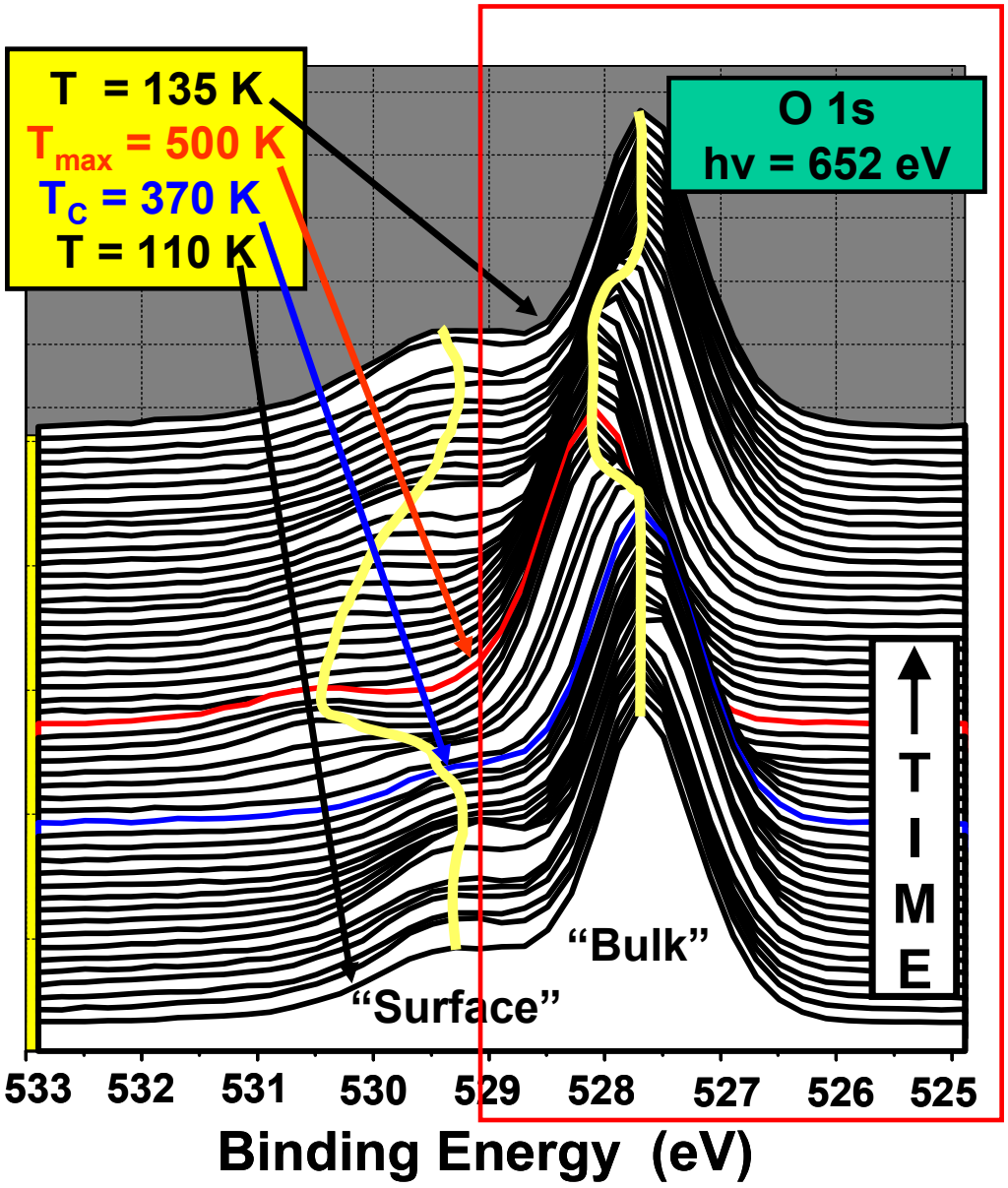

N. Mannella et al., Phys. Rev. Lett. 92, 166401 (2004)

Core and valence photoemission

$La_{0.6}Sr_{0.4}MnO_3$

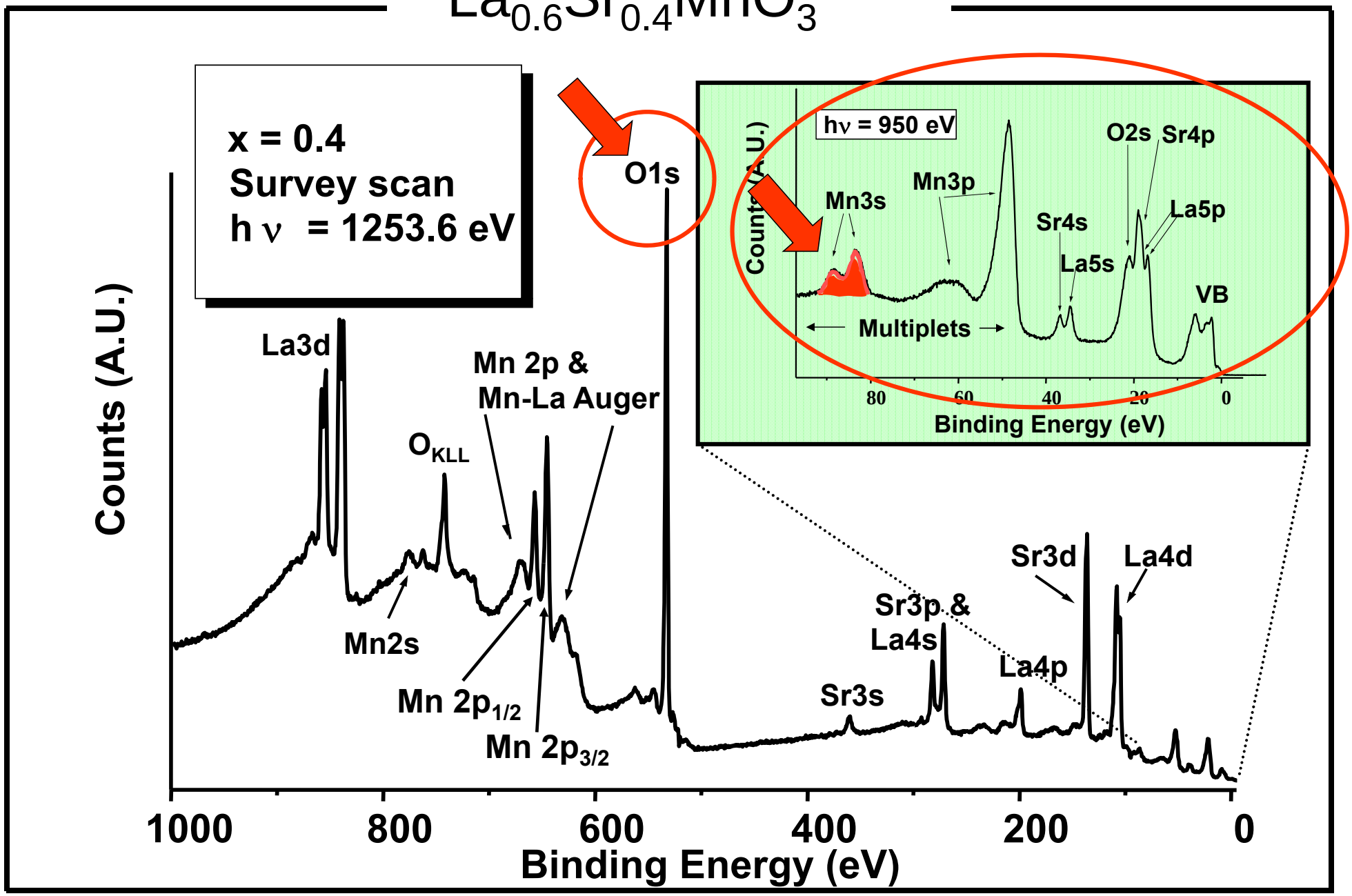

N. Mannella et al., Phys. Rev. Lett. 92, 166401 (2004)

Basic Concepts:

A Little Electronic Structure
The X-Ray-Based Experiments
X-Ray Sources, Synchrotron Radiation, Free Electron Lasers

Core-Level Photoemission

Intensities and Quantitative Analysis, the 3-Step Model
Varying Surface and Bulk Sensitivity
Chemical Shifts

Multiplet Splittings
Electron Screening and Satellite Structure
Magnetic and Non-Magnetic Dichroism
Resonant Photoemission
Photoelectron Diffraction and Holography

Valence-Level Photoemission

Band-Mapping in the Ultraviolet Photoemission Limit
Densities of States in the X-Ray Photoemission Limit

Some New Directions

Photoemission with Hard X-Rays (throughout lectures)
Photoemission with Standing Wave Excitation
Photoemission with: Higher Pressures→multi-Torr→Atmosphere?
Spatial Resolution-Photoelectron Microscopy
Temporal Resolution

Multiplet splitting in core levels of transition metal oxides

$$BE = h\nu - E_{kin} = \underbrace{E^*(N-1)}_{\text{Final state}} - \underbrace{E_0(N)}_{\text{Initial state}}$$

Open 3d shell, net spin S_{Mn}

$h\nu$

$|3s\rangle$

Upon photoemission, two possible final states

$|3s\rangle$

$J^{eff}_{3s,VB(3d)}$

$|3s\rangle$

$$K^{eff}_{3s,VB(3d)} \approx \int \varphi_{3s}(\vec{r}_1)\varphi_{3d}(\vec{r}_2)\frac{e^2}{r_{12}}\varphi_{3d}(\vec{r}_1)\varphi_{3s}(\vec{r}_2)dV_1dV_2$$

The splitting between the two peaks is given by

$\Delta E_{3s} \approx (2S_{Mn} + 1)\, K^{eff}_{3s,VB(3d)}$

(Van Vleck Theorem)

For the cubic manganites in simplest doping model,

$S_{Mn} = 1/2(4-x) \rightarrow$

$\Delta E_{3s} \approx [5-x]\, K^{eff}_{3s,\,VB)3d)}$

with $J^{eff}_{3s,\,VB} \approx 1.1$ eV

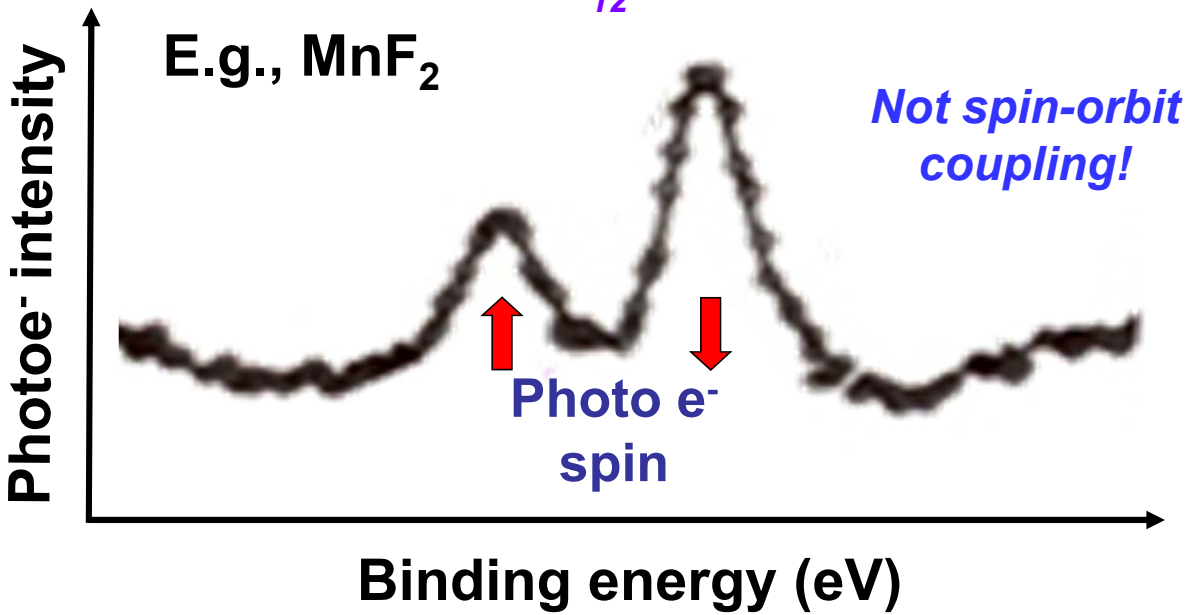

CORE-LEVEL MULTIPLET SPLITTINGS IN Mn COMPOUNDS

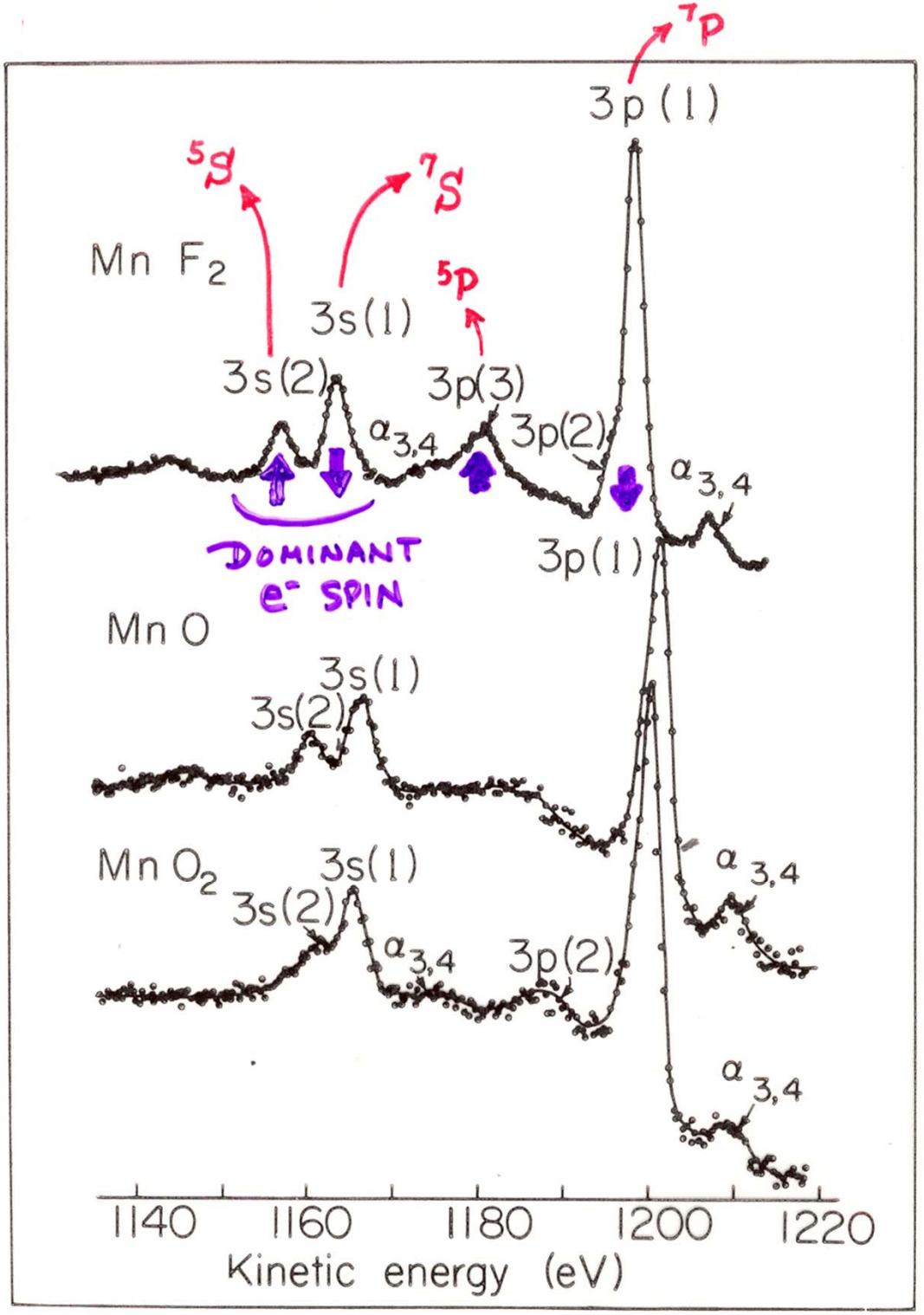

"Basic Concepts of XPS"
Figure 31

Intensities in photoelectron spectra in the sudden approximation

- GENERAL: FINAL STATE K (k-SUBSHELL + ALL OTHER DESIG.)

$$\text{INT.}_K \propto \left| \hat{e} \cdot \langle \Psi^f_{tot}(N,K) | \sum_{i=1}^{N} \vec{r}_i | \Psi^i(N) \rangle \right|^2 \quad \text{(DIPOLE APPROX.}$$

- BORN-OPPENHEIMER : e⁻'s FAST, VIBRATIONS SLOW

$$\text{INT.}_K \propto \underbrace{\left| \langle \Psi^f_{VIB,v'} | \Psi^i_{VIB,v} \rangle \right|^2}_{\text{FRANCK-CONDON FACTOR}} \left| \hat{e} \cdot \langle \Psi^f_{e^-}(N,K) | \sum_{i=1}^{N} \vec{r}_i | \Psi^i_{e^-}(N) \rangle \right|^2$$

- SUDDEN APPROXIMATION: $\Psi_K \rightarrow \Psi_f$ = PHOTO e⁻ (FAST)

k HOLE → $\varphi_1 \rightarrow \varphi'_1$, …, $\varphi_{k-1} \rightarrow \varphi'_{k-1}$, $\varphi_{k+1} \rightarrow \varphi'_{k+1}$, …, $\varphi_N \rightarrow \varphi'_N$ } (SLOW)

$$\text{INT.}_K \propto \left| \langle \Psi^f_{VIB,v'} | \Psi^i_{VIB,v} \rangle \right|^2 \underbrace{\left| \langle \Psi^f_{e^-}(N-1,K) | \hat{\Psi}^{k\ \text{MISSING}}_K(N-1,K) \rangle \right|^2}_{\text{SAME SUBSHELL COUPLING + TOTAL L,S} \rightarrow \text{"MONOPOLE"}} \left| \hat{e} \cdot \langle \varphi_f | \vec{r} | \varphi_K \rangle \right|^2$$

↳ NORMAL $\frac{d\sigma_K}{d\Omega}$

- SLATER DETS. FOR $\Psi^f_{e^-} = \det(\varphi'_1 \varphi'_2 \cdots \varphi'_{k-1} \varphi'_{k+1} \cdots \varphi'_N)$

$$\Psi_K = \det(\varphi_1 \varphi_2 \cdots \varphi_{k-1} \varphi_{k+1} \cdots \varphi_N)$$

$$\text{INT.}_K \propto \left| \langle \Psi^f_{VIB,v'} | \Psi^i_{VIB,v} \rangle \right|^2 \underbrace{\left| \langle \varphi'_1 | \varphi_1 \rangle \right|^2 \left| \langle \varphi'_2 | \varphi_2 \rangle \right|^2 \cdots \left| \langle \varphi'_{k-1} | \varphi_{k-1} \rangle \right|^2 \left| \langle \varphi'_{k+1} | \varphi_{k+1} \rangle \right|^2 \cdots \left| \langle \varphi'_N | \varphi_N \rangle \right|^2}_{(N-1)e^- \text{ SHAKE-UP/ SHAKE-OFF} \rightarrow \text{"MONOPOLE"}} \cdot \left| \hat{e} \cdot \langle \varphi_f | \vec{r} | \varphi_K \rangle \right|^2$$

1e- DIPOLE → $d\sigma/d\Omega$

- PLUS DIFFRACTION EFFECTS IN φ_f ESCAPE

ORIGIN OF MULTIPLET SPLITTINGS IN Mn^{2+}: "ONE-ELECTRON" THEORY

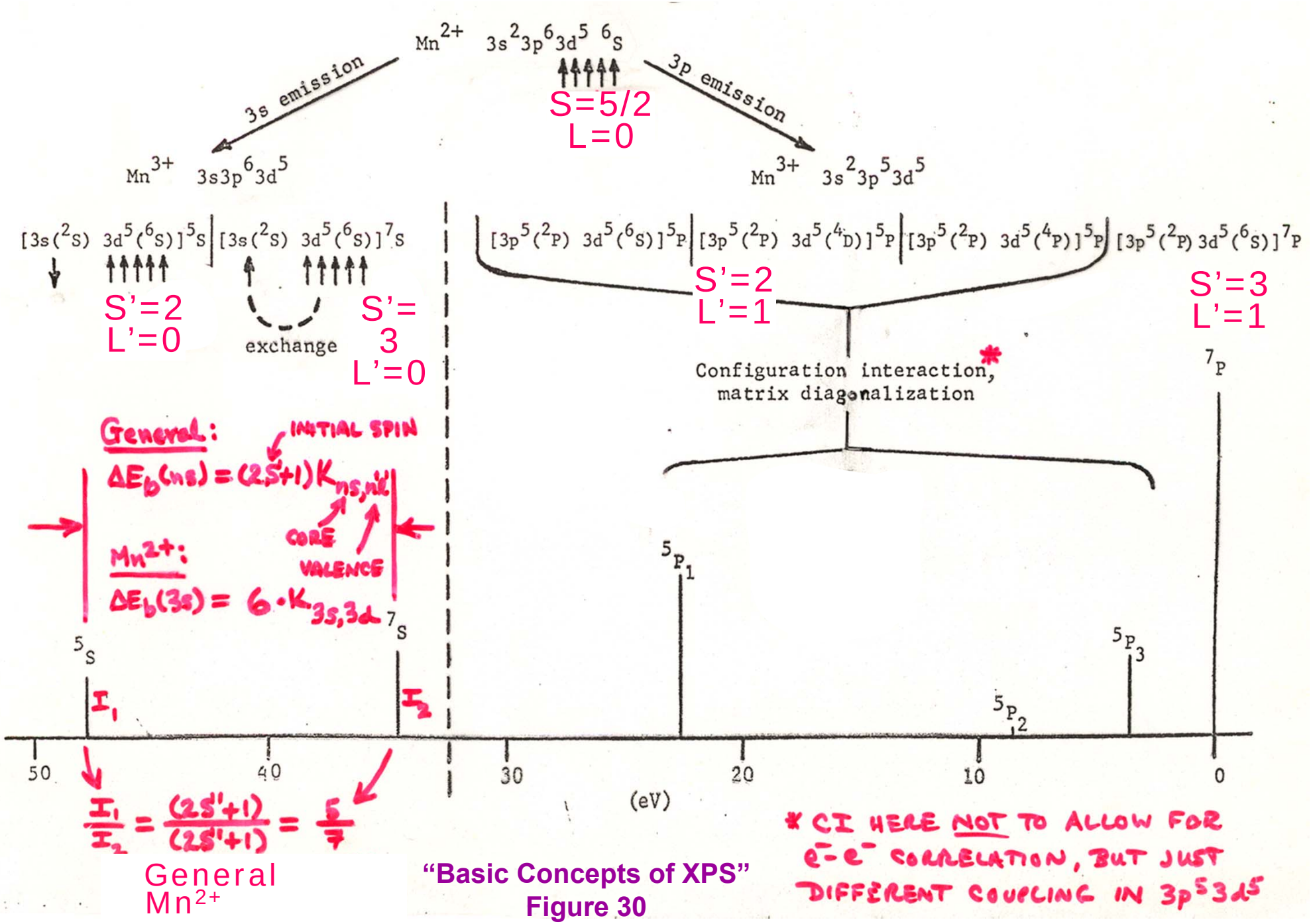

General Mn^{2+}

"Basic Concepts of XPS"
Figure 30

ORIGIN OF MULTIPLET SPLITTINGS IN Mn^{2+}: "ONE-ELECTRON" THEORY

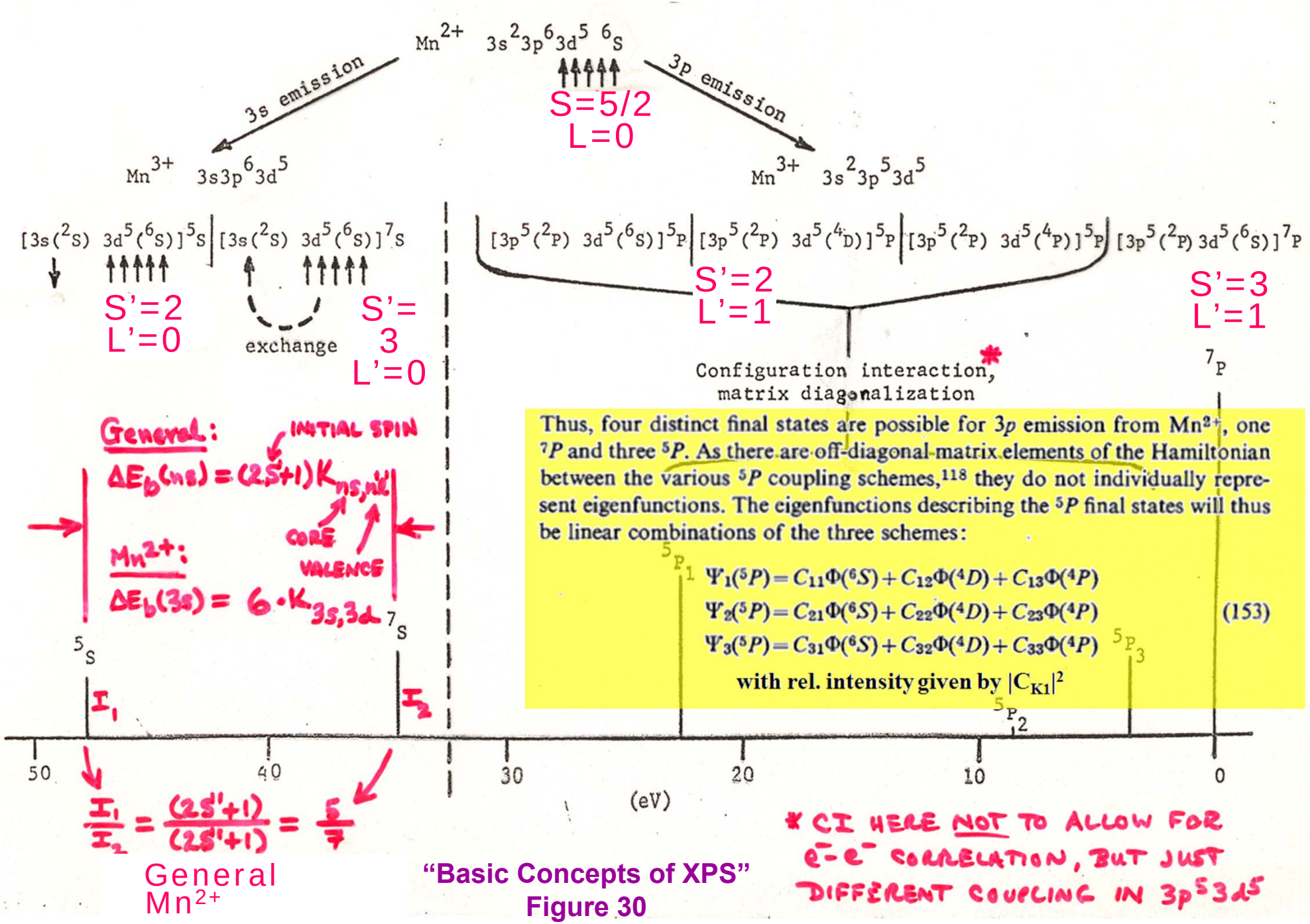

General Mn^{2+}

"Basic Concepts of XPS"
Figure 30

in order for relaxation to occur in forming the lowest-binding-energy "primary" or "adiabatic" final state corresponding to the ionic ground state, excited ionic states corresponding to binding energies higher than $-\epsilon_k$ must also arise. The peaks due to these states have been variously called "shake-up", "shake-off", "many-electron transitions", "configuration-interaction satellites", or "correlation peaks", and more specific illustrations are given in Section V.D. The high-intensity lowest-binding-energy peak has often been associated with a "one-electron transition", although this name is unduly restrictive in view of the inherently many-electron nature of the photoemission process. Thus, the intimate relationship between relaxation and correlation is demonstrated, although it still is possible to determine uniquely a relaxation energy with initial- and final-state Hartree–Fock wave functions that are often assumed to be uncorrelated in the sense that E_{corr} is measured relative to them. The second sudden-approximation sum rule deals with intensities, and it states that the sum of all intensities associated with the states $\Psi^f(N-1, K)$ is given by

$$I_{\text{tot}} = \sum_K I_K = C \sum_K |\langle \phi^f(1) | \hat{t} | \phi_k(1) \rangle|^2 |\langle \Psi^f(N-1, K) | \Psi_R(N-1) \rangle|^2$$
$$= C |\langle \phi^f(1) | \hat{t} | \phi_k(1) \rangle|^2 \quad (78)$$

where C is a constant for a given photon energy. One experimental consequence of this sum rule is that matrix elements and cross-sections calculated with unrelaxed final-state orbitals and thus using Eq. (76) apply only to absolute intensities summed over all states $\Psi^f(N-1, K)$, as was first pointed out by Fadley.[137] Thus, absolute photoelectron intensities for the usually-dominant ionic-ground-state peaks may be below those predicted by unrelaxed or frozen-orbital cross-sections, as has been noted experimentally by Wuilleumier and Krause;[139] by contrast, x-ray absorption coefficients, which inherently sum over all final states for a given $k \rightarrow f$ excitation, are well predicted by unrelaxed cross-sections.[137]

At a higher level of accuracy than any of the approximations discussed up to this point, configuration-interaction wave functions can also be used in the calculation of matrix elements and cross-sections.[91, 127] In particular, Manson[91] has discussed in a general way the effects that this can have, pointing out several mechanisms by which calculated intensities can be significantly modified by the inclusion of CI in the initial-state wave function and the final-state wave function. For computational convenience, it is customary (although not essential) to use the same set of orthonormal one-electron orbitals $\phi_1, \phi_2, \ldots, \phi_M$ $(M > N)$ in making up the configurations of both initial and final states. This apparent lack of allowance for relaxation in the final state can be more than compensated by using a large number of configurations with mixing coefficients C_j^i and C_j^f that are optimized for

both states:

$$\Psi^i(N) = \sum_j C_j^i \Phi_j^i(N) \quad (79)$$

$$\Psi^f(N) = \sum_m C_m^f \Phi_m^f(N) \quad (80)$$

The exact expressions for matrix elements determined with such wave functions are rather complex, particularly if more than one continuum orbital is included, corresponding to an allowance for continuum CI (also referred to as interchannel coupling or close coupling).[91] Although such continuum effects may be important in certain special cases (see Section V.D.5), several many-electron phenomena noted in XPS spectra can be well explained in terms of only initial-state CI and final-state-ion CI. In visualizing these effects, it is thus useful to take a sudden approximation point of view, in which a single primary $k \rightarrow f$ transition is considered and the individual configurations $\Phi_j^i(N)$ and $\Phi_m^f(N)$ are thus written as antisymmetrized products with forms analogous to Eqs (66) and (67):

$$\Phi_j^i(N) = \hat{A}(\phi_k(1)\chi_k(1), \Phi_j^i(N-1)) \quad (81)$$

$$\Phi_m^f(N) = \hat{A}(\phi^f(1)\chi^f(1), \Phi_m^f(N-1)) \quad (82)$$

In these equations, the $(N-1)$-electron factors can if desired be indexed identically, so that, for the fixed one-electron basis set, $\Phi_j^i(N-1) = \Phi_m^f(N-1)$ if $j=m$ and thus also $\langle \Phi_j^i(N-1) | \Phi_m^f(N-1) \rangle = \delta_{jm}$. Matrix elements in this limit are then given by repeated application of Eq. (68) as

$$\langle \Psi(N) | \sum_{i=1}^{N} \hat{t}_i | \Psi^i(N) \rangle = \langle \phi^f(1) | \hat{t} | \phi_k(1) \rangle [\sum_j (C_j^f)^* C_j^i] \quad (83)$$

Thus, the mixing of various configurations into either the initial or final states can affect the observed intensity of a given final state appreciably, as it is only if a certain configuration has a non-zero coefficient in both states that it will contribute a non-zero $(C_j^f)^* C_j^i$ product. For the useful limiting case in which a single configuration $j=1$ dominates the initial state, then $C_j^i \approx 1{\cdot}0$, $C_j^i \approx 0$ for $j \neq 1$, and the square of the matrix element (83) for transitions to a given final state is simply

$$\left| \langle \Psi^f(N) | \sum_{i=1}^{N} \hat{t}_i | \Psi^i(N) \rangle \right|^2 \propto |C_1^f|^2 \quad (84)$$

(If relaxation is permitted in the final-state one-electron orbitals, then overlap integrals of the form $\langle \Phi_m^f(N-1) | \Phi_j^i(N-1) \rangle \equiv S_{jm}$ must be computed,[14] and Eqs (83) and (84) become more complex. However, in general $S_{jm} \approx \delta_{jm}$.) Such CI effects are important in understanding the simplest forms of multiplet

COMPARISON OF GAS-PHASE AND SOLID-STATE SPECTRA

EXPT.: (a), (b), (d), HERMSMEIER ET AL., PHYS. REV. LETT. 61, 2592 (1988) (OUR GROUP)

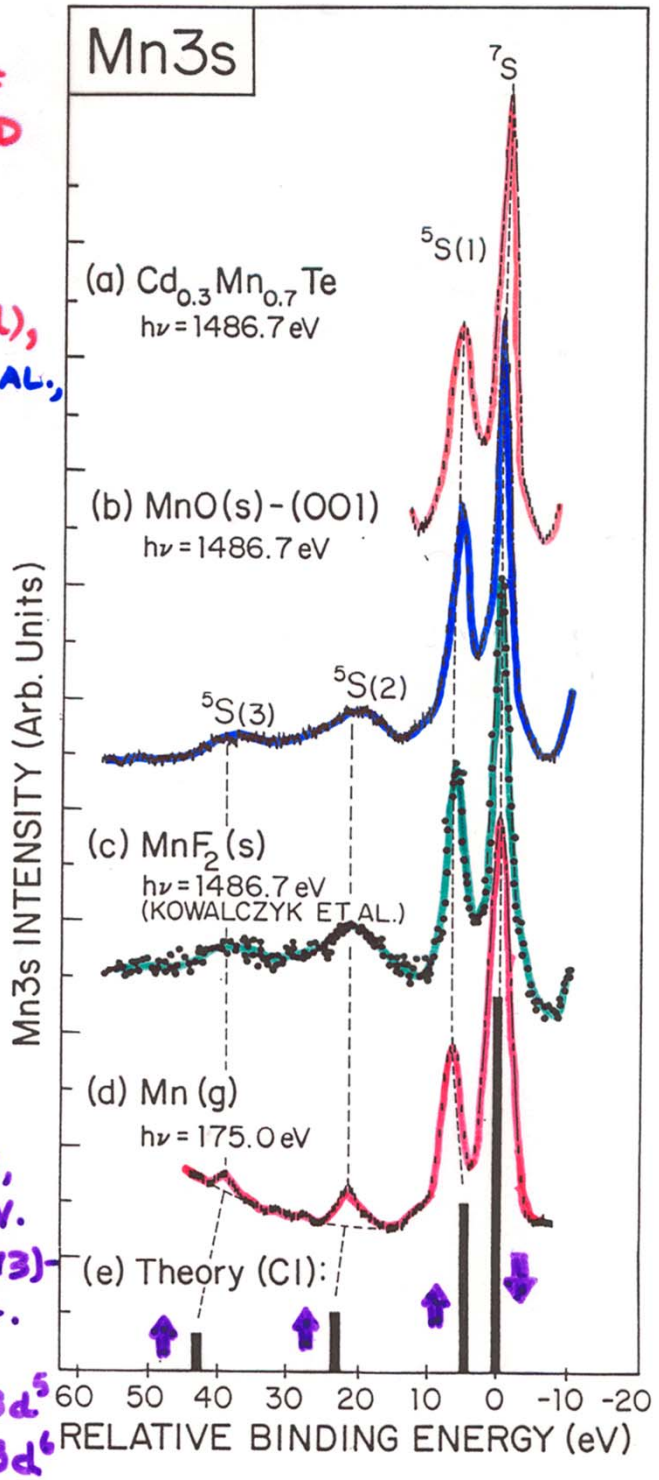

Correlation effects through configuration interaction (CI):

$\Psi_{CI} = \sum_{Config.i} \Phi_i$, **better wave function**

$= \Phi(Mn^{3+}...3s^1 3p^6 3d^5) + \Phi(Mn^{3+}...3s^2 3p^4 3d^6)$

esp. anti-parallel electrons

THEORY: BAGUS, FREEMAN, SASAKI, PHYS. REV. LETT. 30, 850 (1973) - ATOMIC CONFIG. INT. IN $Mn^{3+}...3s^1...3d^5$ + $Mn^{3+}...3s^2 3p^4 3d^6$

"Basic Concepts of XPS" Figure 33

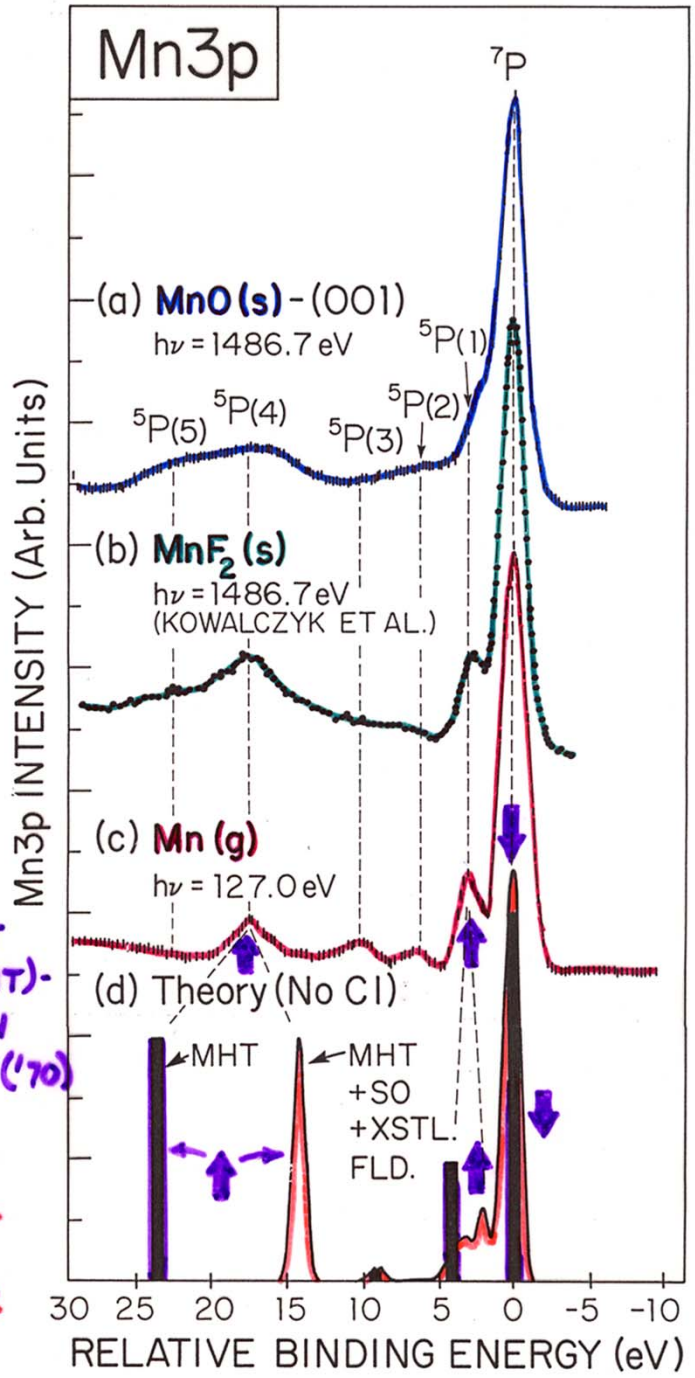

THEORY: NO CI

SIMPLE MULTIPLET HOLE THEORY (MHT) - FADLEY, SHIRLEY PHYS. REV. A2, 1109 ('70)

EMPIRICAL MHT WITH SPIN ORBIT & CRYSTAL FIELD - SUGANO ET AL., J. PHYS. C 15, 2625 (1982)

HERMSMEIER ET AL., P.R.L. 61, 2592 ('88)

Case study: Temperature dependence of Mn3s and O1s spectra in a colossal magnetorestive (CMR) oxide: $La_{0.7}Sr_{0.3}MnO_3$

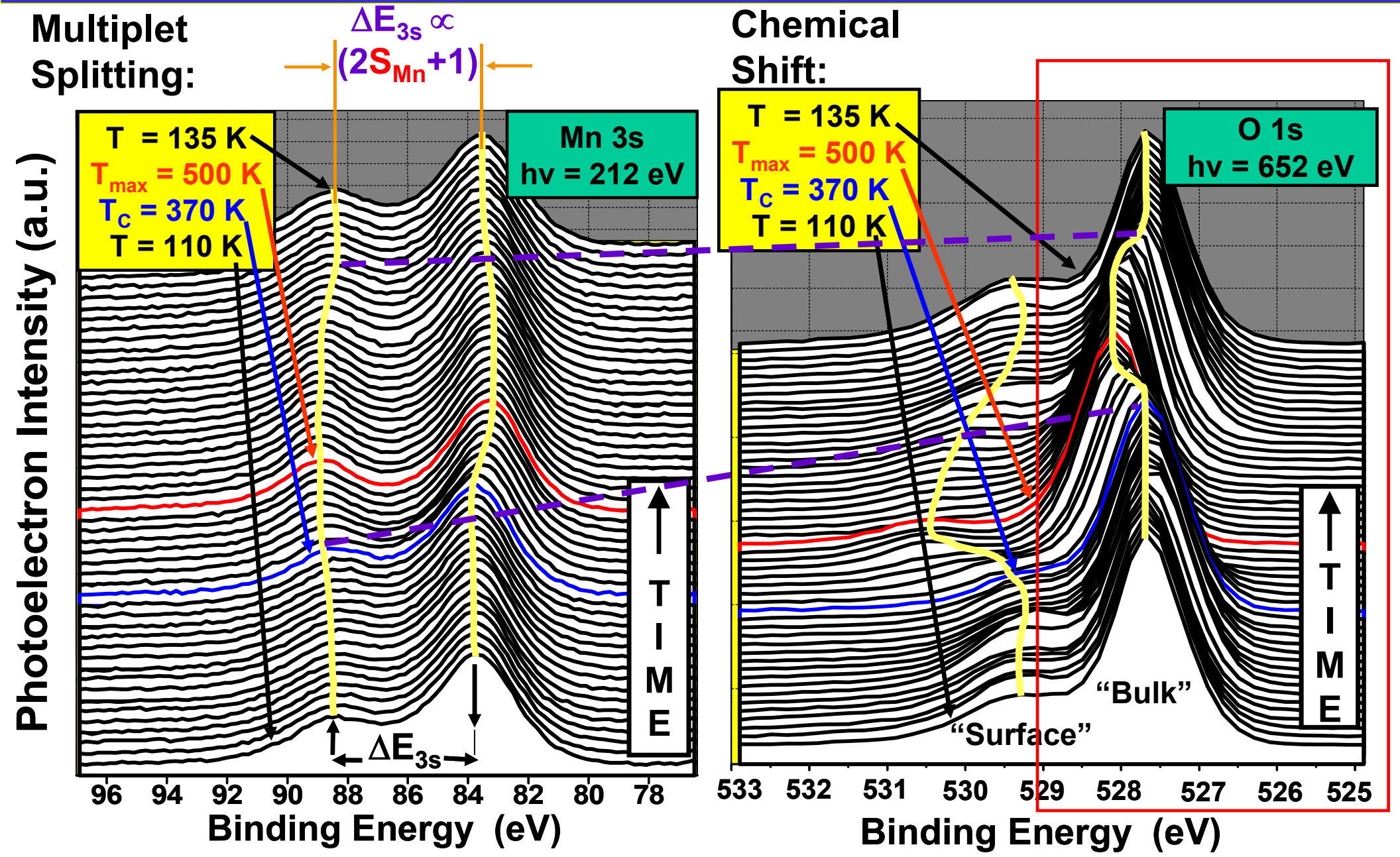

se of the Mn3s splitting-reversible

Increase of O1s BE-reversible

Suggested scenario

Jahn-Teller distortion

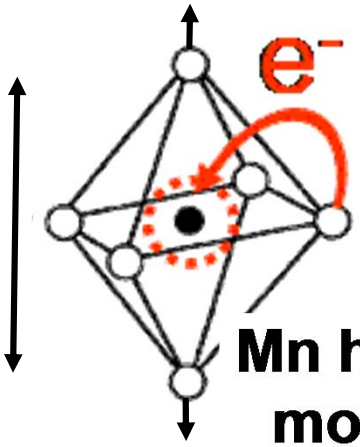

O more positive

Mn higher spin, more negative

T_C

Mixed Mn^{3+}- Mn^{4+}

T_{sat}

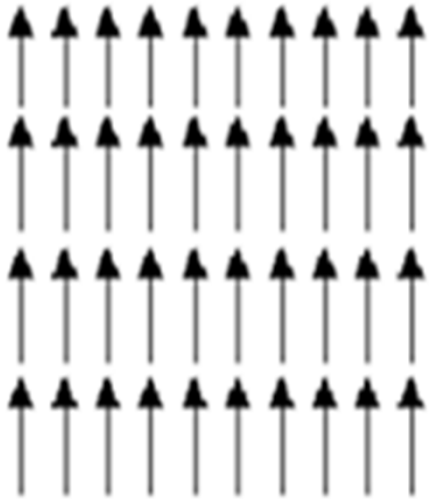

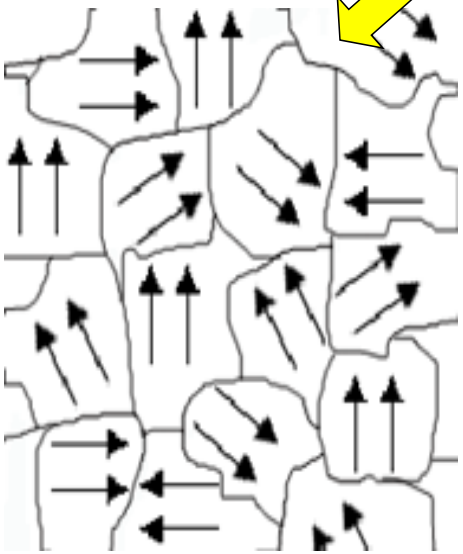

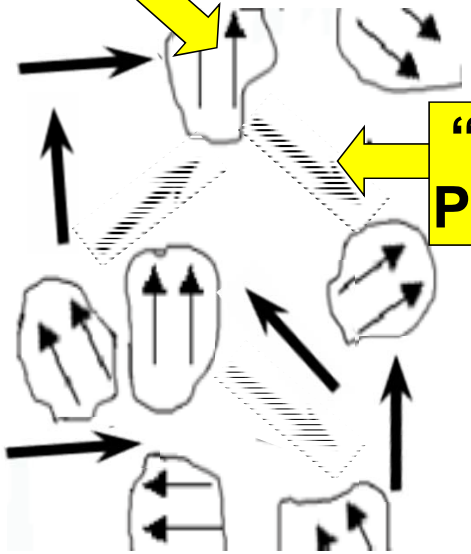

"Polaronic" Phase—Mn^{3+}

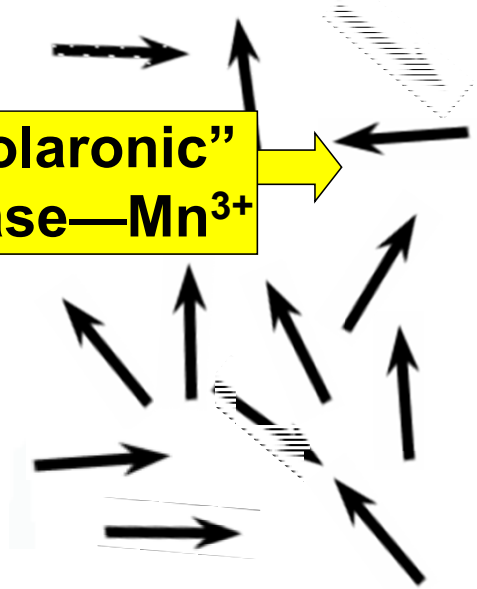

Long-range ferromagnetic order

Loss of long - range order at T_C

Short - range order above T_C up to T_{sat} Jahn-Teller distortion

N. Mannella et al., PRL 92, 166401 ('04); PRB 70, 224433 ('04), PRB 77, 125134 ('08); Offi et al., PRB 77, 174422 ('08)

Basic Concepts:

A Little Electronic Structure
The X-Ray-Based Experiments
X-Ray Sources, Synchrotron Radiation, Free Electron Lasers

Core-Level Photoemission

Intensities and Quantitative Analysis, the 3-Step Model
Varying Surface and Bulk Sensitivity
Chemical Shifts
Multiplet Splittings

Electron Screening and Satellite Structure
Magnetic and Non-Magnetic Dichroism
Resonant Photoemission
Photoelectron Diffraction and Holography

Valence-Level Photoemission

Band-Mapping in the Ultraviolet Photoemission Limit
Densities of States in the X-Ray Photoemission Limit

Some New Directions

Photoemission with Hard X-Rays (throughout lectures)
Photoemission with Standing Wave Excitation
Photoemission with: Higher Pressures→multi-Torr→Atmosphere?
Spatial Resolution-Photoelectron Microscopy
Temporal Resolution

Photoemission: The correct energy picture

$$h\nu = E^{Vacuum}_{binding} + E_{kinetic} = E^{Fermi}_{binding} + \varphi_{spectrometer} + E_{kinetic}$$

$$E^{Vacuum}_{binding}(Qn\ell\, j, K) = E_{final}(N-1, Qn\ell\, j\ hole, K) - E_{initial}(N)$$

= a difference of final and initial state energies

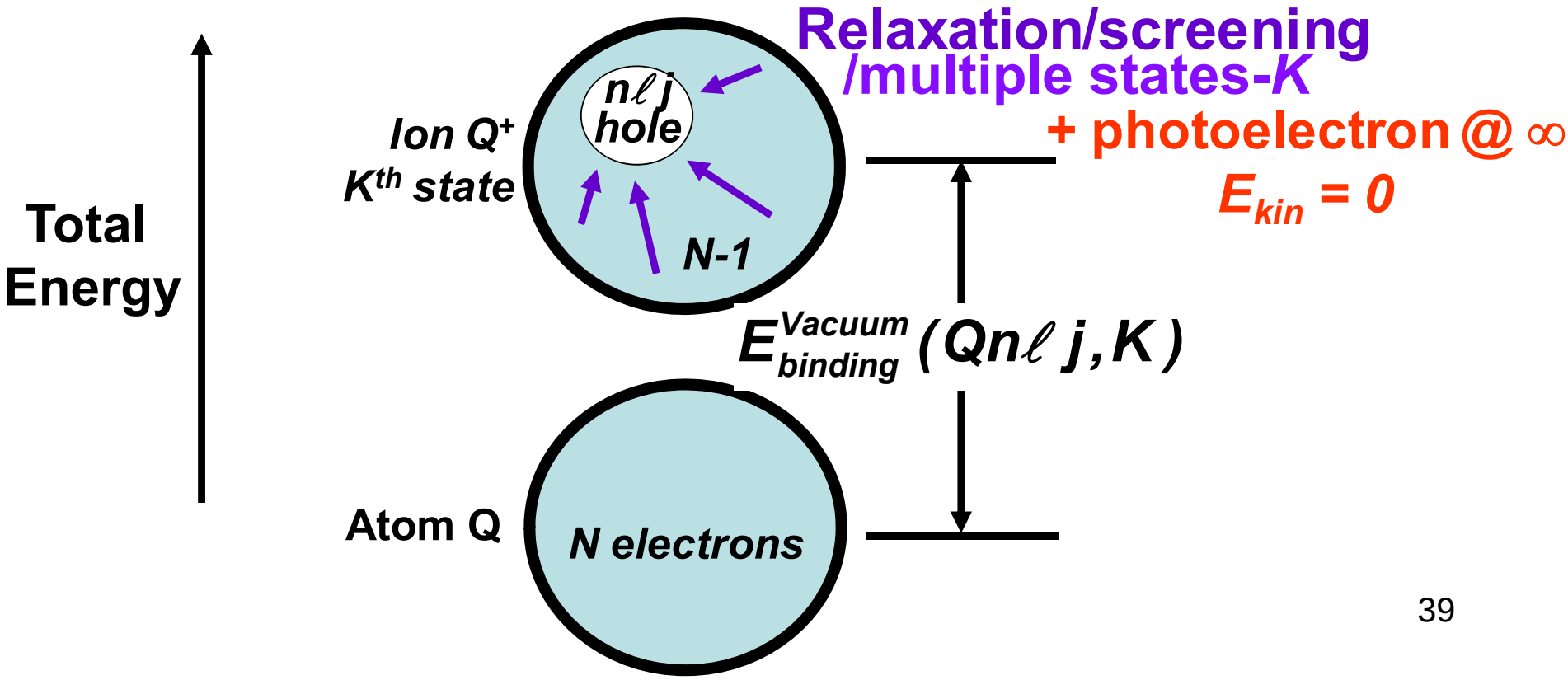

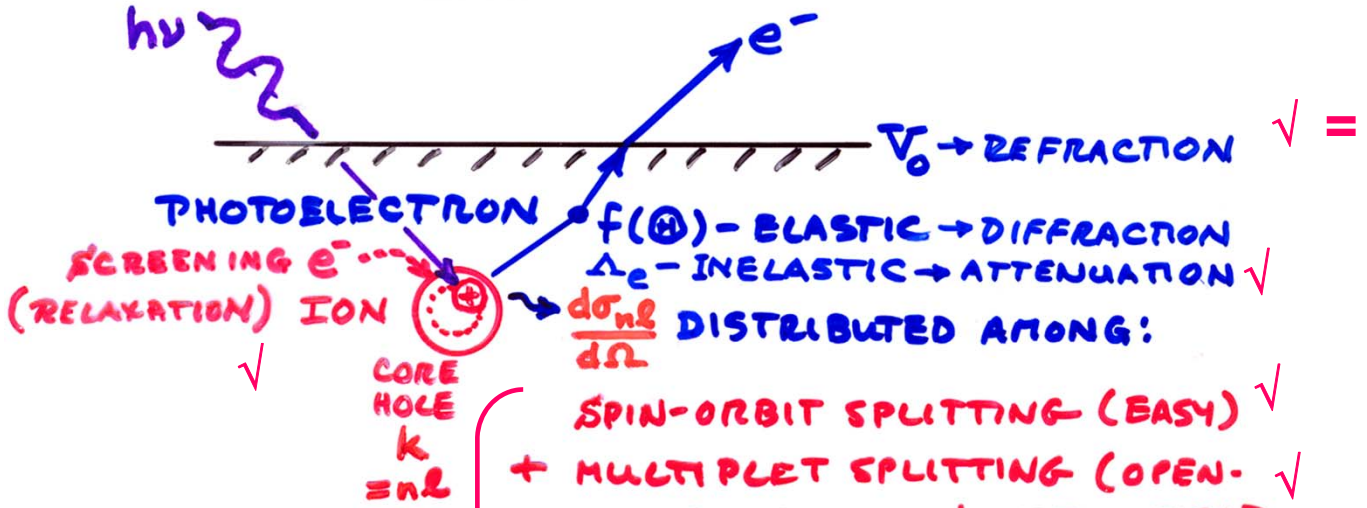

√ = covered so far

ADDITIONAL SOURCES OF STRUCTURE (AND INFORMATION!) IN SPECTRA BEYOND CHEMICAL SHIFTS

- SPIN-ORBIT SPLITTING (EASY) √
- + MULTIPLET SPLITTING (OPEN-SHELL SYSTEMS), XSTAL FIELD √
- + CORRELATION / CONFIGURATION INTERACTION √
- + SHAKE-UP / SHAKE-OFF / e^--HOLE
- + SCREENING / NON-SCREENING: CONFIGURATION INTERACTION
- + VIBRATIONAL EXCITATIONS
- + RESONANT PHOTOEMISSION ($h\nu \approx E_{b,n\ell'}$) √

REALLY ALL AT ONCE, BUT SUM RULES + THEORY HELP

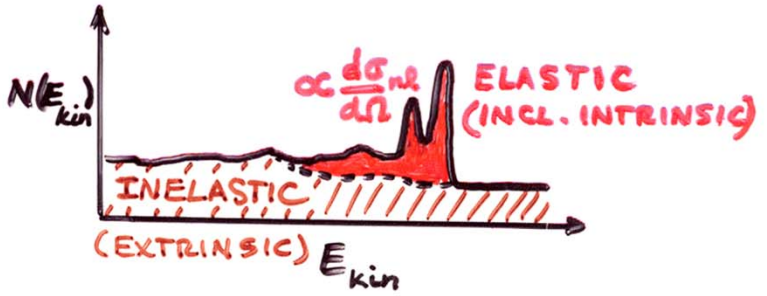

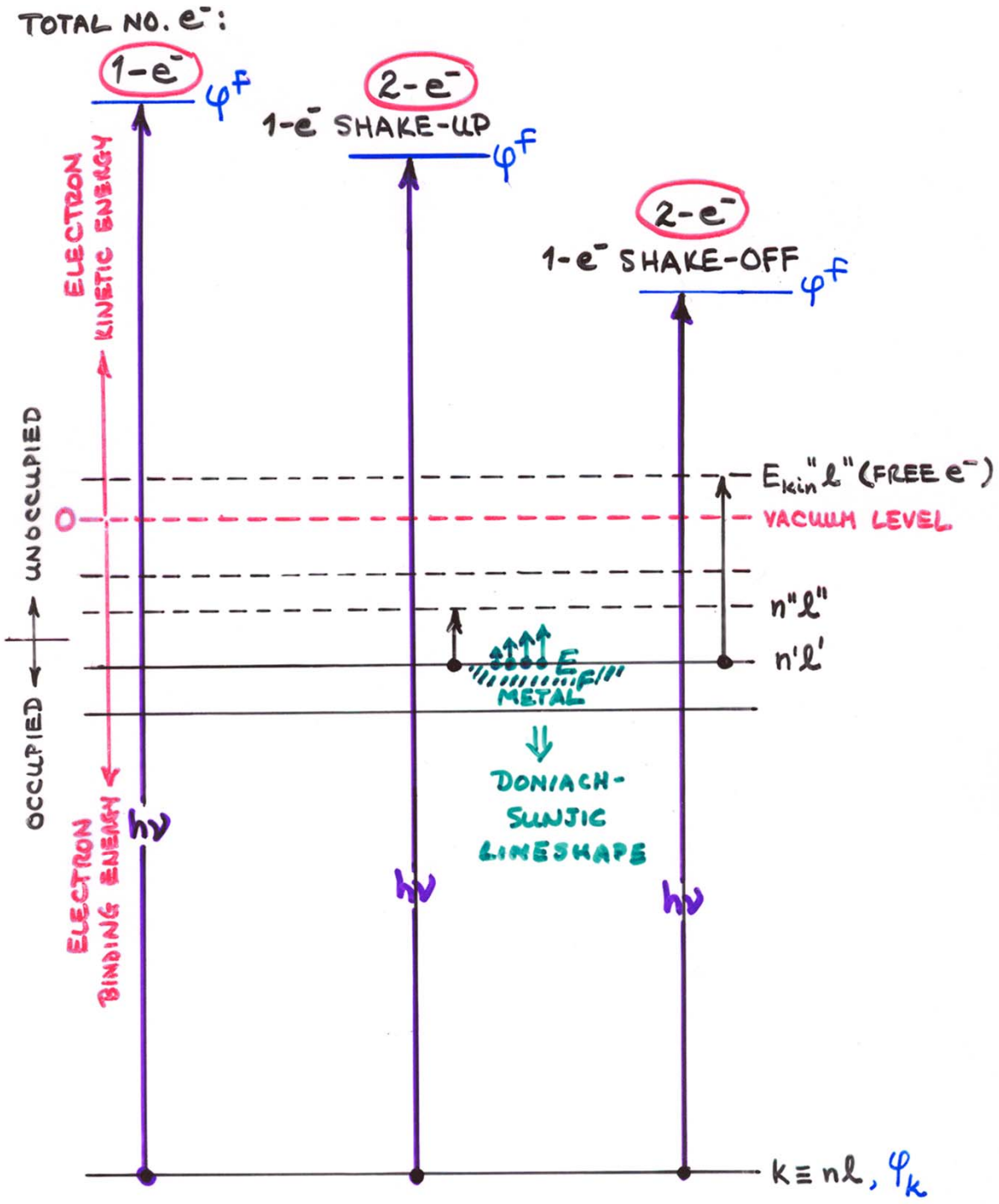

MULTIELECTRON EFFECTS IN CORE EMISSION

Intensities in photoelectron spectra in the sudden approximation

- GENERAL: FINAL STATE K (k-SUBSHELL + ALL OTHER DESIG.)

$$\text{INT.}_K \propto \left| \hat{e} \cdot \langle \Psi^f_{tot}(N,K) | \sum_{i=1}^{N} \vec{r}_i | \Psi^i(N) \rangle \right|^2 \quad \text{(DIPOLE APPROX.}$$

- BORN-OPPENHEIMER: e^-'s FAST, VIBRATIONS SLOW

$$\text{INT.}_K \propto |\langle \Psi^f_{VIB,v'} | \Psi^i_{VIB,v} \rangle|^2 \left| \hat{e} \cdot \langle \Psi^f_{e^-}(N,K) | \sum_{i=1}^{N} \vec{r}_i | \Psi^i_{e^-}(N) \rangle \right|^2$$

$|\langle \Psi^f_{VIB,v'} | \Psi^i_{VIB,v} \rangle|^2$: FRANCK-CONDON FACTOR

- SUDDEN APPROXIMATION: $\Psi_K \rightarrow \Psi_f$ = PHOTO e^- (FAST)

k HOLE → $\varphi_1 \rightarrow \varphi'_1$, …, $\varphi_{k-1} \rightarrow \varphi'_{k-1}$, $\varphi_{k+1} \rightarrow \varphi'_{k+1}$, …, $\varphi_N \rightarrow \varphi'_N$ (SLOW)

$$\text{INT.}_K \propto |\langle \Psi^f_{VIB,v'} | \Psi^i_{VIB,v} \rangle|^2 \left| \langle \Psi^f_{e^-}(N-1,K) | \overset{\uparrow}{\Psi_K}(N-1,K) \rangle \right|^2$$

k MISSING

$$\left| \hat{e} \cdot \langle \varphi_f | \vec{r} | \varphi_K \rangle \right|^2$$

↳ NORMAL $\frac{d\sigma_K}{d\Omega}$

SAME SUBSHELL COUPLING + TOTAL L,S → "MONOPOLE"

- SLATER DETS. FOR $\Psi^f_{e^-} = \det(\varphi'_1 \varphi'_2 \cdots \varphi'_{k-1} \varphi'_{k+1} \cdots \varphi'_N)$

$$\Psi_K = \det(\varphi_1 \varphi_2 \cdots \varphi_{k-1} \varphi_{k+1} \cdots \varphi_N)$$

$$\text{INT.}_K \propto |\langle \Psi^f_{VIB,v'} | \Psi^i_{VIB,v} \rangle|^2 |\langle \varphi'_1 | \varphi_1 \rangle|^2 |\langle \varphi'_2 | \varphi_2 \rangle|^2 \cdots$$
$$|\langle \varphi'_{k-1} | \varphi_{k-1} \rangle|^2 |\langle \varphi'_{k+1} | \varphi_{k+1} \rangle|^2 \cdots |\langle \varphi'_N | \varphi_N \rangle|^2 \cdot$$

$$\left| \hat{e} \cdot \langle \varphi_f | \vec{r} | \varphi_K \rangle \right|^2$$

1e- DIPOLE → $d\sigma/d\Omega$

$(N-1)e^-$ SHAKE-UP/ SHAKE-OFF → "MONOPOLE"

- PLUS DIFFRACTION EFFECTS IN φ_f ESCAPE

Neon 1s shake-up and shake-off

"Basic Concepts of XPS"
Figure 36

$Ne\ 1s^2 2s^2 2p^6\ {}^1S \xrightarrow{-e^-} Ne^+\ 1s^1 2s^2 2p^6\ {}^2S$

1-e^- SHAKE-UP: ($Ne^+\ 1s^1 2s^2 2p^5 np^1\ (n = 3,4,5,\dots)\ {}^2S$
$Ne^+\ 1s^1 2s^1 2p^6 ns^1\ (n = 3,\dots)\ {}^2S$

2-e^- SHAKE-UP: $Ne^+\ 1s^1 2s^2 2p^4 3p^2\ {}^2S$

2p SHAKE-OFF: $Ne^+\ 1s^1 2s^2 2p^5, E_{kin}\ "p"\ {}^2S$

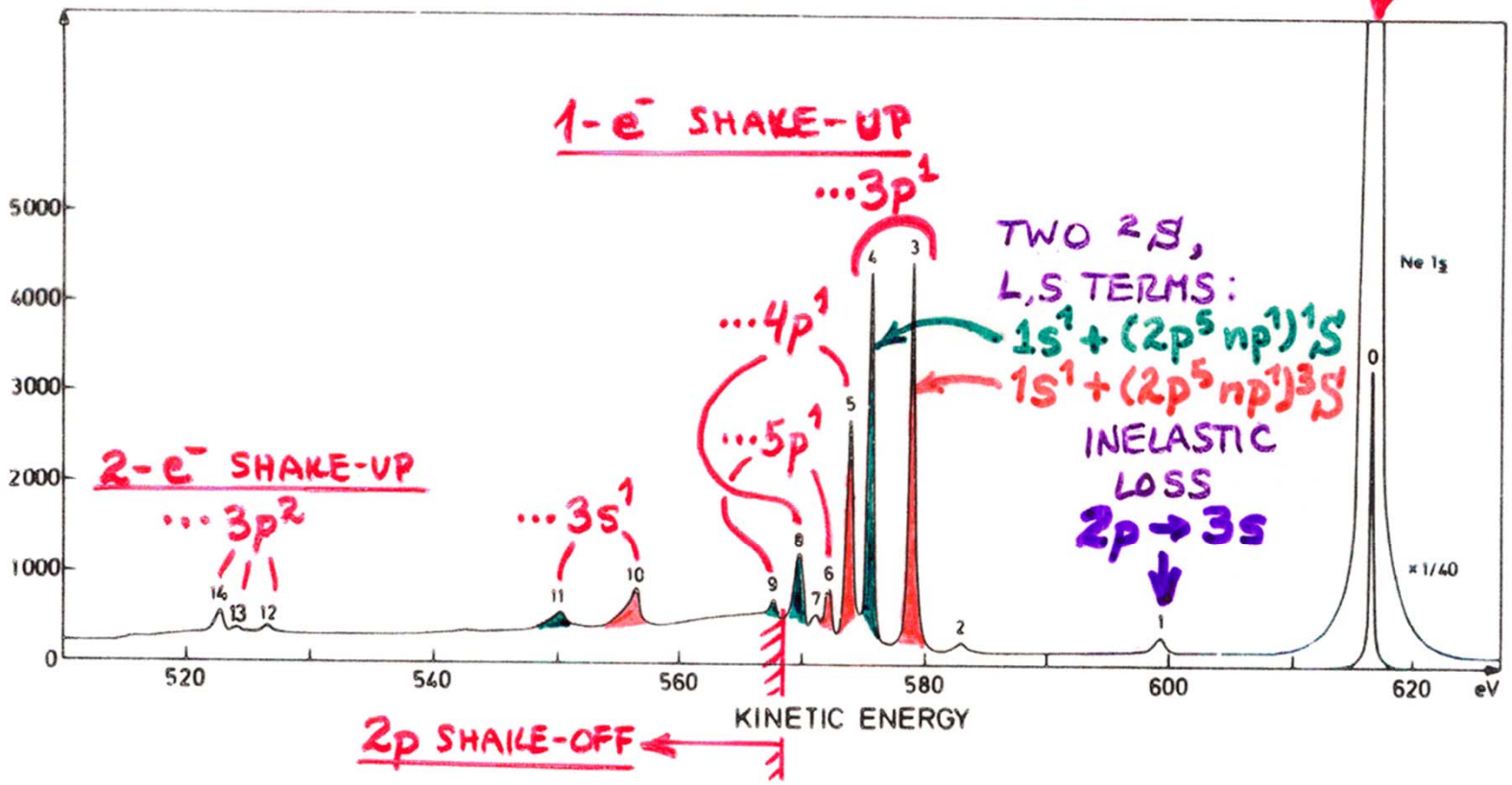

OVERALL: ~12% SHAKE-UP + 16% SHAKE-OFF ≈ 28% OF EVENTS

BAND THEORY—D.O.S:

Shake-up like excitations in metals

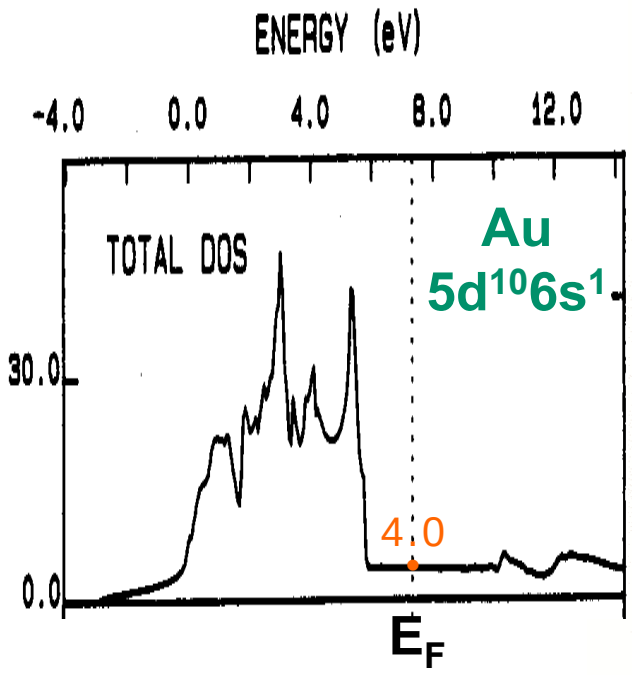

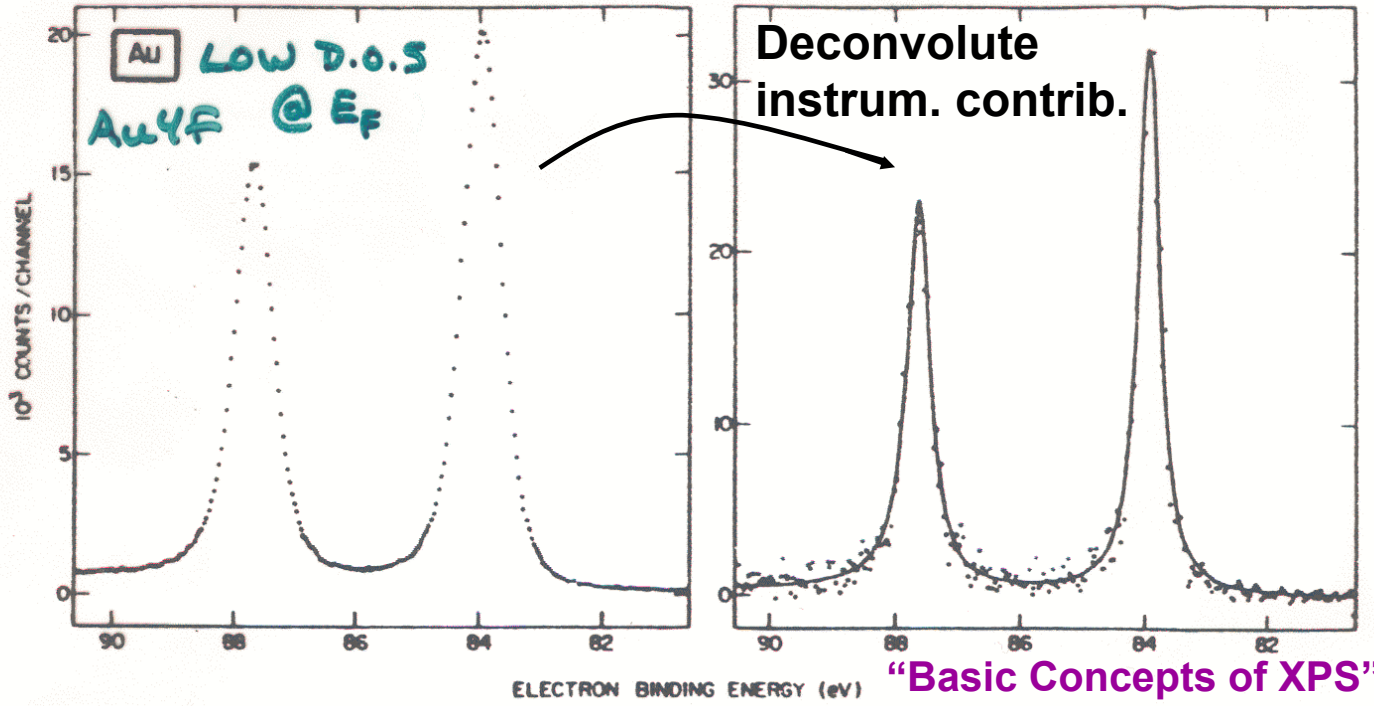

"Basic Concepts of XPS"
Figure 10

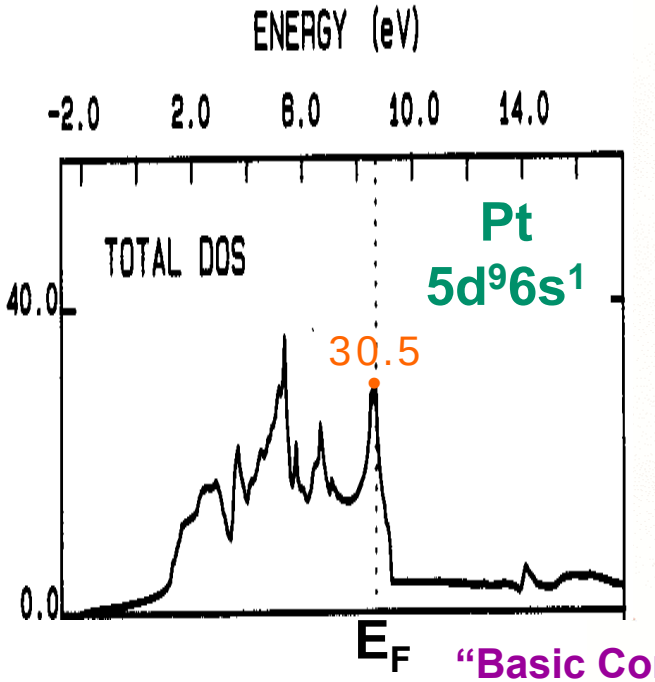

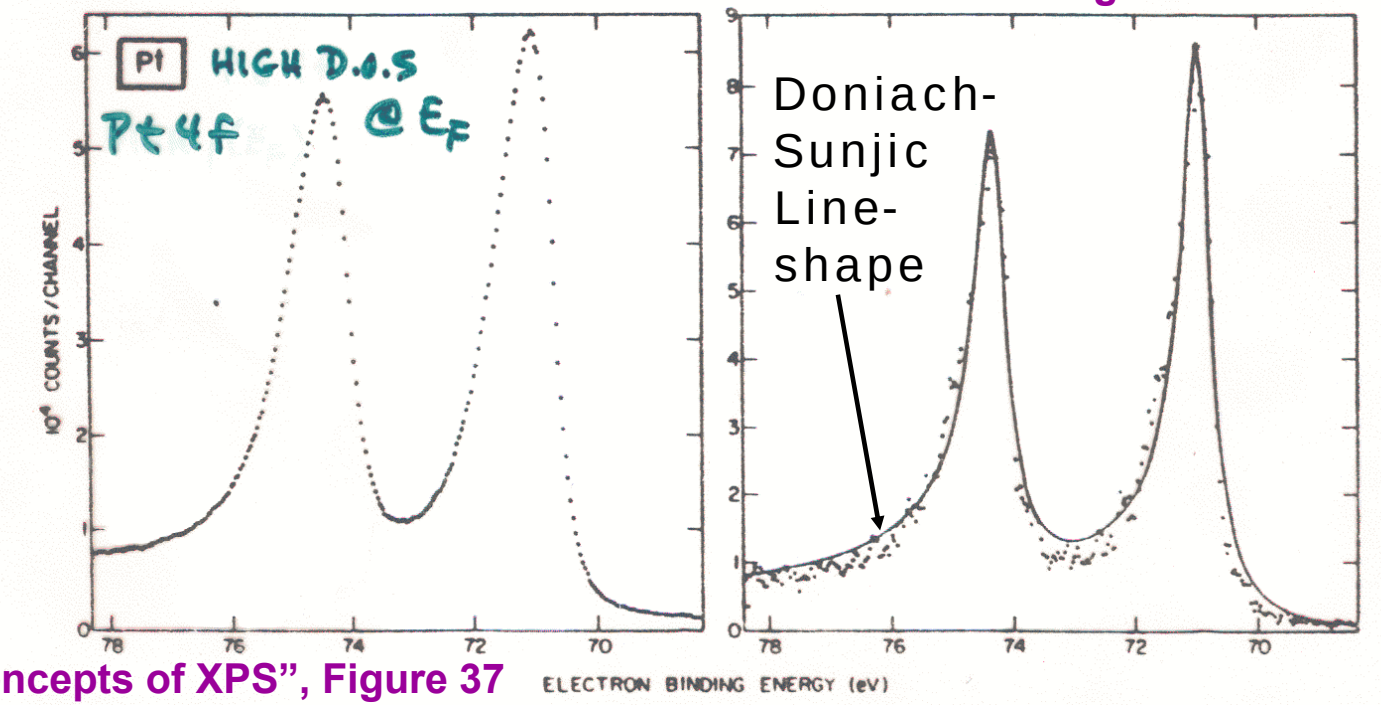

"Basic Concepts of XPS", Figure 37

Global sum rules and many-electron description of photoemission

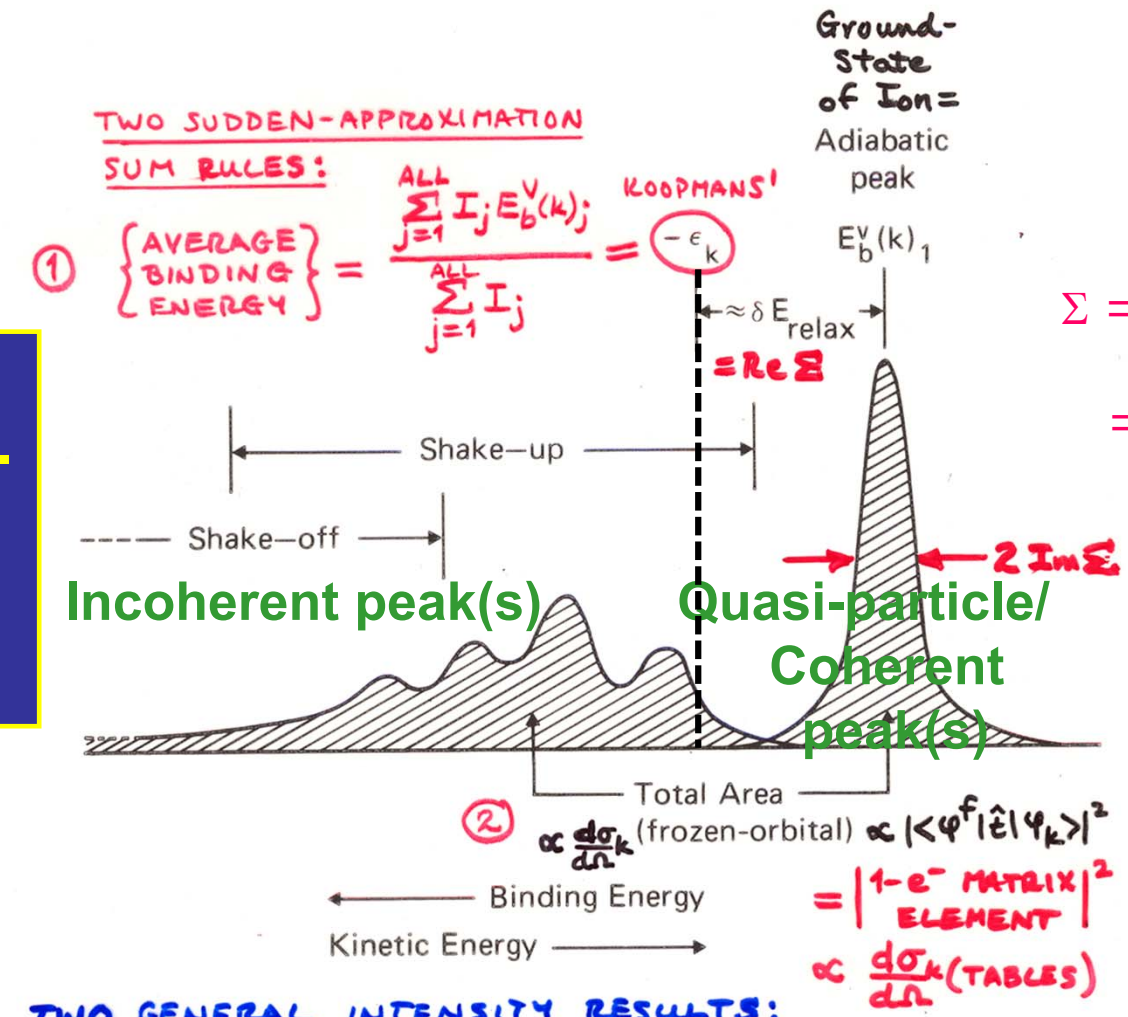

Σ = many-body "self energy"
= $Re\Sigma + iIm\Sigma$

$= \Delta E$

$\Delta E \tau_{lifetime} \approx \hbar/2$

TWO GENERAL INTENSITY RESULTS:

① $I_j \propto |\langle \varphi^f(1) | \hat{\epsilon} | \varphi_k(1) \rangle|^2 |\langle \Psi^F(N-1,j) | \Psi_R(N-1) \rangle|^2$
$k\,e^-$ MISSING

Figure 8 -- Schematic illustration of a photoelectron spectrum involving shake-up and shake-off satellites. The weighted average of all binding energies yields the Koopmans' Theorem binding energy $-\epsilon_k$ (sum rule (77)), and the sum of all intensities is proportional to a frozen-orbital cross section σ_k (sum rule (78)). The adiabatic peak corresponds to formation of the ground-state of the ion ($E_b(k)_1 \equiv E_b(K=1)$).

② (TOTAL SHAKE-UP + SHAKE-OFF) $= 1 - |\langle \Psi^f(N-1,1) | \Psi_R(N-1) \rangle|^2$
$\approx$ 15-25 % FOR ATOMS/MOLEC.

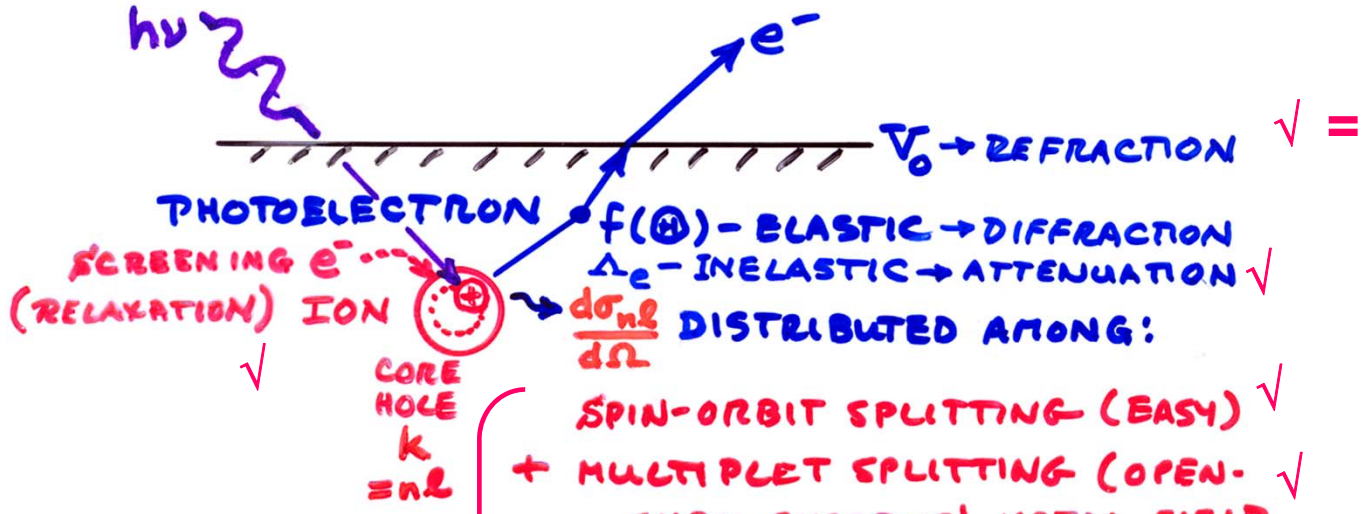

√ = covered so far

ADDITIONAL SOURCES OF STRUCTURE (AND INFORMATION!) IN SPECTRA BEYOND CHEMICAL SHIFTS

REALLY ALL AT ONCE, BUT SUM RULES + THEORY HELP

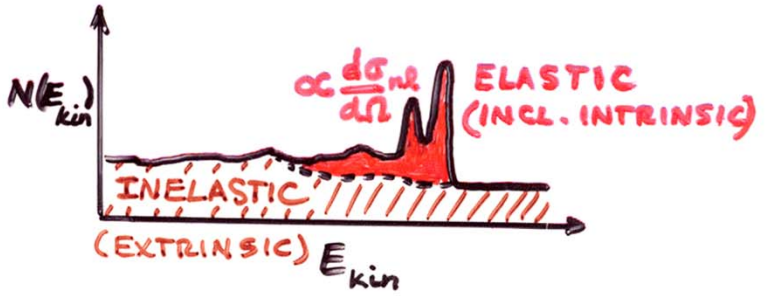

Basic energetics—Many e- & many atom picture

$$h\nu = E^{Vacuum}_{binding} + E_{kinetic} = E^{Fermi}_{binding} + \varphi_{spectrometer} + E_{kinetic}$$

$$E^{Vacuum}_{binding}(Qn\ell\, j, K) = E_{final}(N-1, Qn\ell\, j\ hole, K) - E_{initial}(N)$$

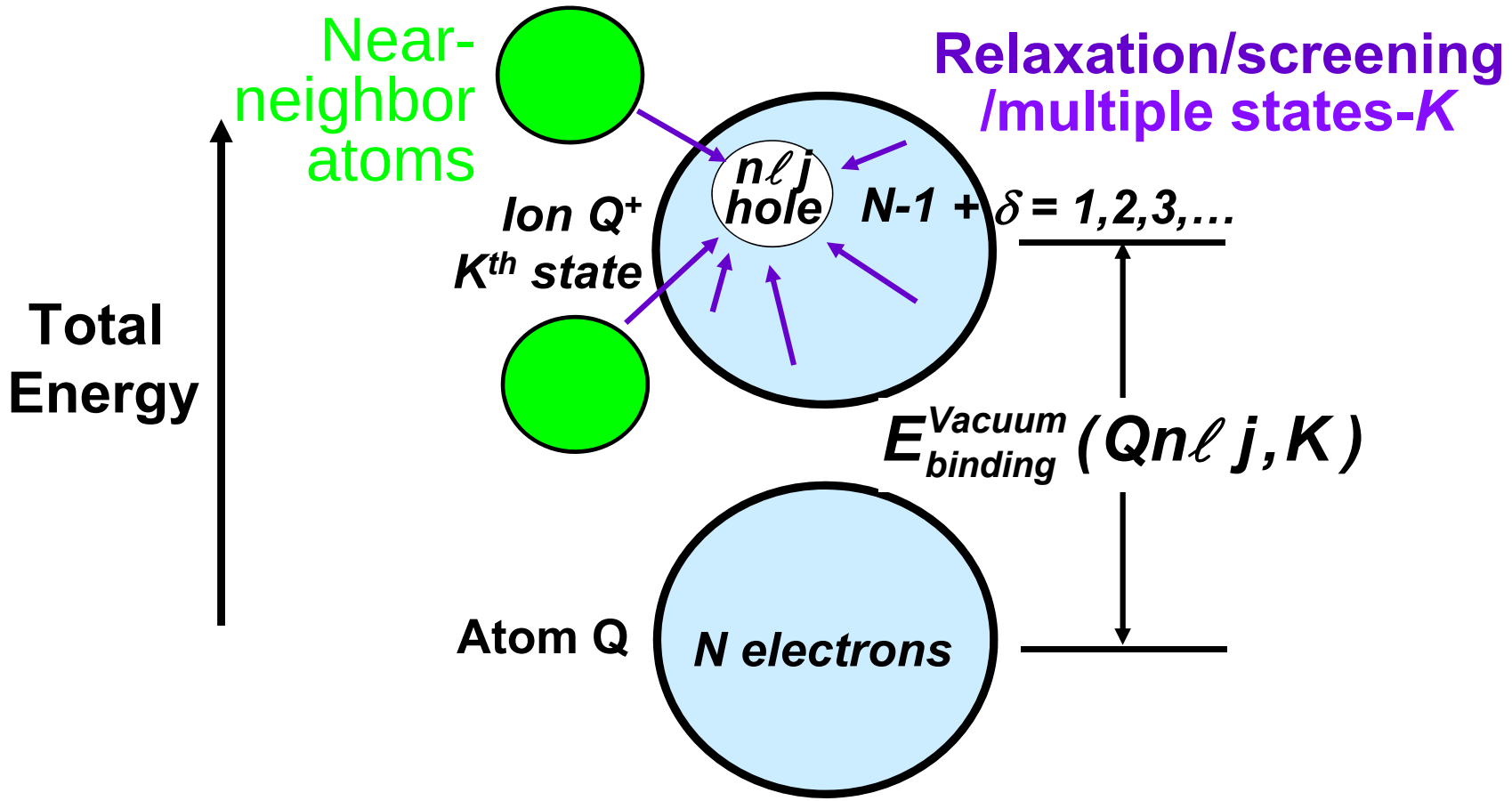

Satellites & charge-transfer screening

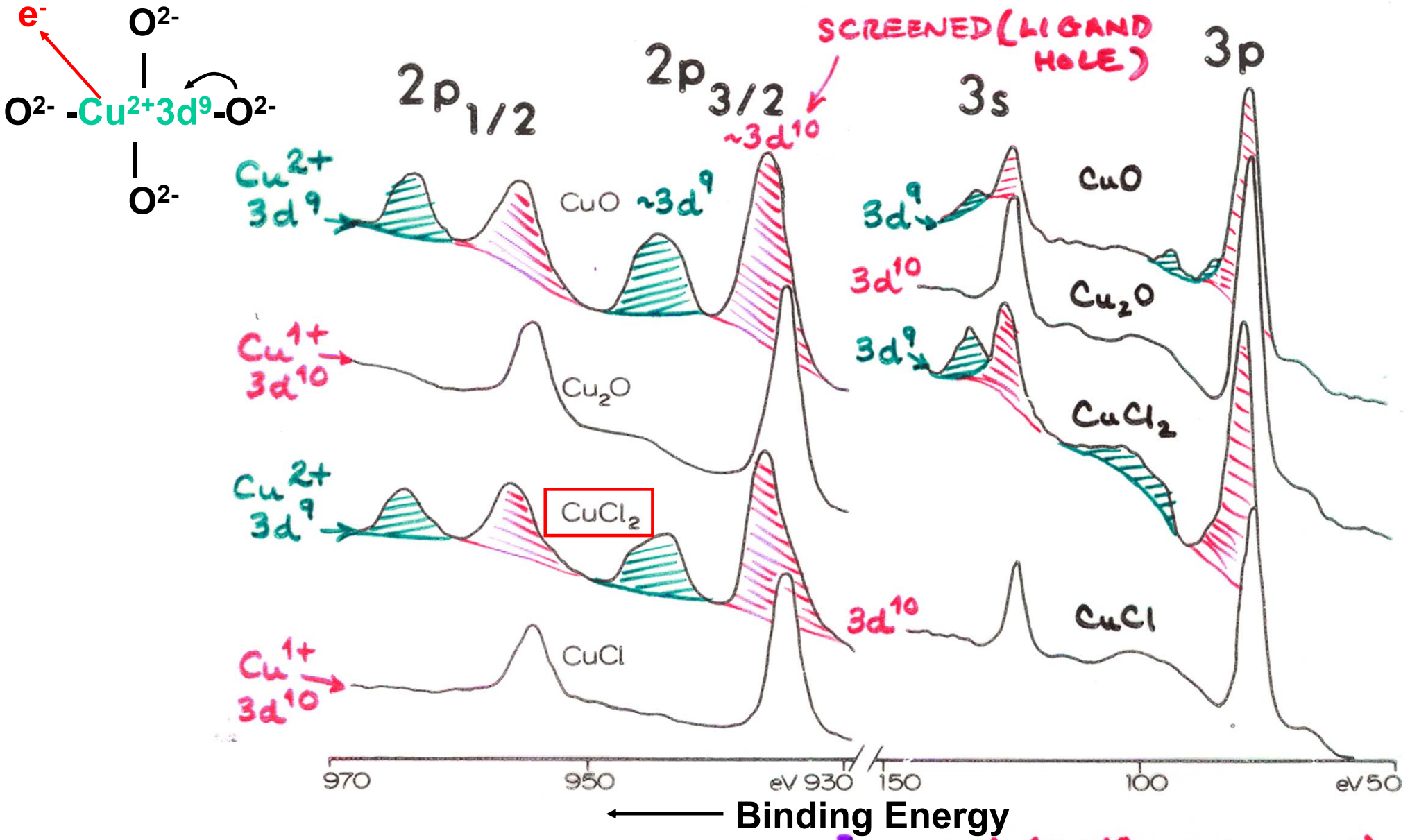

ACTUAL FINAL STATE $\Psi \approx C_1\Phi_1$ (3d10 - SCREENED)
+ $C_2\Phi_2$ (3d9 - UNSCREENED)

"Basic Concepts of XPS"
Figure 38

Cu 2p emission from $CuCl_2$

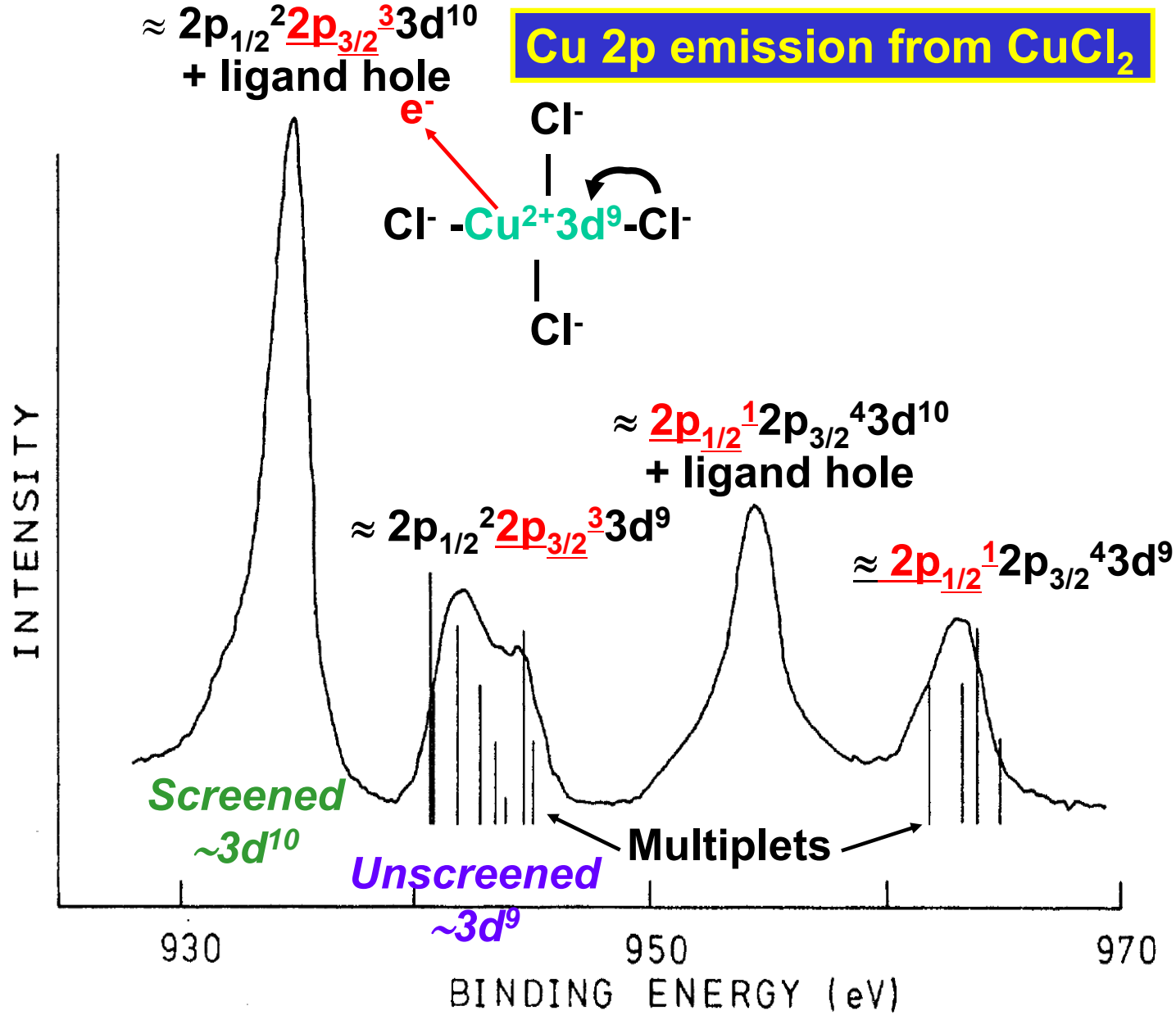

$$\Psi_{final,K}(N-1) = C_{1,K}(2p_{1/2}^2 2p_{3/2}^3 3d^{10} + C\ell\ hole) + C_{2,K}(2p_{1/2}^2 2p_{3/2}^3 3d^9)$$

$$I_{final,K}(N-1) \propto \left| C_{2,K}(2p_{1/2}^2 2p_{3/2}^3 3d^9) \right|^2$$

Van der Laan et al., Phys. Rev. B 23 (1981) 4369

Screening depends on Ionicity/covalency→ satellite intensities can be used to measure interaction parameters

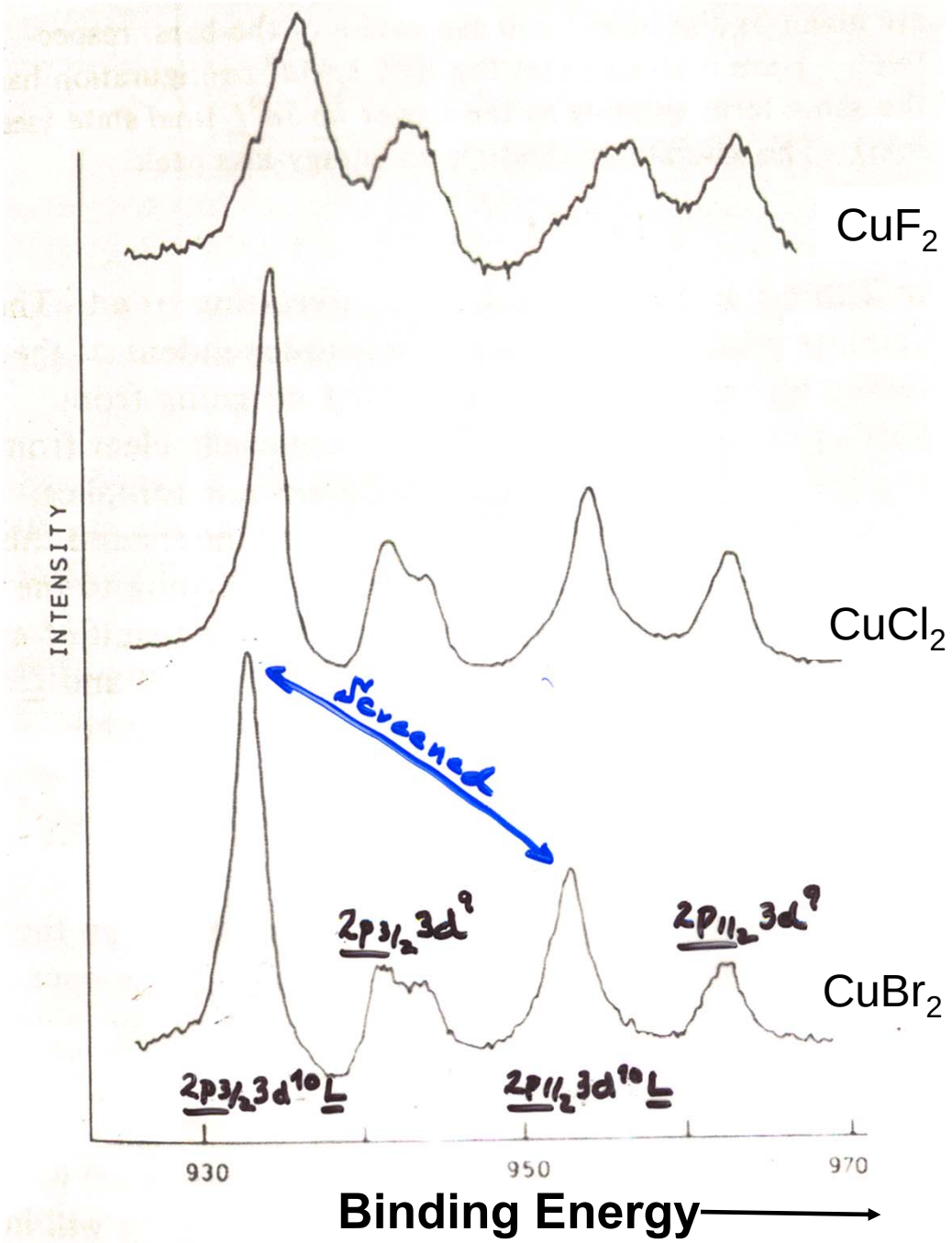

FIG. 1. Cu 2*p* photoelectron spectra of Cu dihalides. The lines leading to a final state with a ligand hole (*L*) show a chemical shift.

More Ionic

More Covalent

Many-electron and screening effects: $La_{0.7}Sr_{0.3}MnO_3$, hν = 7700 eV

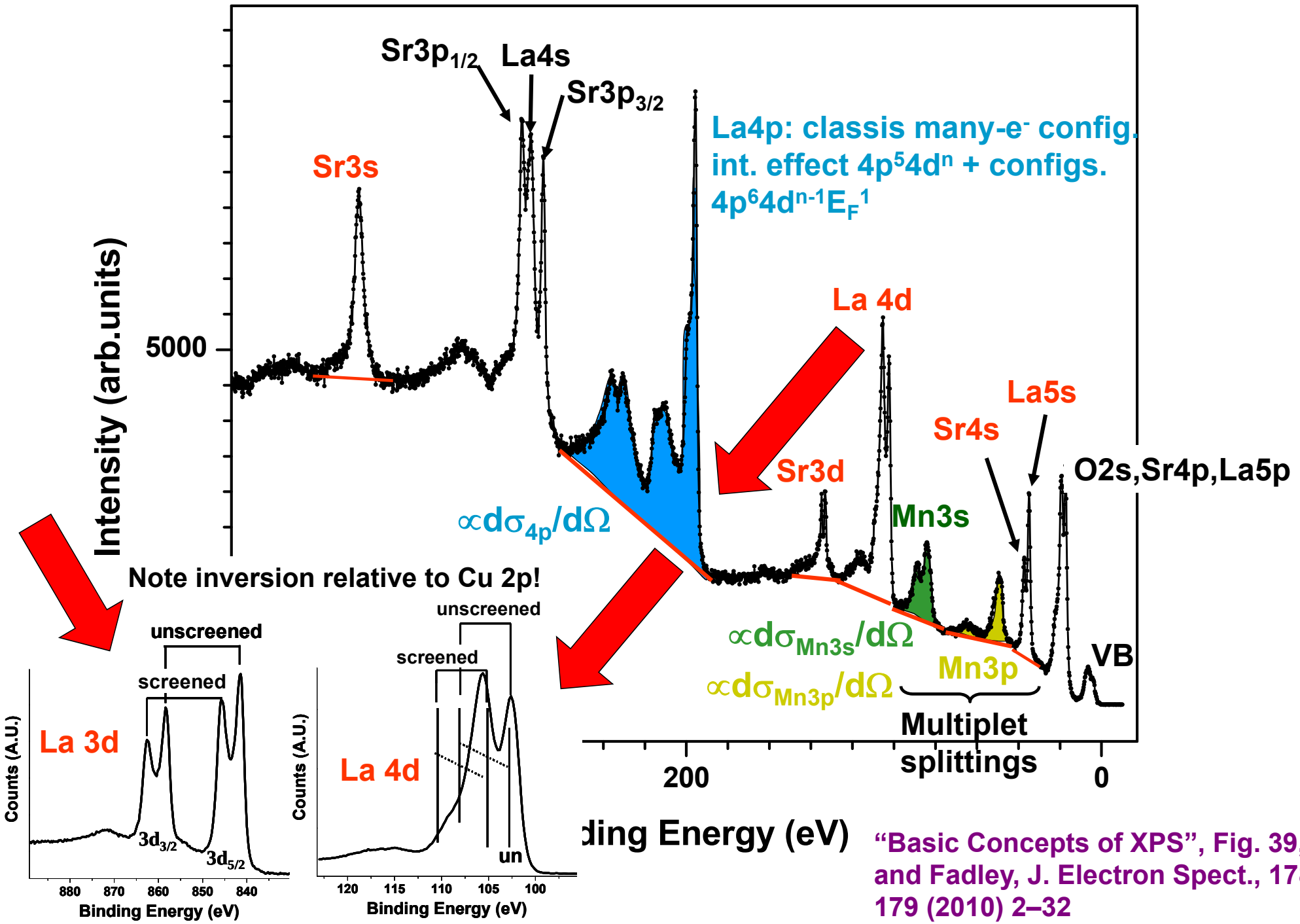

"Basic Concepts of XPS", Fig. 39, and Fadley, J. Electron Spect., 178–179 (2010) 2–32

ATOMIC (CORE) PHOTOELECTRON INTENSITIES: THE "FOUR-STEP" MODEL

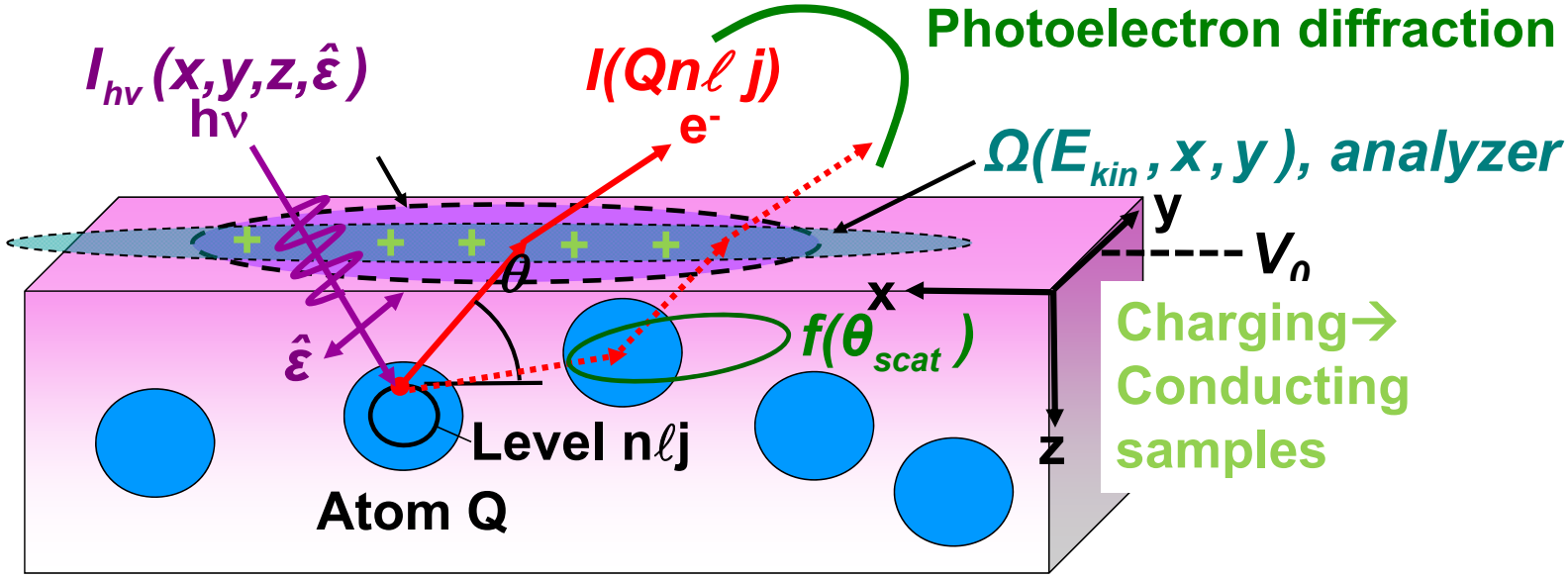

$I(Qn\ell\, j)$ = → Non-dipole effects* and resonant interchannel#

$$C\int_0^{\infty} I_{h\nu}(x,y,z,\hat{\varepsilon})\rho_Q(x,y,z)\frac{d\sigma_{Qn\ell j}(h\nu,\hat{\varepsilon})}{d\Omega}\exp\left[-\frac{z}{\Lambda_e(E_{kin})\sin\theta}\right]\Omega(E_{kin},x,y)\,dxdydz$$

Energy dependent factors needing calibration at usual XPS energies ~1 keV

$I_{h\nu}(x,y,z,\hat{\varepsilon})$ = x-ray flux, $\hat{\varepsilon}$ = polarization

$\rho_Q(x,y,z)$ = density of atoms Q → quantitative analysis

$\frac{d\sigma_{Qn\ell j}(h\nu,\hat{\varepsilon})}{d\Omega}$ = energy-dependent differential photoelectric cross section for subshell $Qn\ell\, j$

$\Lambda_e(E_{kin})$ = energy-dependent inelastic attenuation length + elastic scattering: $f(\theta_{scatt})$

→ Effective Attenuation Length (EAD) → Mean Emission Depth (MED)

$\Omega(E_{kin},x,y)$ = energy-dependent analyzer acceptance solid angle = transmission function

V_0 = inner potential

#Guilleumin et al., Radiation Physics and Chemistry 75, 2258 (2006)
#Drube et al., J. Phys. B: At. Mol. Opt. Phys. 46, 245006 (2013)

Quantitative analysis of peak intensities using theoretical cross sections (Scofield) and hard x-ray excitation: $La_{0.7}Sr_{0.3}MnO_3$, hν = 7700 eV

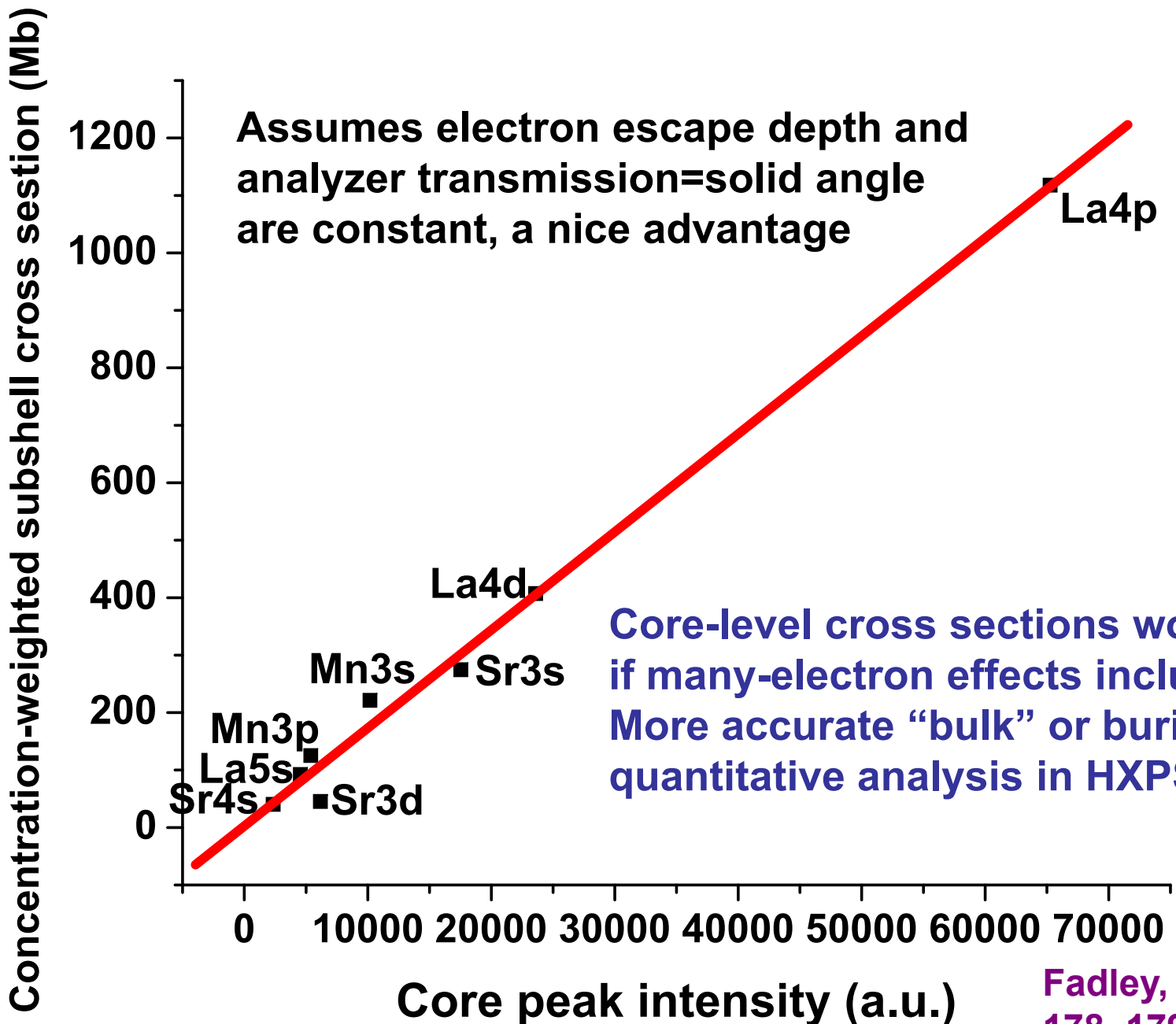

Core-level cross sections work very well, if many-electron effects included→
More accurate "bulk" or buried layer quantitative analysis in HXPS

Fadley, J. Electr. Spect. 178–179 (2010) 2–32

Screening depends on Ionicity/covalency→ satellite intensities can be used to measure interaction parameters

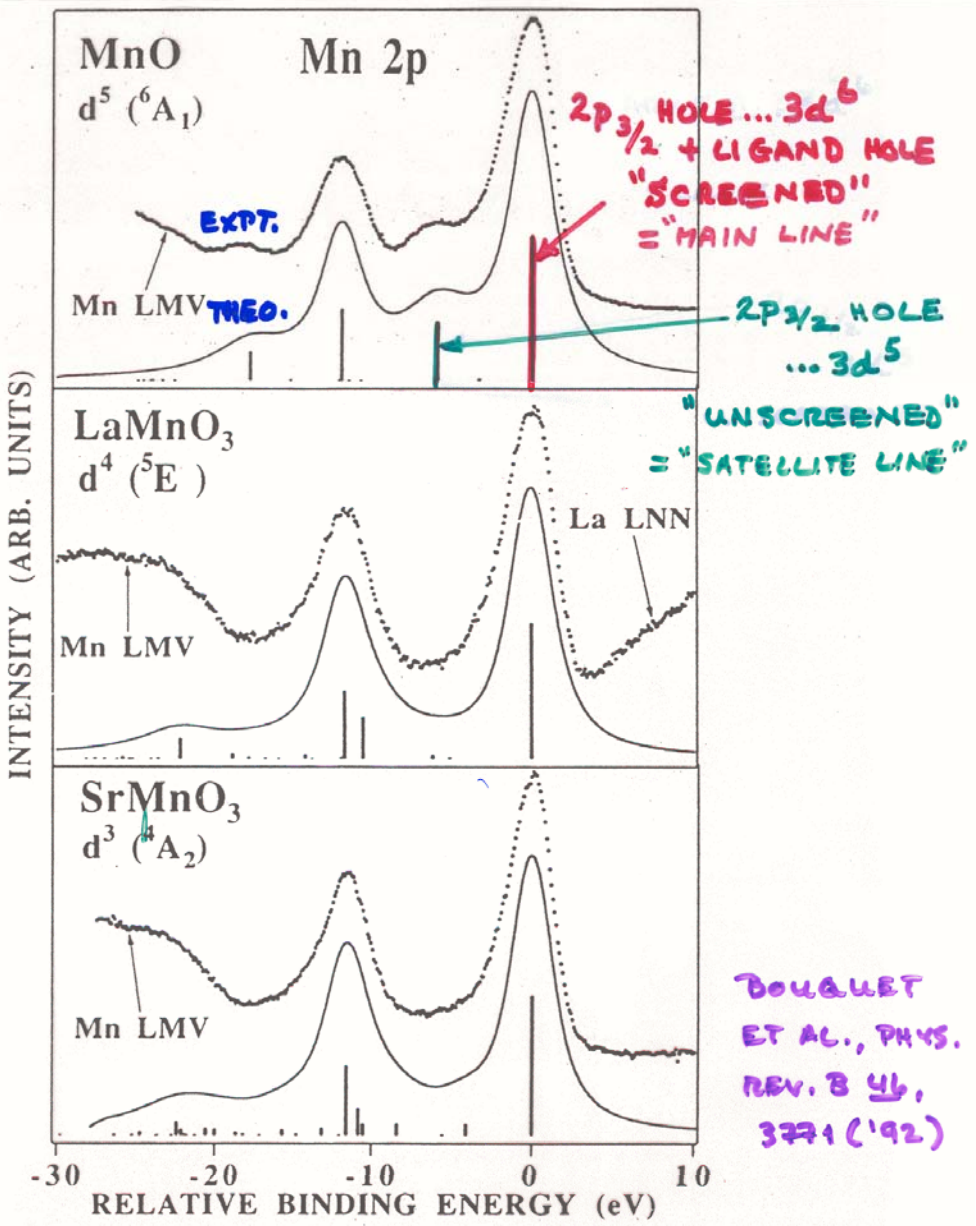

FIG. 1. Theoretical $2p$ core-level XPS spectra (solid line) compared with experimental data (dots) after background subtraction for Mn cations with varying valence. Emission due to the Mn *LMV* Auger peak is observed on the high-binding-energy side of the $2p_{1/2}$ spin-orbit peak, partially obscuring the $2p_{1/2}$ satellite structure.

Localized configuration interaction approach to spectrum simulation: Hubbard Model→Anderson impurity model for PS, XAS, XES

(SUGANO, LARSSON ~> SAWATZKY, VAN DER LAAN, FUJIMORI, OH, ET AL.)

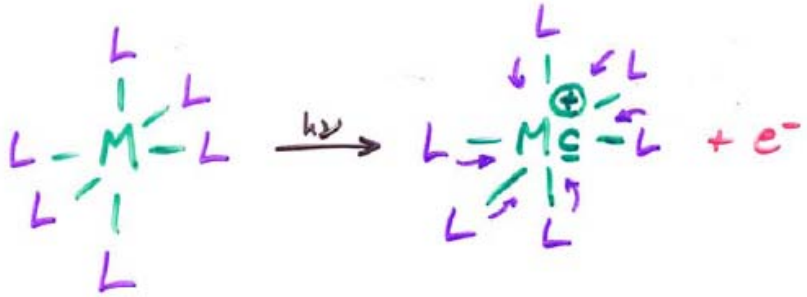

$\underline{c}$ = CORE HOLE ON METAL

$\underline{L}$ = VALENCE ($\underline{\nu}$) HOLE ON LIGAND

$$\psi_i = a_0|d^n\rangle + \sum_m a_m|d^{(n+m)}\underline{L}^m\rangle$$

$$\psi_f = b_0|\underline{c}\,d^n\rangle + \sum_m b_m|\underline{c}\,d^{(n+m)}\underline{L}^m\rangle$$

WITH INTERACTIONS OF:

$10Dq$ = CRYSTAL FIELD (OFTEN NEGLECTED)

Δ = LIGAND-TO-METAL CHARGE TRANSF. ENERGY
= $E(d^{n+1}\underline{L}) - E(d^n)$

$U_{dd} = U$ = d-d COULOMB REPULSION ENERGY
= $E(d^{n-1}) + E(d^{n+1}) - 2E(d^n) \approx J_{dd}$

T = LIGAND P-TO-METAL d HYBRIDIZATION
= $\langle d_\alpha|\hat{H}|p_\alpha\rangle$ (α = SAME SYMMETRY)

$U_{cd} = Q$ = CORE-HOLE-TO-d INTERACTION: $\langle \underline{c}|\hat{H}|d\rangle \approx J_{cd}$ = **coulomb integral**

Good discussion of model: Bocquet & Fujimori, J. Elect. Spect. & Rel. Phen. 82, 87 (1996)-at course website

$$\rho(e_k) = \sum_f |\langle \Psi_f|c|\Psi_g\rangle|^2 \delta(h\nu - e_k - E_f)$$

By now: CTM4XAS program for calculating this for some cases:

http://www.anorg.chem.uu.nl/CTM4XAS/Updates

WITH INTENSITIES FROM SUDDEN APPROX.

AS:

$$I(E_{kin}) \propto \sum_{f,k} |\langle \psi_f(N-1,k)|\psi_g(N-1,\underline{k})\rangle|^2 \cdot \delta(h\nu - E_f - E_{kin})$$

($\underline{k}$ = $\underline{c}$ = CORE HOLE)

WHERE: $\psi_g(N-1,\underline{k}) = \psi_i$ (N WITH $\underline{k}$ HOLE = $\underline{c}$)

http://www.physics.ucdavis.edu/Classes/Physics243A/CTM4XAS.MiniManual.pdf

E.g.—Crystal field in Mn^{3+} with negative octahedral ligands

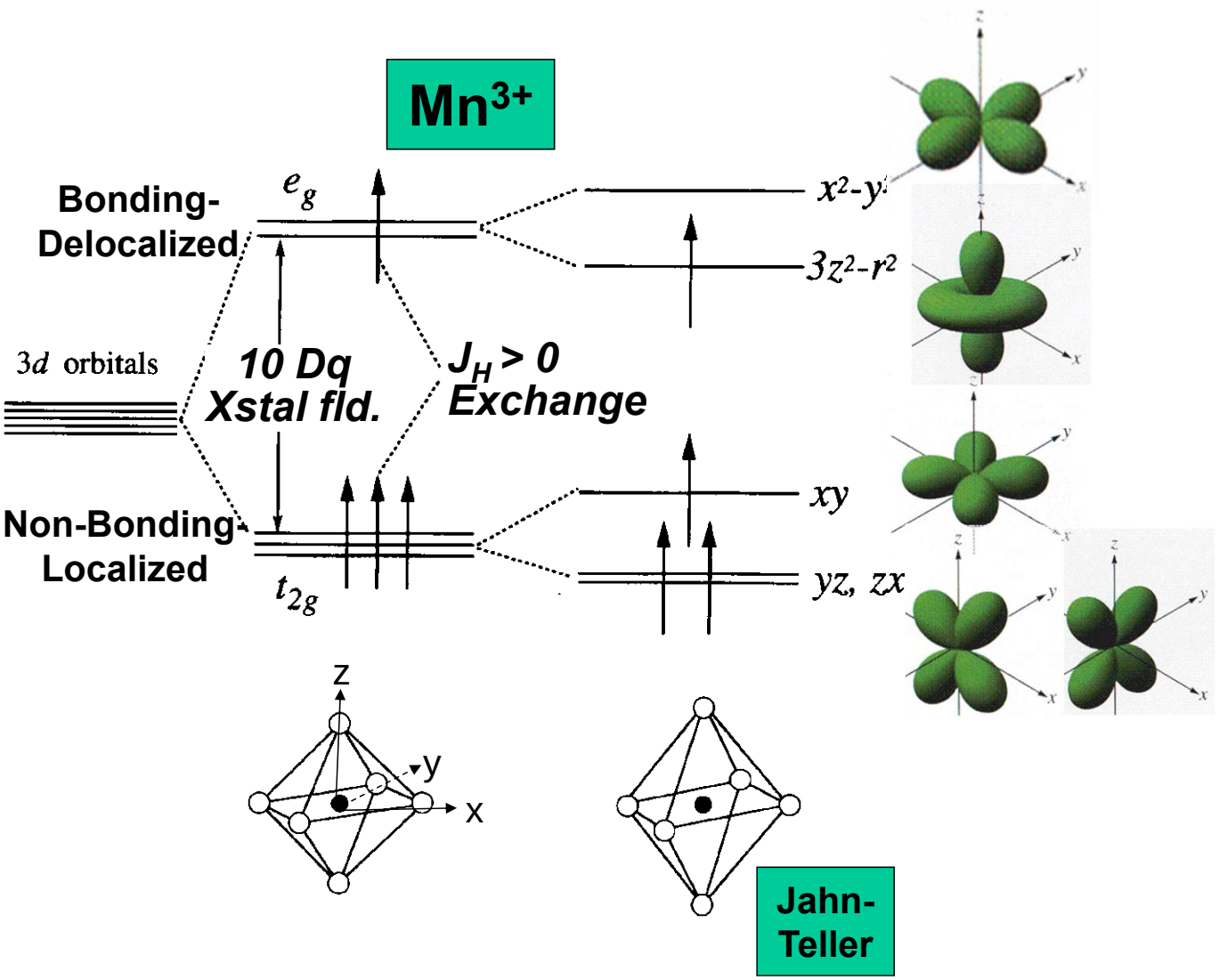

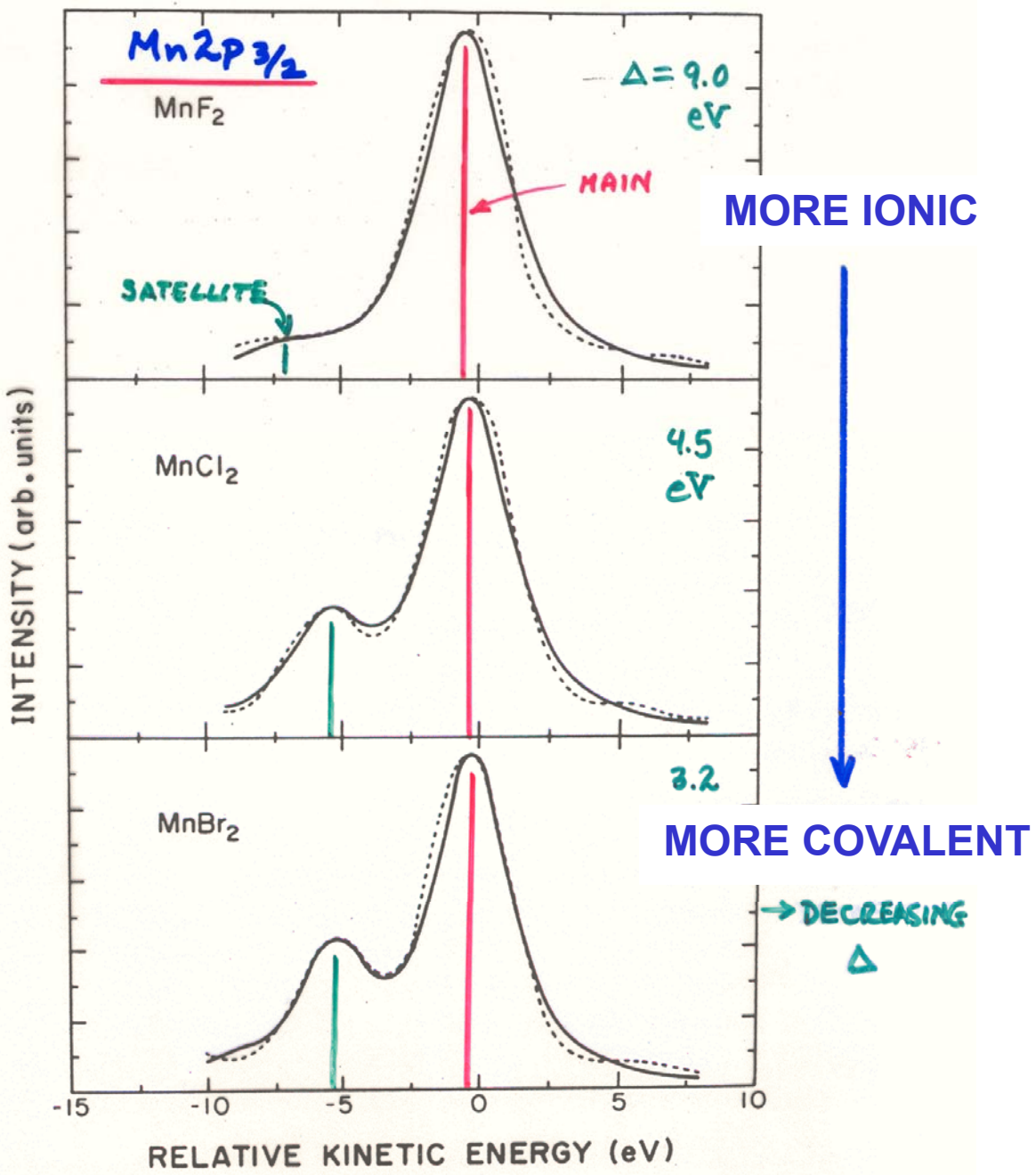

FIG. 6. Fits of the cluster model results with the experimental $2p_{3/2}$ spectra of the manganese dihalides. The parameters used are listed in Table II. A Lorentzian broadening is 2.6–3.0 eV, and a Gaussian broadening of 1.2 eV (FWHM) was used.

ANALYSIS VIA ANDERSON IMPURITY MODEL

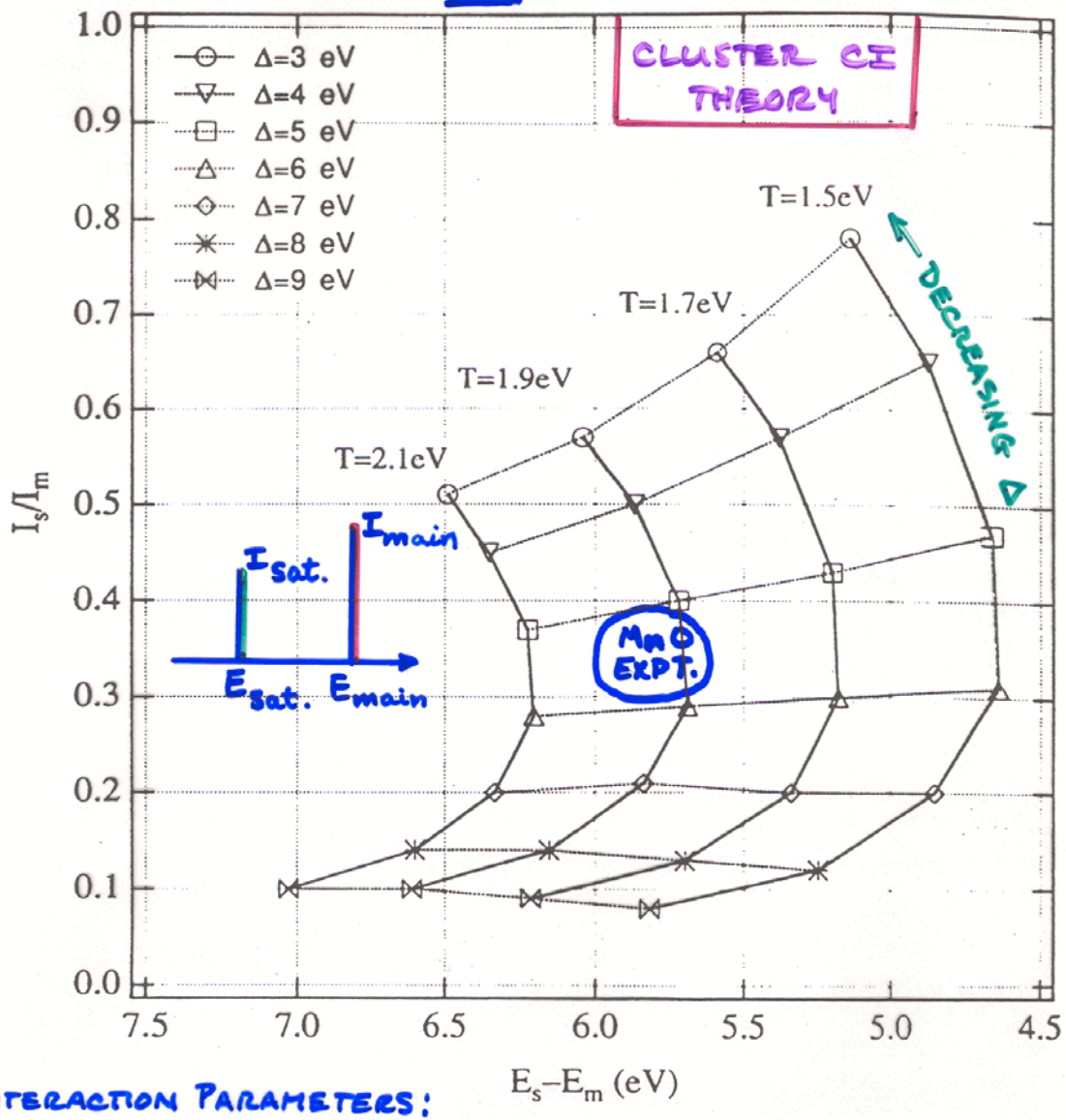

INTERACTION PARAMETERS:

U = 3d-3d COULOMB REPULSION ENERGY

Δ = LIGAND-TO-METAL CHARGE TRANSFER ENERGY

T = LIGAND p — METAL 3d HYBRIDIZATION ENERGY

Q = CORE HOLE-3d COULOMB

BOUQUET ET AL., J. EL. SP. 82, 87 (1996)

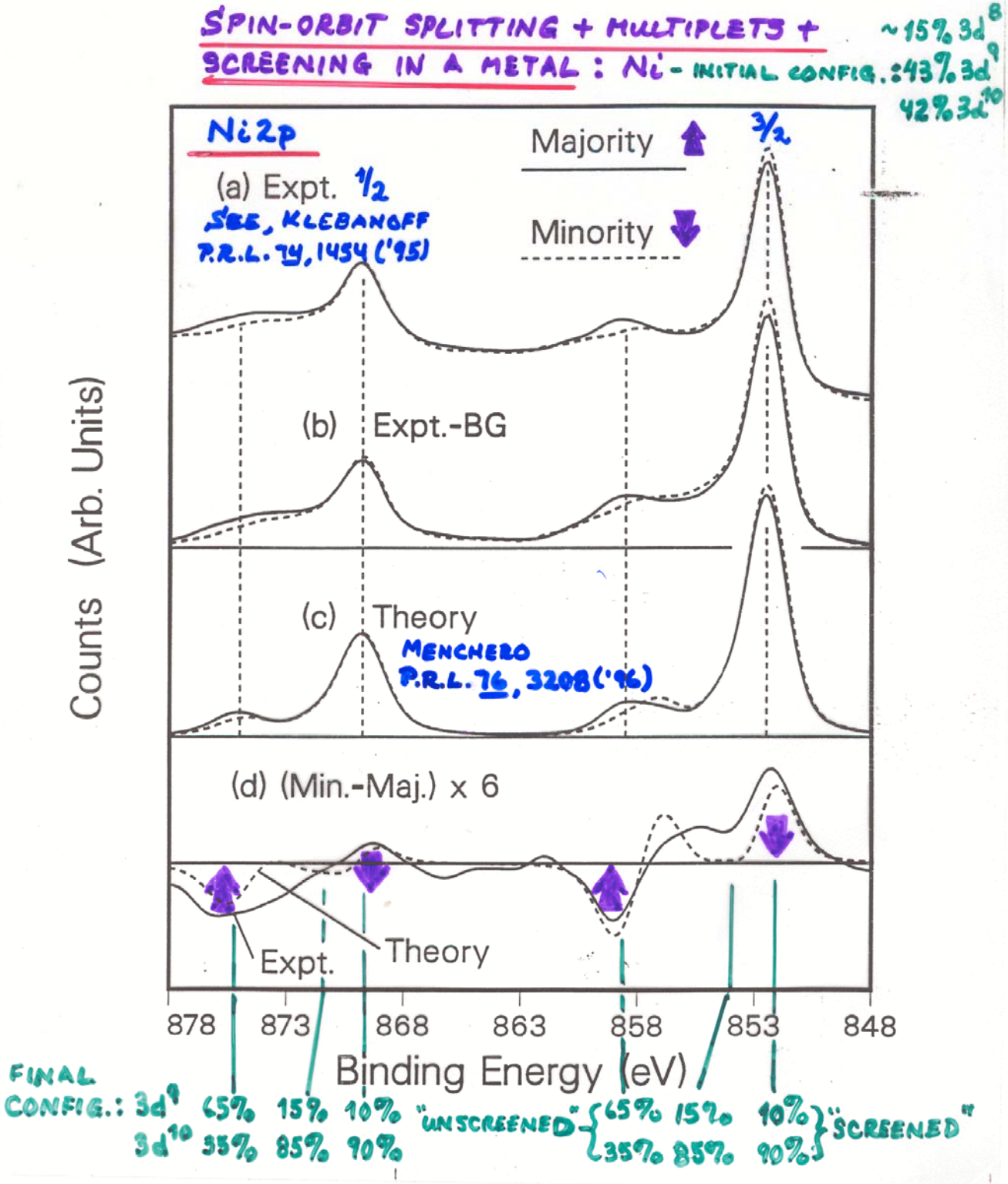
SPIN-ORBIT SPLITTING + MULTIPLETS + SCREENING IN A METAL : Ni - INITIAL CONFIG.: ~15% 3d^8 43% 3d^9 42% 3d^10
Ni 2p
Majority
Minority
3/2
1/2
(a) Expt.
SEE, KLEBANOFF P.R.L. 74, 1454 ('95)
(b) Expt.-BG
(c) Theory
MENCHERO P.R.L. 76, 3208 ('96)
(d) (Min.-Maj.) x 6
Expt.
Theory
Counts (Arb. Units)
878
873
868
863
858
853
848
Binding Energy (eV)
FINAL CONFIG.: 3d^9 65% 15% 10% "UNSCREENED" {65% 15% 10%} "SCREENED"
3d^10 35% 85% 90% {35% 85% 90%}

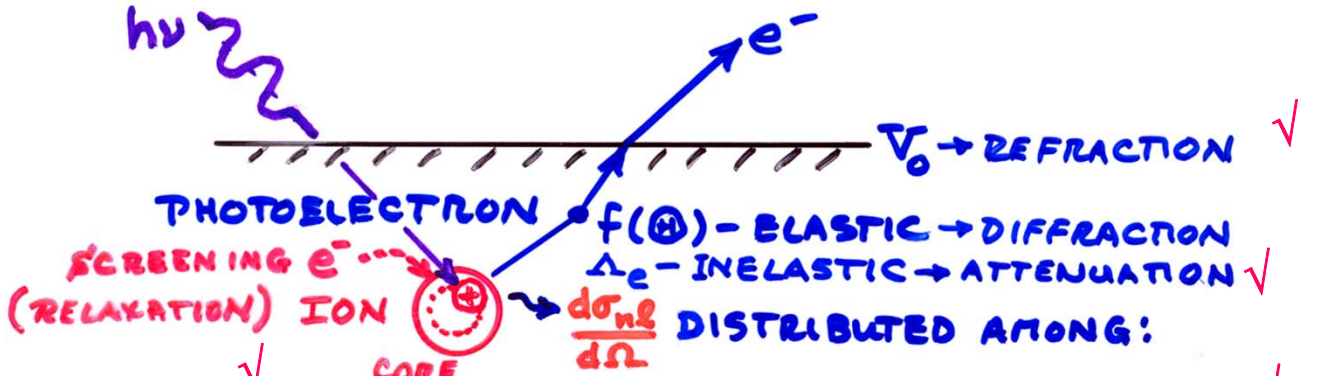

√ = covered so far

ADDITIONAL SOURCES OF STRUCTURE (AND INFORMATION!) IN SPECTRA BEYOND CHEMICAL SHIFTS

- SPIN-ORBIT SPLITTING (EASY) √
- + MULTIPLET SPLITTING (OPEN-SHELL SYSTEMS), XSTAL FIELD √
- + CORRELATION / CONFIGURATION INTERACTION √
- + SHAKE-UP / SHAKE-OFF / e^--HOLE √
- + SCREENING / NON-SCREENING: CONFIGURATION INTERACTION √
- + VIBRATIONAL EXCITATIONS
- + RESONANT PHOTOEMISSION ($h\nu \approx E_{b,n\ell'}$) √

REALLY ALL AT ONCE, BUT SUM RULES + THEORY HELP

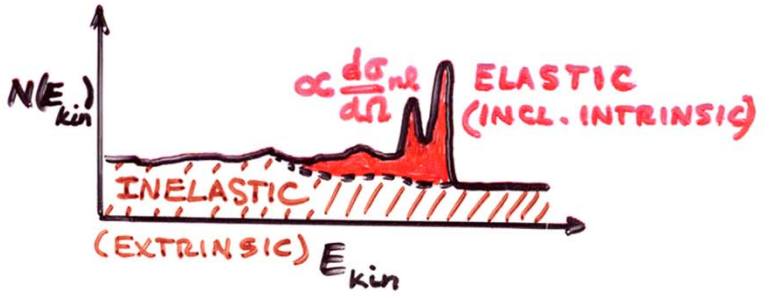

Intensities in photoelectron spectra in the sudden approximation

- GENERAL: FINAL STATE K (k-SUBSHELL + ALL OTHER DESIG.)

$$\text{INT.}_K \propto \left| \hat{e} \cdot \langle \Psi^f_{tot}(N,K) | \sum_{i=1}^{N} \vec{r}_i | \Psi^i(N) \rangle \right|^2 \quad \text{(DIPOLE APPROX.}$$

- BORN-OPPENHEIMER: e⁻'s FAST, VIBRATIONS SLOW

$$\text{INT.}_K \propto \underbrace{|\langle \Psi^f_{VIB,v'} | \Psi^i_{VIB,v} \rangle|^2}_{\text{FRANCK-CONDON FACTOR}} \left| \hat{e} \cdot \langle \Psi^f_{e^-}(N,K) | \sum_{i=1}^{N} \vec{r}_i | \Psi^i_{e^-}(N) \rangle \right|^2$$

- SUDDEN APPROXIMATION: $\Psi_K \rightarrow \Psi_f$ = PHOTO e⁻ (FAST)

k HOLE → $\varphi_1 \rightarrow \varphi'_1$, …, $\varphi_{k-1} \rightarrow \varphi'_{k-1}$, $\varphi_{k+1} \rightarrow \varphi'_{k+1}$, …, $\varphi_N \rightarrow \varphi'_N$ } (SLOW)

$$\text{INT.}_K \propto |\langle \Psi^f_{VIB,v'} | \Psi^i_{VIB,v} \rangle|^2 \underbrace{|\langle \Psi^f_{e^-}(N-1,K) | \Psi_K(N-1,K) \rangle|^2}_{\text{SAME SUBSHELL COUPLING + TOTAL L,S} \rightarrow \text{"MONOPOLE"}} \; \overset{k \text{ MISSING}}{\uparrow}$$

$$|\hat{e} \cdot \langle \varphi_f | \vec{r} | \varphi_K \rangle|^2 \rightarrow \text{NORMAL } \frac{d\sigma_K}{d\Omega}$$

- SLATER DETS. FOR $\Psi^f_{e^-} = \det(\varphi'_1 \varphi'_2 \cdots \varphi'_{k-1} \varphi'_{k+1} \cdots \varphi'_N)$

$$\Psi_K = \det(\varphi_1 \varphi_2 \cdots \varphi_{k-1} \varphi_{k+1} \cdots \varphi_N)$$

$$\text{INT.}_K \propto |\langle \Psi^f_{VIB,v'} | \Psi^i_{VIB,v} \rangle|^2 |\langle \varphi'_1 | \varphi_1 \rangle|^2 |\langle \varphi'_2 | \varphi_2 \rangle|^2 \cdots$$
$$|\langle \varphi'_{k-1} | \varphi_{k-1} \rangle|^2 |\langle \varphi'_{k+1} | \varphi_{k+1} \rangle|^2 \cdots |\langle \varphi'_N | \varphi_N \rangle|^2 \cdot$$

$$|\hat{e} \cdot \langle \varphi_f | \vec{r} | \varphi_K \rangle|^2$$

1e- DIPOLE → dσ/dΩ

(N-1)e⁻ SHAKE-UP/ SHAKE-OFF → "MONOPOLE"

- PLUS DIFFRACTION EFFECTS IN φ_f ESCAPE

VIBRATIONAL STRUCTURE IN VALENCE-LEVEL (MO) SPECTRA

Diatomic A-B example

(Also applies to core-level emission if equilibrium distance changes on forming core hole)

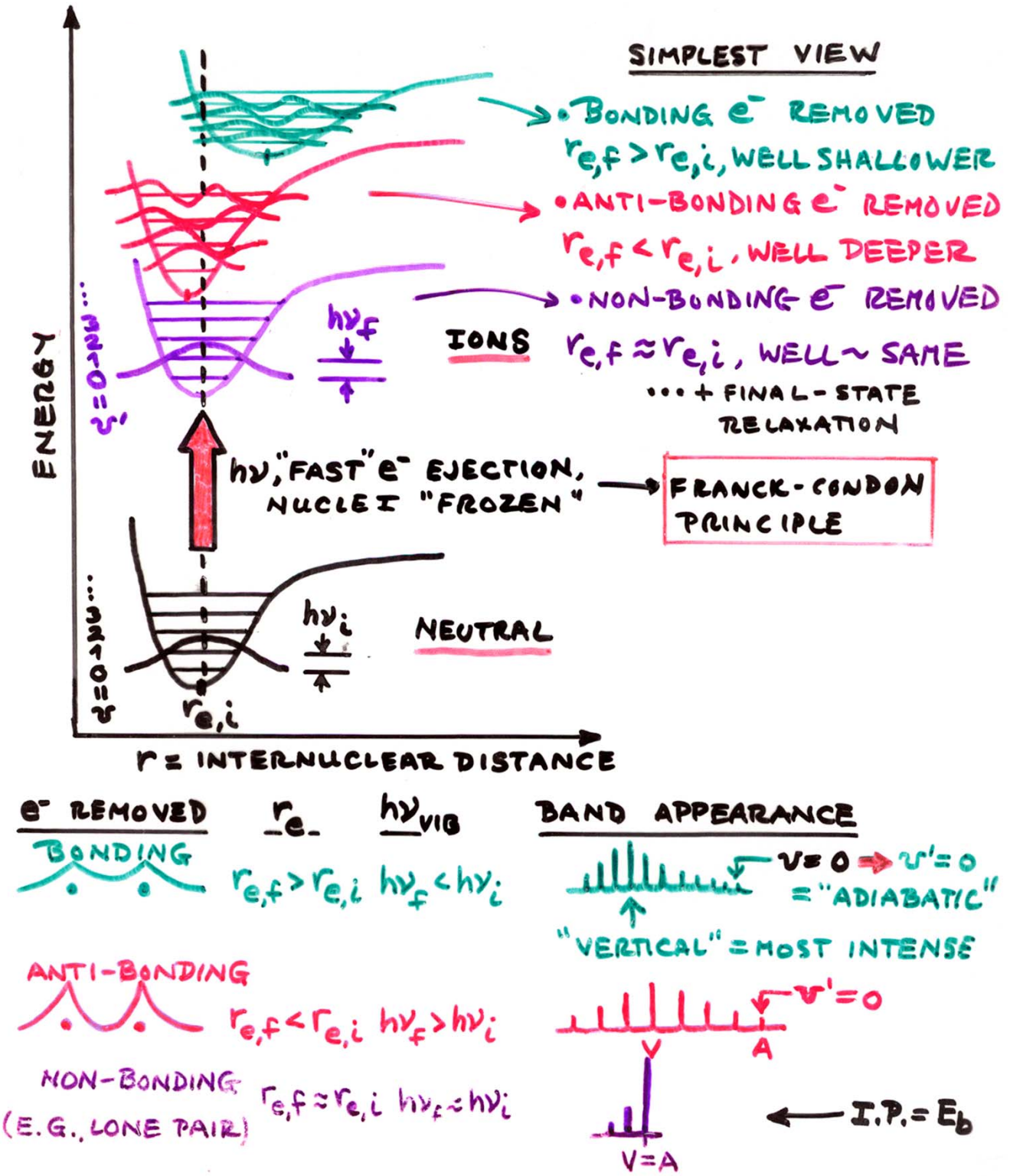

VIBRATIONAL STRUCTURE IN VALENCE-LEVEL (MO) SPECTRA

H_2 Hydrogen

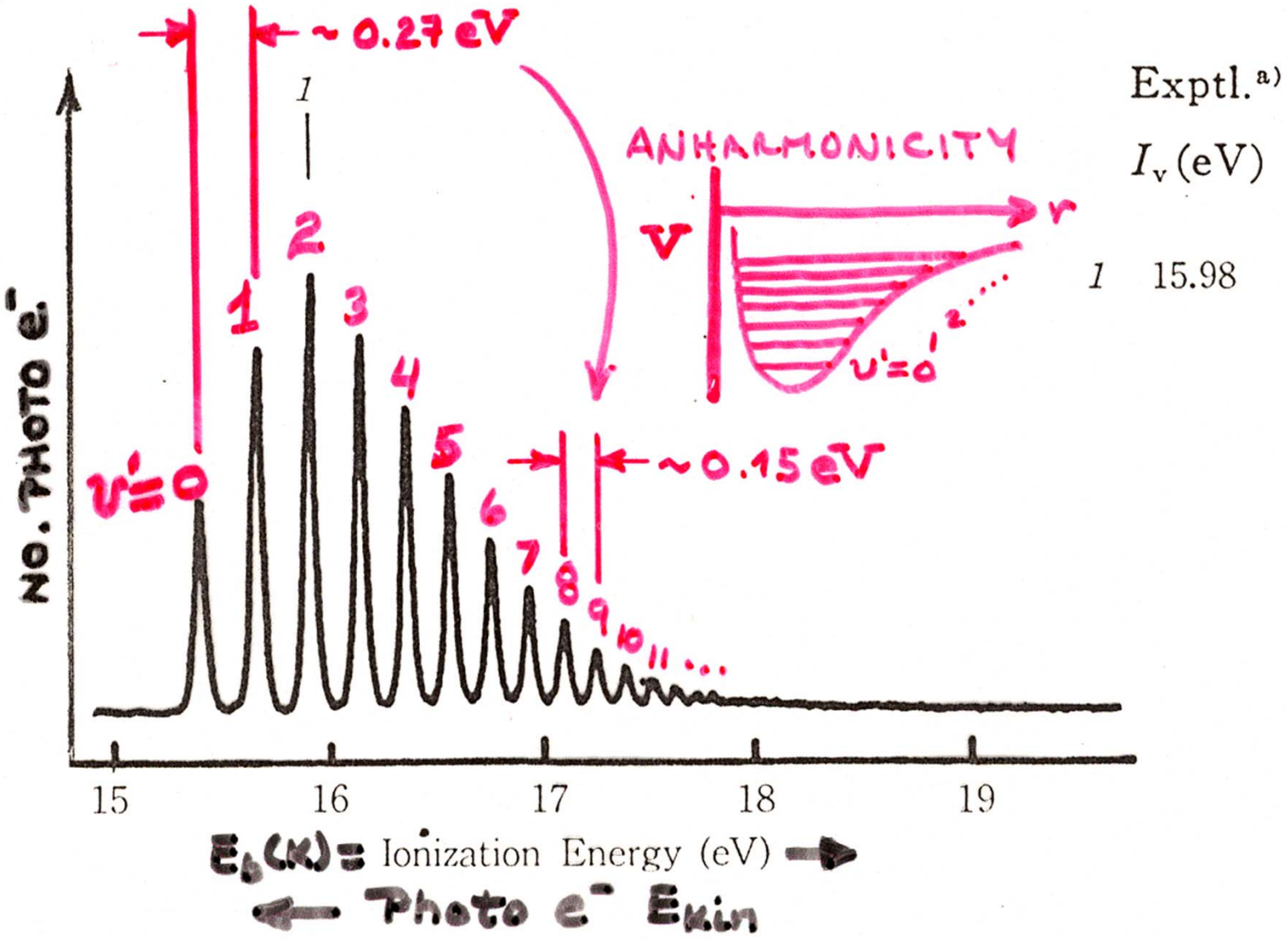

	Exptl.[a] I_v (eV)
1	15.98

Basic Concepts:

A Little Electronic Structure
The X-Ray-Based Experiments
X-Ray Sources, Synchrotron Radiation, Free Electron Lasers

Core-Level Photoemission

Intensities and Quantitative Analysis, the 3-Step Model
Varying Surface and Bulk Sensitivity
Chemical Shifts
Multiplet Splittings
Electron Screening and Satellite Structure
Magnetic and Non-Magnetic Dichroism
Resonant Photoemission
Photoelectron Diffraction and Holography

Valence-Level Photoemission

Band-Mapping in the Ultraviolet Photoemission Limit
Densities of States in the X-Ray Photoemission Limit

Some New Directions

Photoemission with Hard X-Rays (throughout lectures)
Photoemission with Standing Wave Excitation
Photoemission with: Higher Pressures→multi-Torr→Atmosphere?
Spatial Resolution-Photoelectron Microscopy
Temporal Resolution

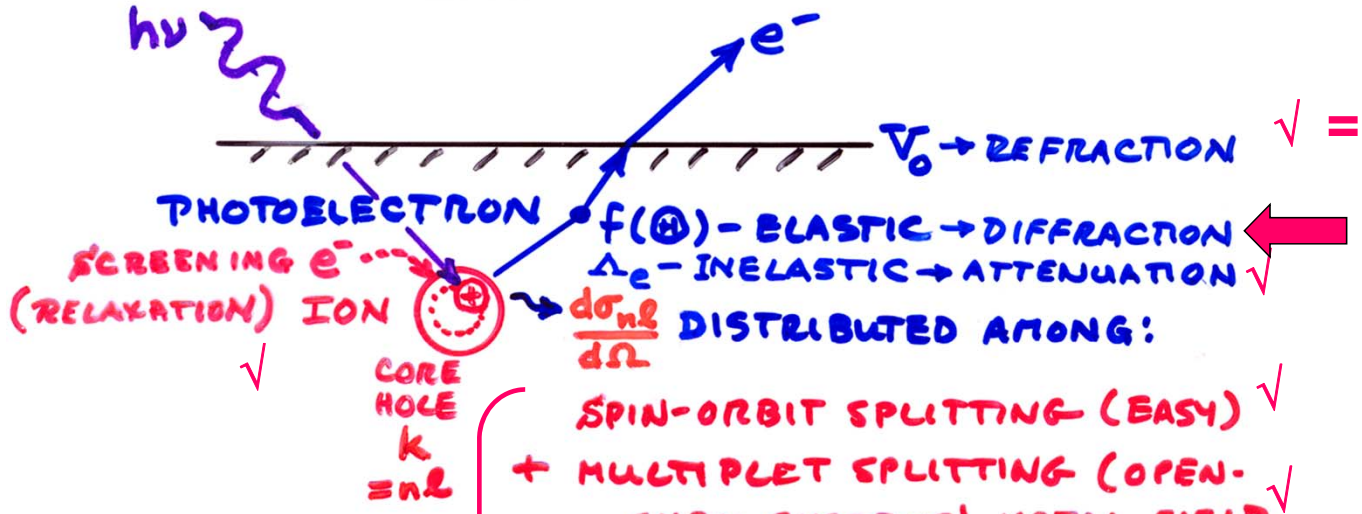

√ = covered so far

ADDITIONAL SOURCES OF STRUCTURE (AND INFORMATION!) IN SPECTRA BEYOND CHEMICAL SHIFTS

- SPIN-ORBIT SPLITTING (EASY) √
- + MULTIPLET SPLITTING (OPEN-SHELL SYSTEMS), XSTAL FIELD √
- + CORRELATION / CONFIGURATION INTERACTION √
- + SHAKE-UP / SHAKE-OFF / e^--HOLE √
- + SCREENING / NON-SCREENING: CONFIGURATION INTERACTION √
- + VIBRATIONAL EXCITATIONS
- + RESONANT PHOTOEMISSION ($h\nu \approx E_{b,n\ell'}$) √

REALLY ALL AT ONCE, BUT SUM RULES + THEORY HELP

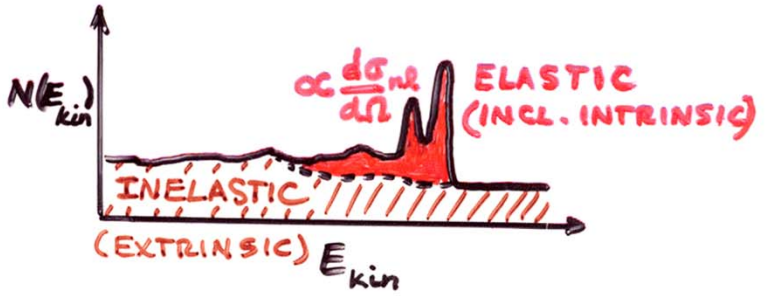

Typical experimental geometry for energy- and angle-resolved photoemission measurements

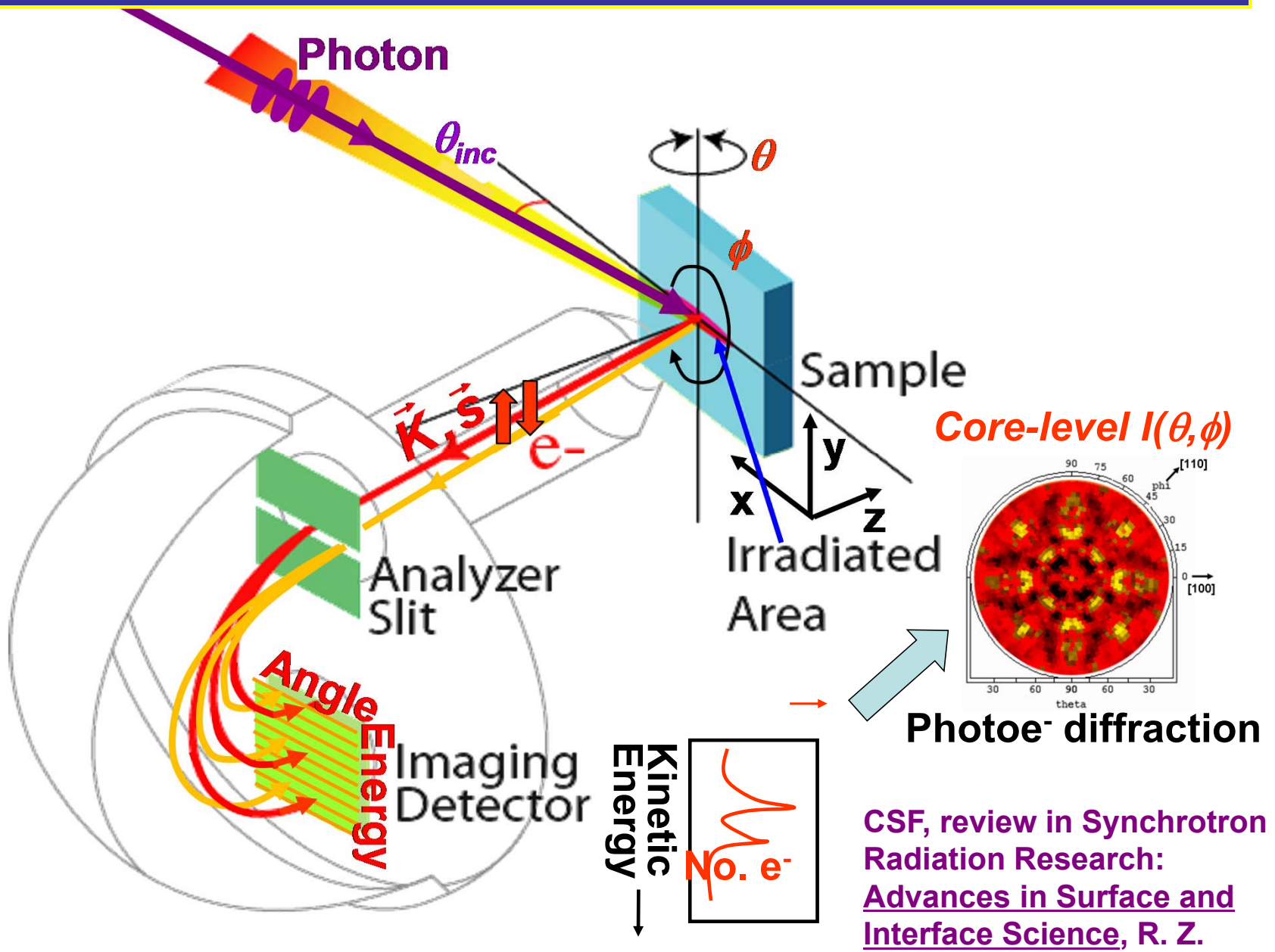

CSF, review in Synchrotron Radiation Research: Advances in Surface and Interface Science, R. Z. Bachrach, Ed. (Plenum Press, New York, 1992).

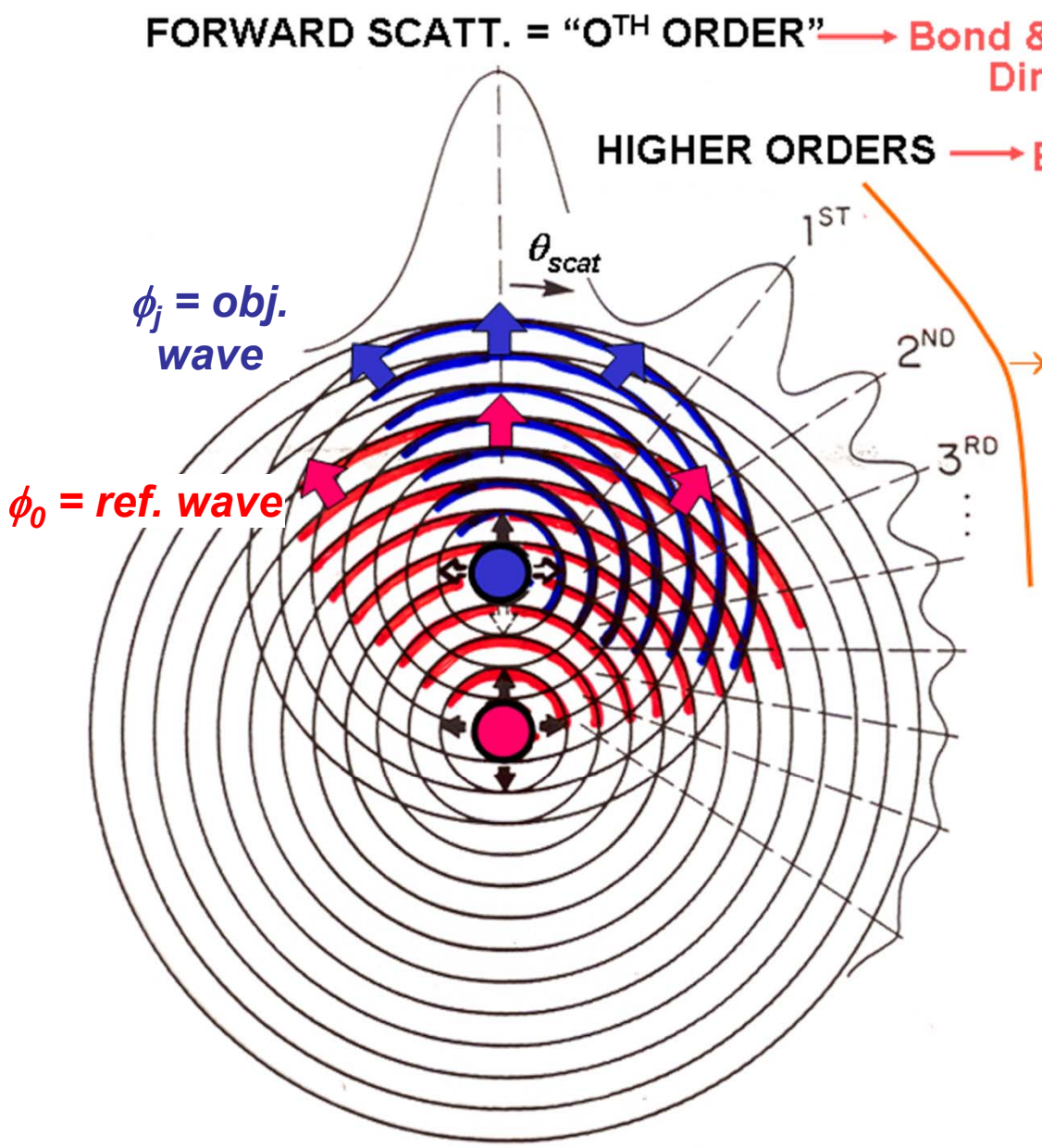

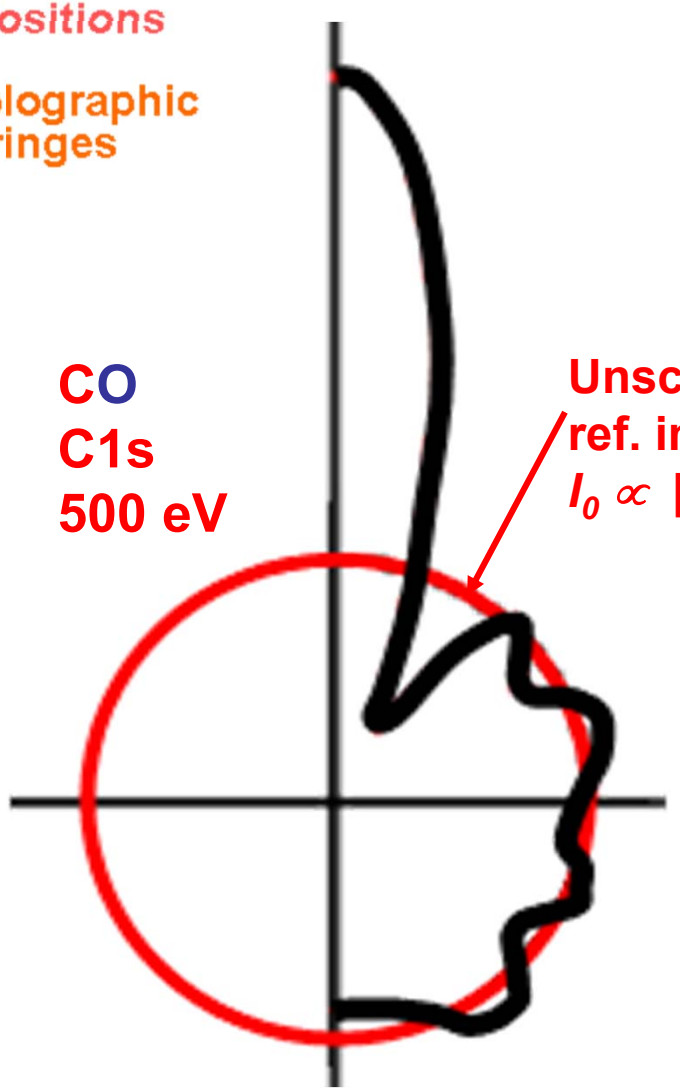

Photoelectron Diffraction

EDAC photoelectron diffraction program: Javier Garcia de Abajo:
http://garciadeabajos-group.icfo.es/widgets/edac/index.html

Photoelectron Diffraction: Single Scattering Theory

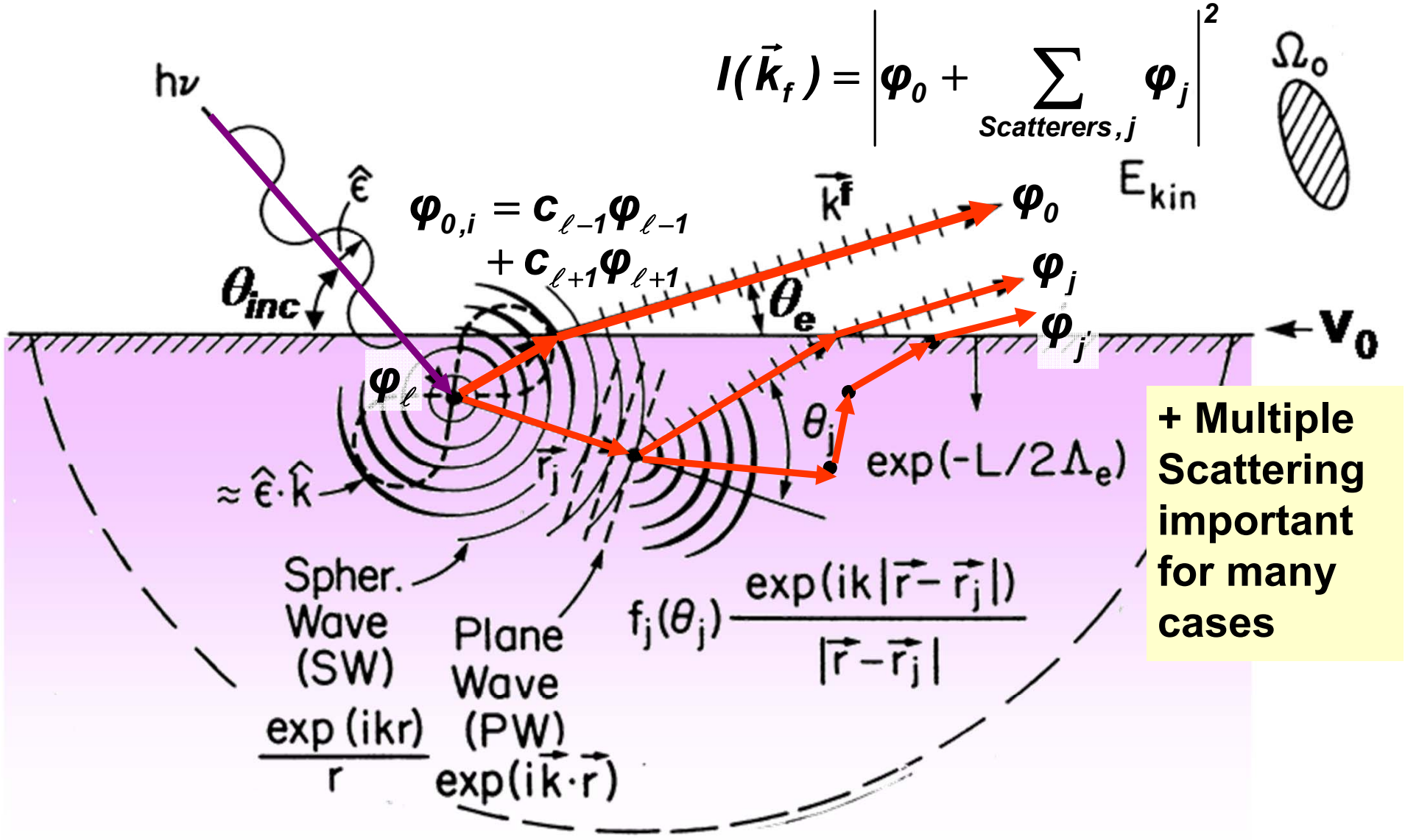

+ Multiple Scattering important for many cases

CALCULATION OF e^--ATOM SCATTERING FACTORS:

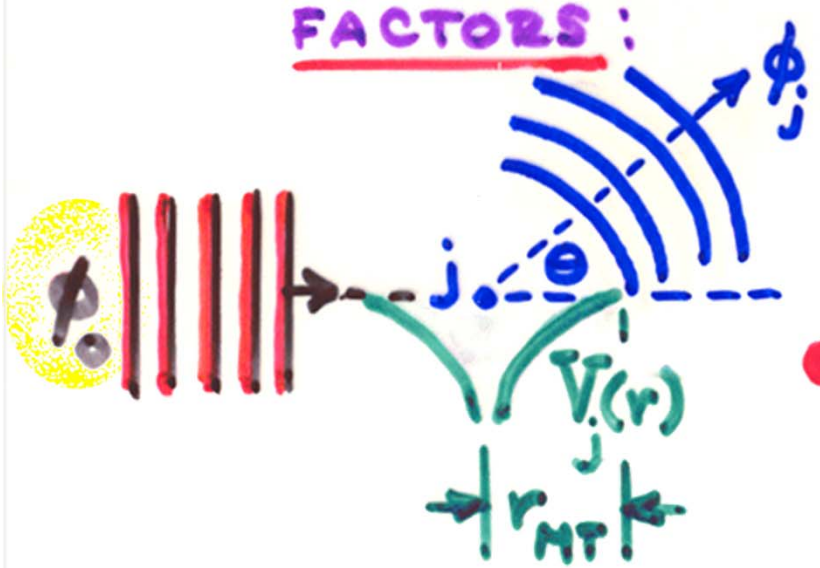

PLANE-WAVE SCATTERING: PARTIAL-WAVE METHOD†

$$f_j^{PW}(\theta) = \frac{1}{k}\sum_{\ell=0}^{\ell_{max}} (2\ell+1)\, e^{i\delta_\ell} \sin\delta_\ell\, P_\ell(\cos\theta)$$

δ_ℓ: PHASE SHIFT

$$\ell_{max} \approx k r_{MT}$$

† ANY TEXTBOOK ON SCATTERING

COMPARE THE OUTGOING PHOTOELECTRON WAVE

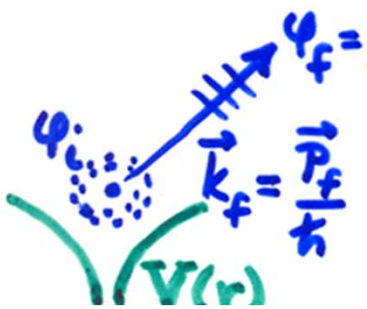

$$\varphi_f(\vec{r},\vec{k}_f) = \varphi_{E_f}(\vec{r},\vec{k}_f)\begin{Bmatrix}\alpha(\sigma)\\ \beta(\sigma)\end{Bmatrix}$$

$$= 4\pi \sum_{\ell_f, m_f} i^{\ell_f} e^{-i\delta_{\ell_f}} Y^*_{\ell_f m_f}(\theta_{k_f}, \phi_{k_f})\, Y_{\ell_f m_f}(\theta,\phi)\, R_{E_f,\ell_f}(r)\begin{Bmatrix}\alpha(\sigma)\\ \beta(\sigma)\end{Bmatrix}$$

δ_{ℓ_f}: PHASE SHIFT OF ℓ_f WAVE IN $V(r)$

Same phase shifts involved

ENERGY DEPENDENCE OF ELECTRON ELASTIC SCATTERING

$$f(\theta) = |f(\theta)| e^{i\psi(\theta)}$$

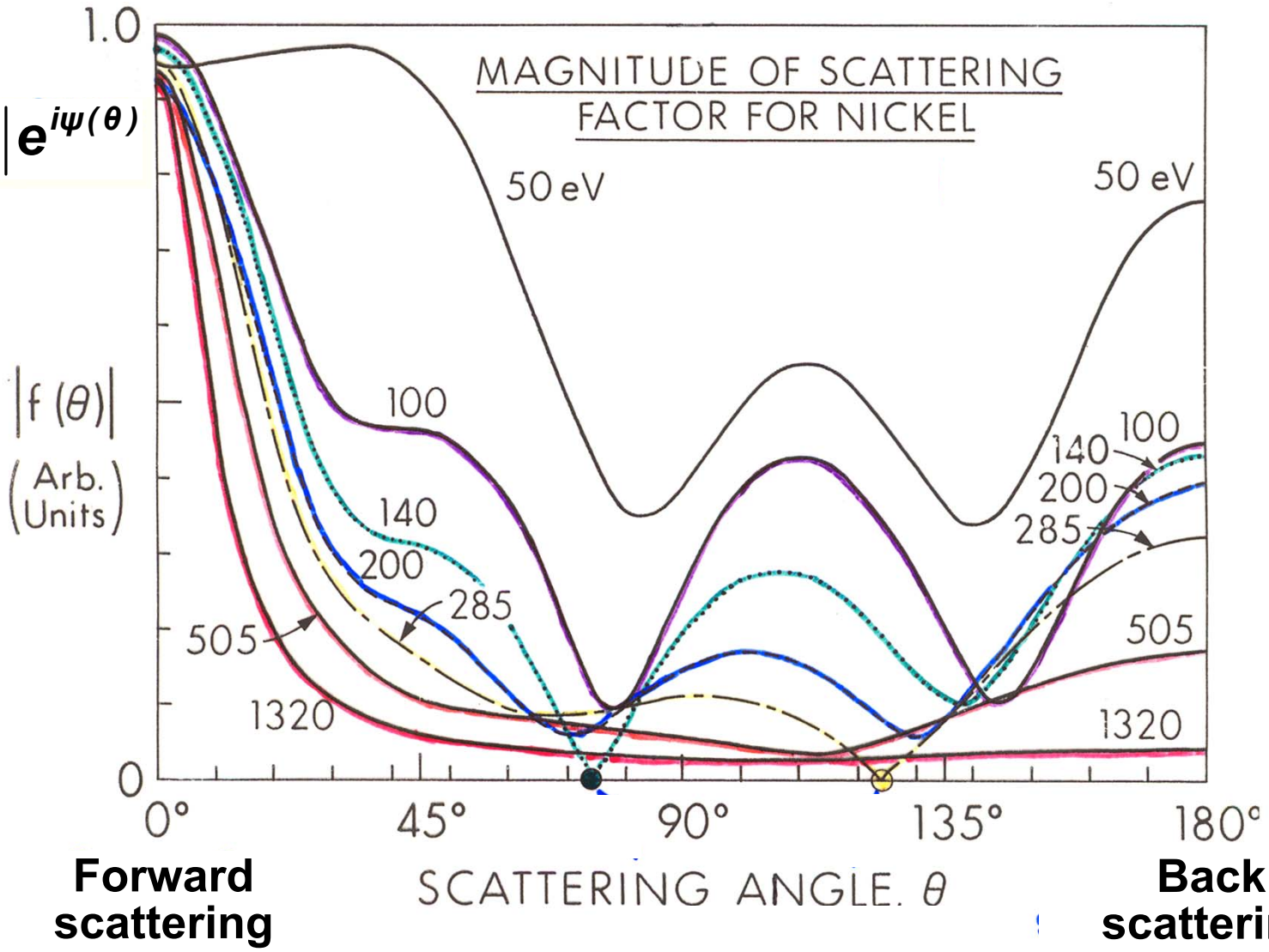

Sagurton et al.
Surf. Sci. 182, 287 ('84)

ENERGY DEPENDENCE OF ELECTRON ELASTIC SCATTERING

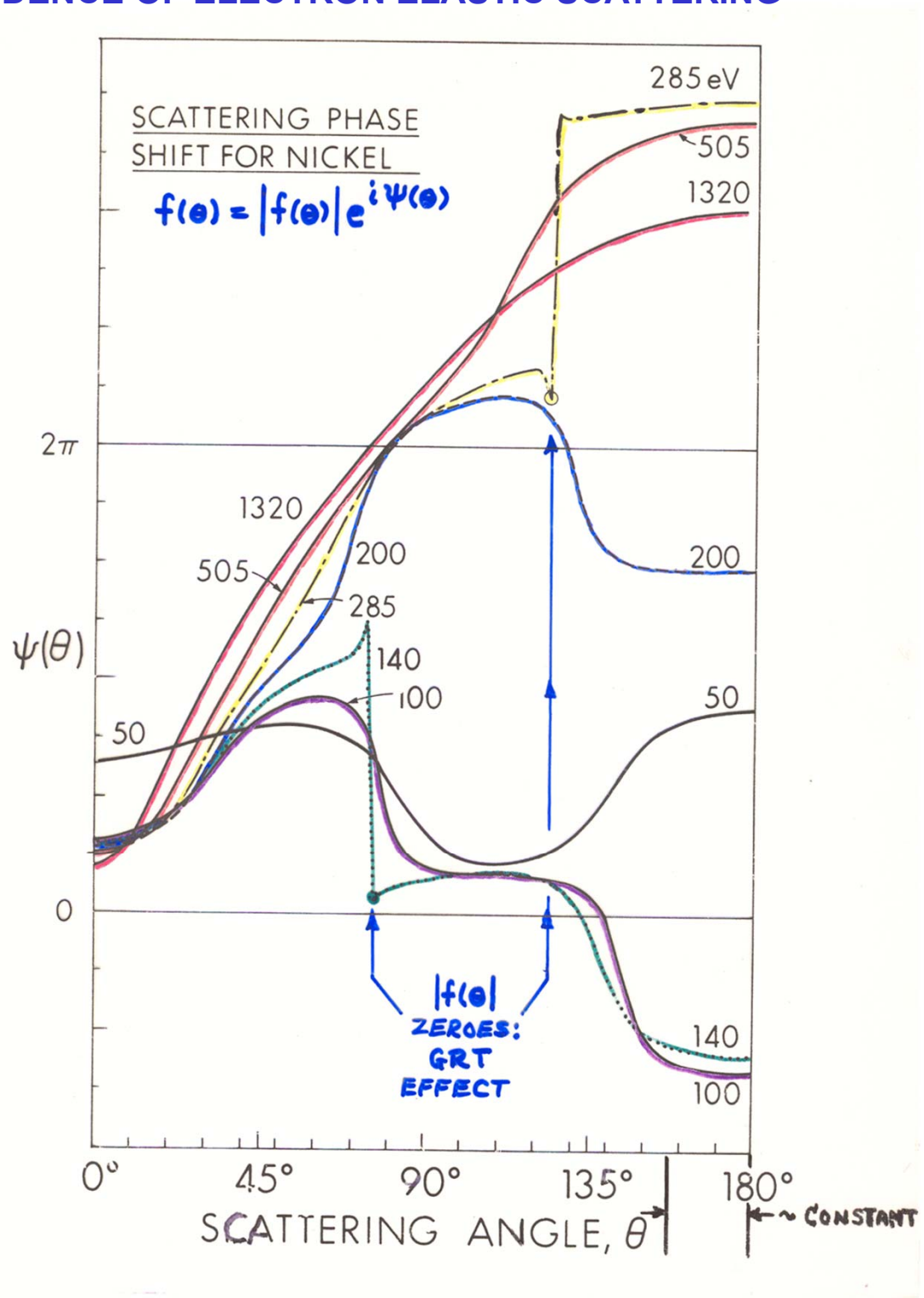

Energy dependence of photoelectron diffraction: Theory

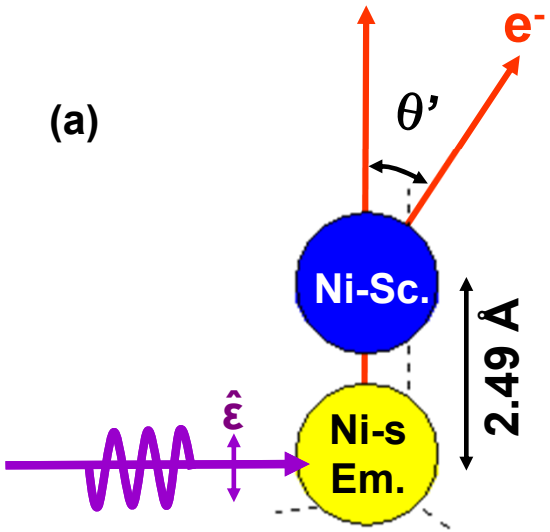

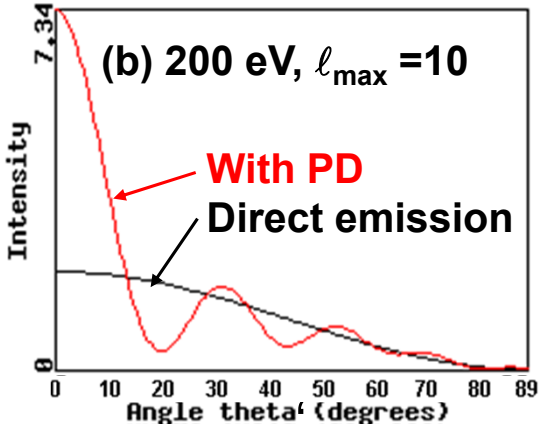

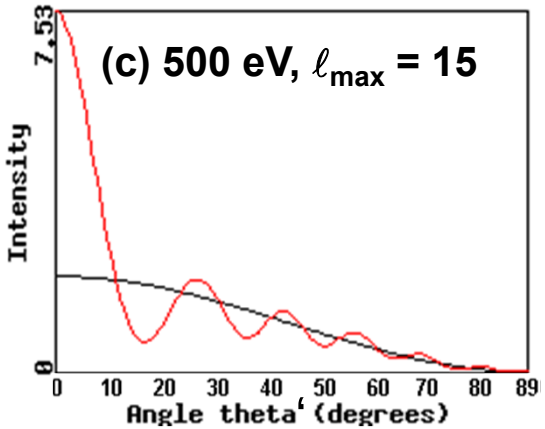

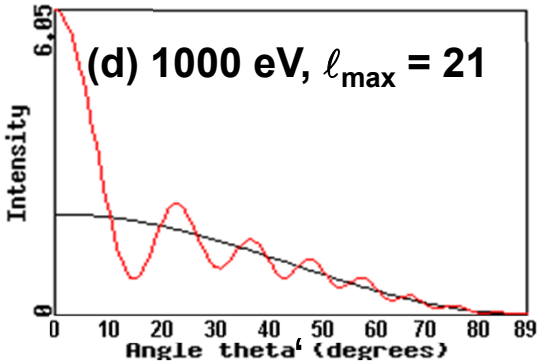

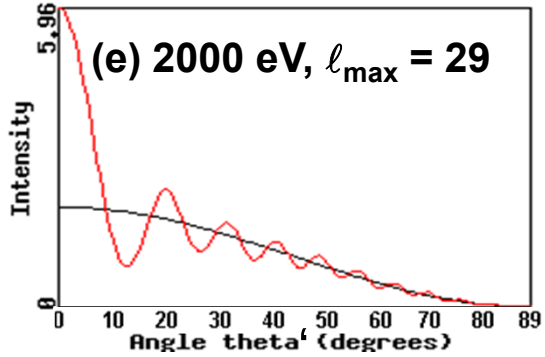

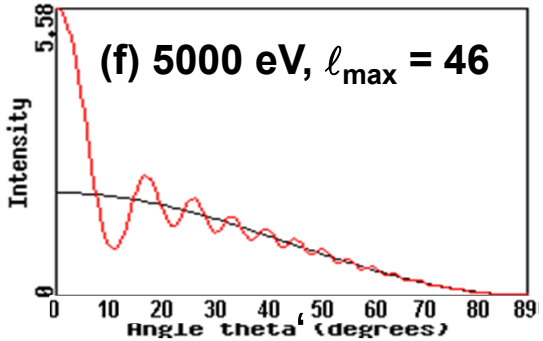

Much more forward peaked at higher energy, weaker in directions away from forward

X-ray Photoelectron Diffraction:1ML FeO on Pt(111)

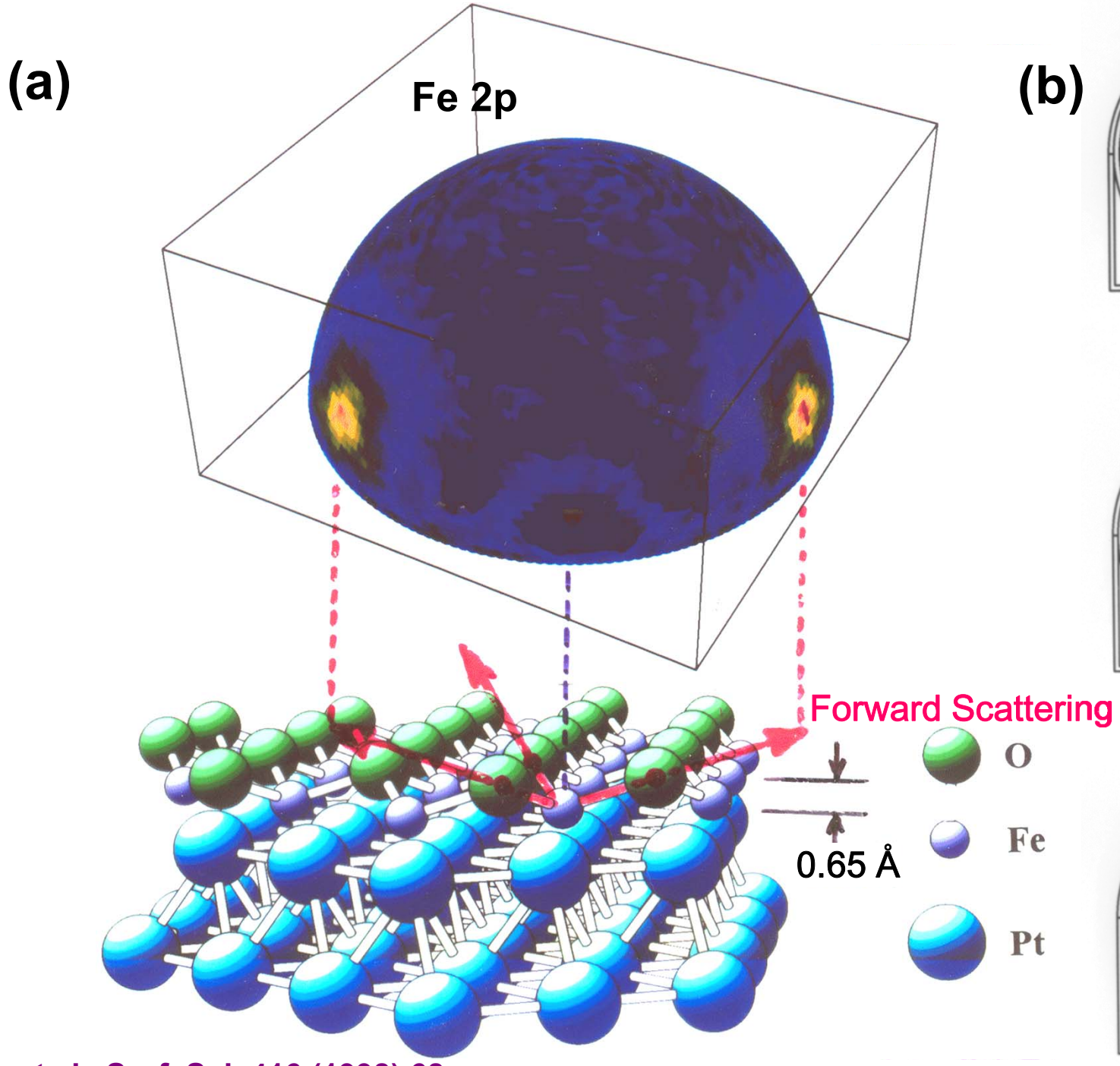

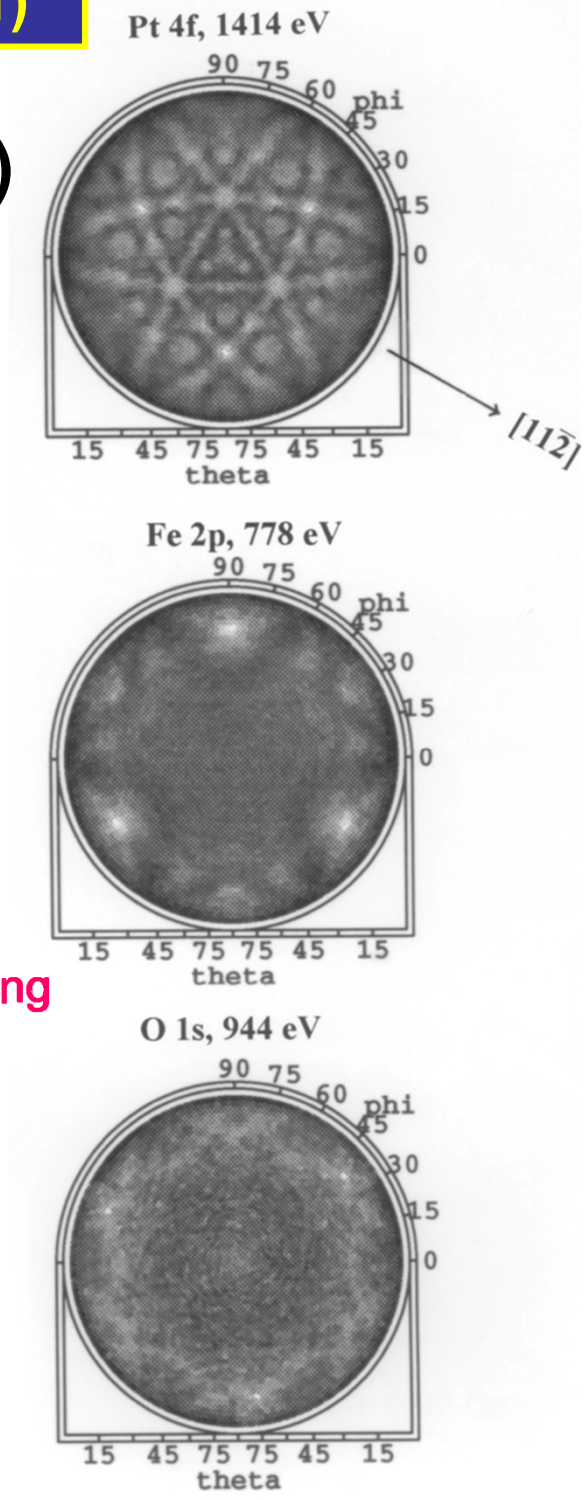

Kim et al., Surf. Sci. 416 (1998) 68

X-ray Photoelectron Diffraction:1ML FeO on Pt(111)

Experiment:
In stereographic projection

Theory:
Single-scatttering cluster model

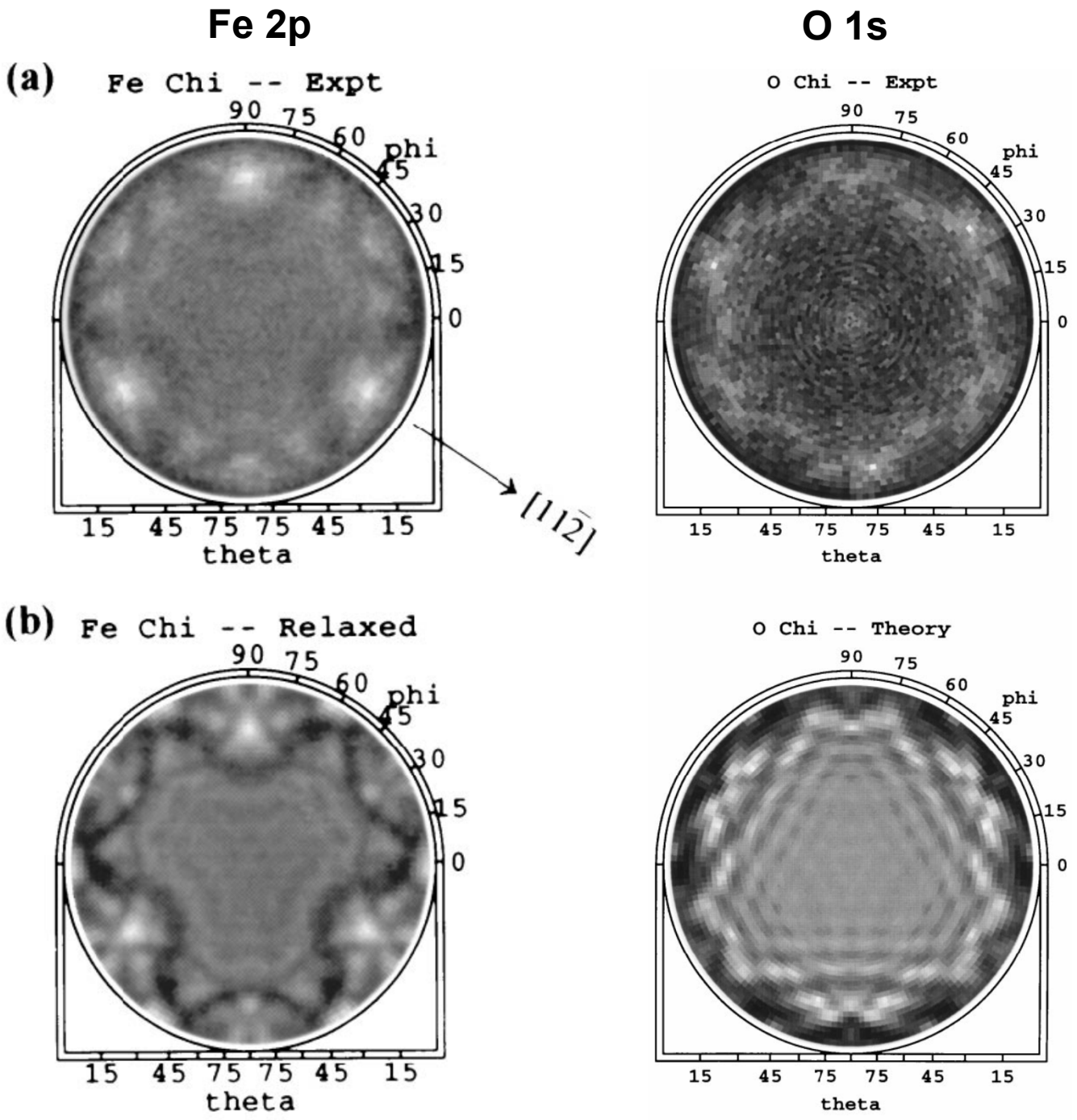

Online calculation of photoelectron diffraction patterns:

EDAC output for CO/Fe(001)

Click on the figure to download data.

http://garciadeabajos-group.icfo.es/widgets/edac/index.html

Oxygen 1st order diff. ring

7 atoms:

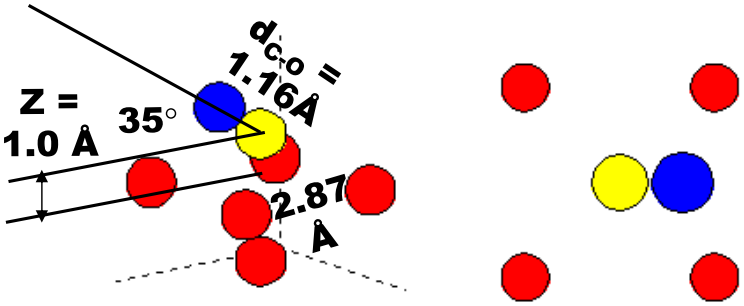

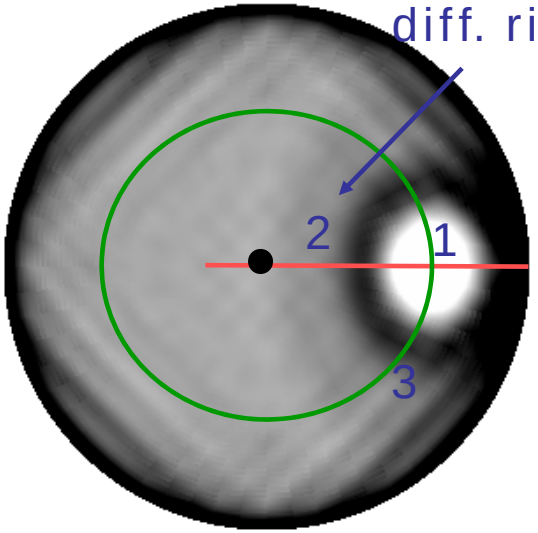

Left: representation of the cluster rocking around a line parallel to the *z* direction and passing by the **emitter (yellow atom)**. The dashed lines stand for the *xyz* axes. **Right:** top view of the cluster, where the *x*/*y* direction (not plotted) runs along the horizontal/vertical screen direction. Different atomic species have been assigned the colors O, Fe.

Polar scan of photoemission intensity (logarithmic scale). White/black regions correspond to high/low intensity. The orientation is the same as in the top-view of the cluster. The distance to the center of the figure is proportional to the polar angle θ. The polar angle range is (0.0, 89.0) (in degrees).

Parameters used in the calculation:

N=7 atoms
Iteration order=4
l_{max}=25
V_0=10.5 eV
Photoelecton energy=1202 eV
p-polarized light
z_0=1.435 Å
Recursion iteration method

X 4 domains rotated by 90°

User friendly web-based program for PD calculations by Javier Garcia de Abajo, DIPC, Donostia-San Sebastian, Spain

Electron Diffraction in Atomic Clusters

for Core Level Photoelectron Diffraction Simulations

http://nanophotonics.csic.es/widgets/edac/index.html

Created by F. Javier García de Abajo (CSIC and DIPC, San Sebastian, Spain)
in collaboration with M. A. Van Hove and C. S. Fadley (LBNL, Berkeley, and UCD, Davis, California)

This site allows performing on-line photoelectron diffraction calculations. Multiple scattering (MS) of the photoelectron is carried out for a cluster representing a solid or molecule. Select the corresponding parameters and click on the "Calculate" button below to perform the actual calculation and to produce a plot of the calculated data (a separate window pops out to display it). A numerical data table can be downloaded by clicking on the resulting plot. Click on the different parameter names in blue to see fuller explanations. Click on the "Preview Cluster" button to display the currently selected atomic cluster (but without performing a MS calculation) or the button "Download Cluster" to download the currently selected cluster. Notice that the scattering phase shifts and excitation radial matrix elements are calculated internally for each cluster configuration, so that the user does not have to provide them. Please, read the terms of use and the restrictions on input parameters before using this site for the first time.

Terms and conditions of use

Terms of use Restrictions on input parameters Password: ******** jarabe12

A password is only necessary for large computation times (click here for more details). Leave it blank otherwise.

Title (optional): CO/Fe(001)

Cluster definition

The cluster and the list of emitters are defined by a list of commands with the following format (click here or on the items of this list for further details):

atom symbol *x y z* layer symbol *x y z a b* α_1 α_2

surface symbol *x y z a* type emitter *x y z*

Fill in the text box with these commands according to the cluster specifications that you need. Some examples are provided by clicking here (you may cut and paste them to this page and modify them further).

```
atom O 0.95 0 1.66
atom C 0 0 1.0
surface Fe 1.435 1.435 0 2.87 bcc100
emitter 0 0 1.0
end
```

The cluster consists of a maximum of [7] atoms. (Warning: a finite number of atoms generally introduces symmetry breaking.)

The size of the cluster is determined by the distance d_{max} = [10] Å and the reference point x_0 = [0] Å, y_0 = [0] Å, z_0 = [0] Å.

See cluster shape for more details.

Plot cluster on output? (•) Yes ( ) No

Cluster shape: (•) Parabolic ( ) Spherical

[Preview Cluster*] [Download Cluster*]

Geometry of beam and analyzer

Incoming beam parameters (see figure)

Polar angle θ_i = [0] degrees

Azimuthal angle φ_i = [0] degrees

Polarization:
(•) p-polarization
( ) s-polarization
( ) RCP
( ) LCP

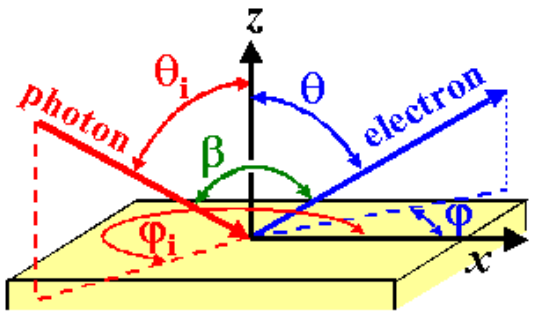

Schematic representation of the geometry

Mobility of cluster beam, and sample (click here for details):
(•) Only the sample moves with constant β = [90] degrees
( ) Only the analyzer moves
( ) Both the sample and the analyzer move

Energy and angle scanning parameters (see figure above)

The following entries will select the range of photoelectron energies and angles of emission.

Energy scans for a given emission angle can be chosen by selecting more than one energy of emission and only one polar angle and one azimuthal angle (the value of each angle is then taken as the lower limit of the selected angular range, and the value of the upper limits are disregarded). In this case, the output is a 1D plot with the photoelectron intensity as a function of photoelectron energy.

Electron energy range: 1 equally-spaced value(s) of the electron energy from 1202 eV to 1202 eV

Polar angle: 50 equally-spaced value(s) of the polar angle θ from 0 degrees to 89 degrees

Azimuthal angle: 61 equally-spaced value(s) of the azimuthal angle φ from 0 degrees to 360 degrees

Type of 2D angular representation: ○ Linear scale ◉ Logarithmic scale

Type of azimuthal of polar angular representation: ◉ Cartesian ○ Polar

Photoelectron detector half-width acceptance angle = 0 degrees. The photoelectron intensities are angle-averaged over a cone with half aperture given by this parameter.

Multiple scattering parameters

Internal code parameters

Maximum orbital quantum number l_{max} = 25

Scattering order = 4

Iteration method: ○ Jacobi (regular MS) ◉ Recursion

Additional solid parameters

Inner potential V_0 = 12.4 eV

8.1 eV from band struct. + work function = 4.3 eV = 12.4 eV

Electronic edge z_0 = 1.435 Å

Inelastic mean free path: either choose a fixed value = 17.8 Å

or (if that last entry is <0) use the TPP-2M formula with parameters ρ = 8.91 g/cm^3, N_v = 10, E_p = 35.45 eV, and E_g = 0 eV

Temperature (K) = 300 and Debye emperature (K) = 450

Photoelectron Diffraction with soft and hard x-ray excitation: two viewpoints

The scattering of photoelectrons from localized sources can be described in real space (multiple scattering cluster) and reciprocal space (dynamical theory of electron diffraction)

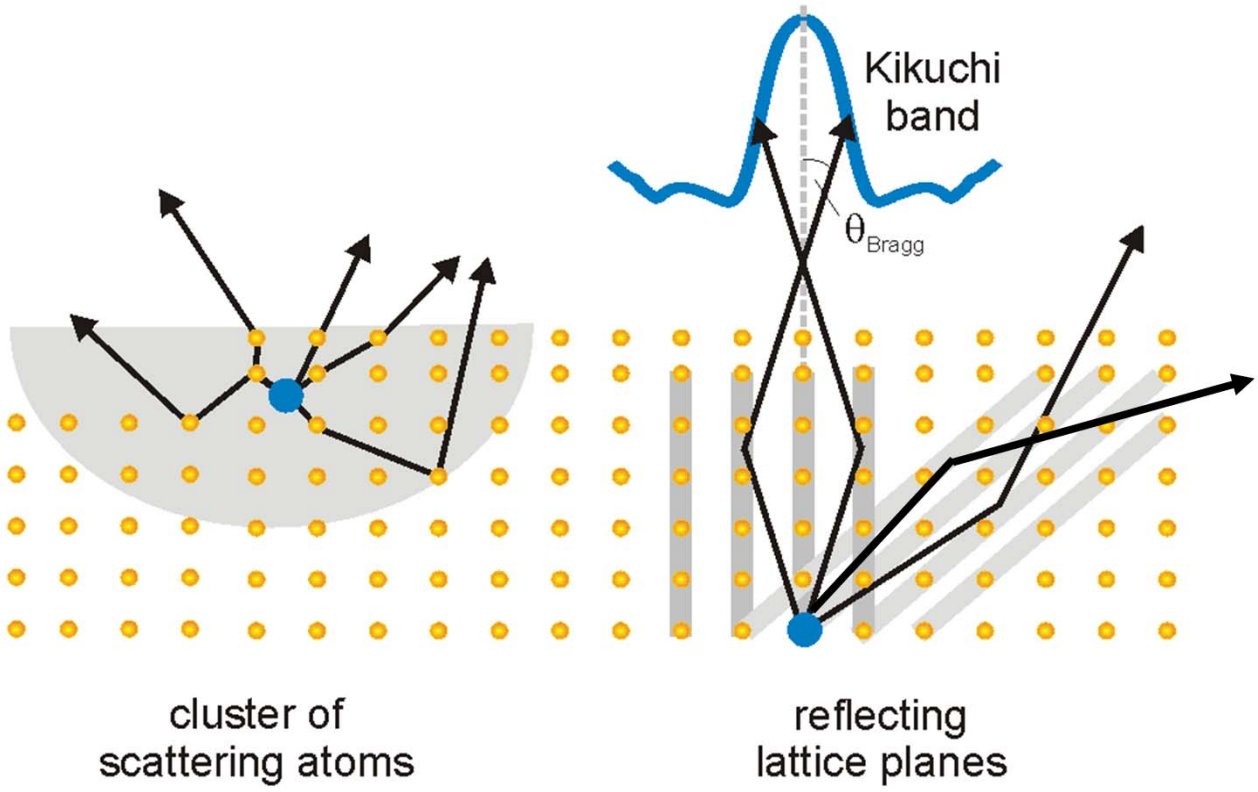

Soft x-ray excitation → Hard x-ray excitation

A. Winkelmann et al, New J. Phys 10 (2008) 113002

Photoelectron Diffraction with soft and hard x-ray excitation: two viewpoints, expt. vs. theory

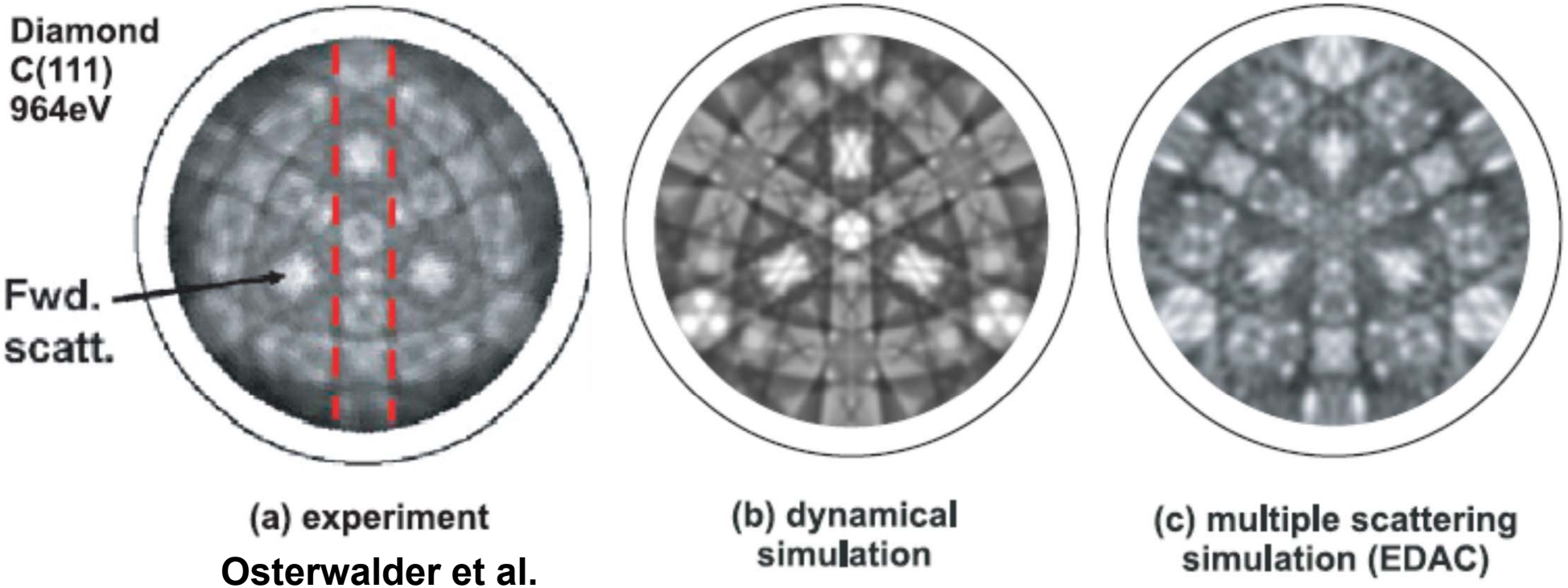

Osterwalder et al.

Easier to use for higher energies, "bulk" or long-range order emission

A. Winkelmann et al, New J. Phys 10 (2008) 113002

Bulk sensitive HXPD of Si 1s

$h\nu$ = 5417 eV

Native SiO_2 /Si(001)

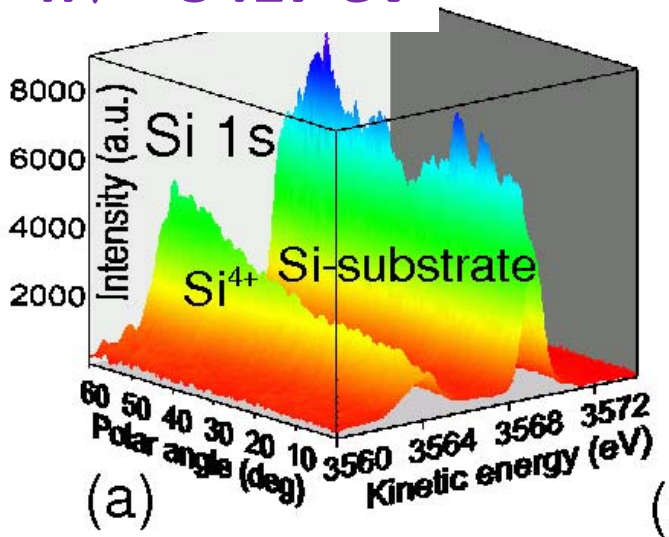

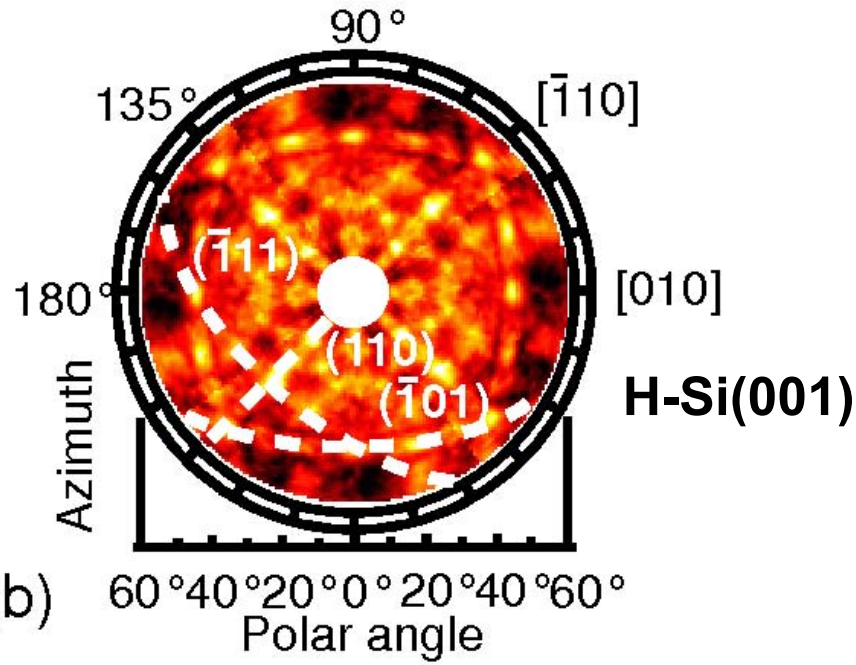

H-Si(001)

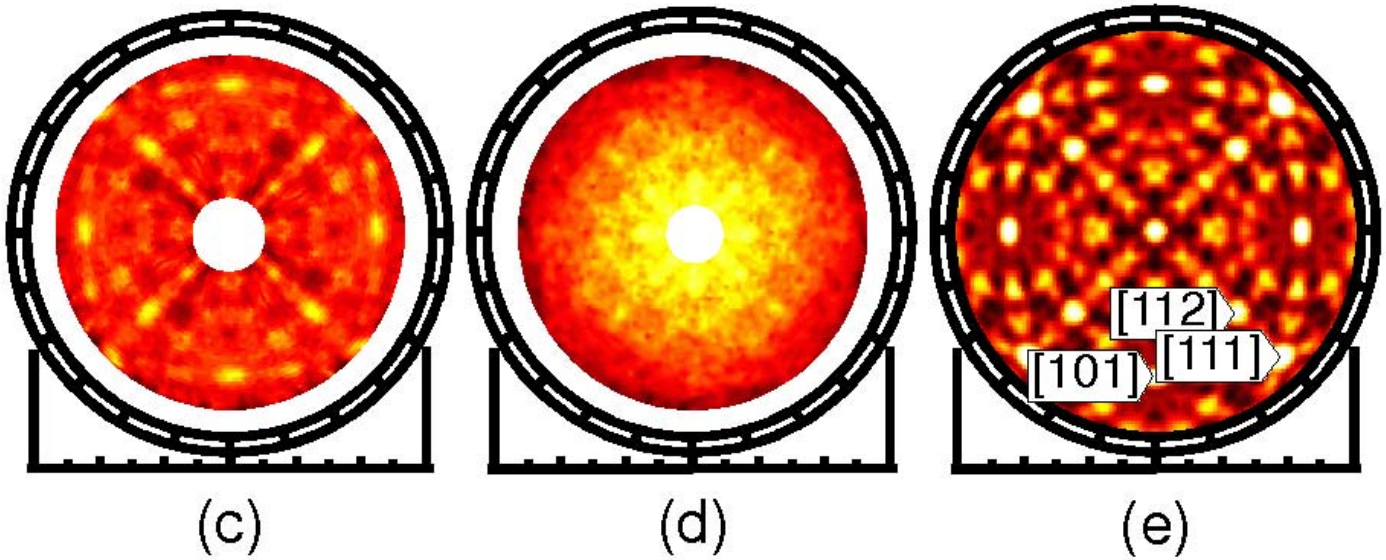

4.1 nm SiO_2/Si(001)

7.0 nmSiO_2/Si(001)

Multiple scattering cluster simulation

Pis et al., Applied Physics Express 3 (2010) 056701;
Kobata et al., SPring8: Surf. Interf. Anal.,http://onlinelibrary.wiley.com/doi/10.1002/sia.3760/pdf

Hard x-ray photoelectron diffraction--Theory: Sensitivity to lattice distortions and atomic site type?

Si(111)-6 keV: Impurity atom on lattice site (Si) vs. tetrahedral interstitial (T)

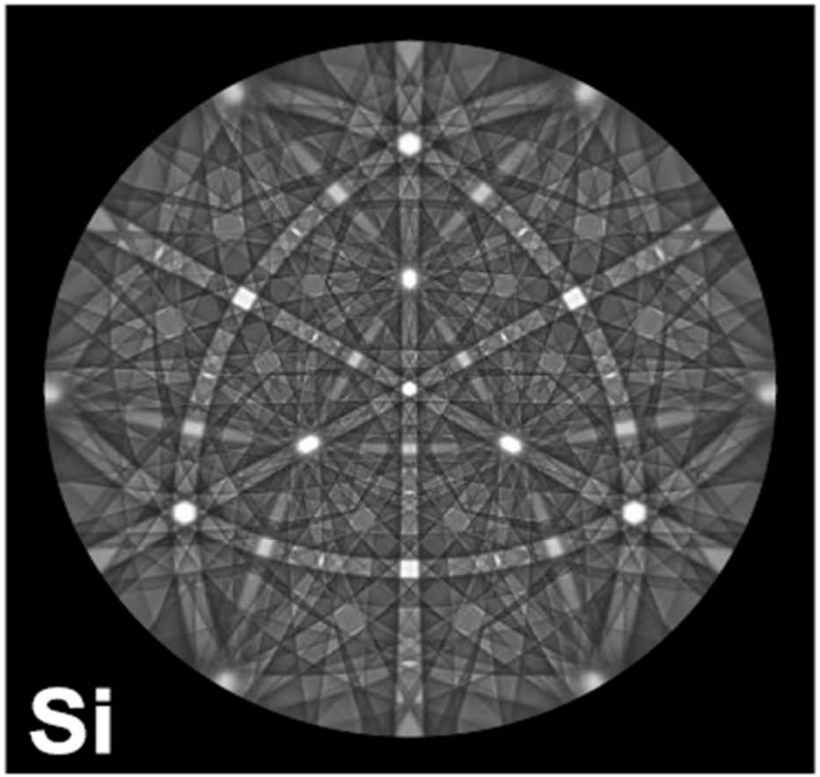

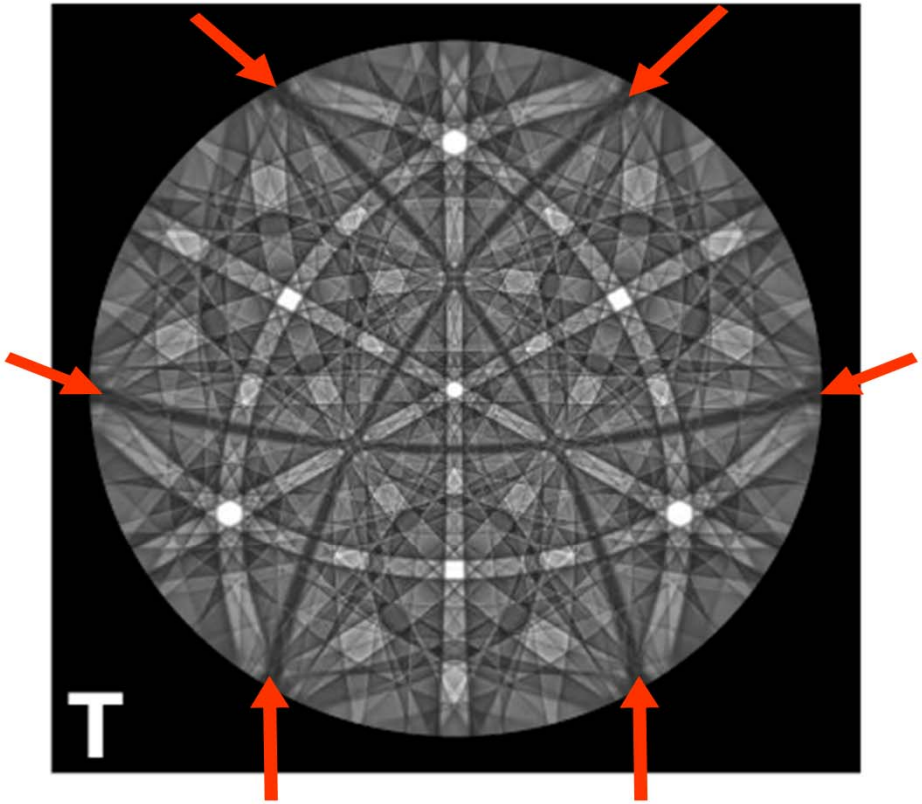

A. Winkelman, J. Garcia de Abajo, MPI Halle, CF, New Journal of Physics 10 (2008) 113002

Missing Kikuchi bands-->"forbidden reflections"

Basic Concepts:

A Little Electronic Structure
The X-Ray-Based Experiments
X-Ray Sources, Synchrotron Radiation, Free Electron Lasers

Core-Level Photoemission

Intensities and Quantitative Analysis, the 3-Step Model
Varying Surface and Bulk Sensitivity
Chemical Shifts
Multiplet Splittings
Electron Screening and Satellite Structure
Magnetic and Non-Magnetic Dichroism
Resonant Photoemission
Photoelectron Diffraction and Holography 

Valence-Level Photoemission

Band-Mapping in the Ultraviolet Photoemission Limit
Densities of States in the X-Ray Photoemission Limit

Some New Directions

Photoemission with Hard X-Rays (throughout lectures)
Photoemission with Standing Wave Excitation
Photoemission with: Higher Pressures→multi-Torr→Atmosphere?
Spatial Resolution-Photoelectron Microscopy
Temporal Resolution

Diffraction and Holography: What's the Difference?

Holography:

Reference and scattered interfere→ phase relation preserved

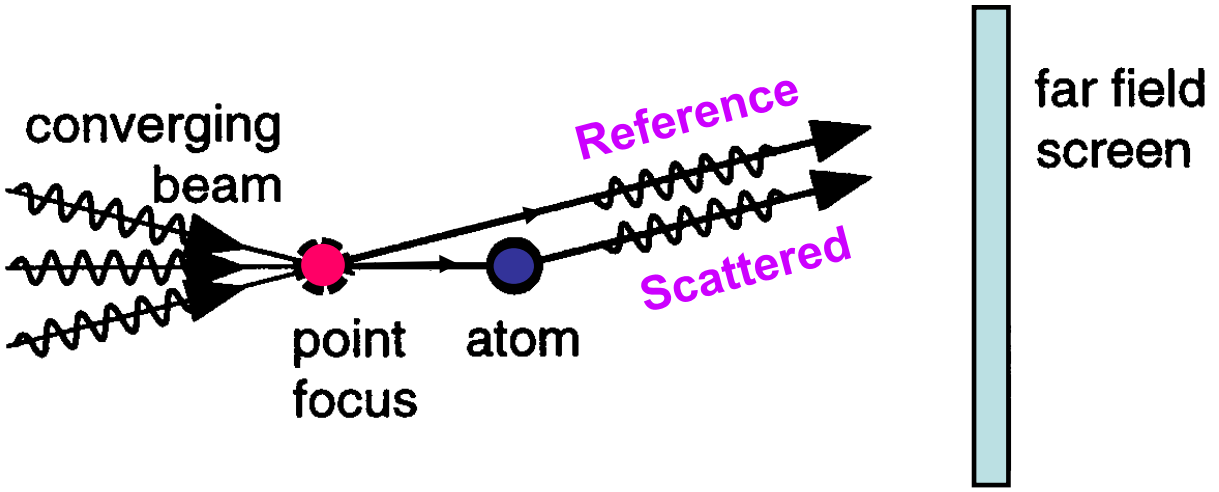

Diffraction:

Reference lost→ "The phase problem": solved for x-rays via "direct methods", multiple anomalous dispersion, isomorphous replacement

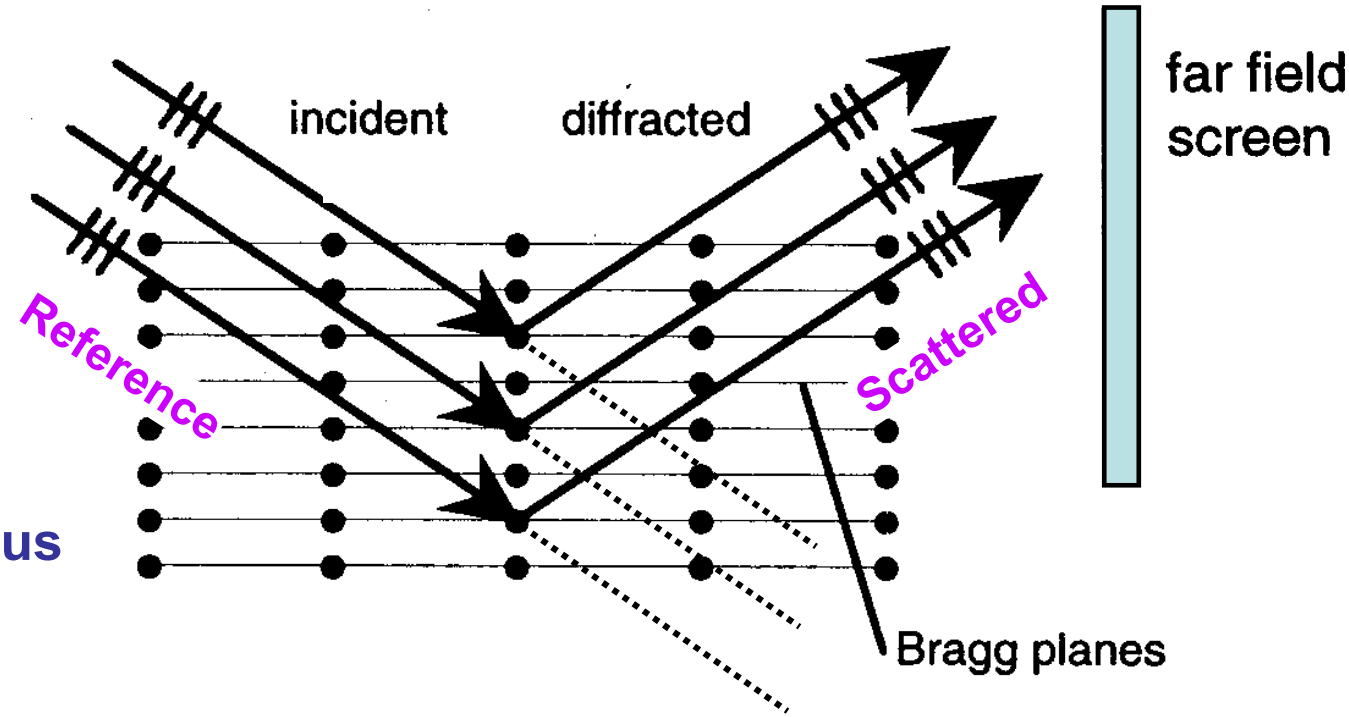

Photoelectron Holography: An Additional Trick

Holography:

Reference and scattered interfere→ phase relation preserved

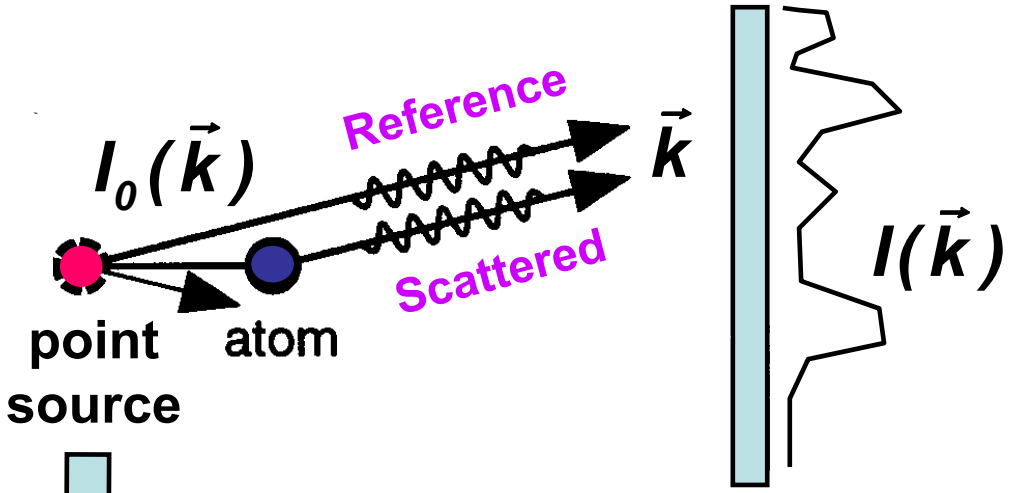

Use an "inside-source": atomic or nuclear emitter (Szöke, in "Short Wavelength Radiation: Generation and Applications", D. Attwood and J. Bokor, Eds., AIP Conference Proceedings No. 147 (1986))

$$\chi(\vec{k}) = [I(\vec{k}) - I_0(\vec{k})] / I_0(\vec{k})$$

Holographic image of scatterers =

$$U(\vec{r}) = \left| \iiint \chi(\vec{k}) \exp[i\vec{k} \bullet \vec{r} - ikr] d^3k \right|$$

Review in: C.S. Fadley, M.A. Van Hove, A. Kaduwela, S. Omori, L. Zhao, and S. Marchesini, J. Phys. Cond. Mat. 13, 10517 (2001)

Differential photoelectron holography in Cu(001) —Cu 3p emission

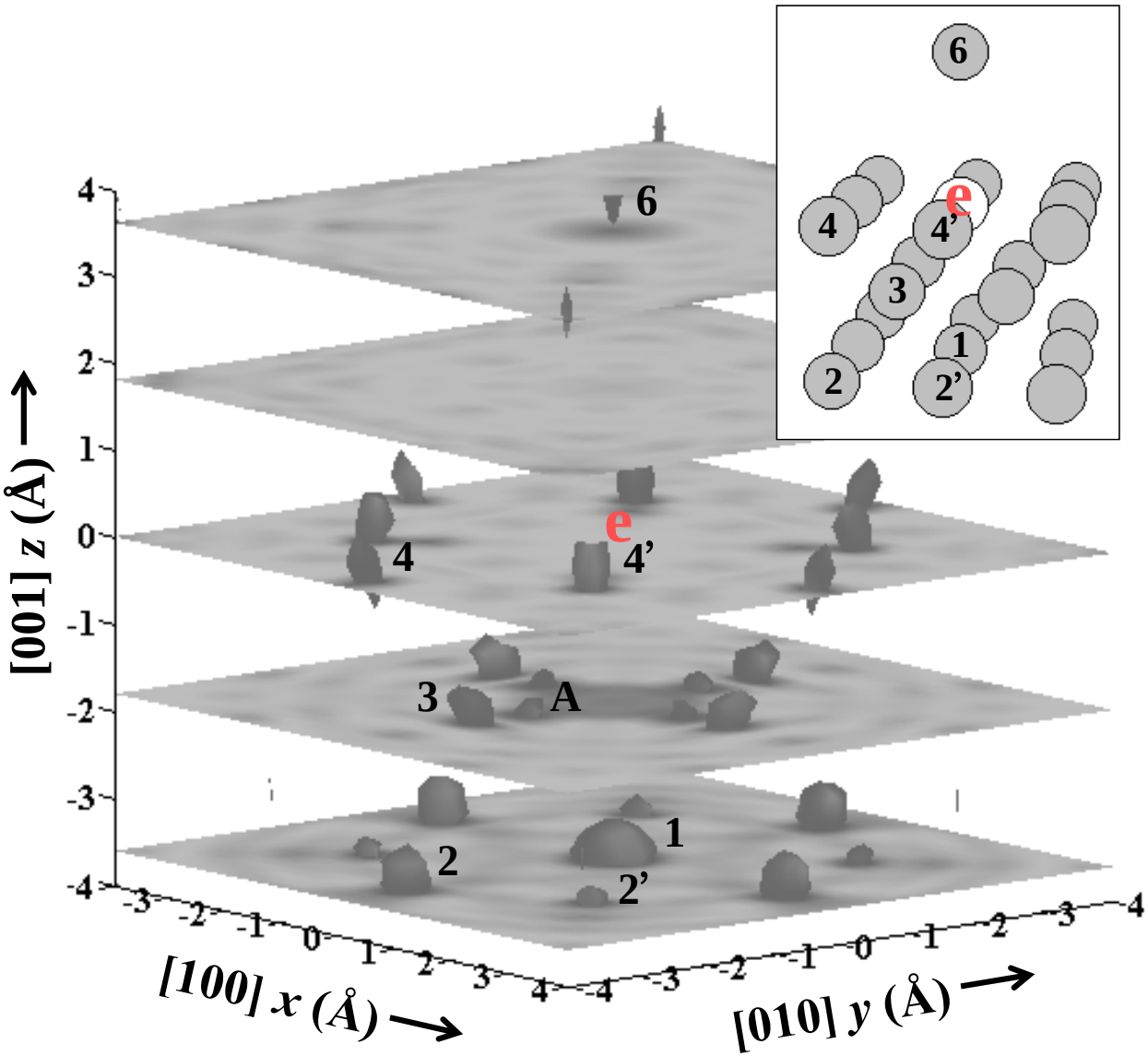

Omori et al., Phys. Rev. Lett. 88 (2002) 5504

Derivative photoelectron holography: As and Si emission from As/Si(111):

$$U(\vec{r}) = \left| \iiint \chi(\vec{k}) \exp[i\vec{k}\cdot\vec{r} - ikr]\, d^3k \right|$$

$$\text{with } \chi = \frac{I(\vec{k}) - I_0}{I_0}$$

and $I(\vec{k})$ from integration of logarithmic derivative

$$L(h\nu, \hat{k}) = \frac{I(h\nu + \delta, \hat{k}) - I(h\nu - \delta, \hat{k})}{\left[I(h\nu + \delta, \hat{k}) + I(h\nu - \delta, \hat{k}) \right] \delta}$$

$$I(\vec{k}) \equiv I(k, \hat{k}) = A \int L(h\nu, \hat{k})\, d^3k$$

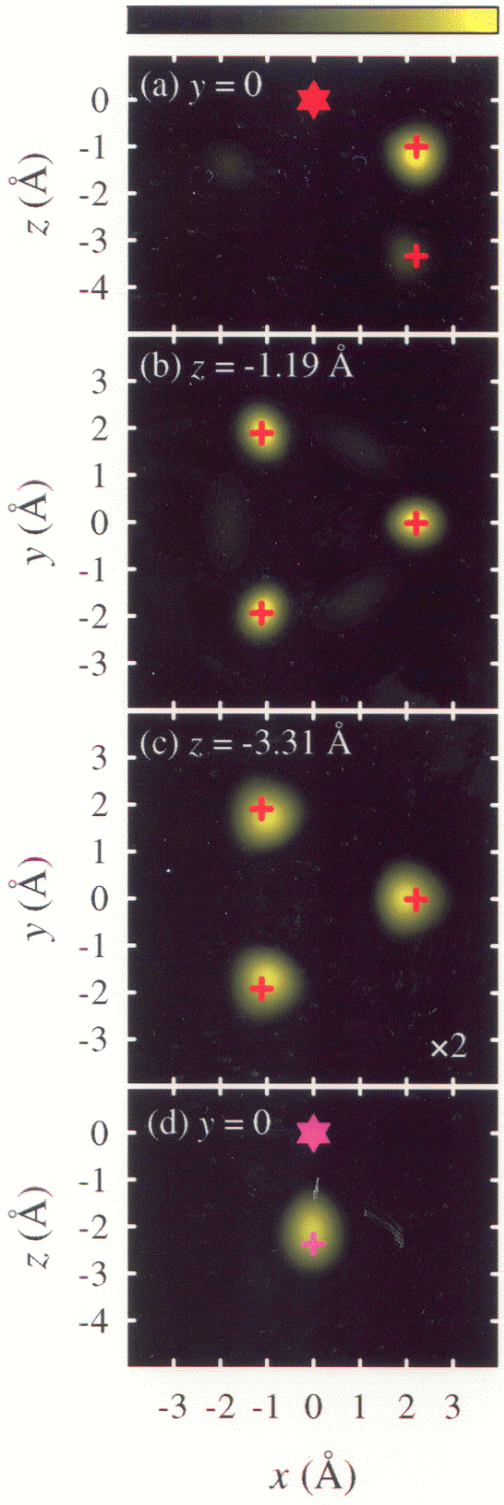

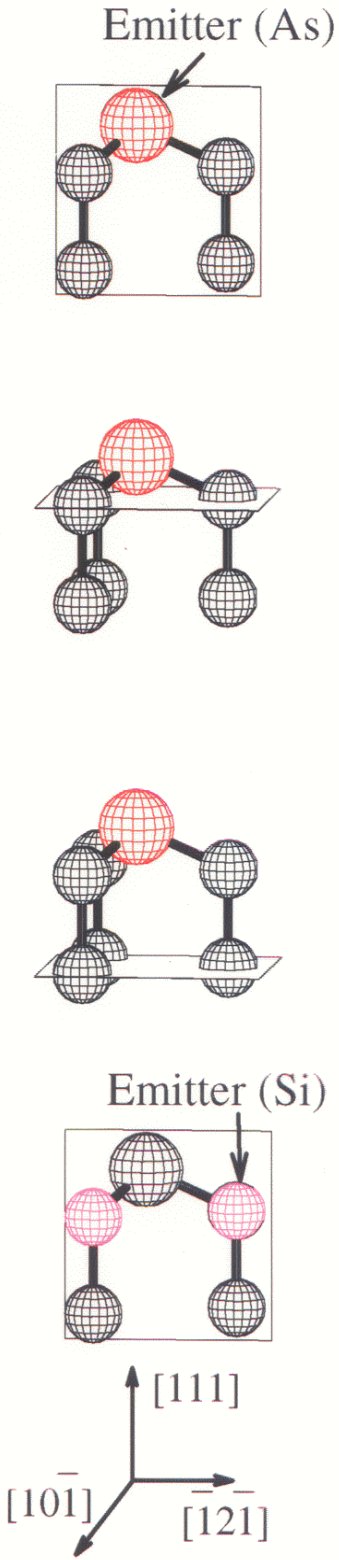

Luh et al. Phys. Rev. Lett., 81, 4160 (1998)

Basic Concepts:

A Little Electronic Structure
The X-Ray-Based Experiments
X-Ray Sources, Synchrotron Radiation, Free Electron Lasers

Core-Level Photoemission

Intensities and Quantitative Analysis, the 3-Step Model
Varying Surface and Bulk Sensitivity
Chemical Shifts
Multiplet Splittings
Electron Screening and Satellite Structure
Magnetic and Non-Magnetic Dichroism
Resonant Photoemission
Photoelectron Diffraction and Holography Model-With Spin

Valence-Level Photoemission

Band-Mapping in the Ultraviolet Photoemission Limit
Densities of States in the X-Ray Photoemission Limit

Some New Directions

Photoemission with Hard X-Rays (throughout lectures)
Photoemission with Standing Wave Excitation
Photoemission with: Higher Pressures→multi-Torr→Atmosphere?
Spatial Resolution-Photoelectron Microscopy
Temporal Resolution

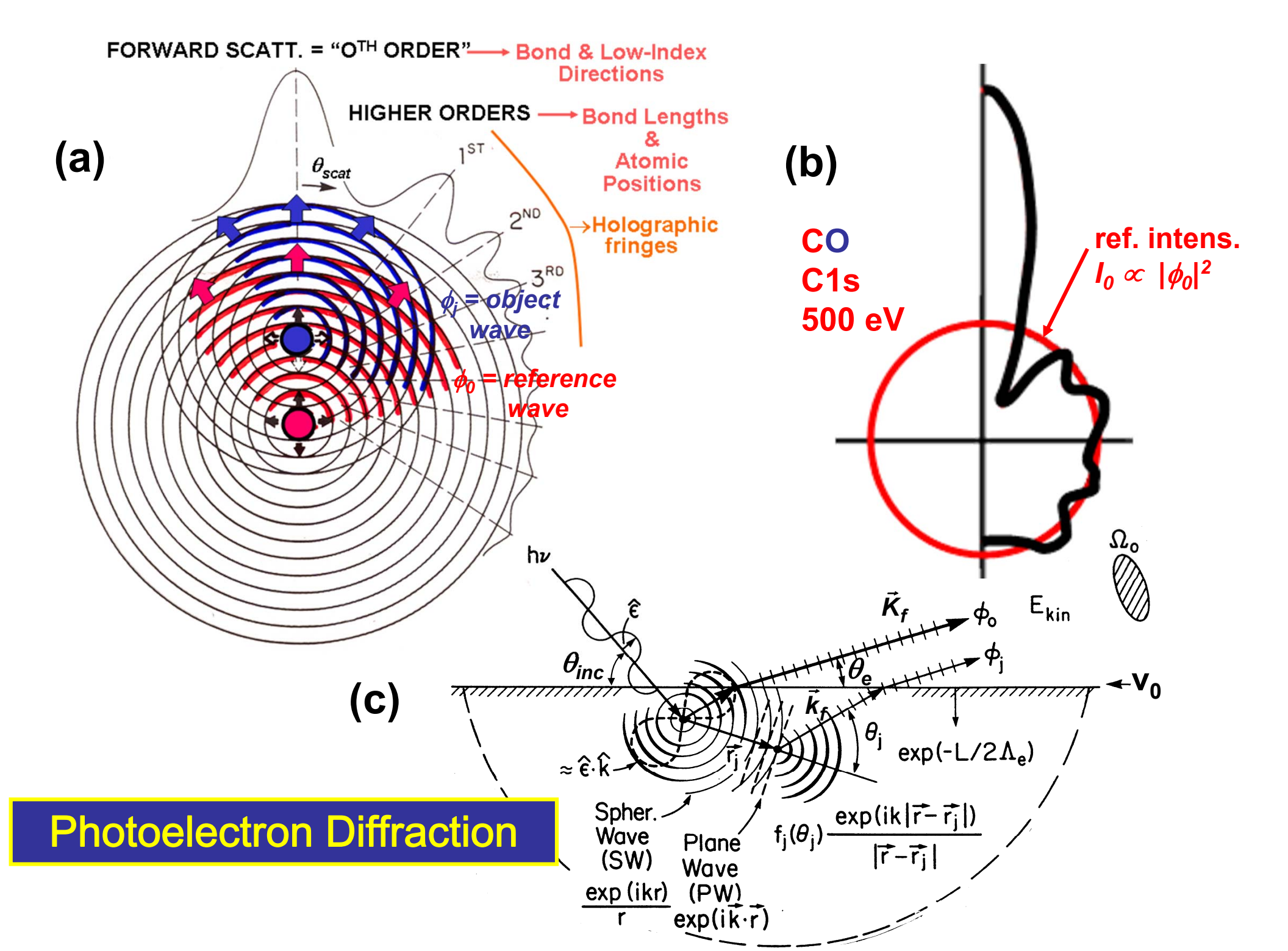
FORWARD SCATT. = "0TH ORDER"
Bond & Low-Index Directions
HIGHER ORDERS
Bond Lengths & Atomic Positions
Holographic fringes
(a)
θscat
1ST
2ND
3RD
φj = object wave
φ0 = reference wave
(b)
CO
C1s
500 eV
ref. intens.
I0 ∝ |φ0|2
Ω0
hν
ε̂
θinc
K̄f
φ0
Ekin
φj
θe
V0
k̄f
θj
≈ ε̂·k̂
r̄j
exp(-L/2Λe)
Spher. Wave (SW)
exp (ikr) / r
Plane Wave (PW)
exp(ik·r̄)
fj(θj) exp(ik|r̄ - r̄j|) / |r̄ - r̄j|
(c)
Photoelectron Diffraction

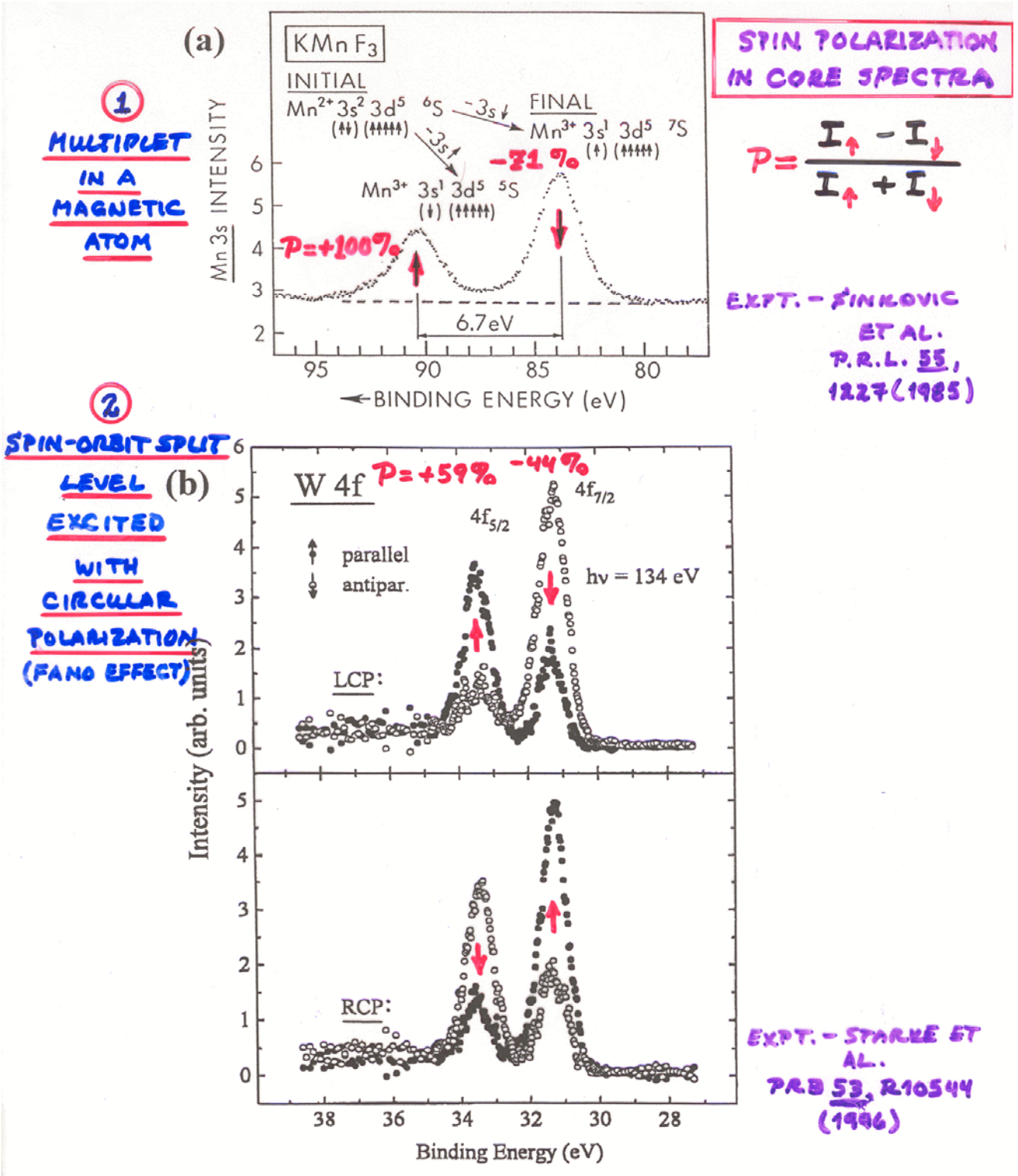

Spin <u>internally</u> referenced to spin of each ion

Spin <u>externally</u> referenced to $\vec{k}_{h\nu}$ and $\vec{M}$ of sample

SPIN-DEPENDENT SCATTERING:

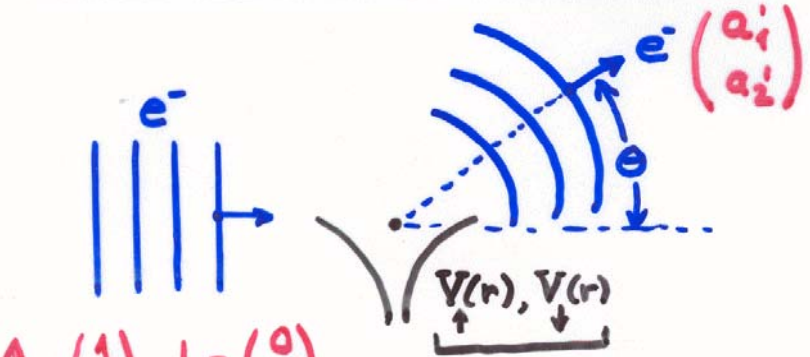

$\uparrow = \begin{pmatrix}1\\0\end{pmatrix}, \downarrow = \begin{pmatrix}0\\1\end{pmatrix},$

OR MIXED $\begin{pmatrix}a_1\\a_2\end{pmatrix}$

DIFF. FOR MAGNETIC ATOMS: EXCHANGE

IN GENERAL:

$$\begin{pmatrix}a_1'\\a_2'\end{pmatrix} = \begin{pmatrix}f_{\uparrow}(\theta) & -g(\theta)e^{-i\Phi(\theta)}\\ g(\theta)e^{i\Phi(\theta)} & f_{\downarrow}(\theta)\end{pmatrix}\begin{pmatrix}a_1\\a_2\end{pmatrix}$$

WITH: $f_{\uparrow\downarrow}(\theta)$ = USUAL COULOMB + EXCHANGE SCATTERING FACTOR (PERHAPS SPIN-DEP.)

$g(\theta), \Phi(\theta)$ = SPIN-ORBIT SCATTERING EFFECTS

Compare: Mott spin detector at 10-100 keV

TYPICAL NOS. FOR Co @ 100 eV:

$$|f(\theta)| \approx 100\,|g(\theta)|$$

(FINK + INGRAM, AT. DATA 4, 129('72))

CORE MULTIPLETS AS INTERNAL SPIN-POLARIZED e⁻ SOURCES

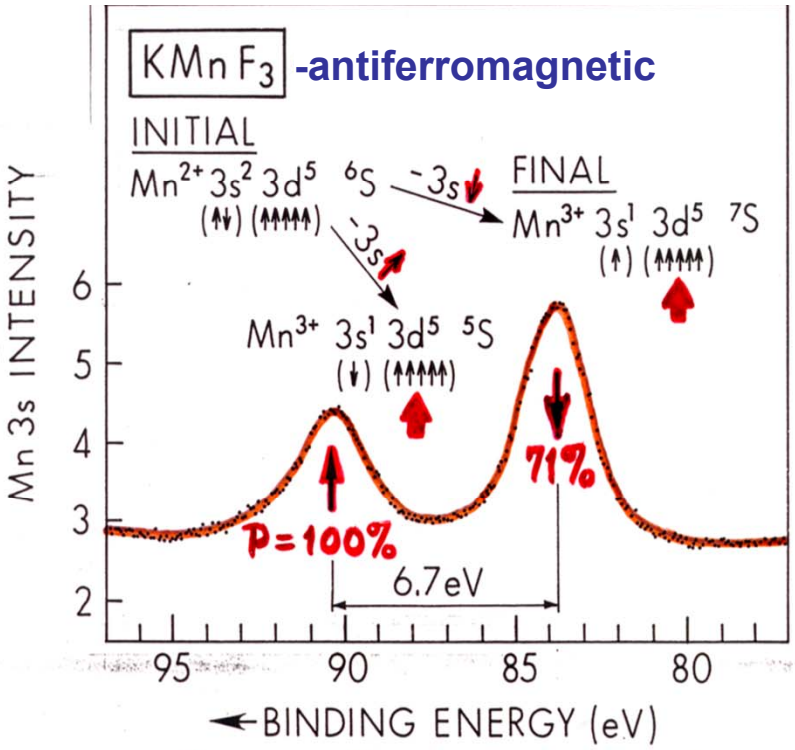

- Peak separation ∝ spin moment
- Peak separation affected by spin-dependent final-state/screening effects
- Peak intensities affected by spin-dependent scattering/diffraction
- No external spin detector required
- Photoe⁻ spin referred to moment of emitting atom:

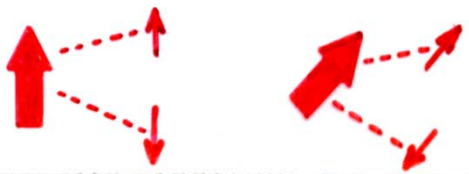

SPIN-POLARIZED PHOTOELECTRON DIFFRACTION

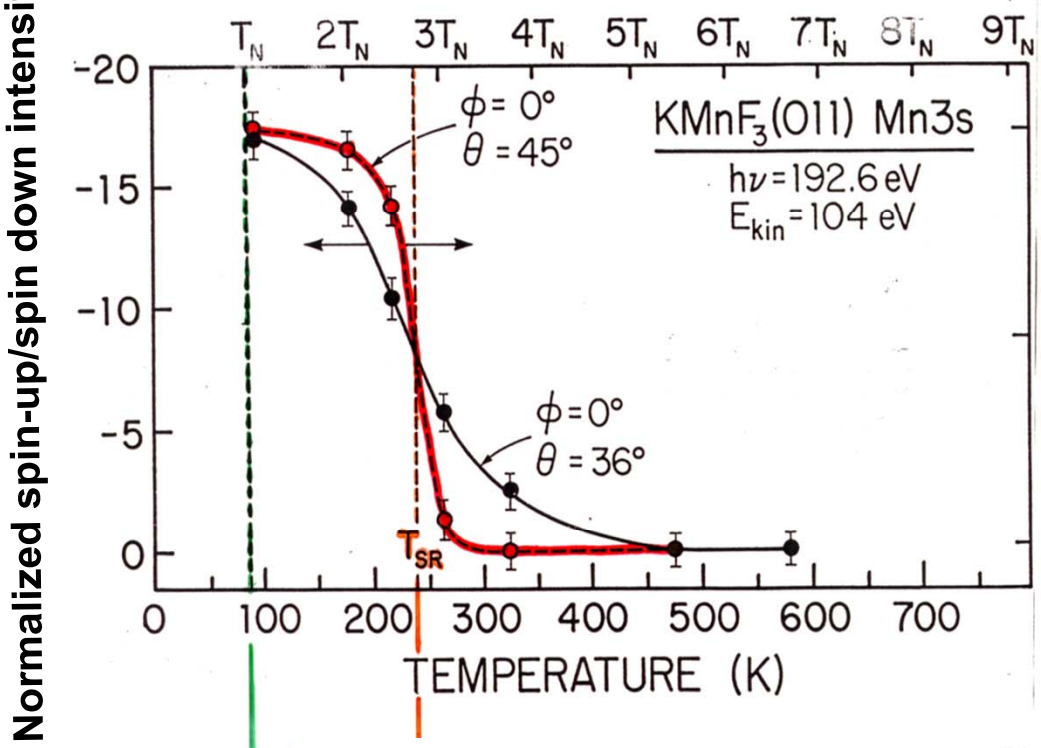

Loss of long-range AF order

Loss or change of short-range AF order (near surface)

Sinkovic, Hermsmeier, Fadley, PRL 55, 1227 (1985)

Future experiment: Spin-polarized photoelectron holography: direct imaging of magnetic moments in 3D?:

Normal image-

$$U(\vec{r}) = \left| \int \chi(\vec{k}) exp\left[-ikr + i\vec{k}\cdot\vec{r}\right] d^3k \right|^2$$

Spin-selective images-

$$\Delta(r) = U_{\uparrow}(r) - U_{\downarrow}(r)$$

$$\Delta'(r) = \left| \begin{array}{l} \int_k exp(-ikr) \times \\ \iint_{\hat{k}} exp\left(i\vec{k}\cdot\vec{r}\right)\left[\chi_{\uparrow}(\vec{k}) - \chi_{\downarrow}(\vec{k})\right] d^3k \end{array} \right|$$

Kaduwela et al. , Phys. Rev. B 50, 9656 (1994); Fadley et al., J. Phys. B Cond. Matt. 13, 10517 (2001)

Simulation: MnO-AF cluster

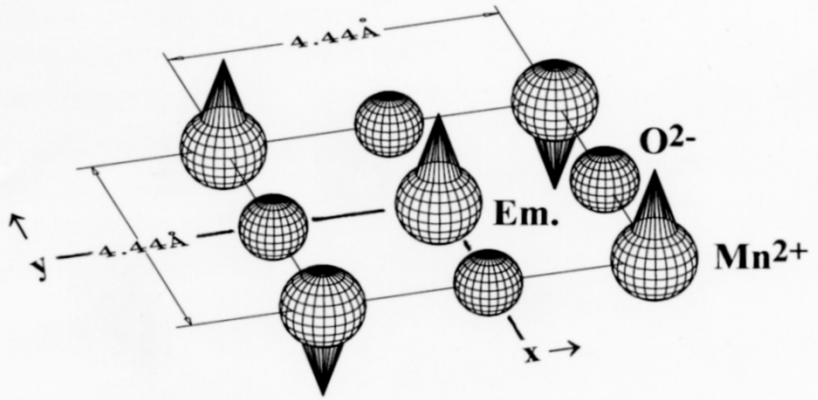

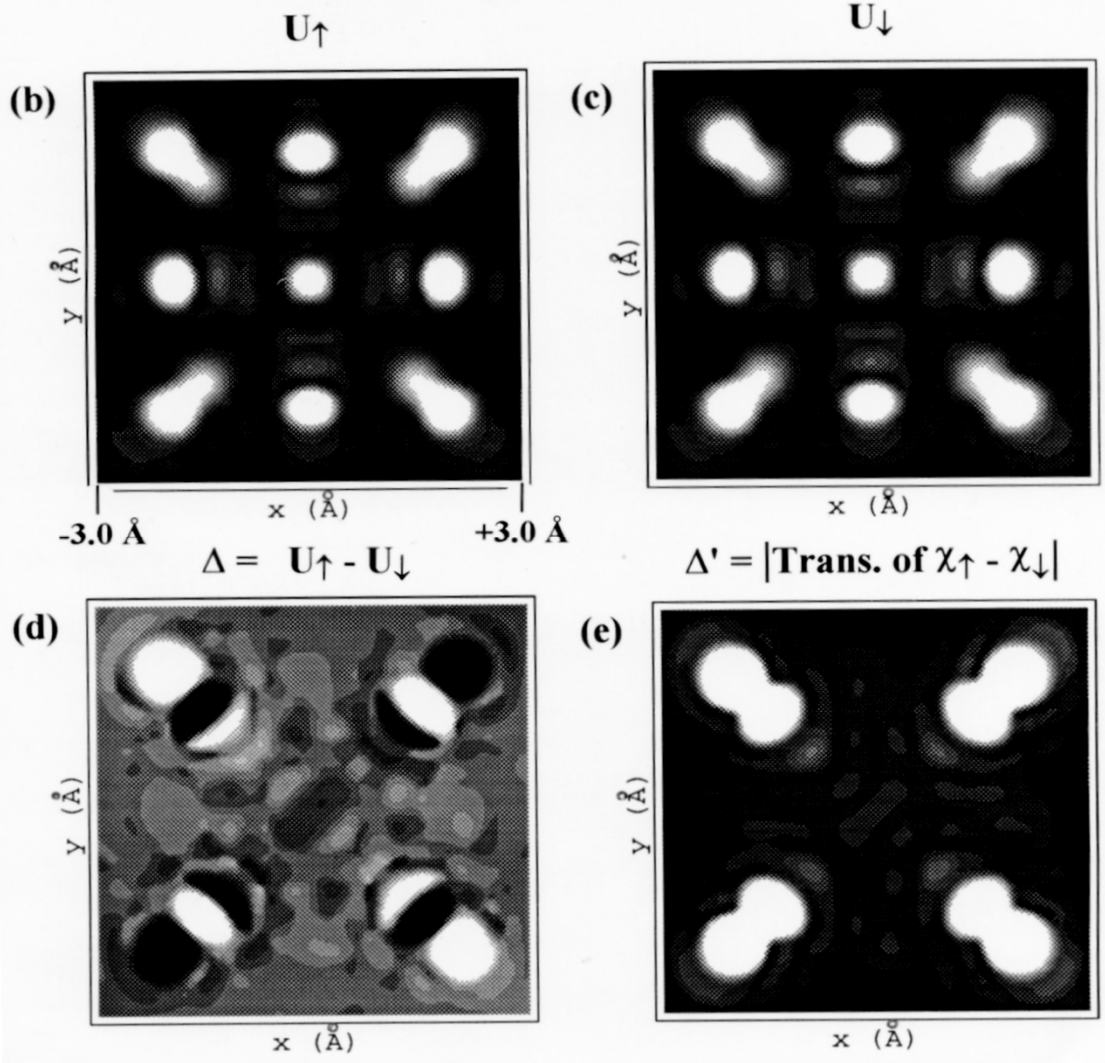

Spin-dependent diffraction and screening during a magnetic transition at the Gd(0001) surface

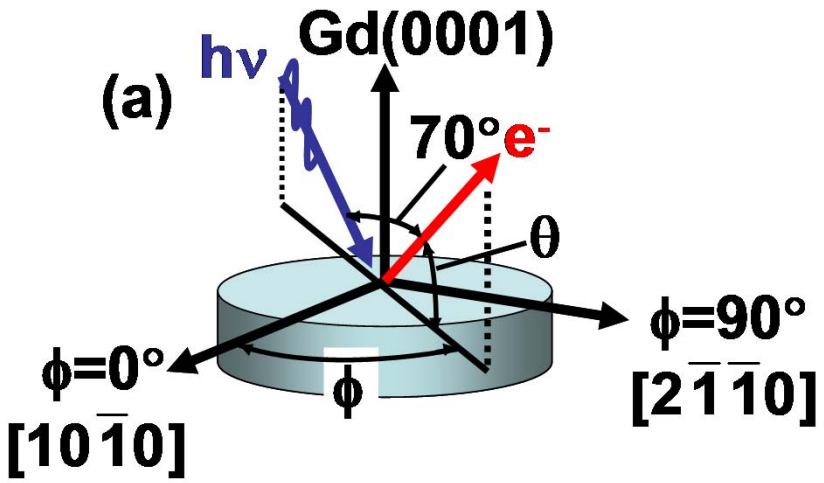

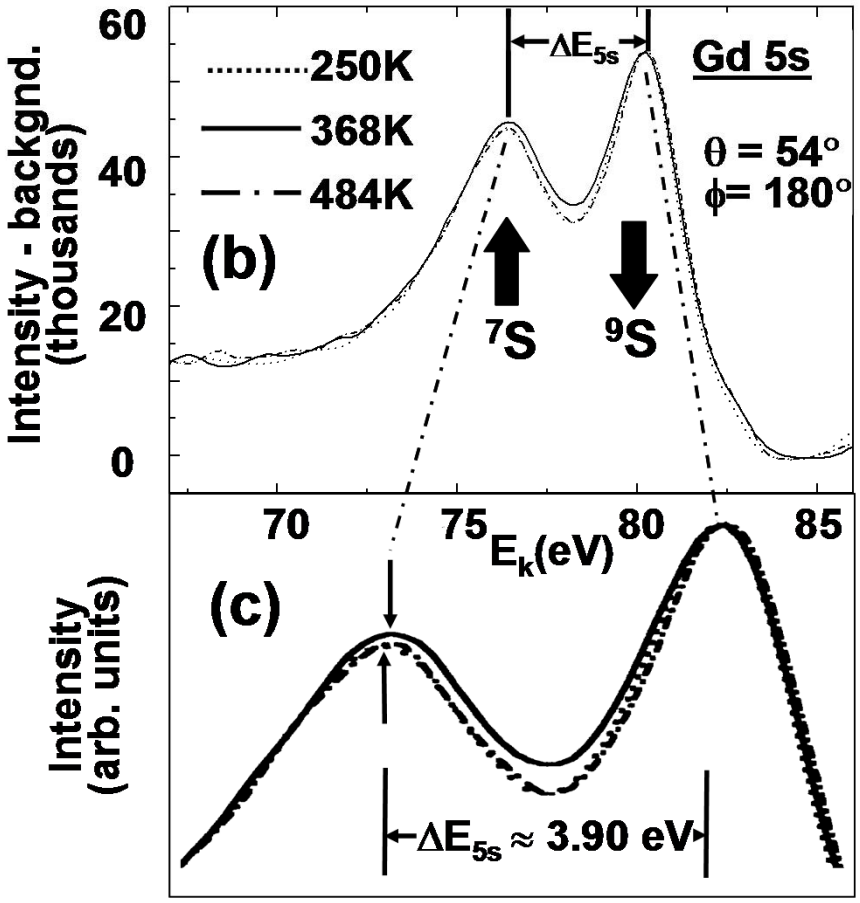

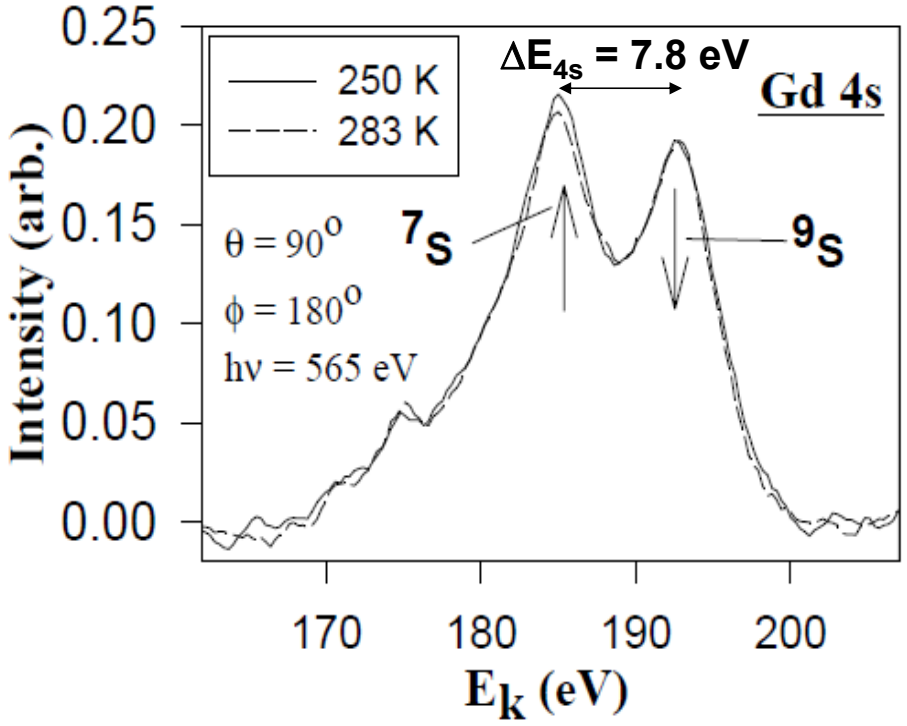

Tober et al., PRL 81, 2360 (1998) and J. Electron Spectrosc. 189, 152– 156 (2013)

Spin-dependent diffraction and screening during a magnetic transition at the Gd(0001) surface

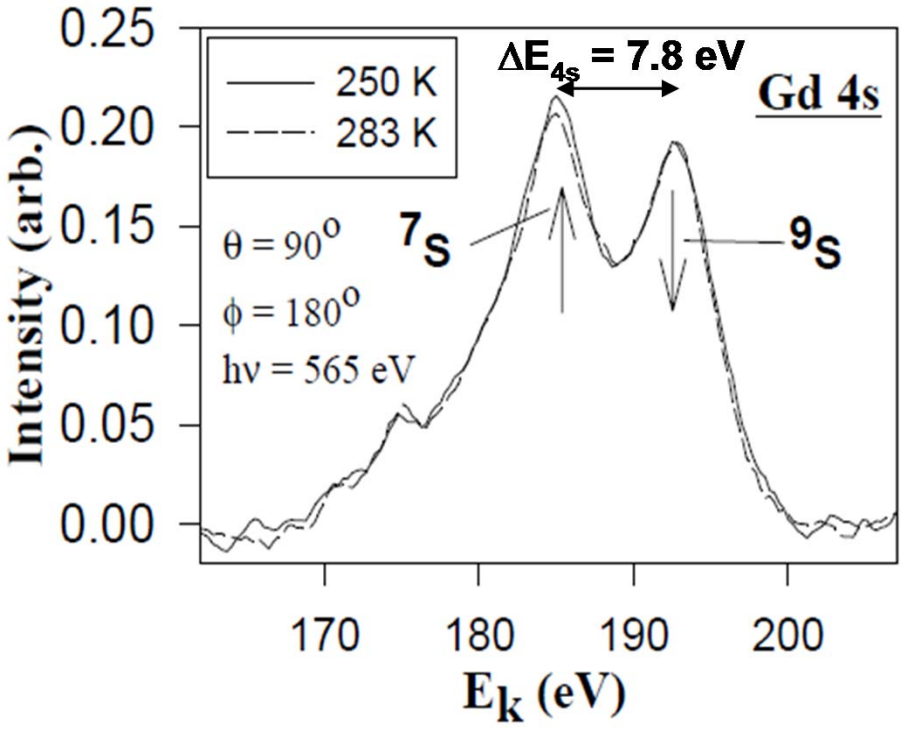

LDA+U calculations for binding energy diff. between FM and PM states: changes too small. Suggests spin-dependent final-state screening. Future: Higher resolution, spin and time-resolved measurements

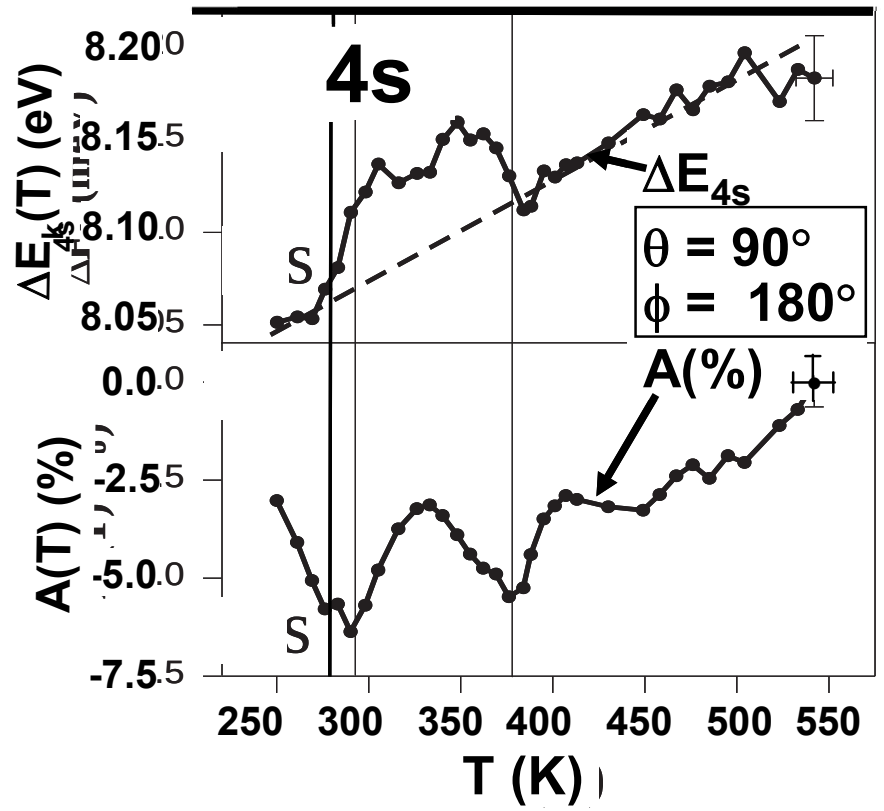

Spin-up/spin-down asymmetry =
$A(T) = [I(^7S)/I(^9S)]_T / [I(^7S)/I(^9S)]_{HT=PM}$

Tober et al., PRL 81, 2360 (1998) J. Electron Spectrosc. 189, 152– 156 (2013)

Basic Concepts:

A Little Electronic Structure
The X-Ray-Based Experiments
X-Ray Sources, Synchrotron Radiation, Free Electron Lasers

Core-Level Photoemission

Intensities and Quantitative Analysis, the 3-Step Model
Varying Surface and Bulk Sensitivity
Chemical Shifts
Multiplet Splittings
Electron Screening and Satellite Structure

Magnetic and Non-Magnetic Dichroism
Resonant Photoemission
Photoelectron Diffraction and Holography

Valence-Level Photoemission

Band-Mapping in the Ultraviolet Photoemission Limit
Densities of States in the X-Ray Photoemission Limit

Some New Directions

Photoemission with Hard X-Rays (throughout lectures)
Photoemission with Standing Wave Excitation
Photoemission with: Higher Pressures→multi-Torr→Atmosphere?
Spatial Resolution-Photoelectron Microscopy
Temporal Resolution

Typical experimental geometry for energy- and angle-resolved photoemission measurements

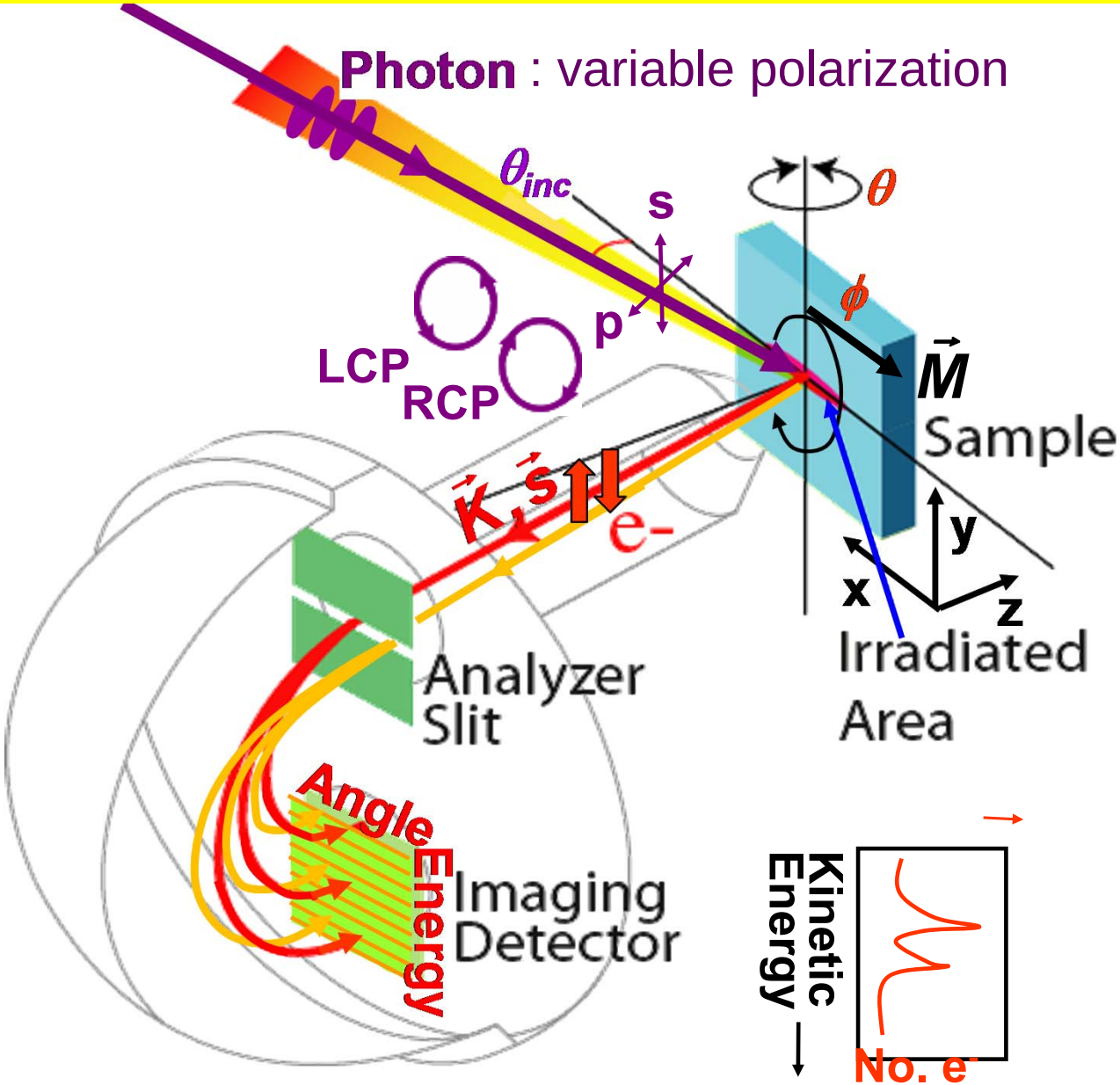

1st Expt. Magnetic Circular Dichroism 1-e- Theo.

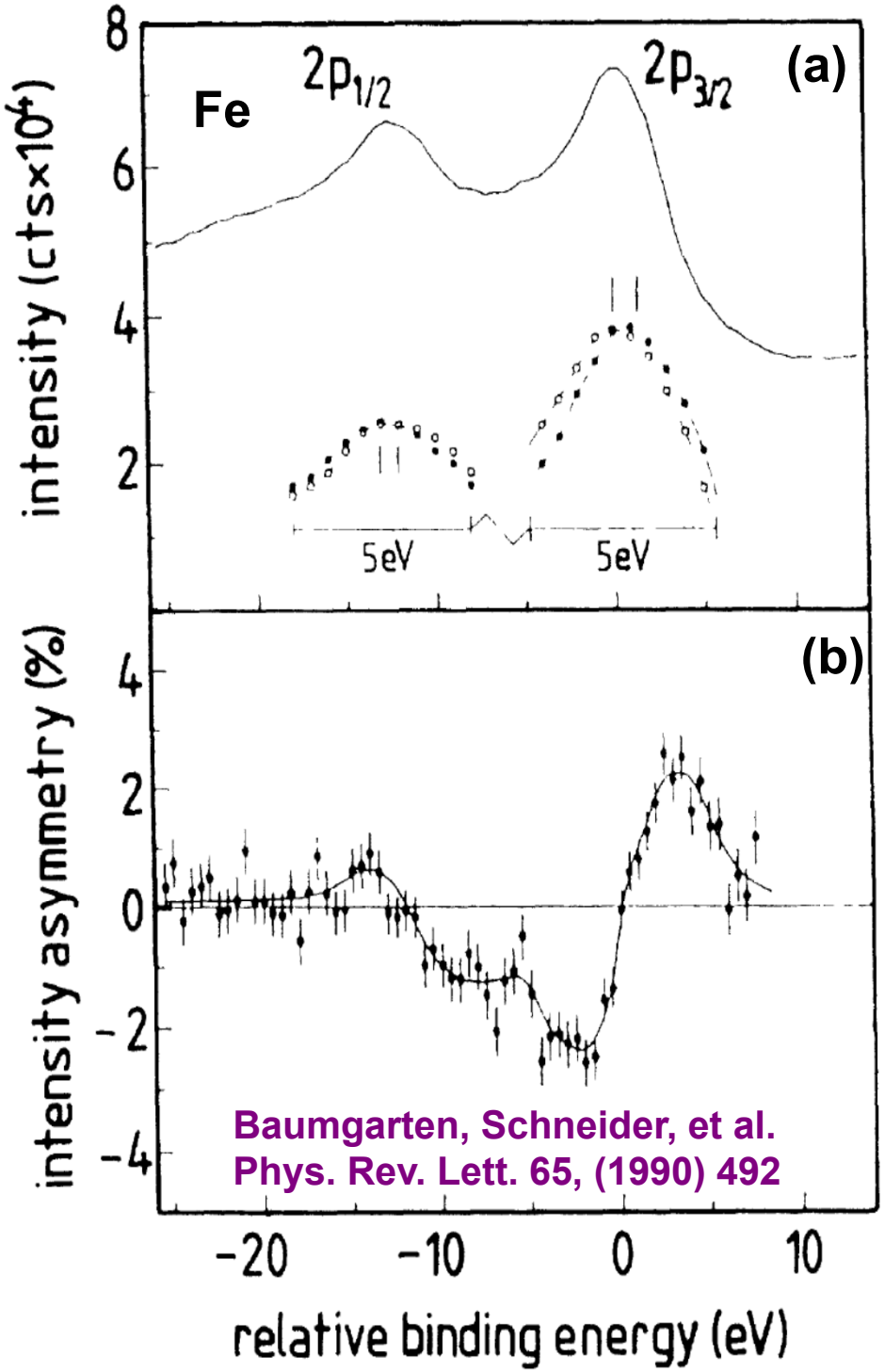

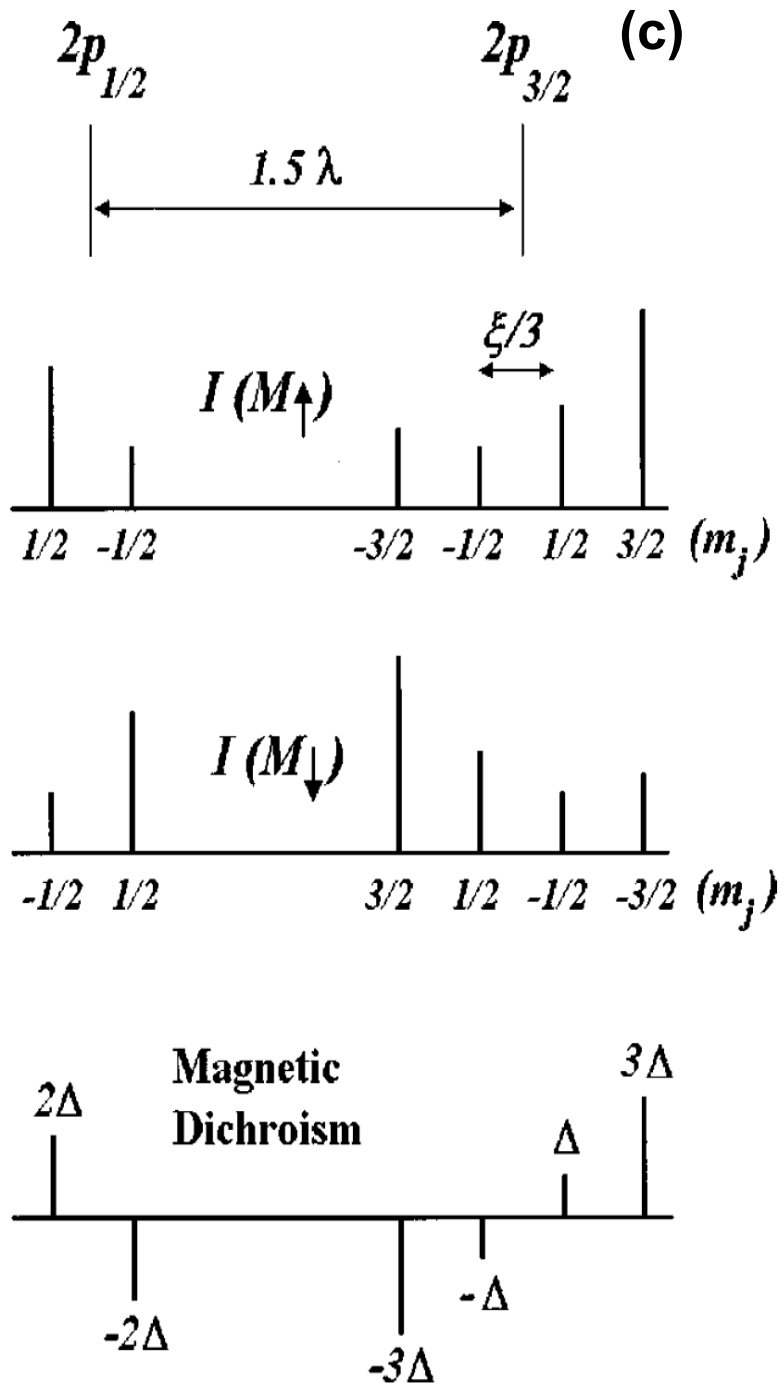

Menchero, Phys. Rev. B 57 (1998)993

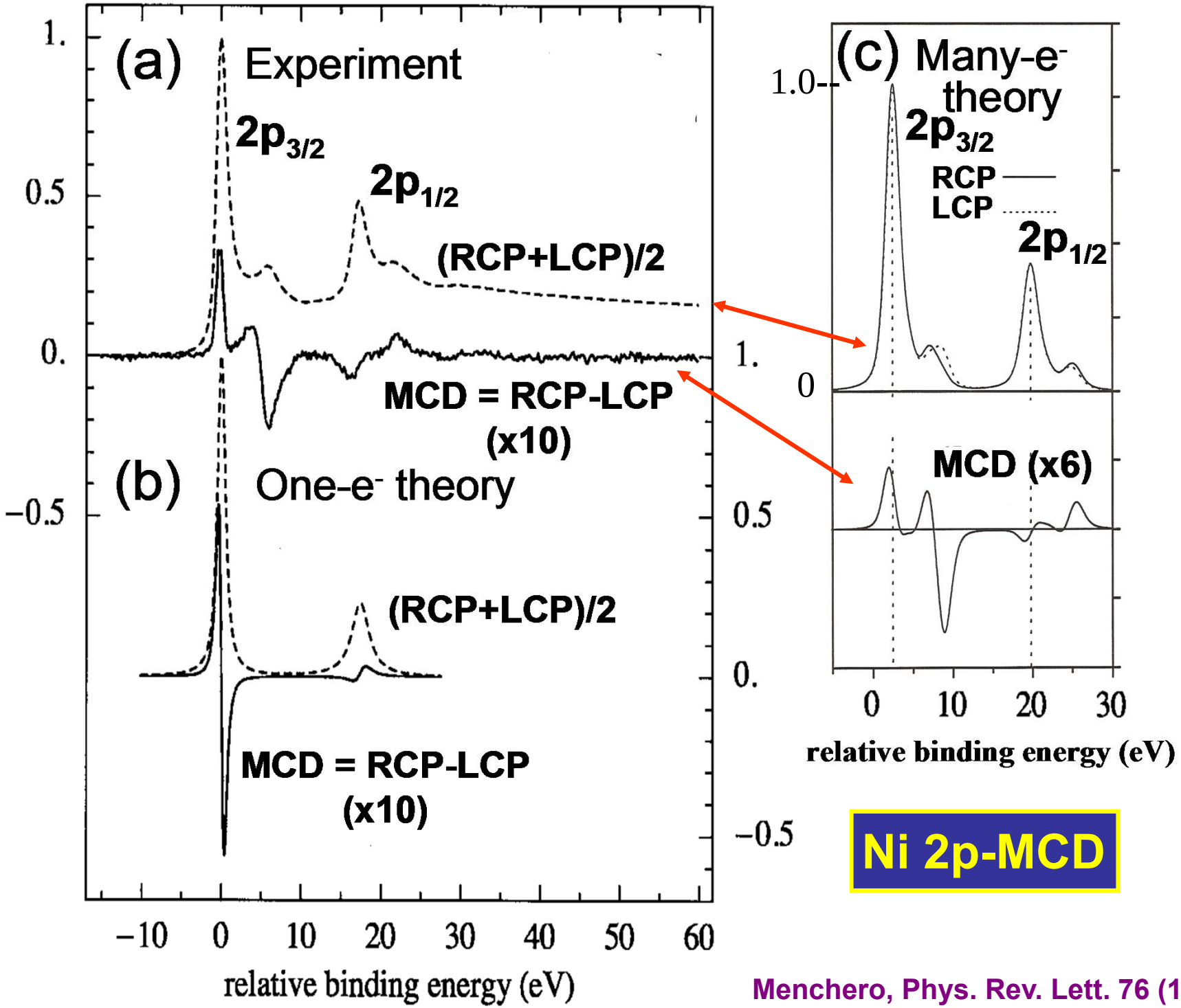

Ni 2p-MCD

Menchero, Phys. Rev. Lett. 76 (1996) 3208

Van der Laan et al., J. Phys. Condens. Matter 12 (2000) L275

Fe 2p Magnetic Circular Dichroism

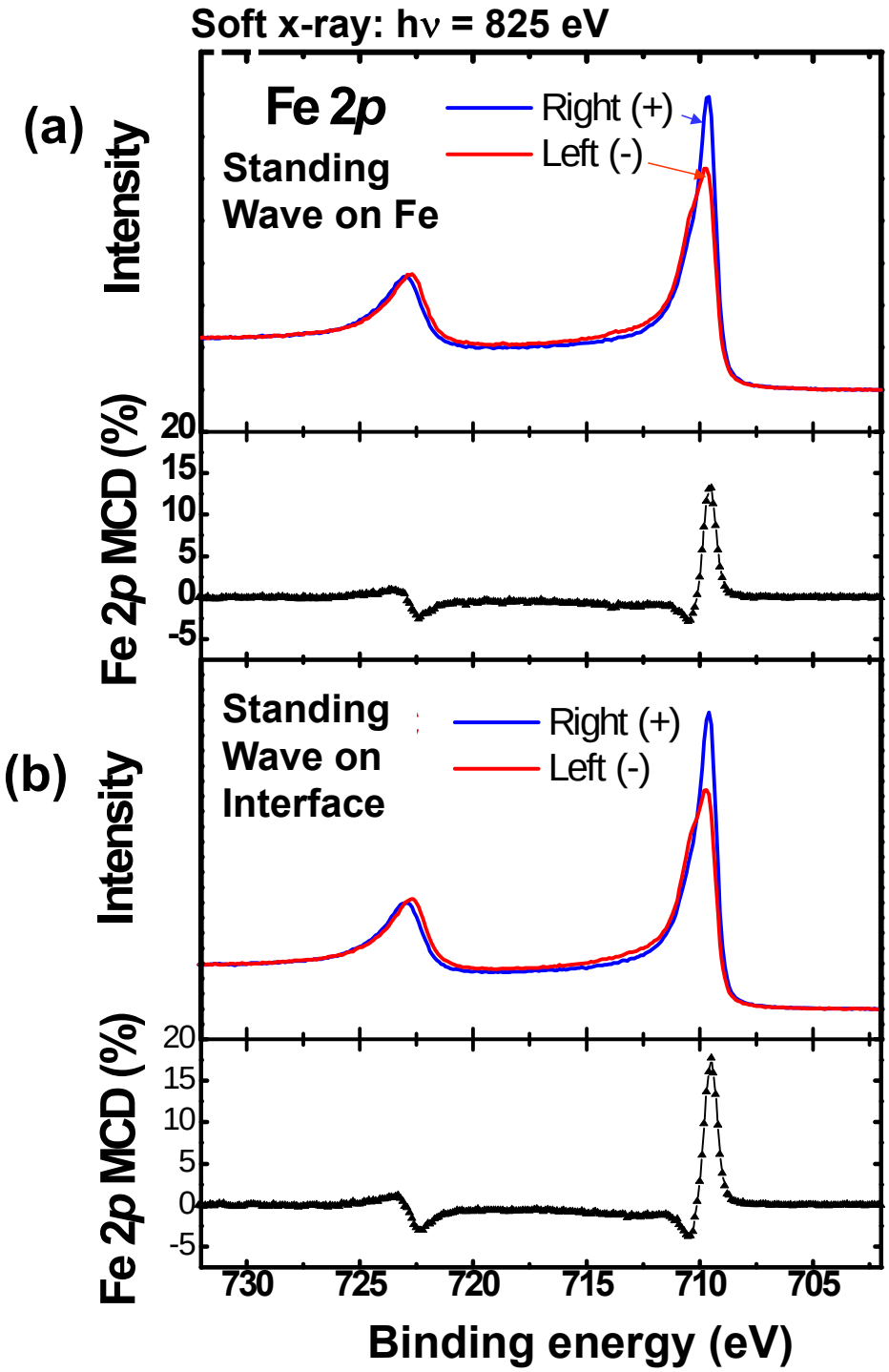

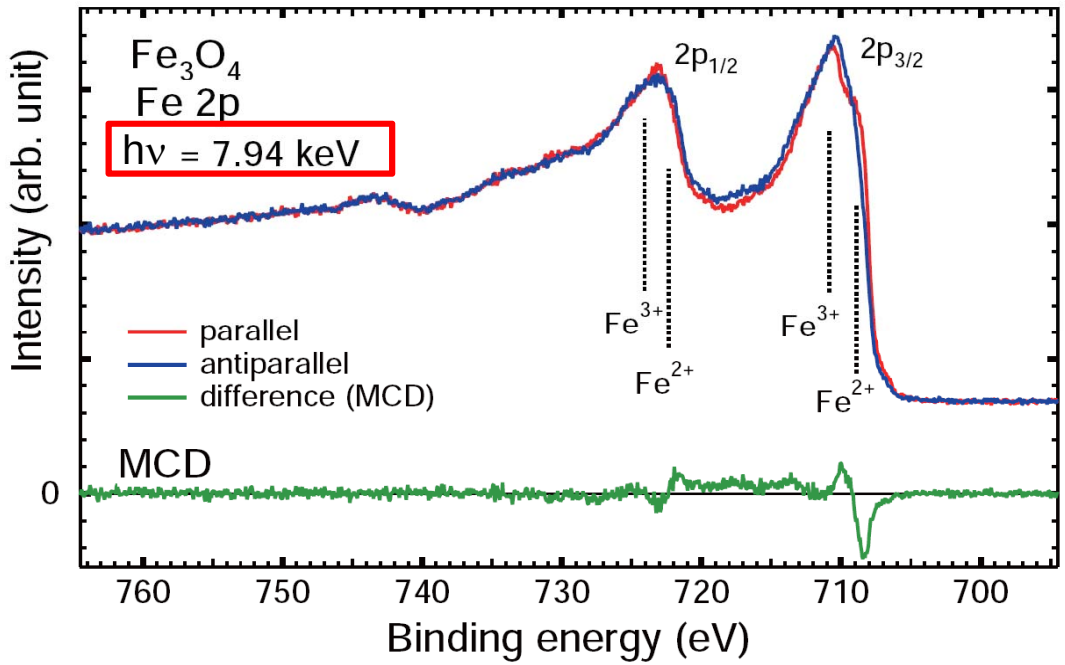

S. Ueda et al., Appl. Phys. Express 1 (2008) 077003

S.-H. Yang, B.S. Mun et al., Condens. Matter 14 (2002) L406.

Magnetic circular dichroism in core-level HXPS

Magnetic circular dichroism from the Heusler compound Co_2FeAl in a deeply buried layer underneath a 10 nm thick MnIr exchange bias layer:

➢multilayer [MgO(001) / Co_2FeAl (30 nm) / MnIr (10nm) / AlO_x -cap (1 nm)]

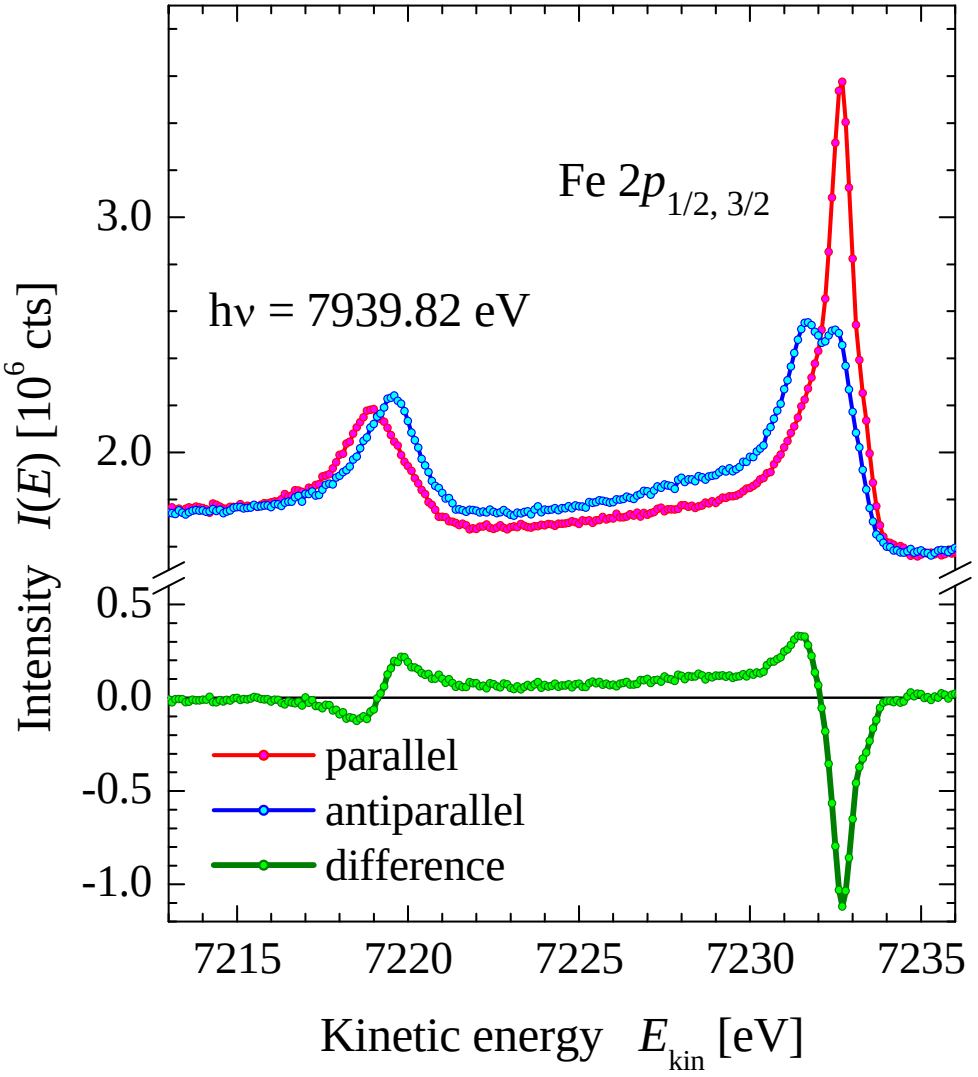

- **Huge dichroism in Fe 2p core level emission is still detected in the deeply buried layer, even at relaxed energy resolution— Asymmetry max.: - 40%**

- **Element-specific magnetism in buried layers and interfaces**

G. Fecher et al., Mainz
Measured at SPring8

Basic Concepts:

A Little Electronic Structure
The X-Ray-Based Experiments
X-Ray Sources, Synchrotron Radiation, Free Electron Lasers

Core-Level Photoemission

Intensities and Quantitative Analysis, the 3-Step Model
Varying Surface and Bulk Sensitivity
Chemical Shifts
Multiplet Splittings
Electron Screening and Satellite Structure
Magnetic and Non-Magnetic Dichroism
Resonant Photoemission
Photoelectron Diffraction and Holography

Valence-Level Photoemission

Band-Mapping in the Ultraviolet Photoemission Limit
Densities of States in the X-Ray Photoemission Limit

Some New Directions

Photoemission with Hard X-Rays (throughout lectures)
Photoemission with Standing Wave Excitation
Photoemission with: Higher Pressures→multi-Torr→Atmosphere?
Spatial Resolution-Photoelectron Microscopy
Temporal Resolution

XPD and circular dichroism in non-magnetic systems

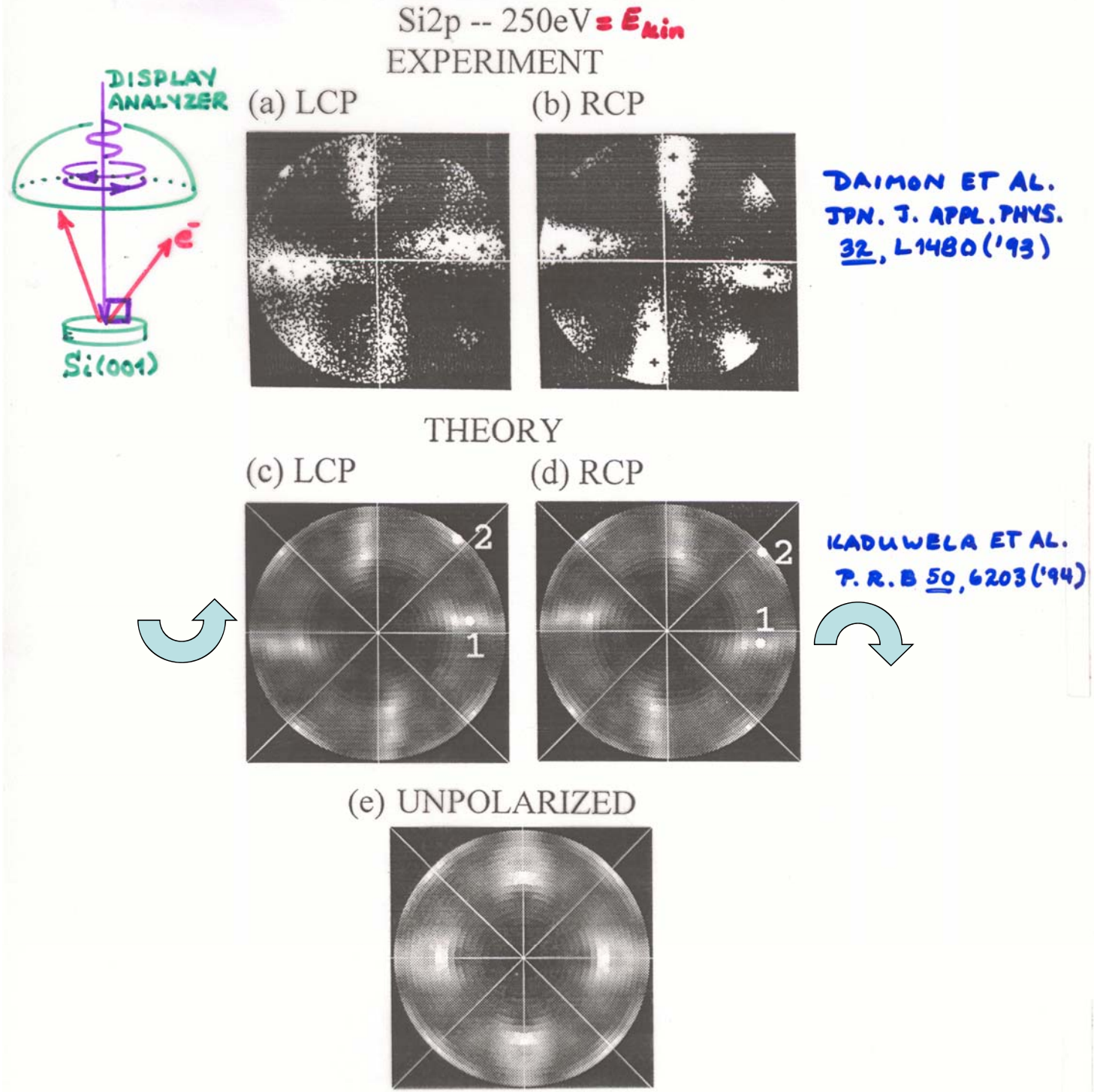

Circular dichroism in photoelectron angular distributions (CDAD)

→ **Non-magnetic dichroism effects due to photoelectron diffraction**

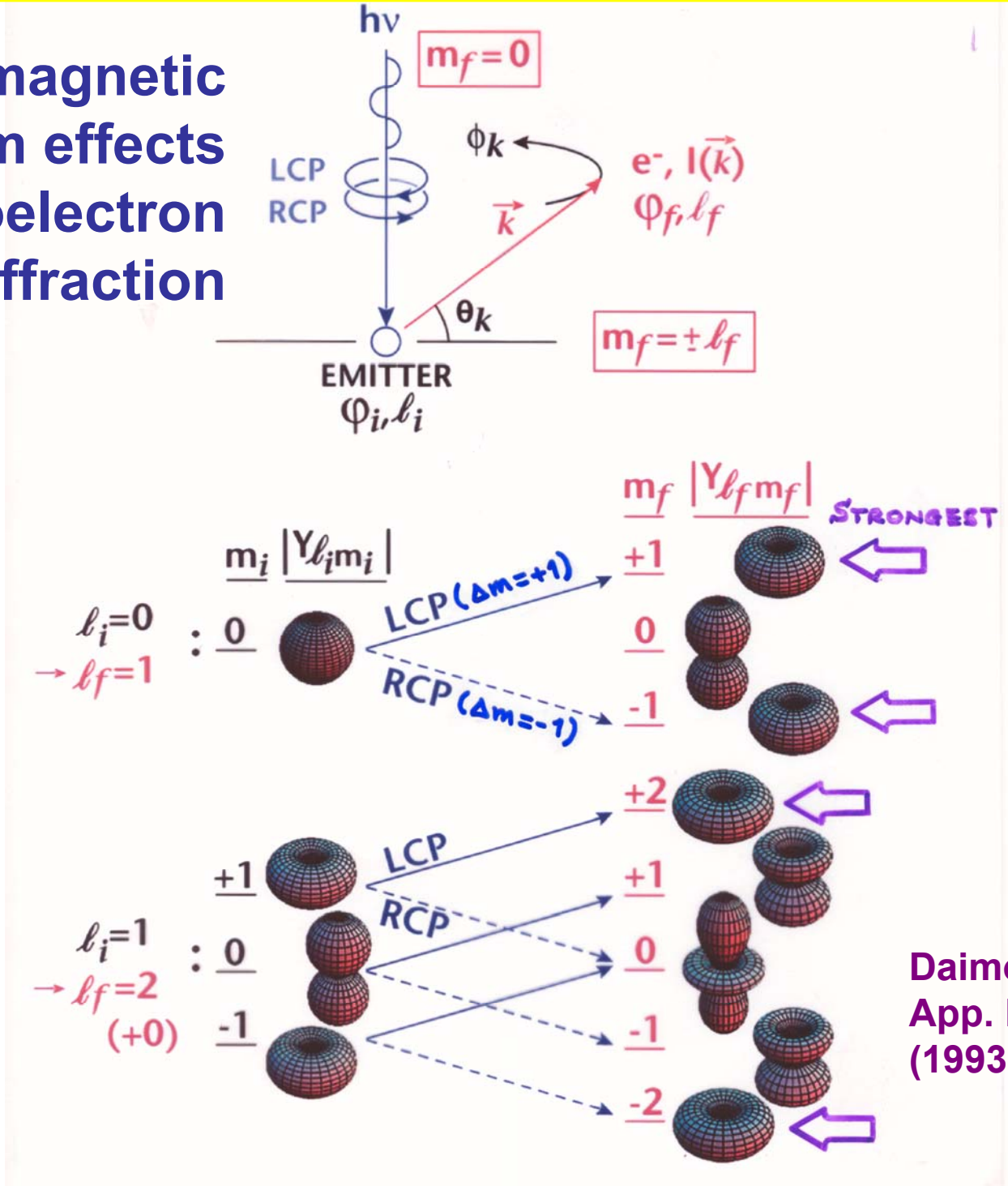

Daimon et al., Jpn. J. of App. Phys. 32, L1480 (1993)

Circular dichroism in photoelectron angular distributions (CDAD)

CONSTANT-PHASE SURFACE OF:

$$\psi_{\text{PHOTOE}^-}(r,\theta,\phi) \propto \frac{e^{ikr}}{r} \Theta_{lm} e^{i m_f \phi}$$

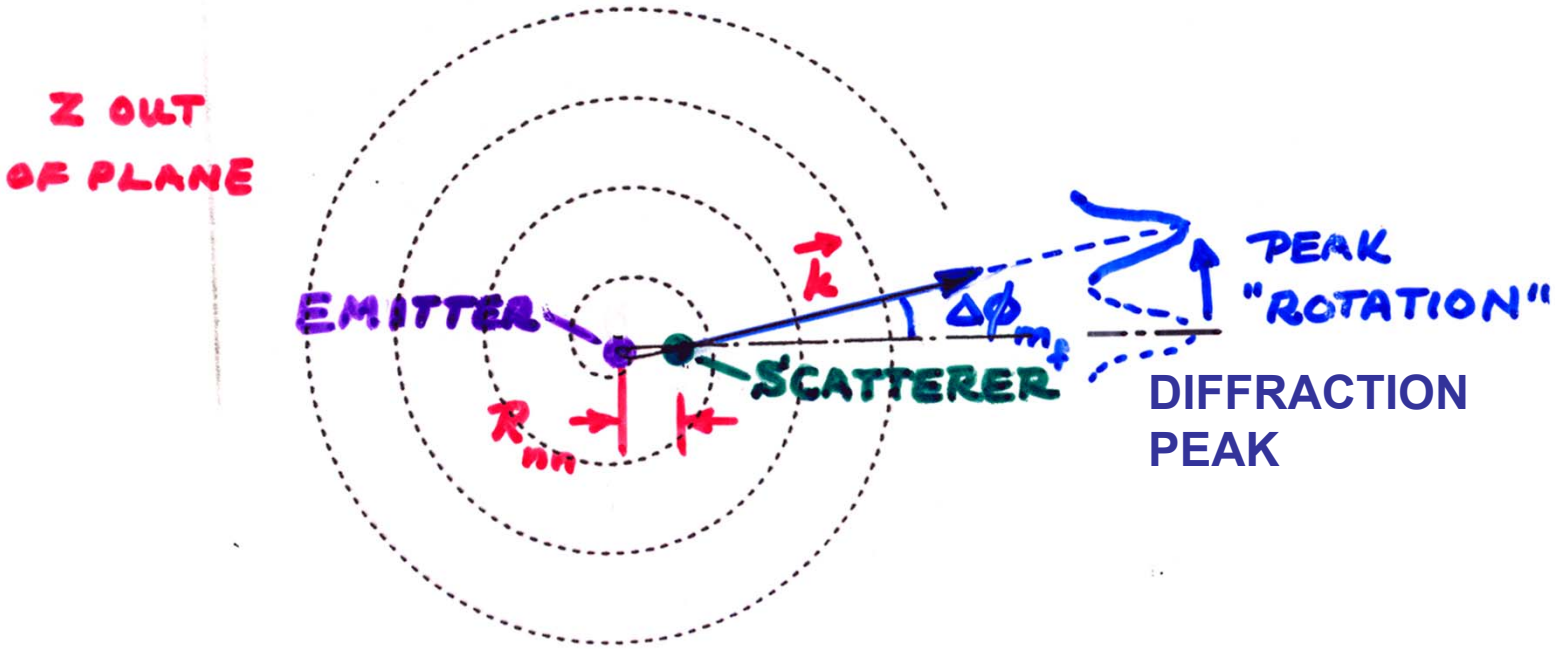

$$\left\| \Delta\phi_{m_f} = \frac{m_f}{R_{nn,\parallel} k_\parallel} \right\|$$

$$\overline{m_f} \approx m_{f,\max}$$

DAIMON ET AL.
JPN. J. APPL. PHYS.
32, L1480 ('93)

Theory: Effect of varying the polarization?: C 1s emission from CO

E_{kin} = 200 eV

Linear p polarization:

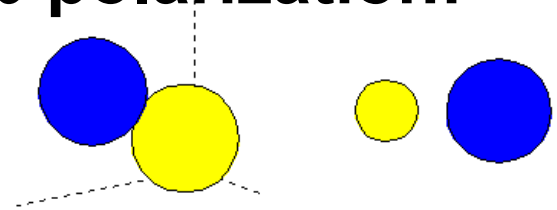

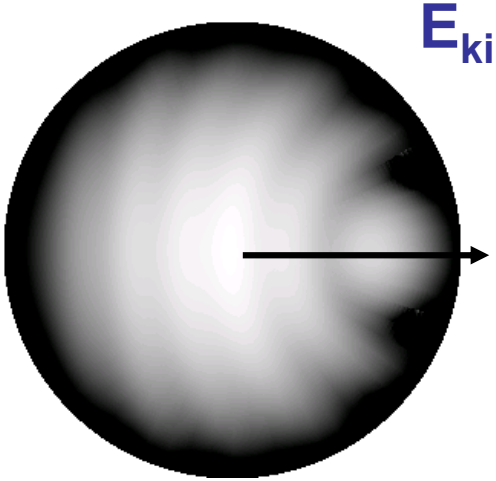

Right circular polarization:

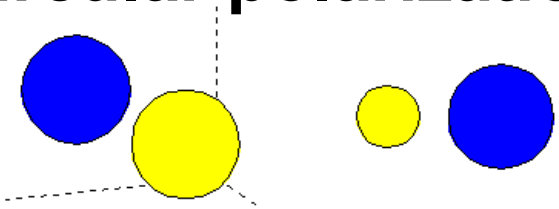

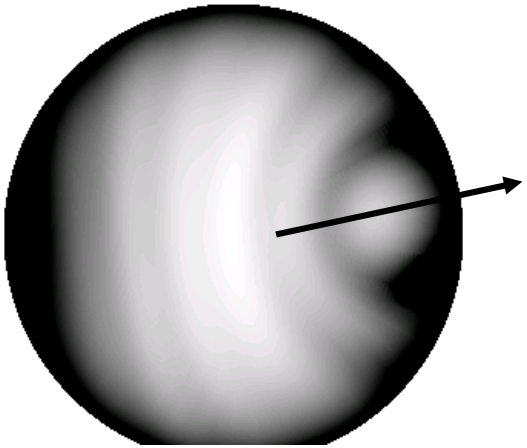

Circular dichroism in angular distributions (CDAD)

Left circular polarization:

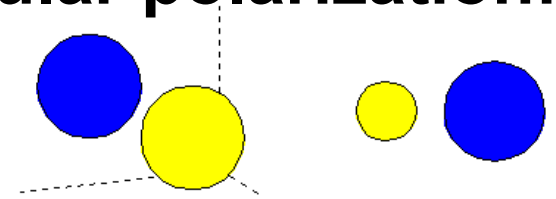

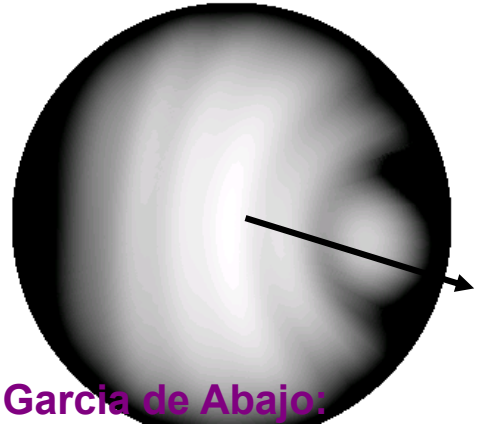

EDAC photoelectron diffraction program: Javier Garcia de Abajo:
http://garciadeabajos-group.icfo.es/widgets/edac/index.html

Fano effect and spin polarization (SP) in core photoelectron spectra—expt.

SPIN-ORBIT SPLIT LEVEL (b) EXCITED WITH CIRCULAR POLARIZATION (FANO EFFECT)

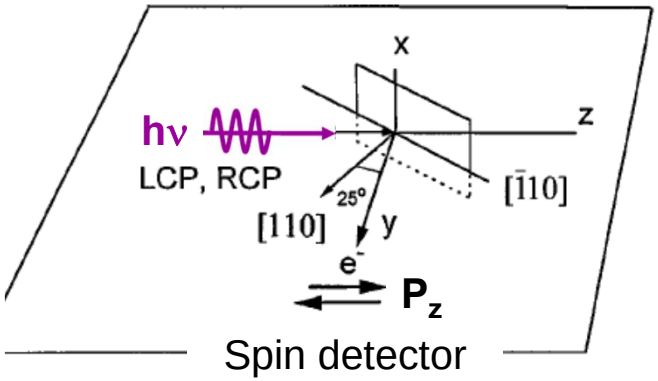

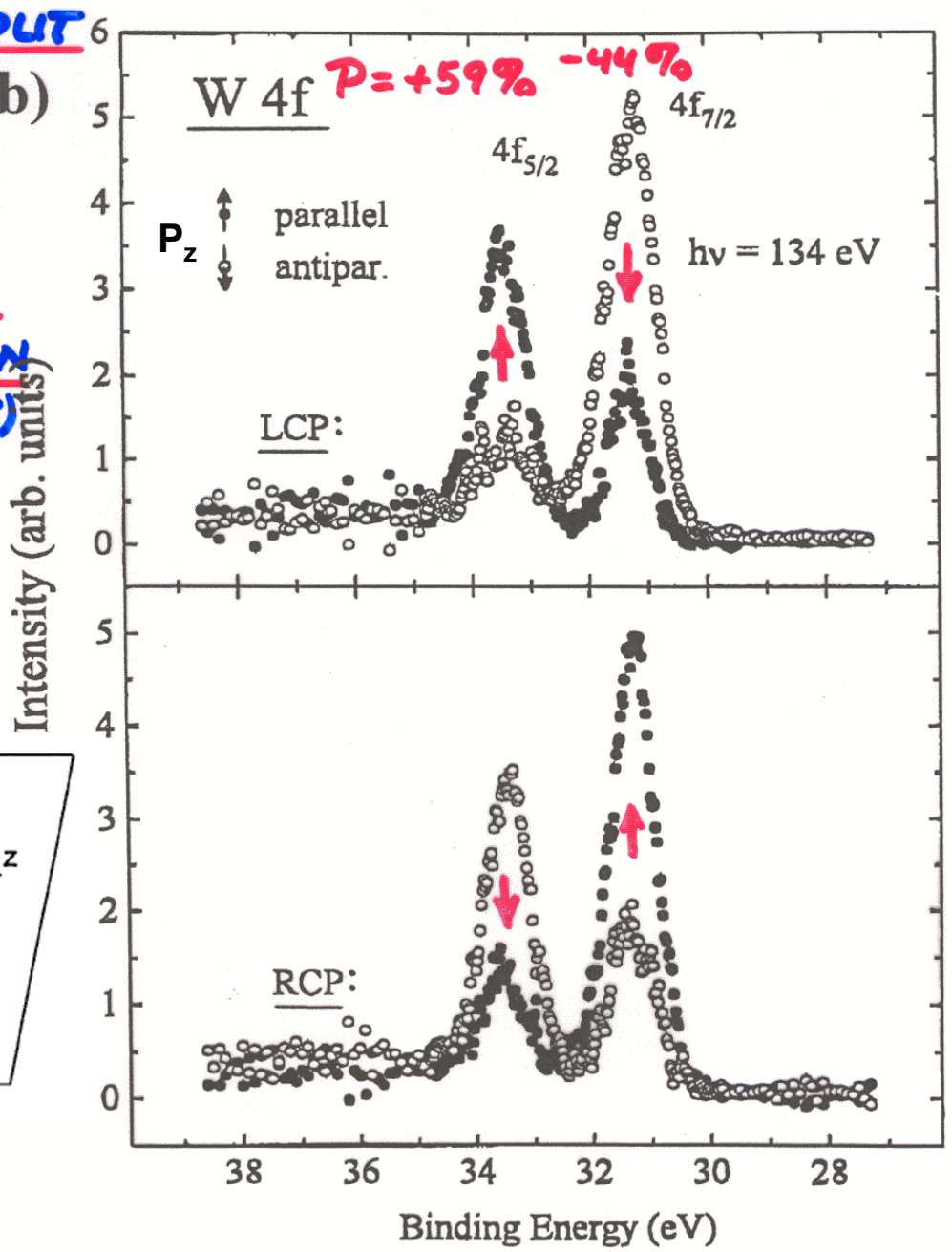

EXPT. – STARKE ET AL. PRB 53, R10544 (1996)

Putting non-magnetic CD (CDAD) together with spin polarization: Theory with proper final-state channel interference: Single Atom

Free Fe $2p_{1/2}$

THEORY (s+d)

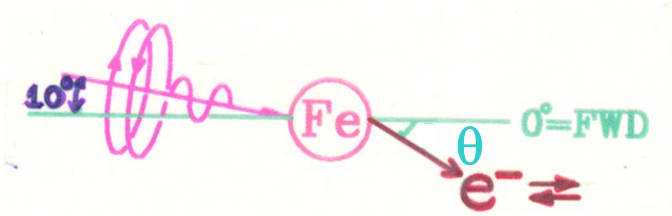

E_{kin} = 145 eV

LCP

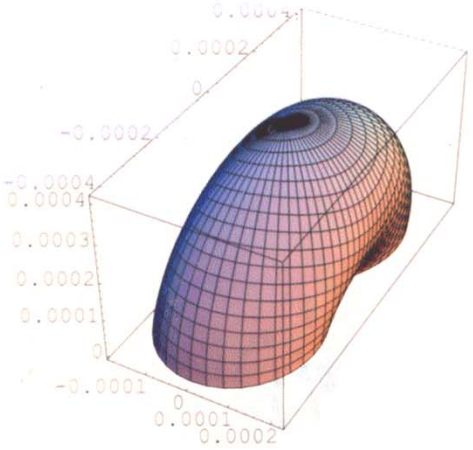

RCP

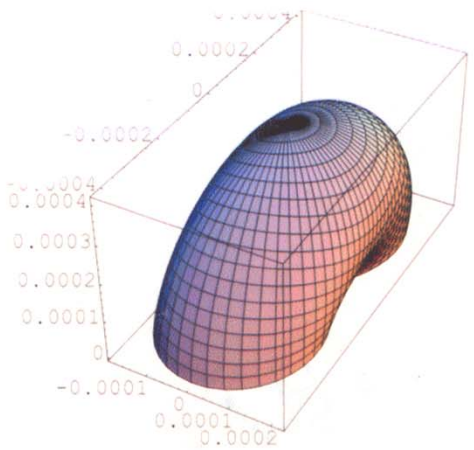

%CDAD

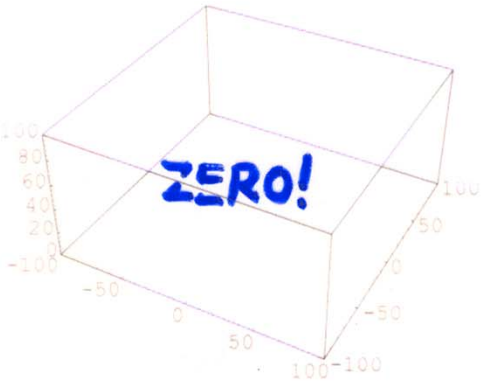

Spin Pol. (LCP)

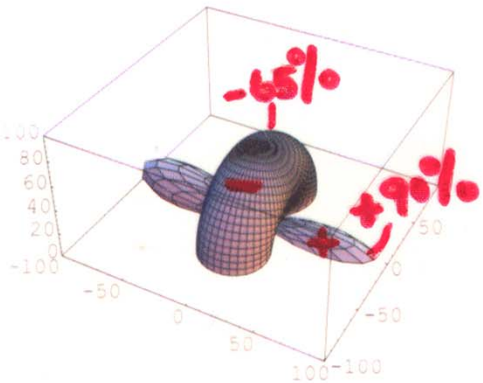

$$\%CDAD = \frac{RCP - LCP}{RCP + LCP} \times 100 \qquad \%P = \frac{LCP(\uparrow) - LCP(\downarrow)}{LCP(\uparrow) + LCP(\downarrow)} \times 100$$

= CIRCULAR DICHROISM IN ANGULAR DISTRIBUTION

A. Kaduwela, C.F., unpublished

Putting non-magnetic CD (CDAD) together with spin polarization: Theory with proper final-state channel interference: Single Atom

Fe $2p_{1/2}$
Ferromagnetic Cluster

THEORY
(s + d)
- ADDS PHOTOELECTRON DIFFRACTION

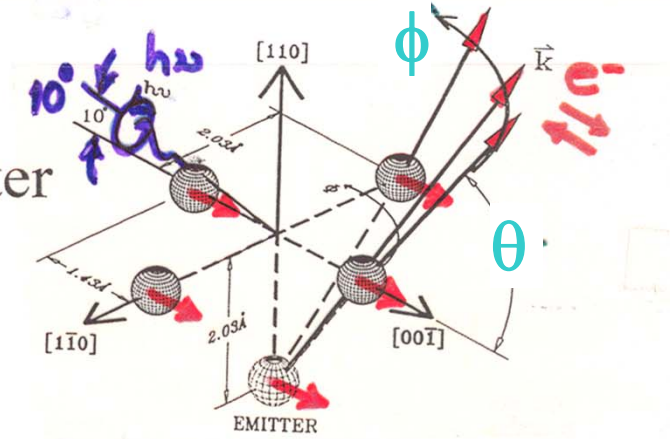

LCP RCP

PEAK "ROTATIONS" (ALA DAIMON ET AL.)

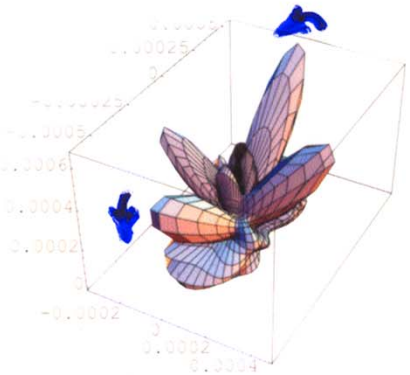

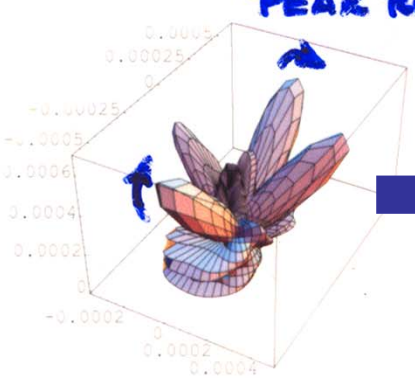

"Circular Dichroism In Angular Distributions" (CDAD

%CDAD Spin Pol. (LCP)

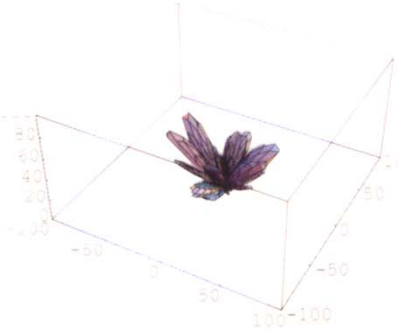

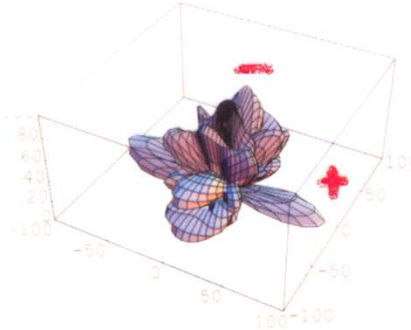

$$\%CDAD = \frac{RCP - LCP}{RCP + LCP} \times 100 \qquad \%P = \frac{LCP(\uparrow) - LCP(\downarrow)}{LCP(\uparrow) + LCP(\downarrow)} \times 100$$

A. Kaduwela, C.F., unpublished

Basic Concepts:

A Little Electronic Structure
The X-Ray-Based Experiments
X-Ray Sources, Synchrotron Radiation, Free Electron Lasers

Core-Level Photoemission

Intensities and Quantitative Analysis, the 3-Step Model
Varying Surface and Bulk Sensitivity
Chemical Shifts
Multiplet Splittings
Electron Screening and Satellite Structure
Magnetic and Non-Magnetic Dichroism
Resonant Photoemission-covered already
Photoelectron Diffraction and Holography

Valence-Level Photoemission

Band-Mapping in the Ultraviolet Photoemission Limit
Densities of States in the X-Ray Photoemission Limit

Some New Directions

Photoemission with Hard X-Rays (throughout lectures)
Photoemission with Standing Wave Excitation
Photoemission with: Higher Pressures→multi-Torr→Atmosphere?
Spatial Resolution-Photoelectron Microscopy
Temporal Resolution

PHOTOELECTRIC CROSS SECTIONS FOR Mn

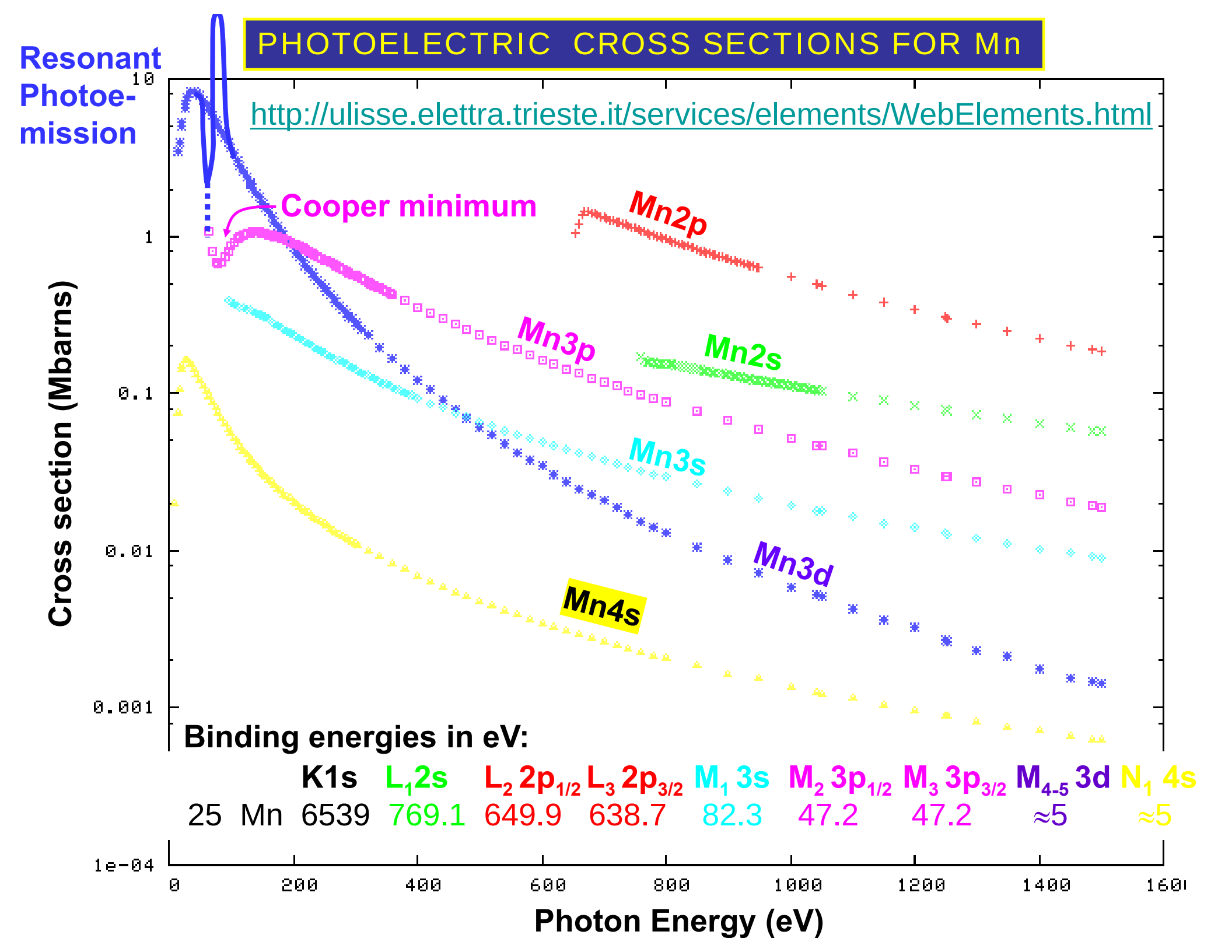

Binding energies in eV:

		K1s	L_1 2s	L_2 $2p_{1/2}$	L_3 $2p_{3/2}$	M_1 3s	M_2 $3p_{1/2}$	M_3 $3p_{3/2}$	M_{4-5} 3d	N_1 4s
25	Mn	6539	769.1	649.9	638.7	82.3	47.2	47.2	≈5	≈5

Resonant Photoemission—Atomic Mn, Mn 3d with Mn 3p

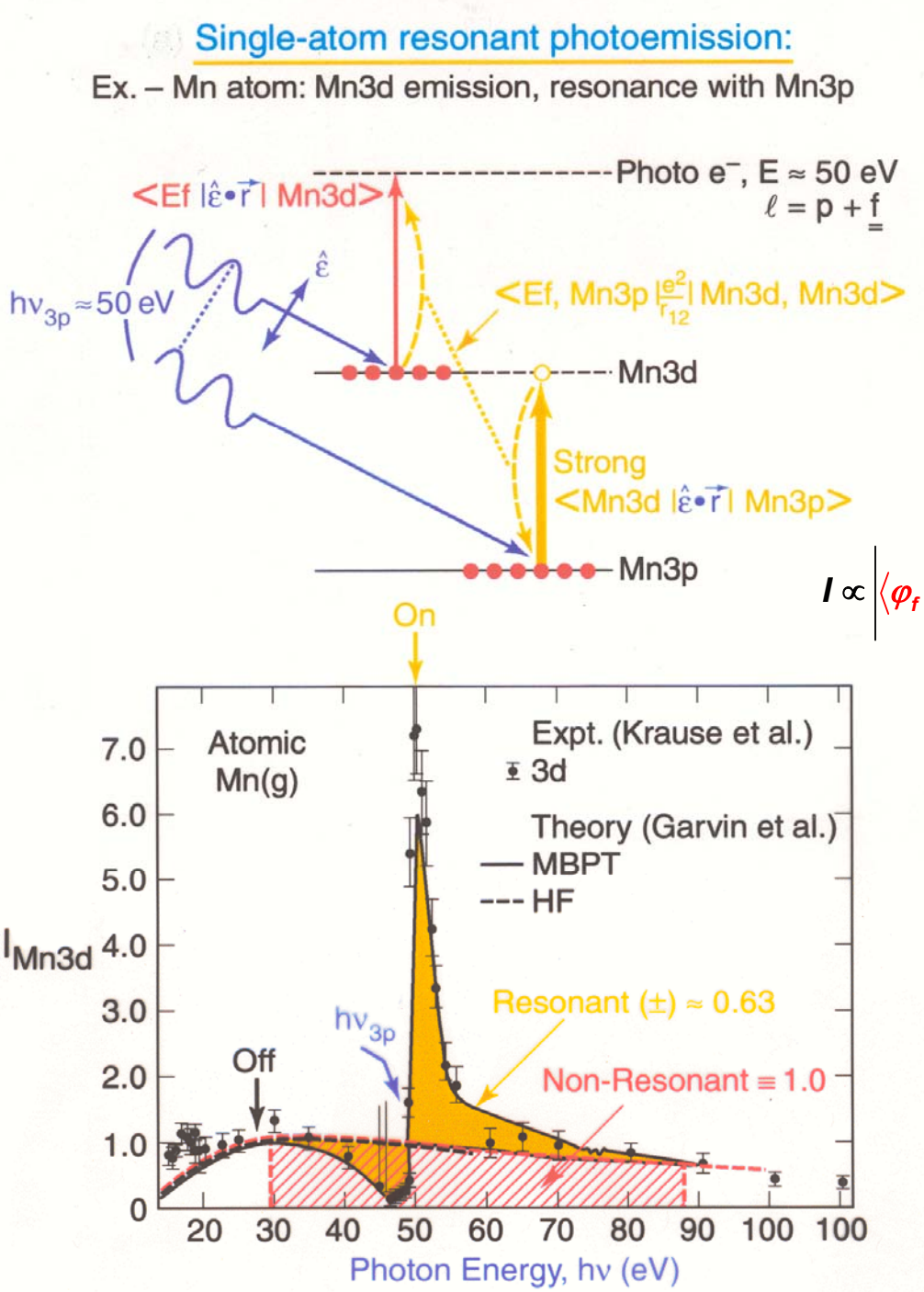

Normal photoemission:

$$I \propto \left| \langle \varphi_f(1) | \hat{e} \bullet \vec{r} | \varphi_i(1) \rangle \right|^2$$

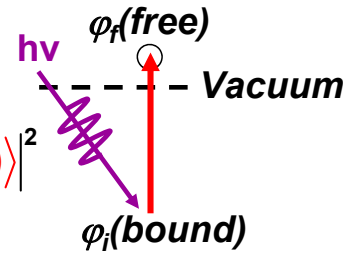

Resonant photoemission:

$$I \propto \left| \langle \varphi_f(1) | \hat{e} \bullet \vec{r} | \phi_i(1) \rangle + \sum_m \langle \varphi_f(1)\varphi_1(2) | \frac{e^2}{r_{12}} | \varphi_i(1)\varphi_m(2) \rangle \langle \varphi_m(1) | \hat{e} \bullet \vec{r} | \varphi_1(1) \rangle \right|^2 \times \delta(h\nu - (E_m - E_1))$$

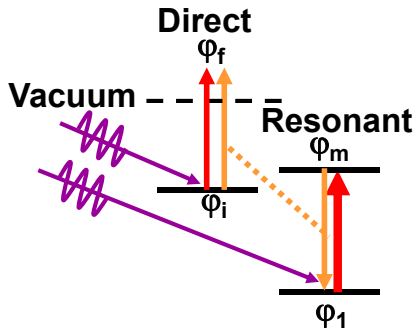

$SrTiO_3$ and $La_{0.67}Sr_{0.33}MnO_3$ band structures and DOS

$SrTiO_3$-insulator

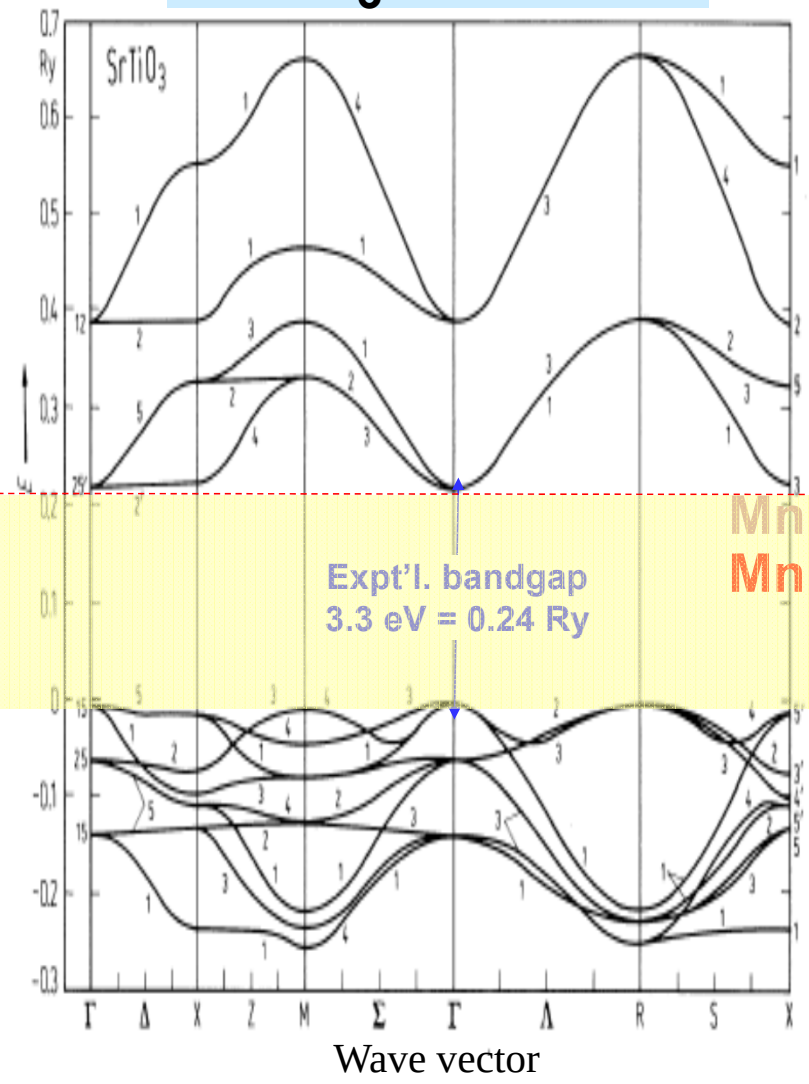

Mattheiss, PRB 6, 4718 (1972)

$La_{0.67}Sr_{0.33}MnO_3$-Half-Metallic Ferromagnetic metal

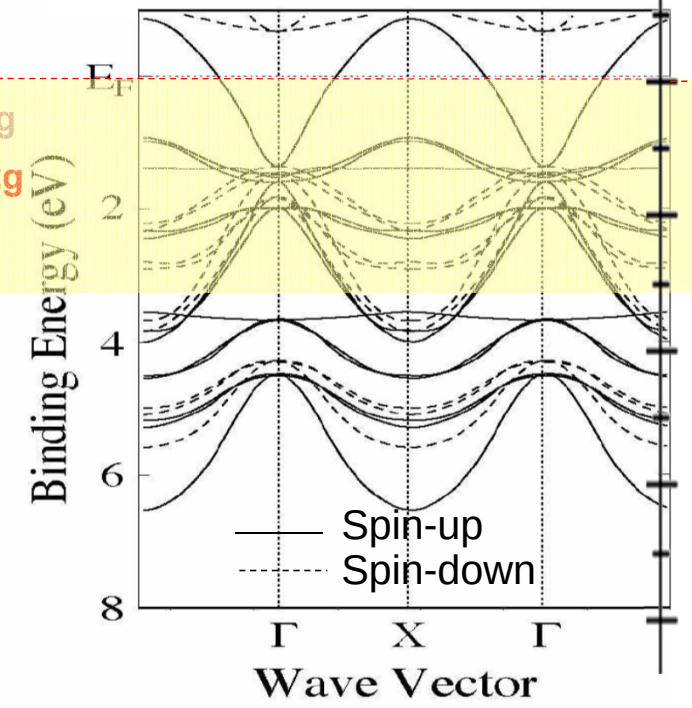

Chikamatsu et al., PRB 73, 195105 (2006)

Zheng, Binggeli, J. Phys. Cond. Matt. 21, 115602 (2009)

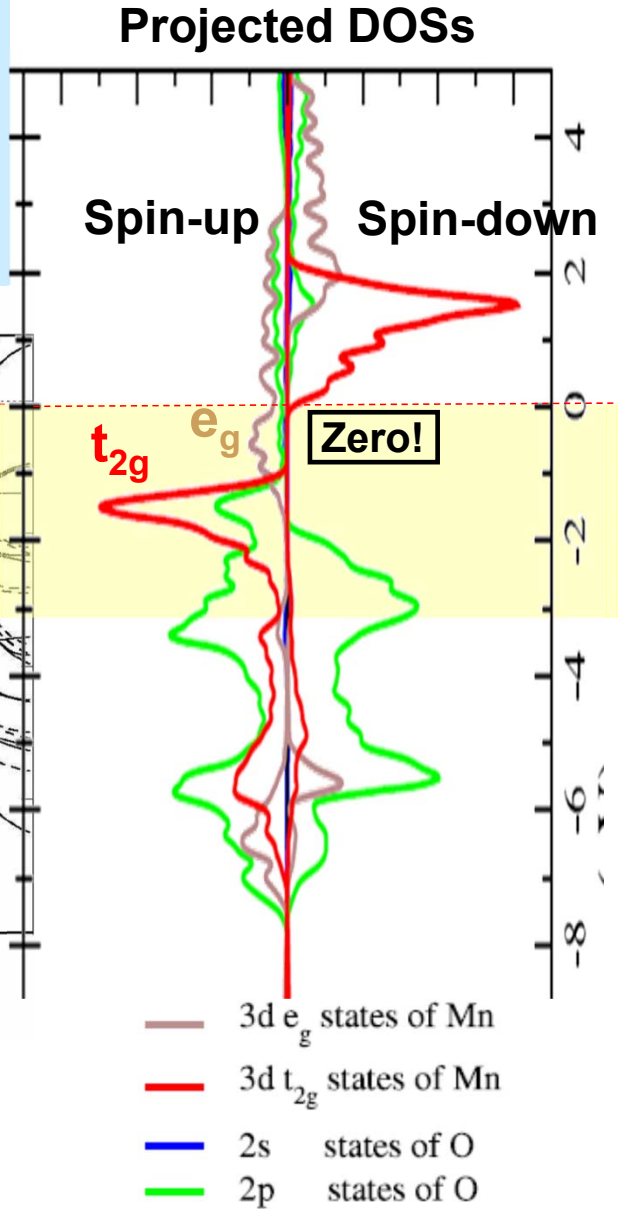

Resonant Photoemission—$La_{0.6}Sr_{0.4}MnO_3$, Mn 3d with Mn 2p

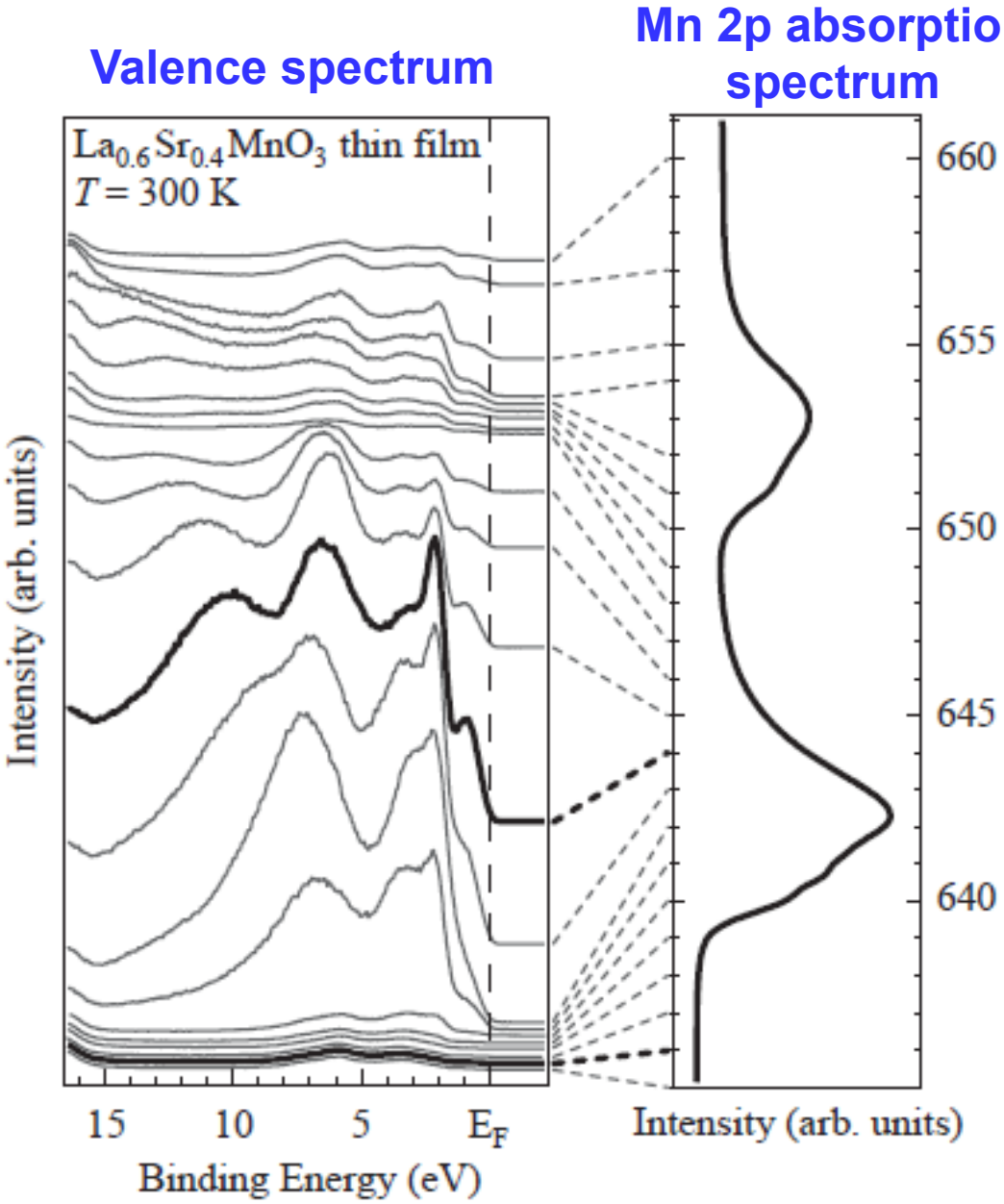

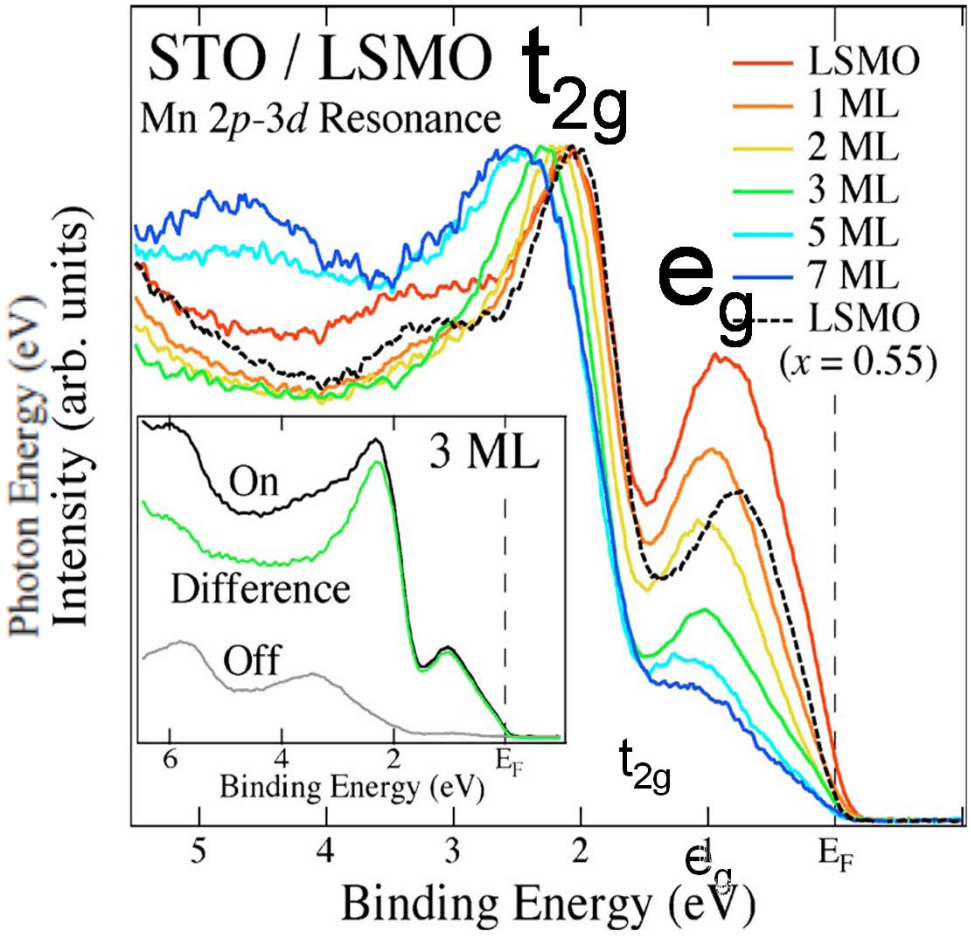

Prior resonant PS: Fujimori et al., J.A.P 99, 08S903 (2006)

K. Horiba et al. / Journal of Magnetism and Magnetic Materials 272–276 (2004) 436–437

Basic Concepts:

A Little Electronic Structure
The X-Ray-Based Experiments
X-Ray Sources, Synchrotron Radiation, Free Electron Lasers

Core-Level Photoemission

Intensities and Quantitative Analysis, the 3-Step Model
Varying Surface and Bulk Sensitivity
Chemical Shifts
Multiplet Splittings
Electron Screening and Satellite Structure
Magnetic and Non-Magnetic Dichroism
Resonant Photoemission
Photoelectron Diffraction and Holography

Valence-Level Photoemission


Band-Mapping in the Ultraviolet Photoemission Limit
Densities of States in the X-Ray Photoemission Limit-Covered already

Some New Directions

Photoemission with Hard X-Rays (throughout lectures)
Photoemission with Standing Wave Excitation
Photoemission with: Higher Pressures→multi-Torr→Atmosphere?
Spatial Resolution-Photoelectron Microscopy
Temporal Resolution

Valence-band photoemission: Angle-Resolved Photoemission (ARPES)

$$E_f(\vec{K}_f) =$$
$$E_f(\vec{k}_f) - V_0 = h\nu - E_i(\vec{k}_i)$$
$$\approx \hbar^2 K_f^2 / 2m_e$$

$$\vec{k}_{f,\parallel} = \vec{K}_{f,\parallel}$$

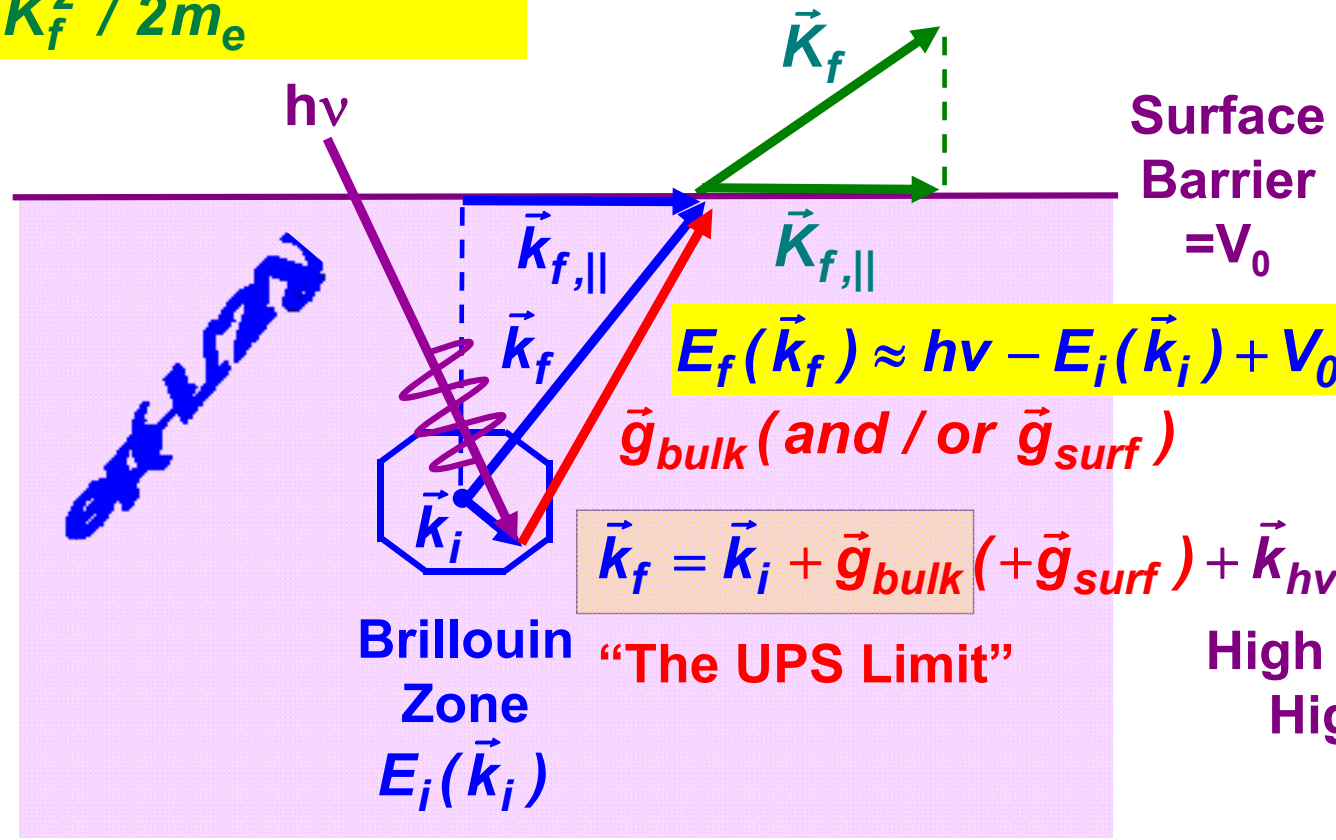

$$E_f(\vec{k}_f) \approx h\nu - E_i(\vec{k}_i) + V_0 \approx \hbar^2 k_f^2 / 2m_e$$

$\vec{g}_{bulk}$ (and / or $\vec{g}_{surf}$)

$$\vec{k}_f = \vec{k}_i + \vec{g}_{bulk} (+\vec{g}_{surf}) + \vec{k}_{h\nu} + \vec{k}_{phonon}$$

"The UPS Limit"

High energy a/o High temp.

$$I(E_f, \vec{k}_f) \propto \left| \hat{\varepsilon} \bullet \left\langle \varphi_{photoe}(E_f = h\nu + E_i, \vec{k}_f = \vec{k}_i + \vec{g}) \middle| \vec{r} \middle| \varphi(E_i, \vec{k}_i) \right\rangle \right|^2$$

"Direct" or k-conserving transitions

ARPES—How high can we go in energy and temperature?

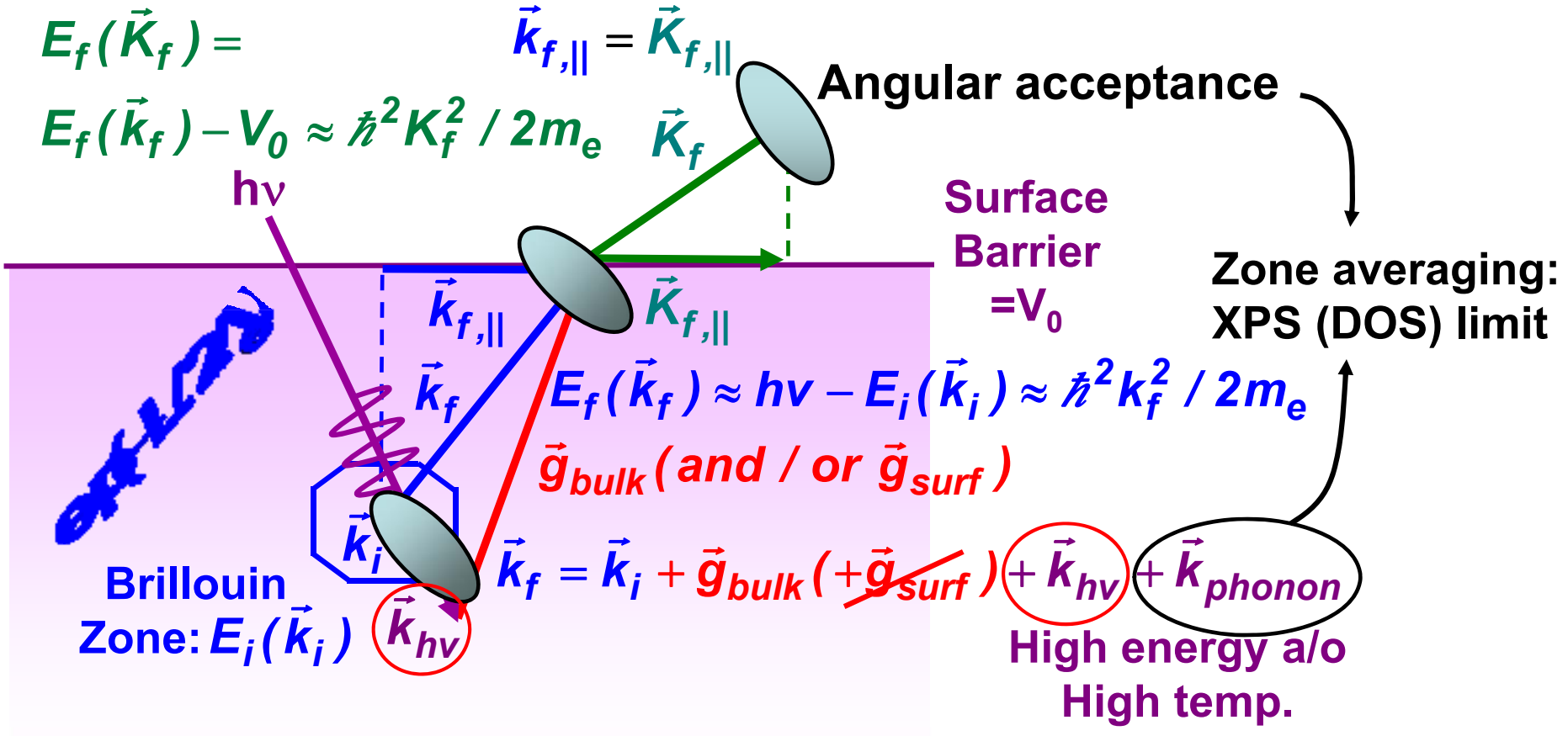

Fraction DTs ≈ Debye-Waller factor = $W(T) \approx \exp[-(k^f)^2 \langle u^2(T) \rangle]$

$\approx \exp[-C_1 (k^f)^2 T/(m\Theta_D^2)] \approx \exp(-C_2 E_{kin} T)$

$W \approx 1$

$W \approx 0$

ARPES→bands, quasiparticles (Low hν, Low T, High angul. Res.)

Shevchik, Phys. Rev. B 16, 3428 (1977)
Hussain….CF, Phys. Rev. B 34 (1986) 5226

XPS→DOS+XPD (High hν, High T, Low angul. Res.)

Angle-Resolved Photoemission at High Energy--

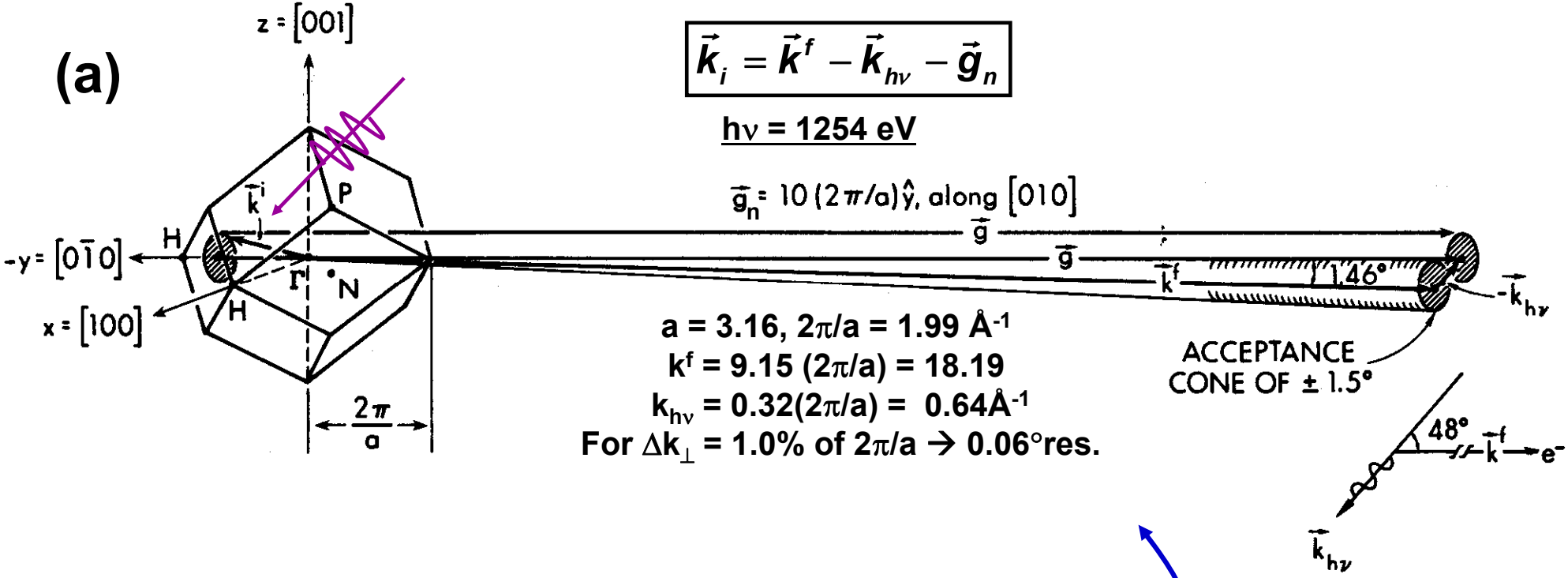

$$\vec{k}_i = \vec{k}^f - \vec{k}_{h\nu} - \vec{g}_n$$

$h\nu$ = 1254 eV

a = 3.16, $2\pi/a$ = 1.99 Å^{-1}

$k^f = 9.15\ (2\pi/a) = 18.19$

$k_{h\nu} = 0.32(2\pi/a) = 0.64$Å^{-1}

For $\Delta k_\perp$ = 1.0% of $2\pi/a$ → 0.06°res.

Hussain et al.....CF, Phys. Rev. B 22 3750 (1980) Phys. Rev. B 34, 5226 (1986)

Shevchik, Phys. Rev. B 16, 3428 (1977)

Additional effects at higher energies:

- Non-dipole--the photon momentum $k_{h\nu}$ →*easy to allow for*
- Angular acceptance→B.Z. averaging →*need better angular res.*
- Lattice recoil→phonon creation→more B.Z. averaging,

Fraction DTs ≈ Debye-Waller factor = $W(T) \approx \exp[-(k^f)^2 \langle u^2(T)\rangle]$

$\approx \exp[-C_1 (k^f)^2 T/(m\Theta_D^2)] \approx \exp(-C_2 E_{kin} T)$ →*need cryocooling*

→the "XPS limit" of full B.Z. averaging and D.O.S. sensitivity

→core-like photoelectron diffraction

Alvarez et al., PR*B* 54, 14703 (1996)

- Recoil →peak shifts and broadening:

$$E_{recoil}(eV) \approx \left[\frac{m_e}{M}\right] E_{kin} \approx 5.5 \times 10^{-4} \left[\frac{E_{kin}(eV)}{M(amu)}\right]$$

Takata et al., Phys. Rev. B 75, 233404 (2007)

ARPES→HARPES-How high can we go? Photoemission Debye-Waller Factors and Recoil Energies

Photon energy for ~50% DTs = O.5 D-W @ 20K

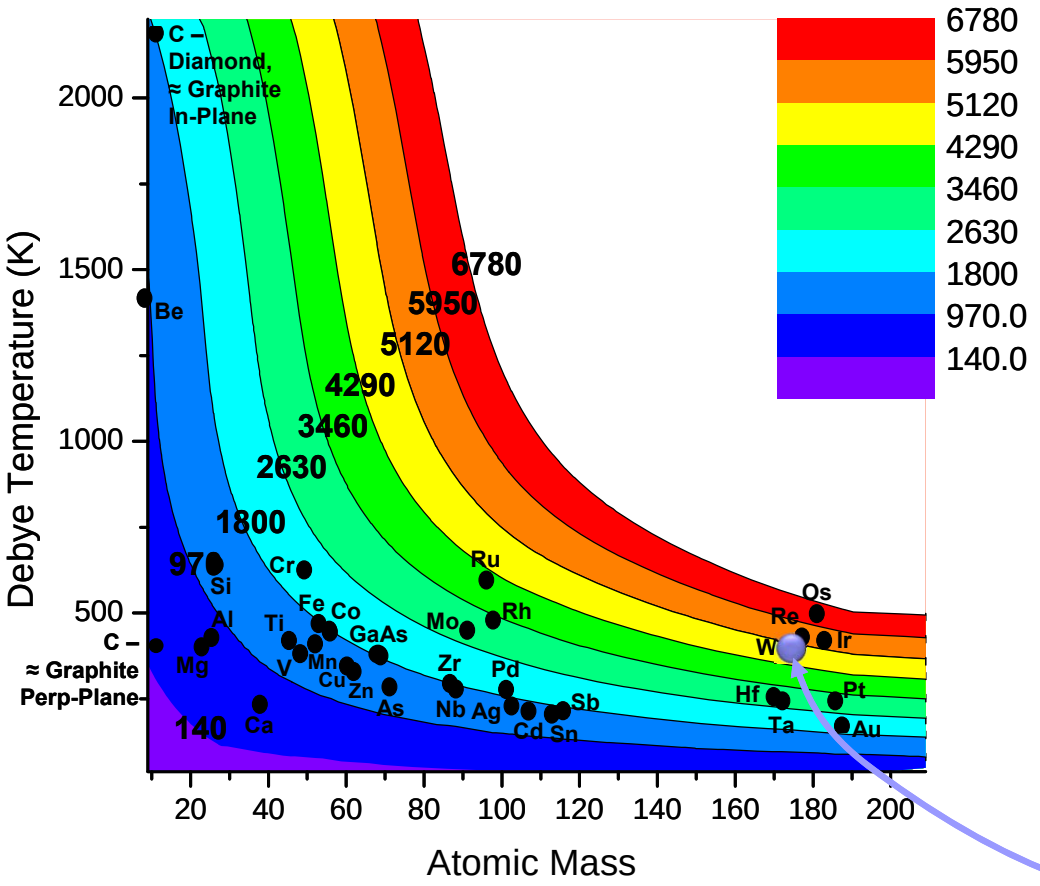

Recoil energy for all atoms and different photon energies

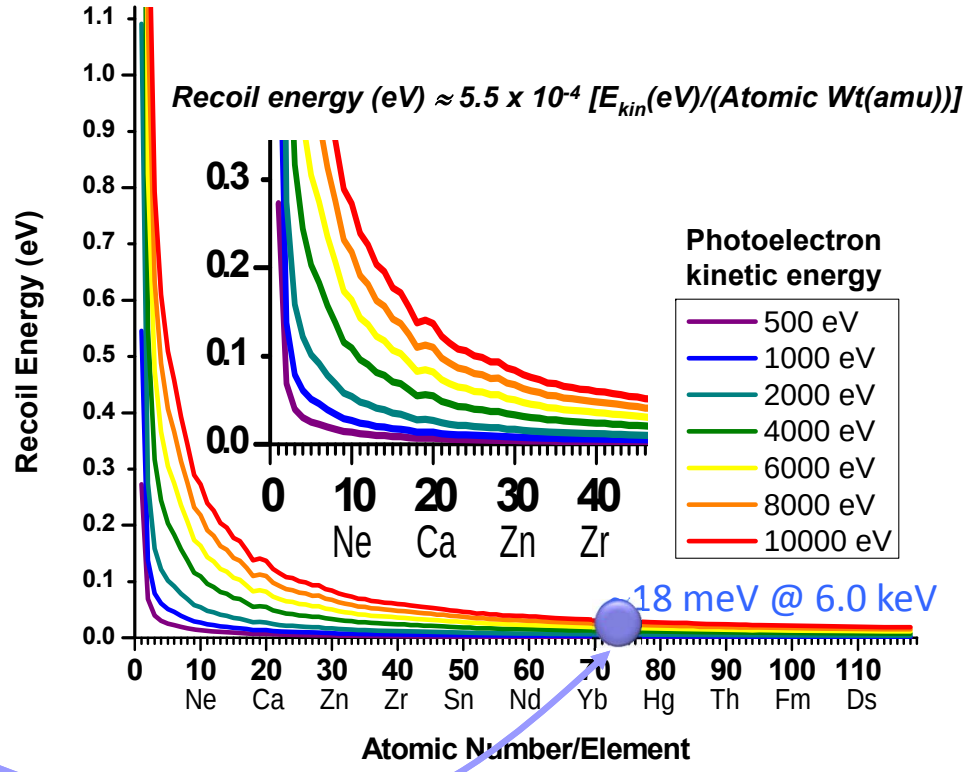

C. Papp. L. Plucinski, et al.,
Phys. Rev. B 84, 045433 (2011)

Hard x-ray ARPES for W(110): 6.0 keV

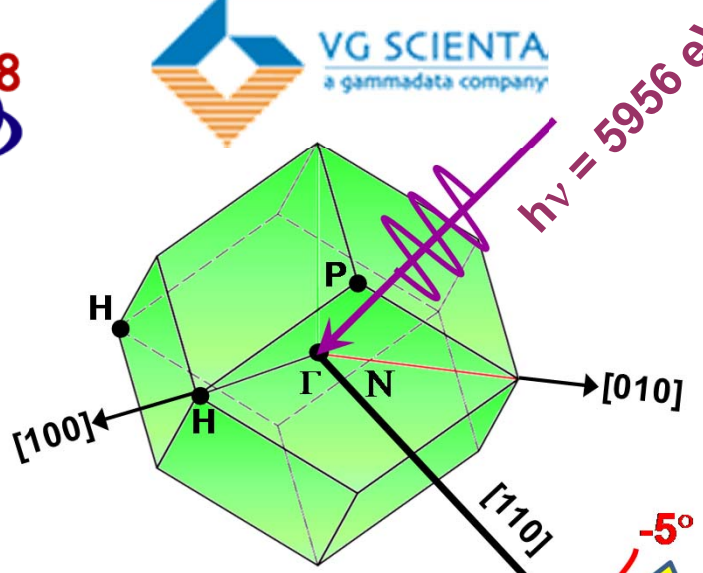

W(110)-air exposed, ~1 year, ~12 Å WO_x, ~3 Å C

Ang. Res.: ~0.2°→0.02° in future

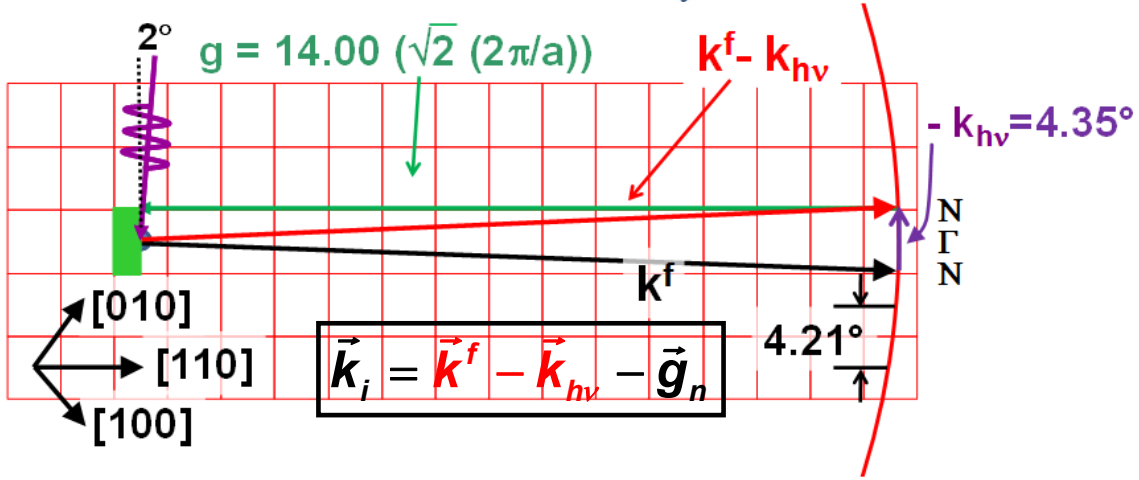

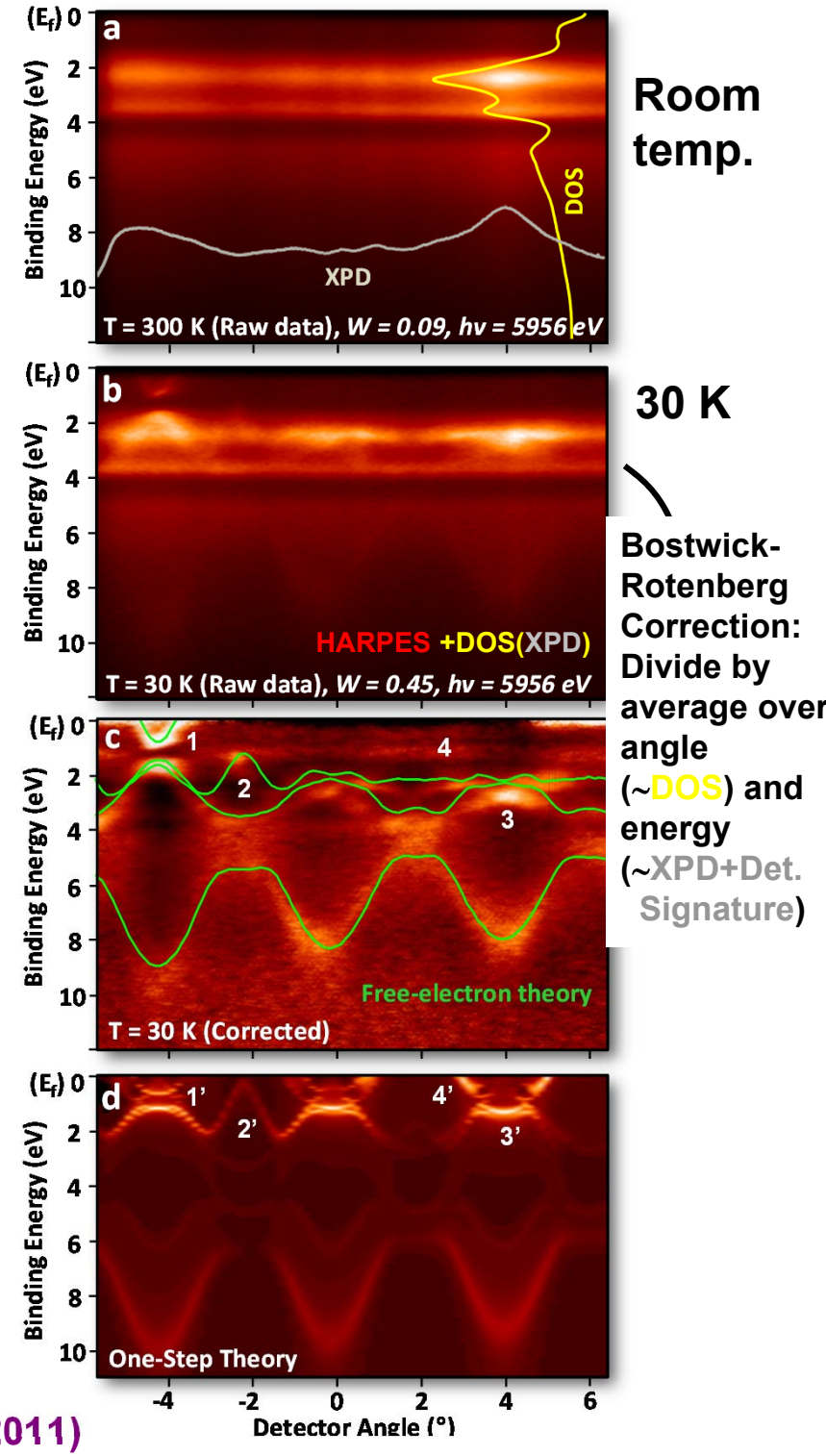

Gray, Minar et al., Nature Mat. 10, 759 (2011);
Plus *News and Views*, Feng, Nature Mat. 10, 729-730 (2011)

ARPES→HARPES-How high can we go? Photoemission Debye-Waller Factors and Recoil Energies

Photon energy for ~50% DTs = O.5 D-W @ 20K

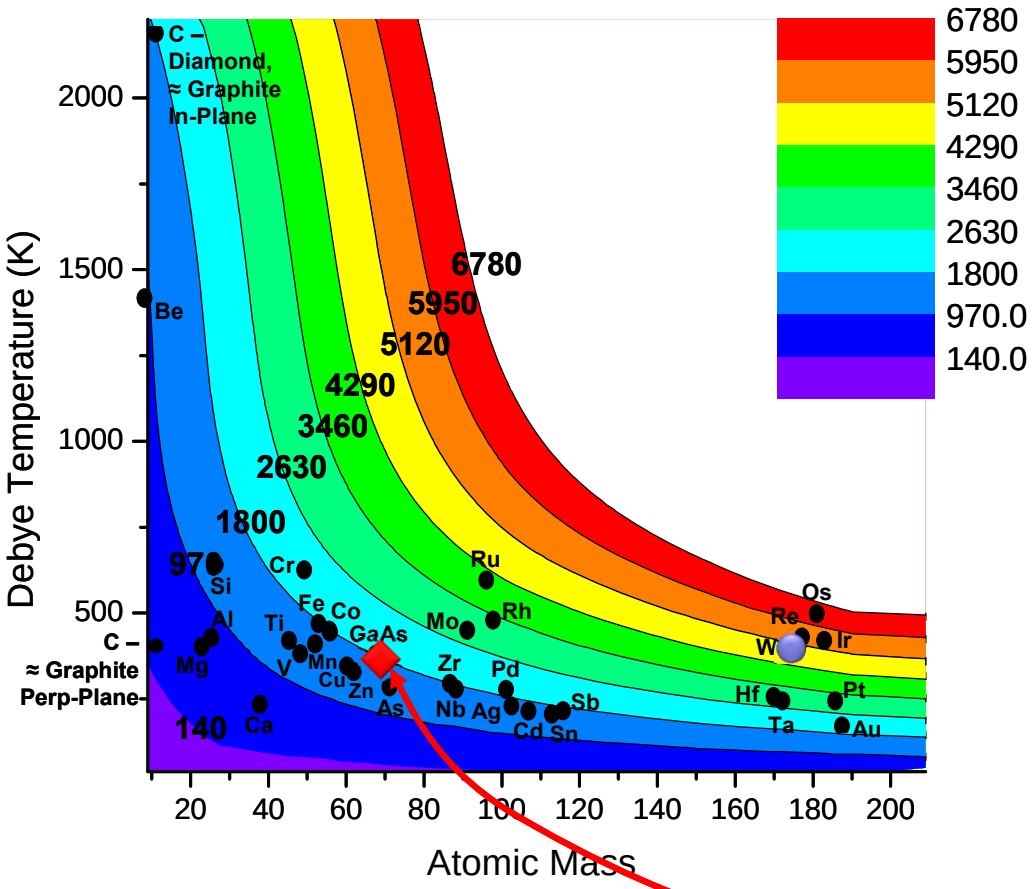

Recoil energy for all atoms and different photon energies

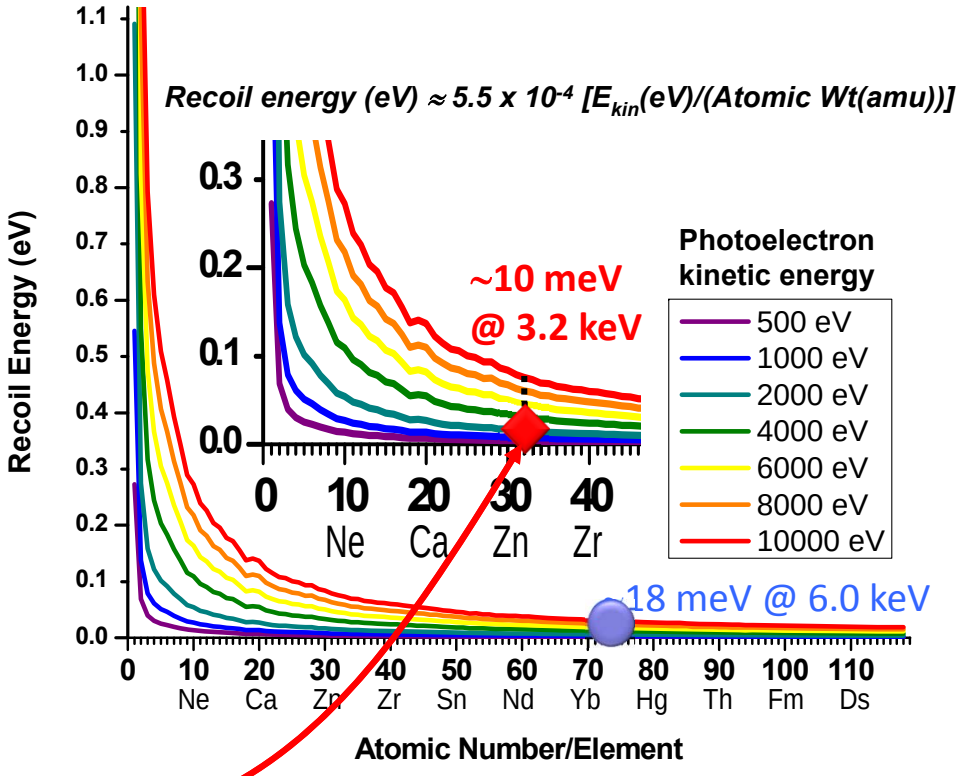

C. Papp. L. Plucinski, et al.,
Phys. Rev. B 84, 045433 (2011)

Hard x-ray ARPES for GaAs(001): 3.2 keV

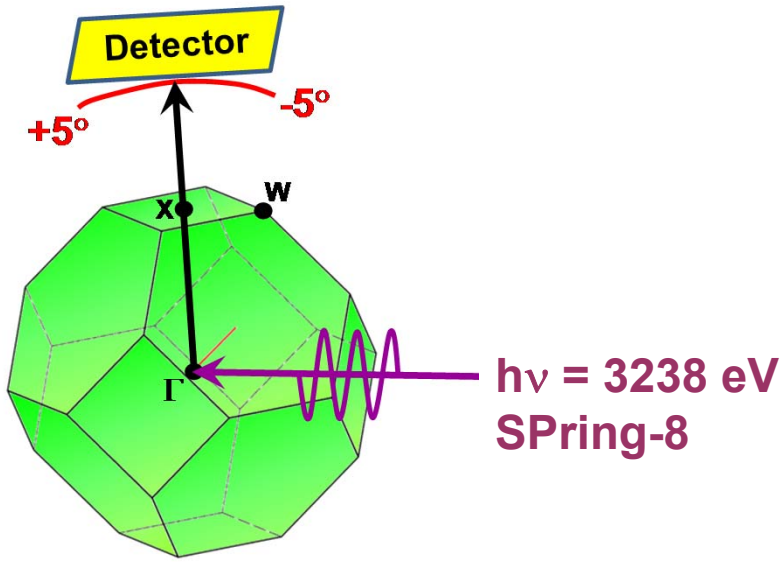

hν = 3238 eV
SPring-8

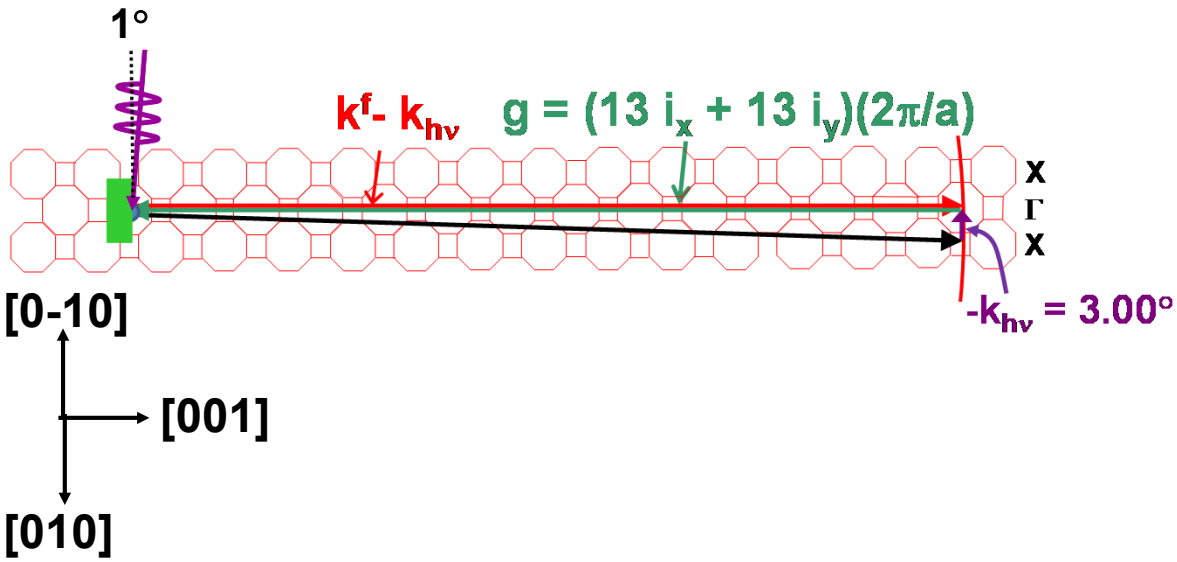

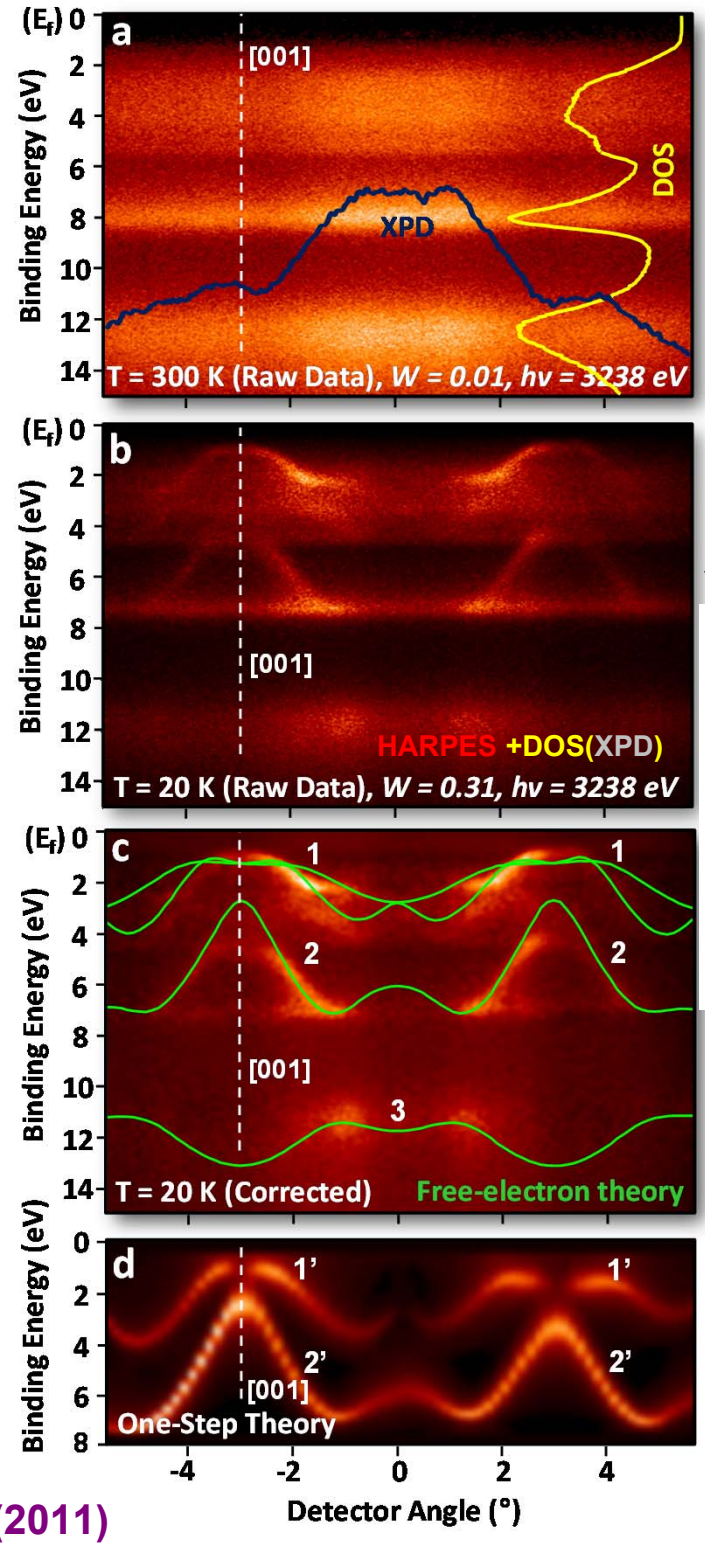

Bostwick-Rotenberg Correction: Divide by average over angle (~DOS) and energy (~XPD)

Gray, Minar et al., Spring-8, Nature Materials 10, 759 (2011)

A first real application of soft x-ray ARPES: Soft x-ray ARPES from $SrCuO_2$ at $h\nu$ = 700 eV and 300K, photoemission Debye-Waller factor of only 0.03-0.04

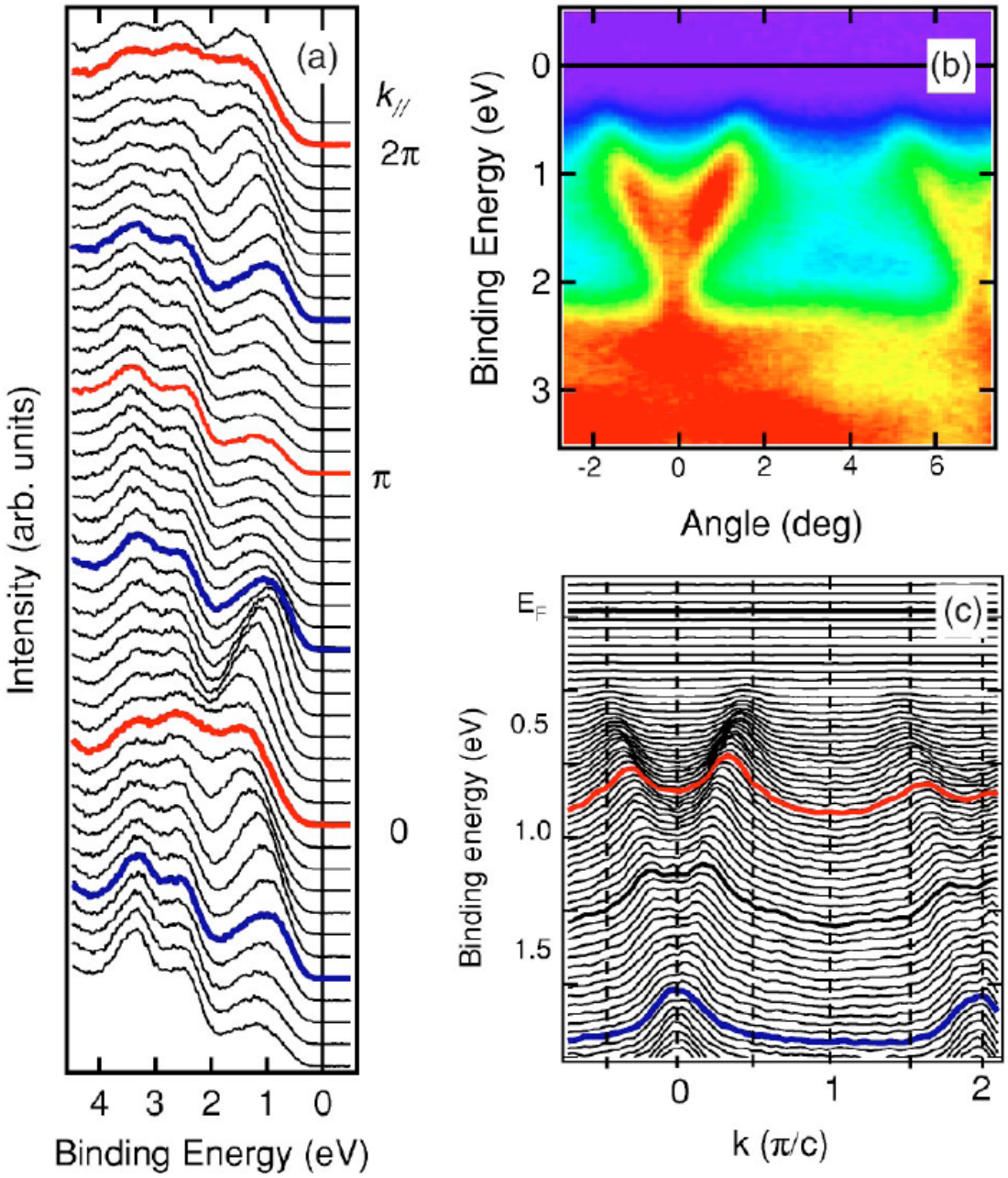

Photoemission DW factors can be too conservative for some systems (lack of correlated vibrations?) →suggests a wider application of SARPES/HARPES

S. Suga, A. Sekiyama, et al., PRB 70, 155106 (2004)

3D band mapping of a "2D" material VSe_2

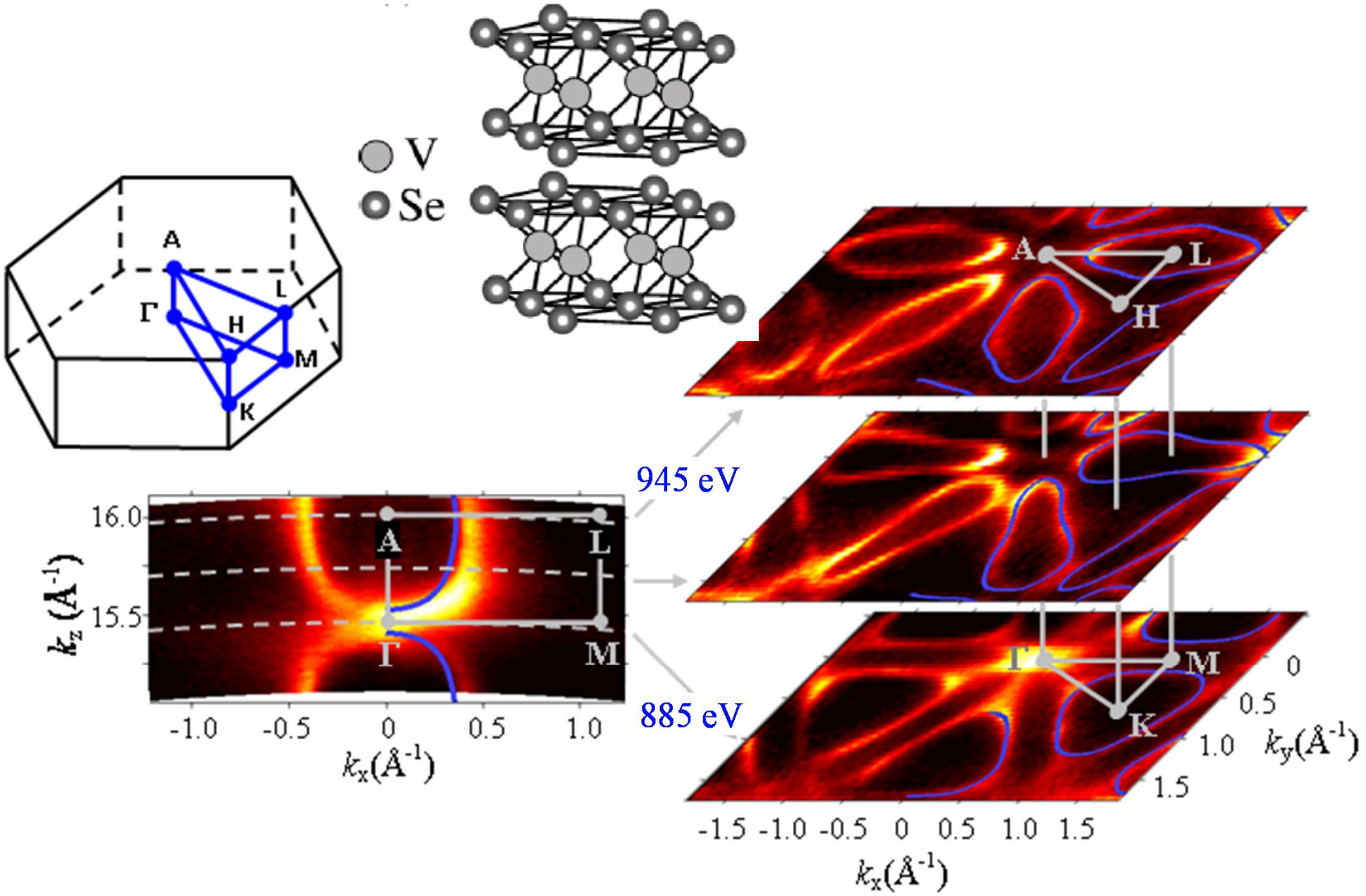

Strocov et al., PRL 109, 086401 (2012)

$\vec{k}_i = \vec{k}_f - \vec{k}_{h\nu} - \vec{g}_n$

Soft→Hard Angle-Resolved Photoemission: Basic Considerations

- + Deeper probing: "bulk" electronic structure, buried layers and interfaces, less surface sensitive
- + Free-electron final state: good approximation

$$E_f(\vec{k}_f) \approx \hbar^2 k_f^2 / 2m_e$$

- + Less $k_\perp$ broadening: $\Delta k_\perp \approx 1/\Lambda_e$*(inelastic)*
- + 3D band mapping: possible with photon energy variation
- + Resonant excitation: enhance a given atom's contribution, move standing wave in sample
- + Standing-wave excitation: possible, multilayers, epi-, single crystal- systems
- + Core-level spectra: provide complementary information on charge states, structure via XPD
- - Phonon smearing: need cryocooling, DW factor as criterion

$$DW(T) \approx \exp[-g_n^2 \langle u^2(T) \rangle]$$

- - Angular resolution: need higher for $\Delta k_{||}$ resolution
- - Non-dipole effects: allowance for photon momentum, but easy

$$\vec{k}_i = \vec{k}_f - \vec{k}_{h\nu} - \vec{g}_n$$

- - Recoil effects: shift and smear energies

$$E_{recoil} \approx \frac{\hbar^2 k_f^2}{2M} \approx 5.5 \times 10^{-4} \left[\frac{E_{kin}\,(eV)}{M\,(amu)} \right]$$

CSF, Synch.Rad. News. 25, 26 (2012); V. Strocov et al., Appl. Phys. Lett. 101, 242103 (2012)

Four levels of interpreting ARPES spectra

[1] Simply looking at the final state as a free electron in an extended-zone scheme, translating it into the first BZ via $\vec{k}_f = \vec{k}_{h\nu} - \vec{g}_n$, and asking qualitatively where it cuts the ground-state band structure

[2] More rigorously requiring energy and *k*-conservation and computing the locus of points in energy and *k* that satisfy it, again ground-state band structure (e.g. Plucinski, et al., Phys. Rev. B 84, 045433 (2011))

[3] Calculating the spectral function to allow for many-body excitations in the sudden approximation, but with no matrix elements:

$$I(\vec{k},\varepsilon) \propto \sum_s \left|\langle N-1,\mathbf{K}\right| c_{\vec{k}} \left|N,0\right\rangle\right|^2 \delta\left(E_{N-1,s} + \varepsilon - E_{N,0} - \hbar\omega\right)$$

$$= A(\vec{k},\varepsilon-\hbar\omega)\cdot f(\varepsilon-\hbar\omega)$$

spectral function

The ARPES signal $I(\vec{k},\varepsilon)$ directly proportional to the removal part of the **spectral function** $A(\vec{k},\omega) = -\frac{1}{\pi} Im\, G\,(\vec{k},\omega)$

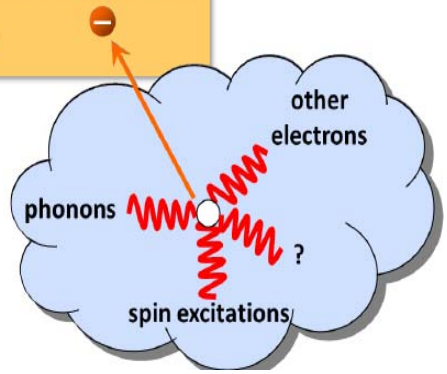

[4] Carrying out full one-step photoemission calculations that include the surface and all matrix elements, so as to be able to accurately represent intensities. For SARPES and HARPES (Minar, Braun, Ebert, J. Elect. Spect. 184, 91 (2011))

LMU LUDWIG-MAXIMILIANS-UNIVERSITÄT MÜNCHEN

SPRKKR method + One-step model

Angle resolved UV and X-ray photoemission
for arbitrary ordered and disordered correlated systems

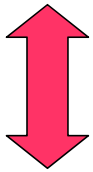

One-step model of photoemission

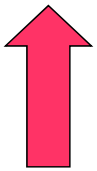

Standing-wave
$|E^2(\text{depth})|$

LSDA

Relativistic
Dirac formalism

Full potential
2D Semi-infinite

DMFT

CPA-Alloys, dopants,
phonons (Debye model)

Model Surface
barrier

Reviews:
KKR: Ebert, Ködderitzsch, Minar, Rep. Prog. Phys. 74, 096501 (2011)
KKR+DMFT: Minar, JPCM Topical Review 23, 253201 (2011)
KKR+One step model: Minar, Braun, Ebert et al., JESRP 184, 91(2011)

Jan Minar
Juergen Braun
Hubert Ebert

Phonon effects in photoemission

- Phonon excitations define fundamental limit to band mapping as energy or temperature is raised because of full BZ averaging Shevchik (1977)

- Photo current can be roughly divided into two contributions:

$$< I^{Tot}(E_F,k,T)> \approx W(T) I^{DT}(E_F,k,T) + [1 - W(T)]\, I^{NDT}(E_F,k,T)$$

- Photoemission Debye-Waller Factor $W(T) = exp(-\Delta k^2 < u^2 >) = exp(-g^2_{hk\ell} < u^2 >)$

- Actual situation: $< I^{Tot}(E_F,k,T)> \approx W(T) < I^{Multiple\ scatt}(E_F,k,T)> + < I^{Atomic}(E_F,k,T)> + < I^{Incoherent}(E_F,k,T)>$

ARPES

MEWDOS, XPD

via t(T) (Larson and Pendry, Feder)

- Improved treatment of phonon effects on LEED state – cluster implementation: Zampieri *et al.* (1996)

- Proper formulation for solids within multiple scattering formalism for high energy regime: Fujikawa and Arai (2009)

Tungsten--Debye-Waller Factors and Recoil Energies

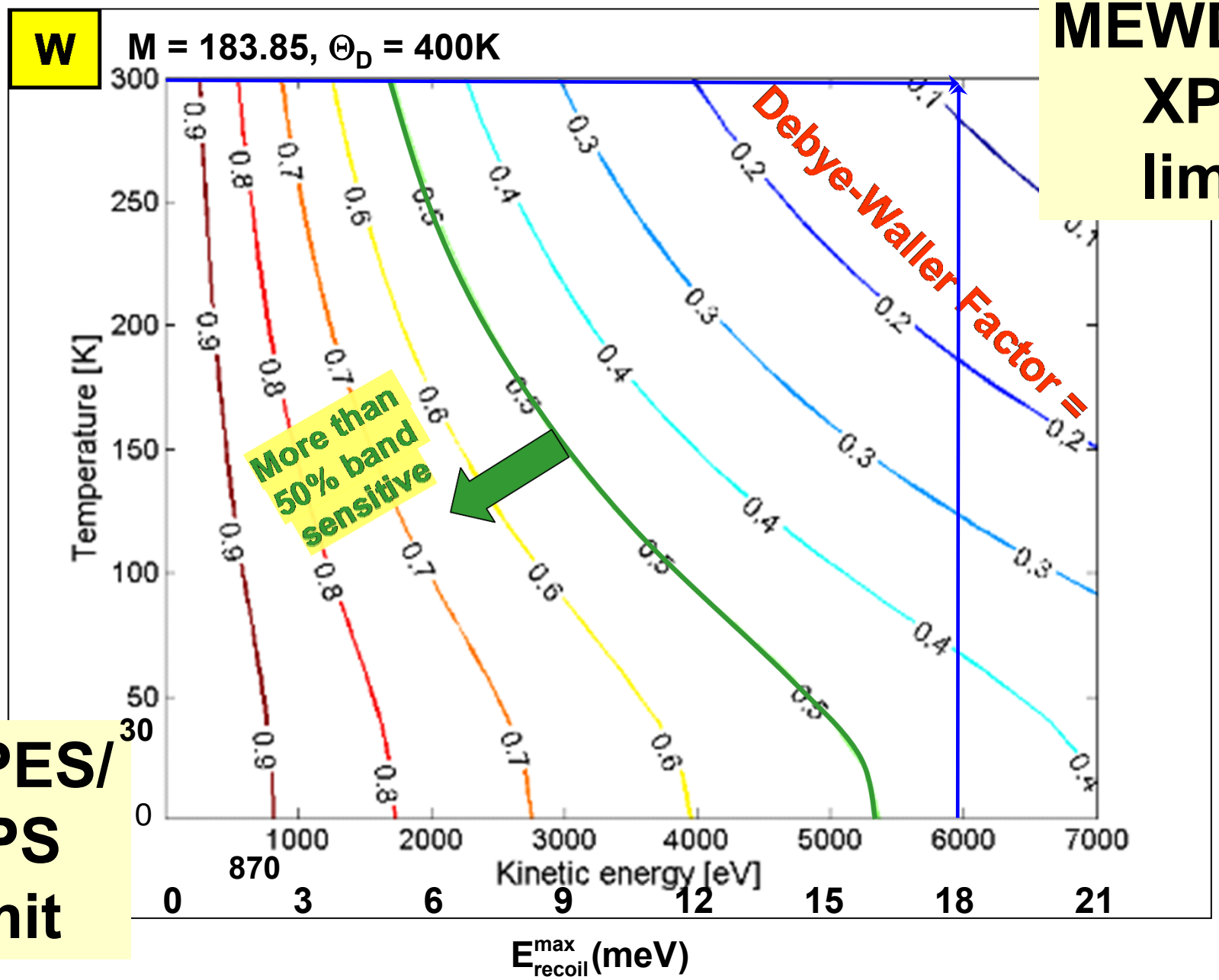

MEWDOS/ XPS limit

ARPES/ UPS limit

Plucinski, et al. PRB 78, 035108 (2008); Phys. Rev. B 84, 045433 (2011)

Hard x-ray ARPES for W(110), 6 keV: One-step theory with phonons (Braun, Minar, Ebert) vs expt. (Gray et al.)

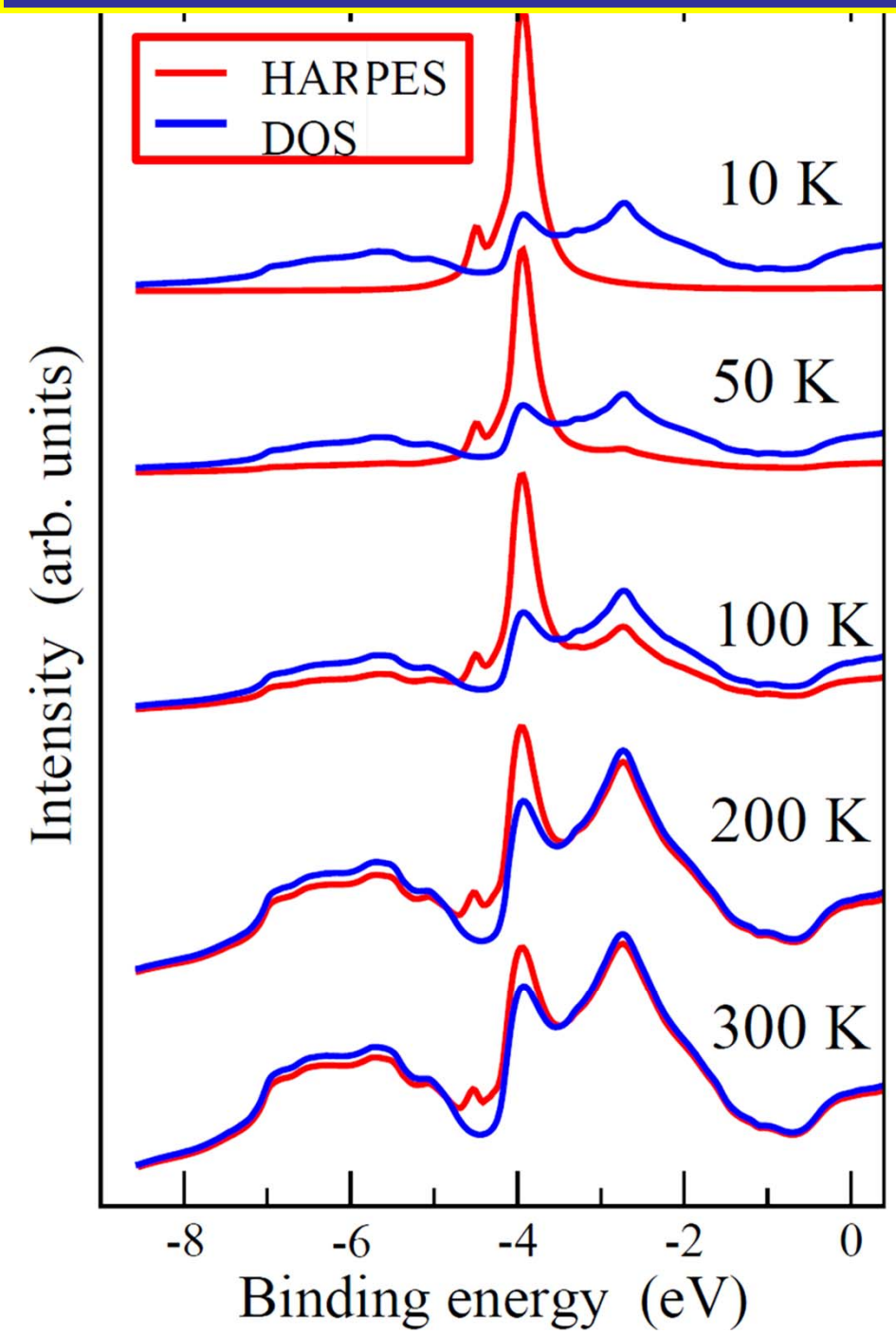

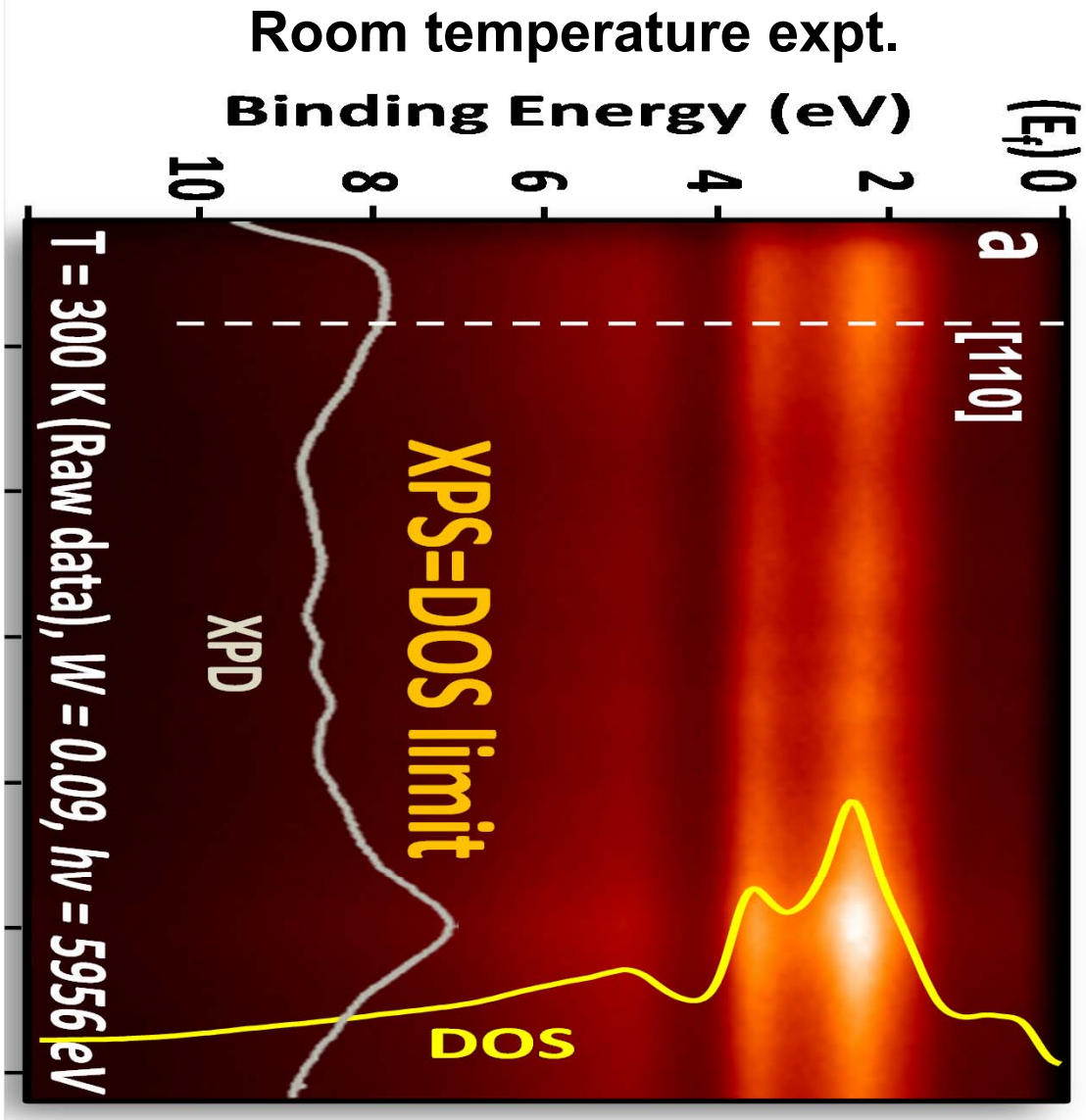

Braun et al., Phys. Rev. B 88, 205409 (2013)

Tungsten--Debye-Waller Factors and Recoil Energies

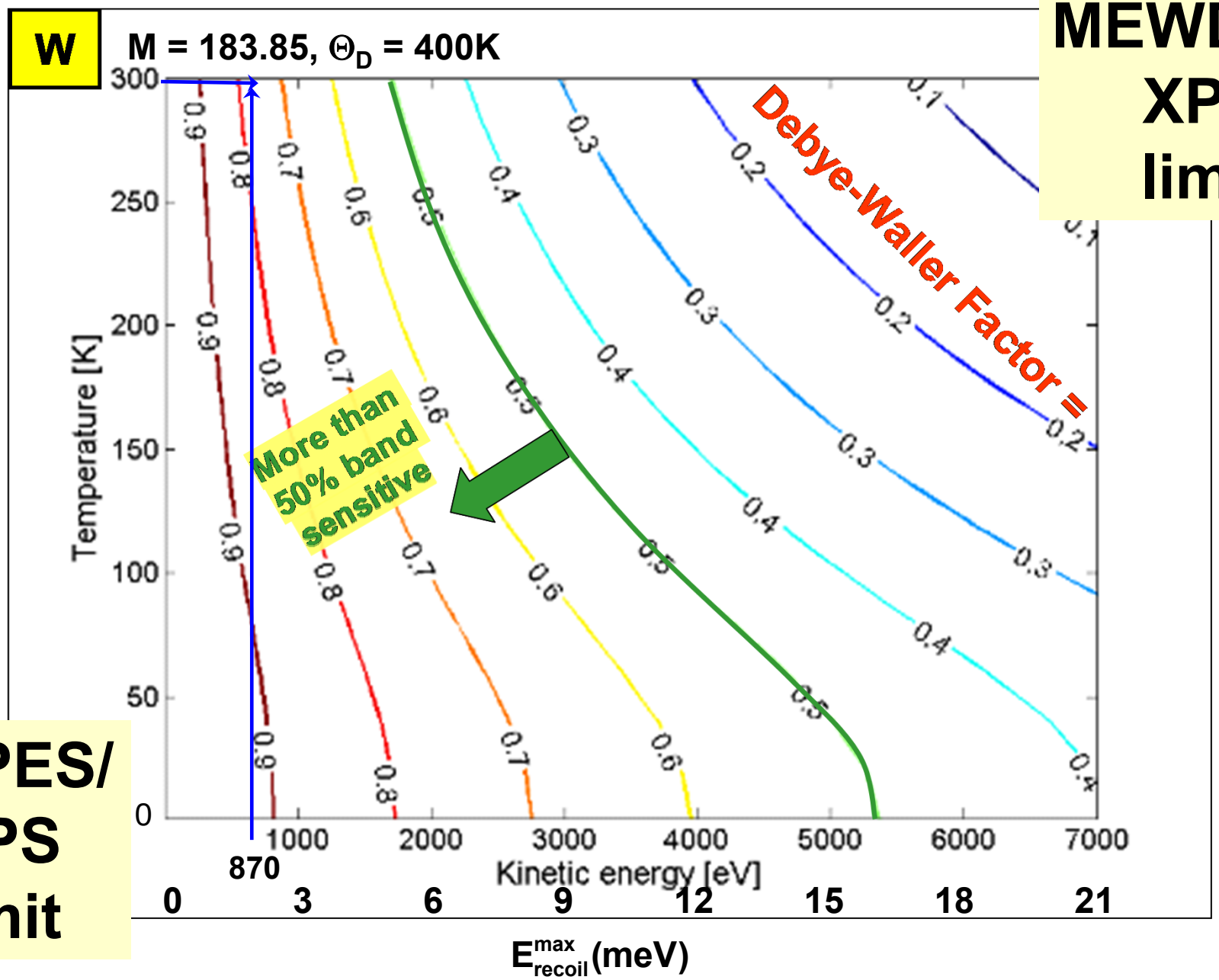

MEWDOS/ XPS limit

ARPES/ UPS limit

Plucinski, et al. PRB 78, 035108 (2008); Phys. Rev. B 84, 045433 (2011)

Phonon effects: Improved theoretical modeling

L. Plucinski, J. Minar, …
PRB 78, 035108 (2008)

One-step, t-reversed LEED, spin-polarized relativistic KKR:

- Phonons via complex phase shifts

- Phonons via the coherent potential model

J. Braun, J. Minar, S. Mankovsky, L. Plucinski, Phys. Rev. B 88, 205409 (2013).

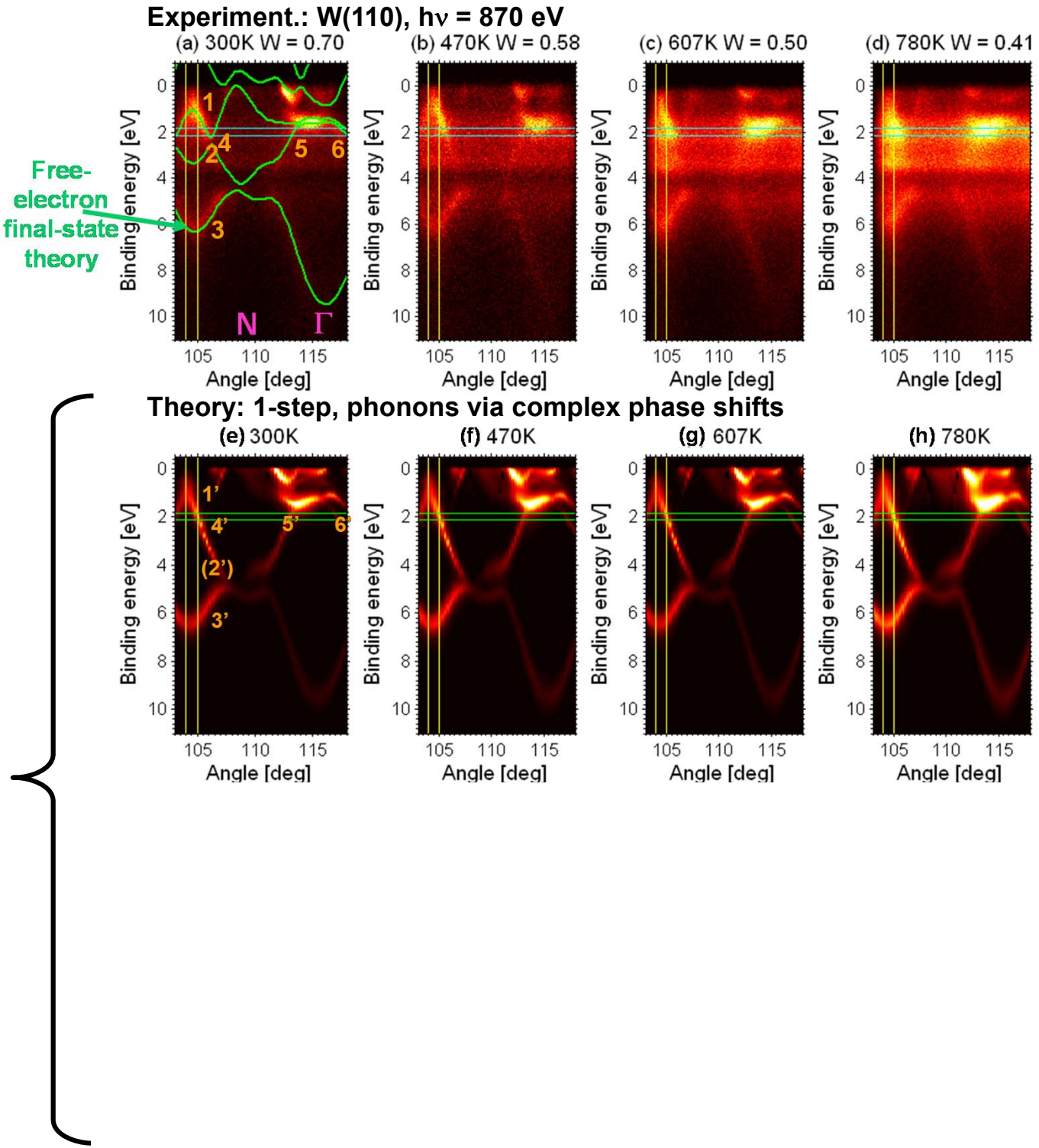

Phonon effects: Improved theoretical modeling

L. Plucinski, J. Minar, …
PRB 78, 035108 (2008)

One-step, t-reversed LEED, spin-polarized relativistic KKR:

- Phonons via complex phase shifts

- Phonons via the coherent potential model

J. Braun, J. Minar, S. Mankovsky, L. Plucinski, Phys. Rev. B 88, 205409 (2013).

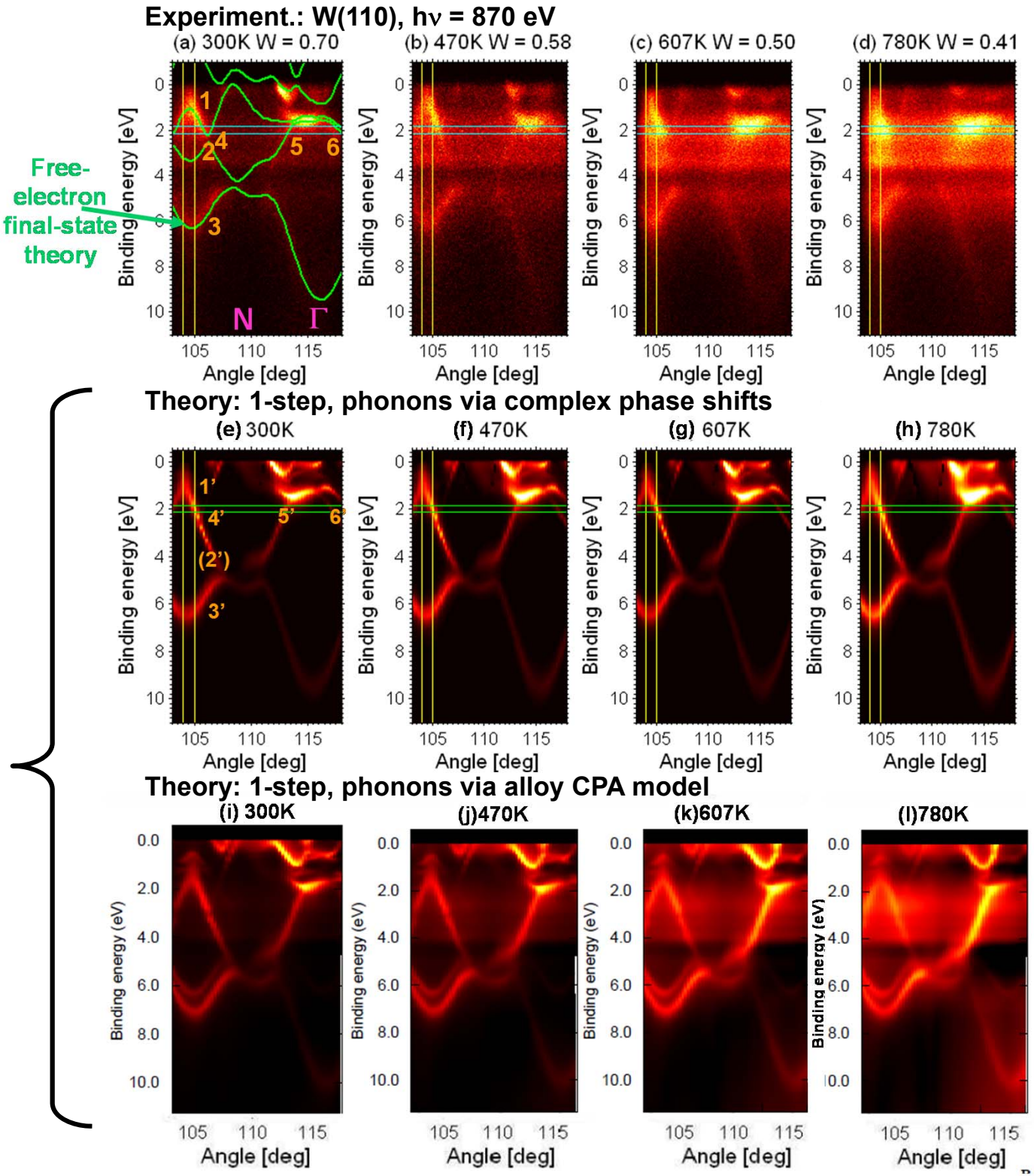

Calc. phonon effects in photoemission, Au soft and hard x-ray: Angle-resolved PES (ARPES)→Angle-integrated PES (XPS/MEWDOS)

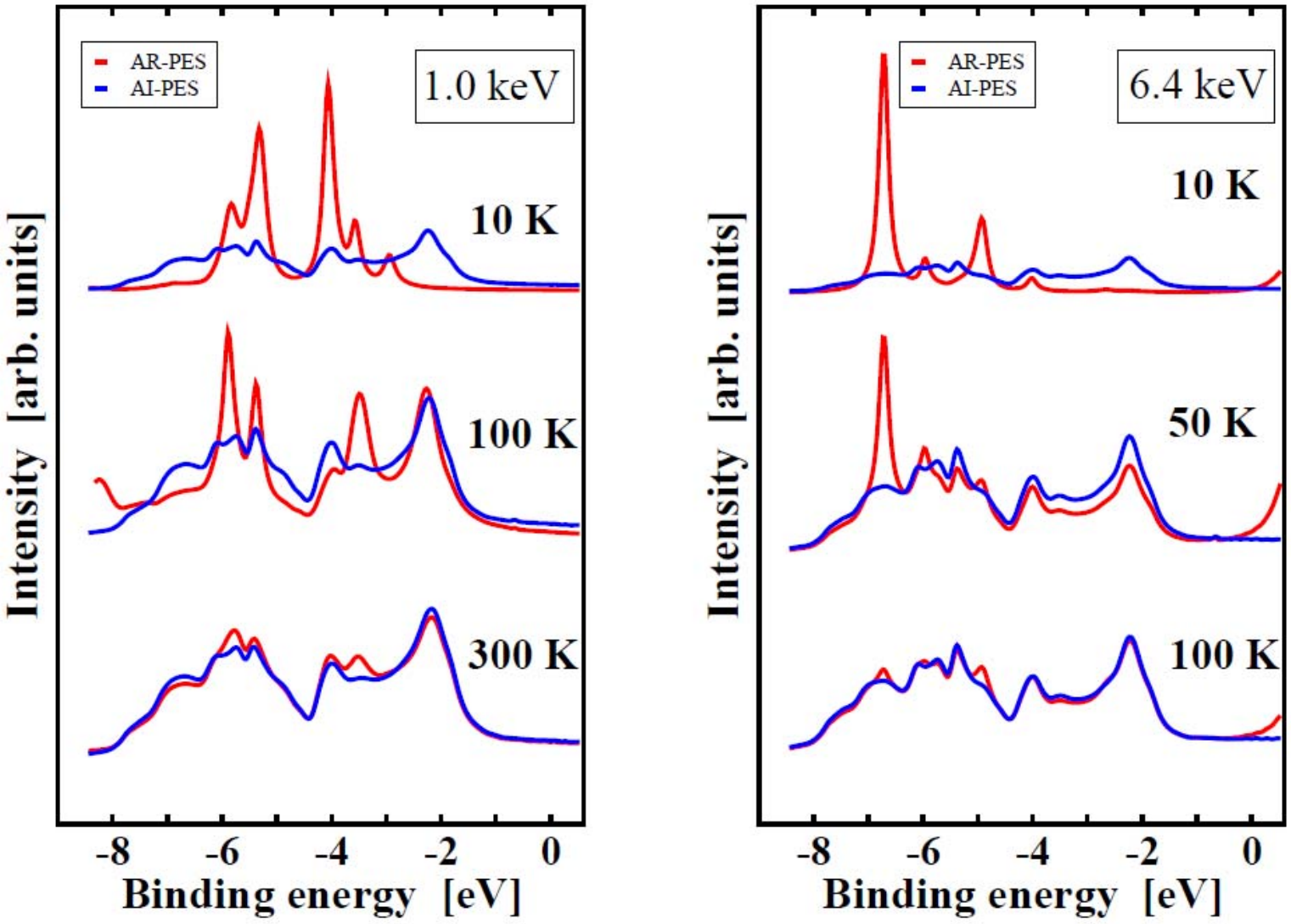

Braun, Minar, et al., Phys. Rev. B 88, 205409 (2013)

A first real application of soft x-ray ARPES: Soft x-ray ARPES from $SrCuO_2$ at hν = 700 eV and 300K, photoemission Debye-Waller factor of only 0.03-0.04

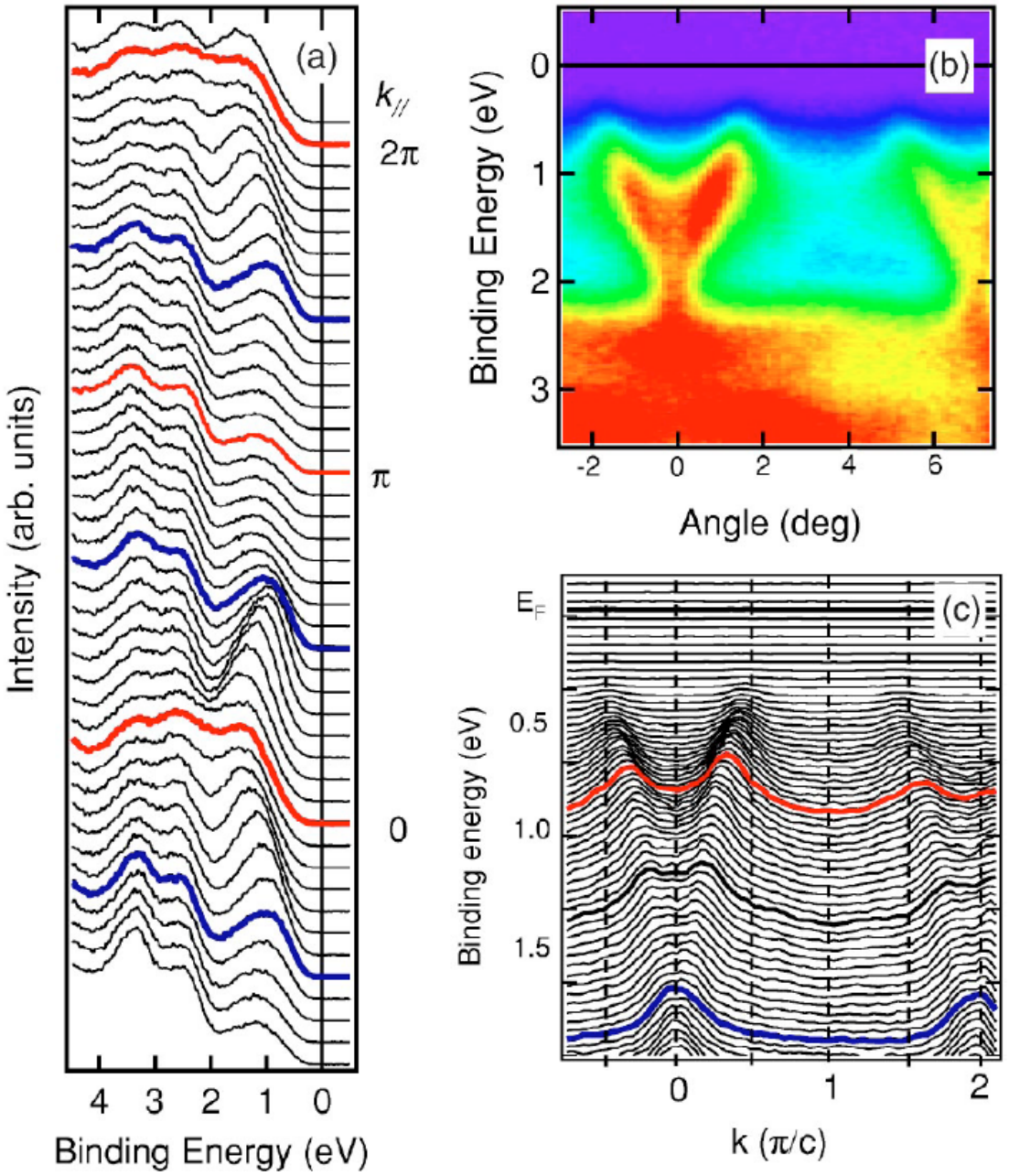

Photoemission DW factors can be too conservative for some systems (lack of correlated vibrations?) →suggests a wider application of SARPES/HARPES

S. Suga, A. Sekiyama, et al., PRB 70, 155106 (2004)

Photon energy for D-W = O.5 @ 20K

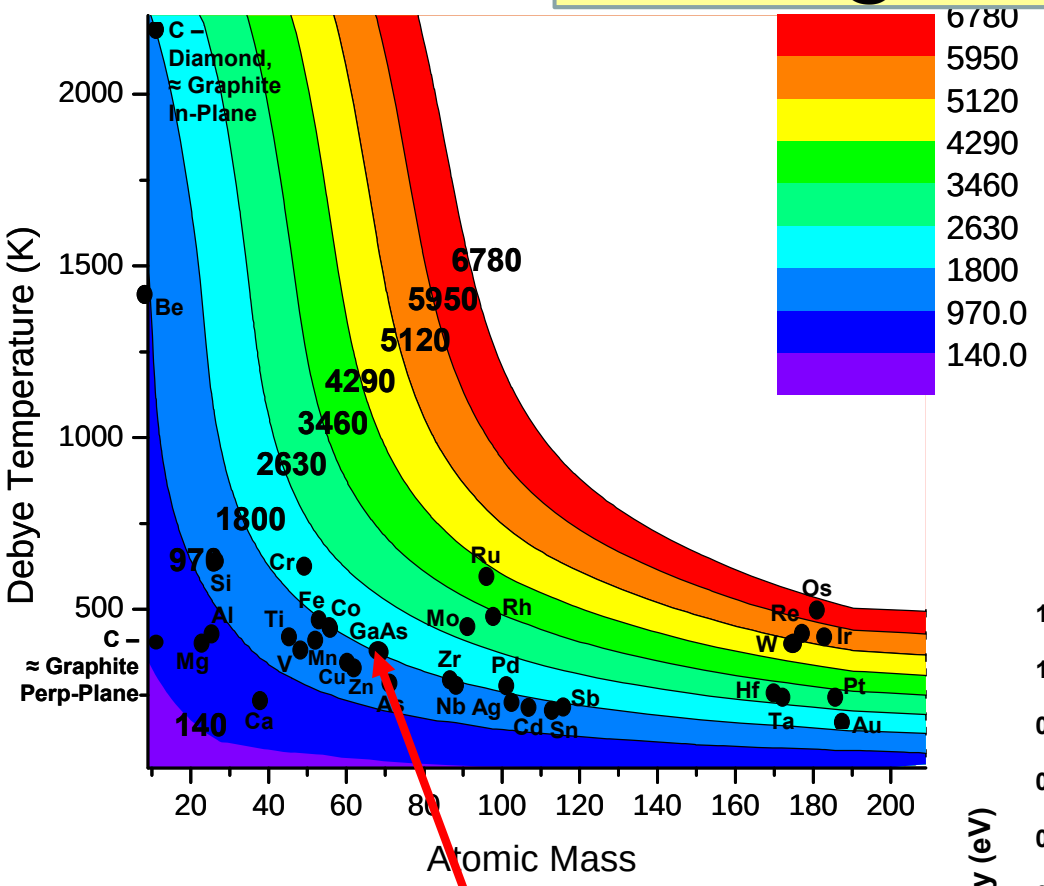

HARPES-How high can we go? Photoemission Debye-Waller Factors and Recoil Energies

E.g.-GaAs

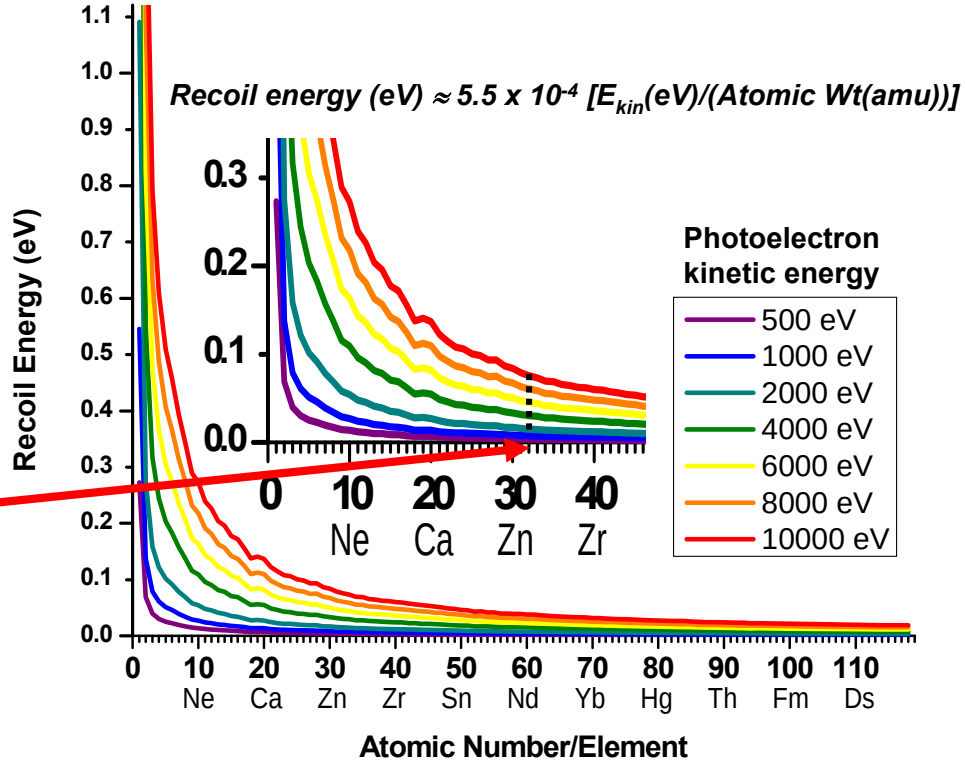

C. Papp. L. Plucinski, et al.,
Phys. Rev. B 84, 045433 (2011)

Looking through an amorphous layer to do ARPES: GaAs @ 11K

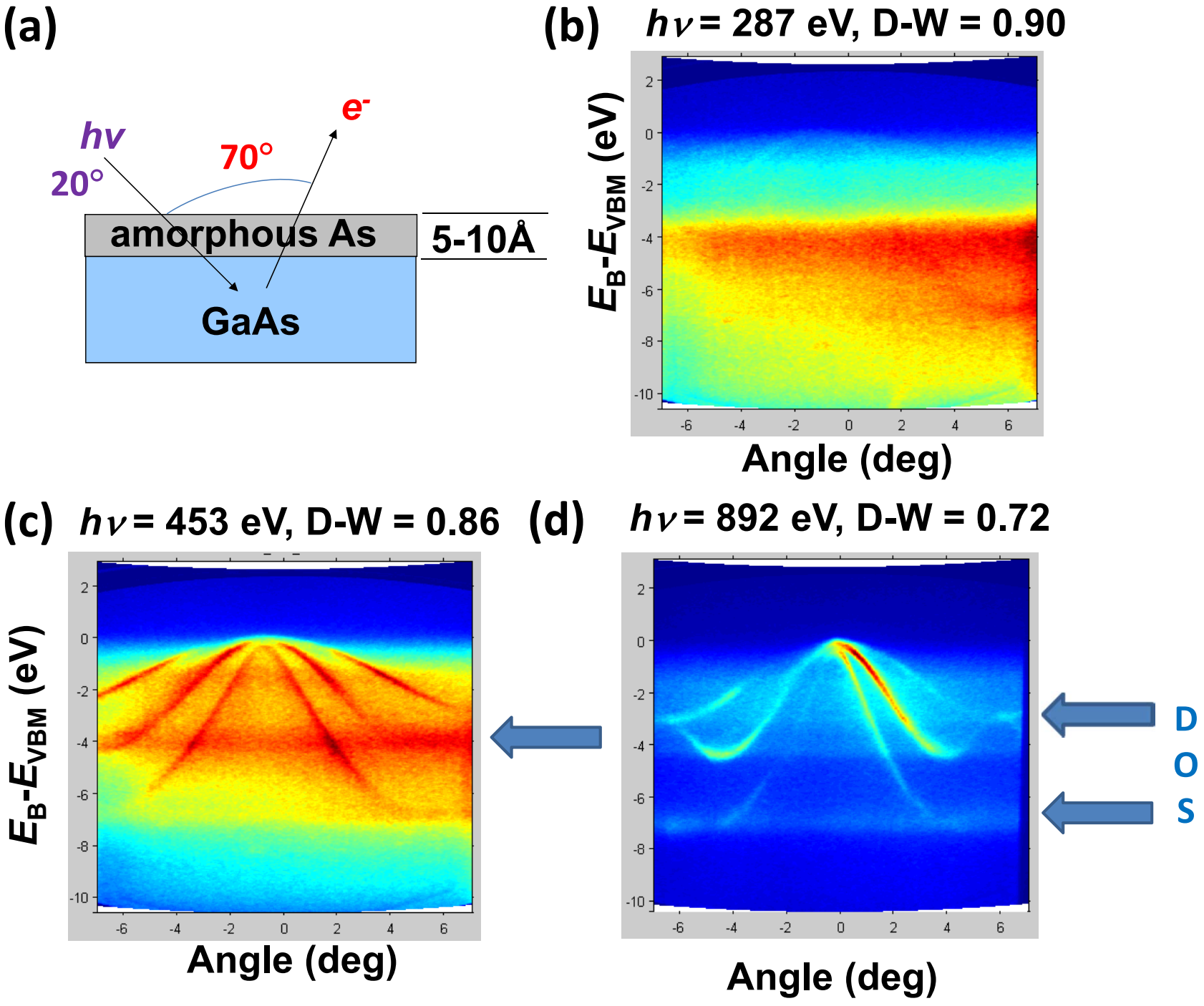

M. Kobayashi, V.N. Strocov et al,, Appl. Phys. Lett. 101, 242103 (2012)

ARPES—How high can we go in energy and temperature?

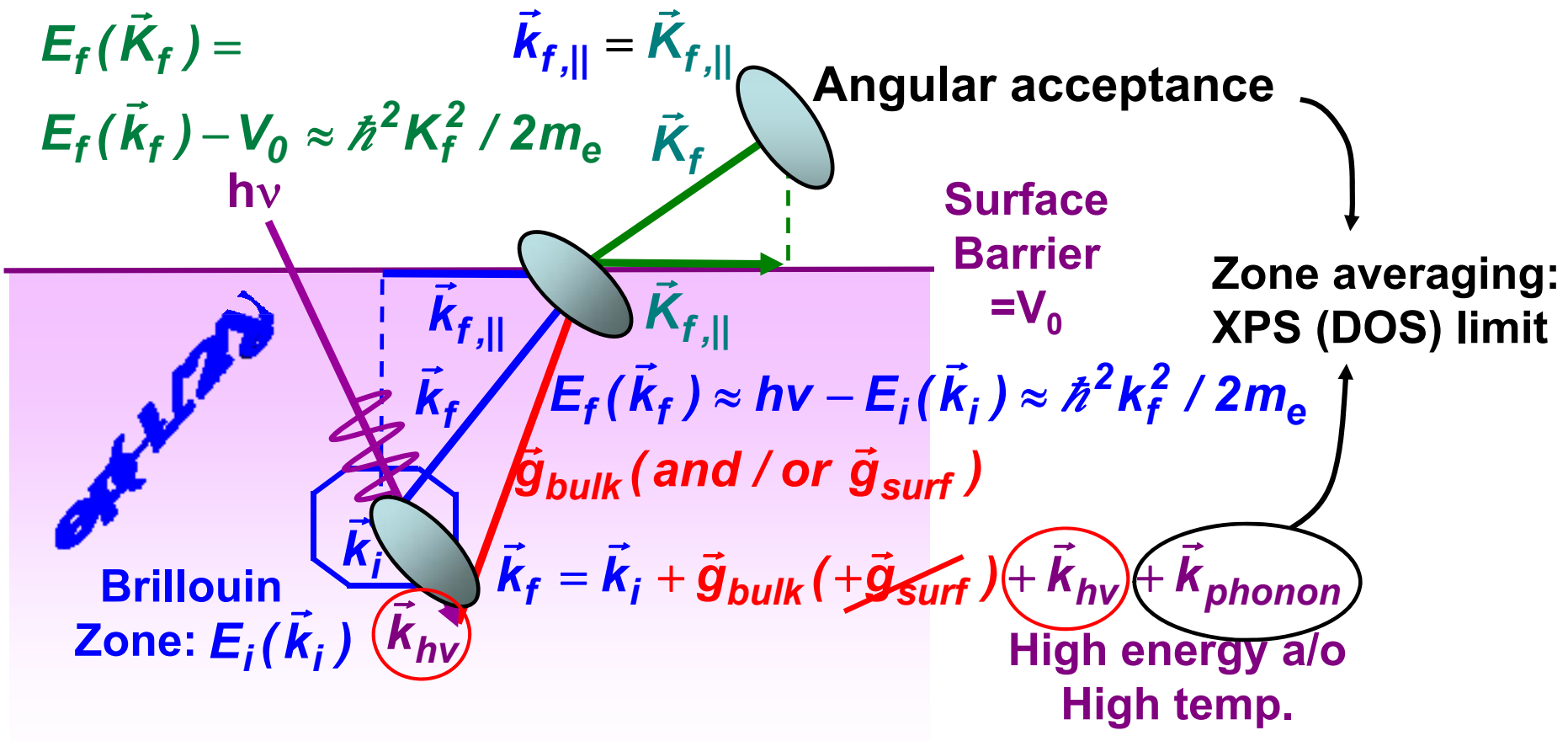

Fraction DTs ≈ Debye-Waller factor = $W(T) \approx \exp[-(k^f)^2 \langle u^2(T) \rangle]$

$\approx \exp[-C_1 (k^f)^2 T/(m\Theta_D^2)] \approx \exp(-C_2 E_{kin} T)$

$W \approx 1$

$W \approx 0.3$

$W \approx 0$

ARPES→bands, quasiparticles (Low hν, Low T, High angul. Res.)

Shevchik, Phys. Rev. B 16, 3428 (1977)
Hussain….CF, Phys. Rev. B 34 (1986) 5226

XPS→DOS+XPD (High hν, High T, Low angul. Res.)

Hard x-ray ARPES--GaAs and the dilute magnetic semiconductor $Ga_{0.97}Mn_{0.03}As$

How does Mn alter the GaAs electronic structure so as to produce ferromagnetic coupling?
Differing views: p-d exchange, double exchange?

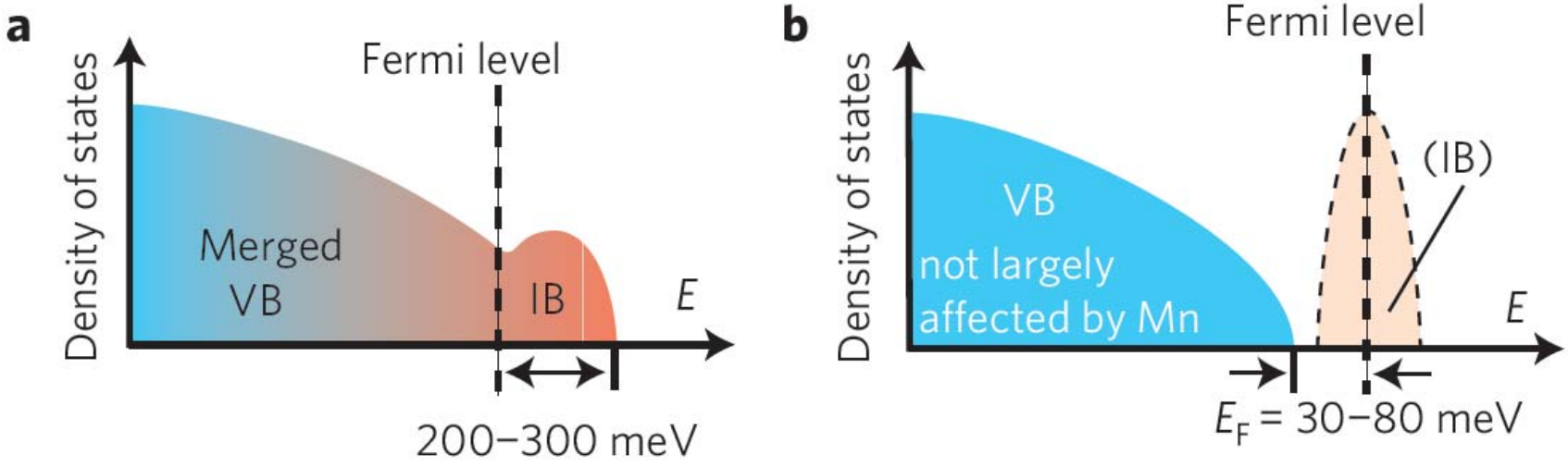

Ohya et al., Nature Physics 7, 342 (2011)

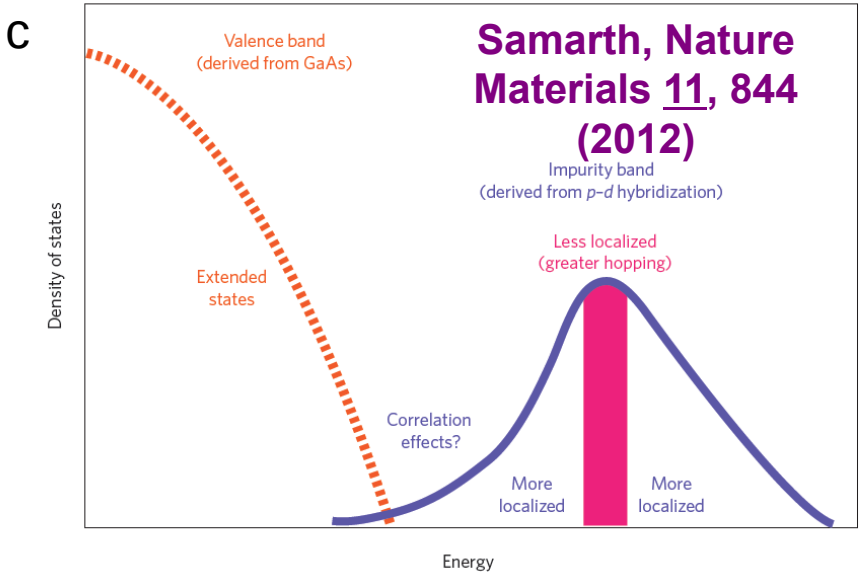

Samarth, Nature Materials 11, 844 (2012)

Hard x-ray ARPES--GaAs and DMS $Ga_{0.97}Mn_{0.03}As$ Comparing Experiment (3.2 keV, 30K) and One-Step KKR Theory

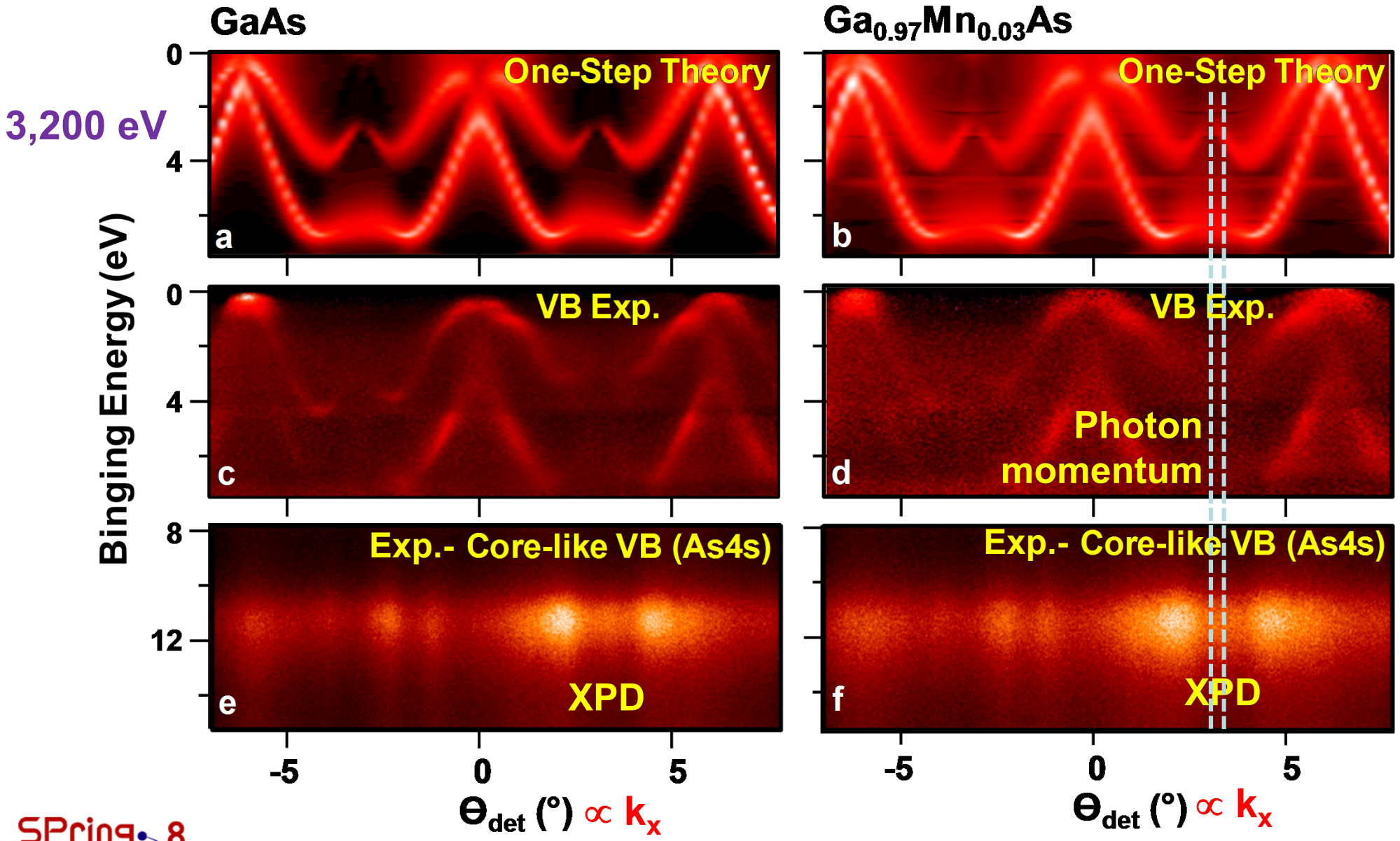

SPring-8

Gray, Minar et al., Nature Materials 11, 957 (2012)

GaAs and $Ga_{0.97}Mn_{0.03}As$ Angle-Integrated Hard X-Ray ARPES @ 3.2 keV Experiment and One-Step KKR Theory

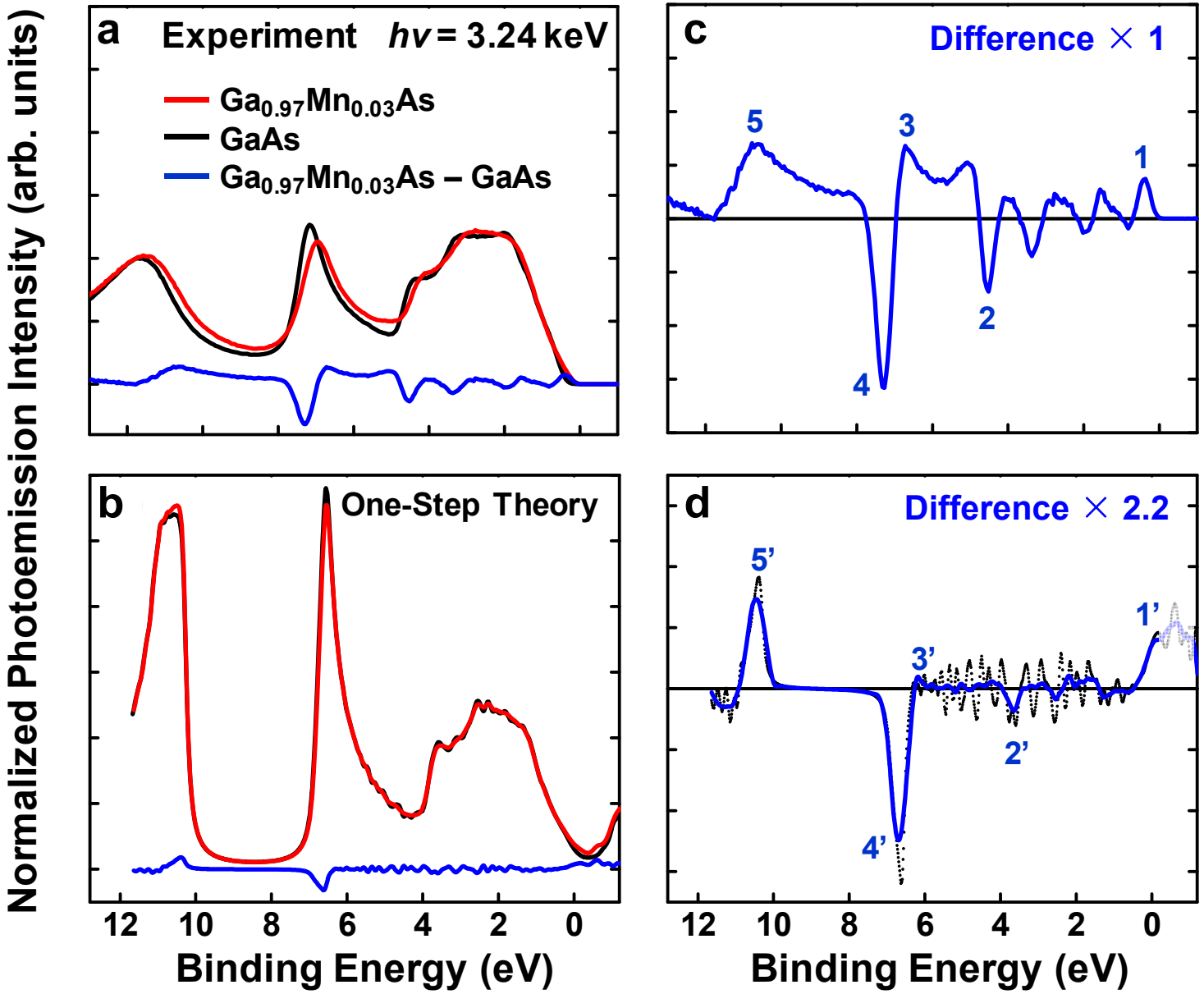

Gray et al., Nature Materials 11, 957 (2012)

Hard x-ray ARPES--GaAs and the dilute magnetic semiconductor $Ga_{0.97}Mn_{0.03}As$

How does Mn alter the electronic structure so as to produce ferromagnetic coupling?
Differing views:

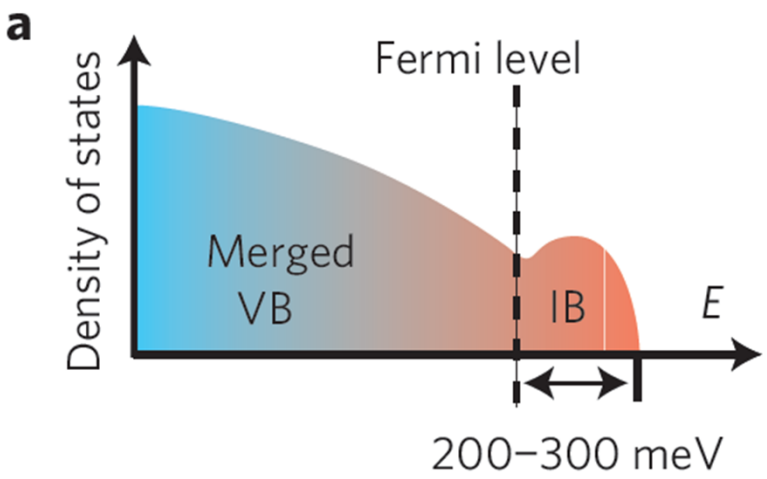

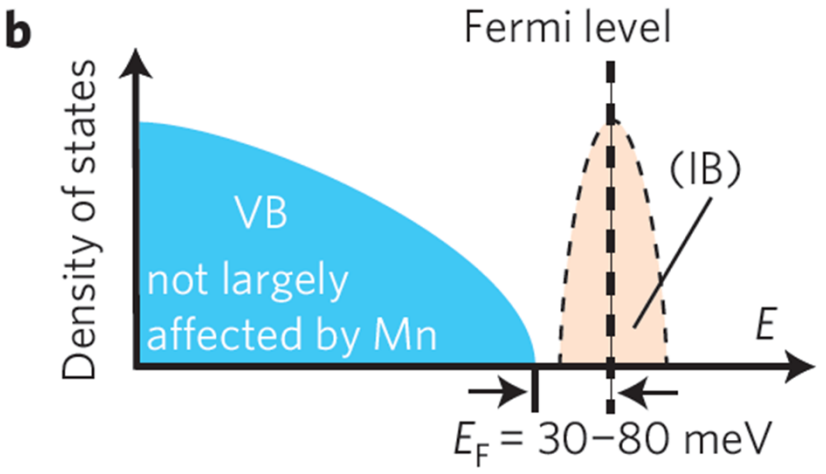

Ohya et al., Nature Physics 7, 342 (2011)

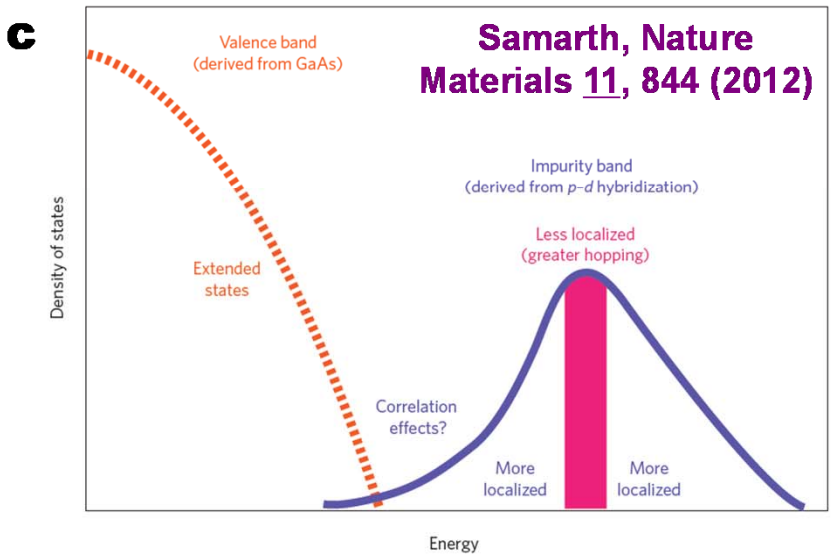

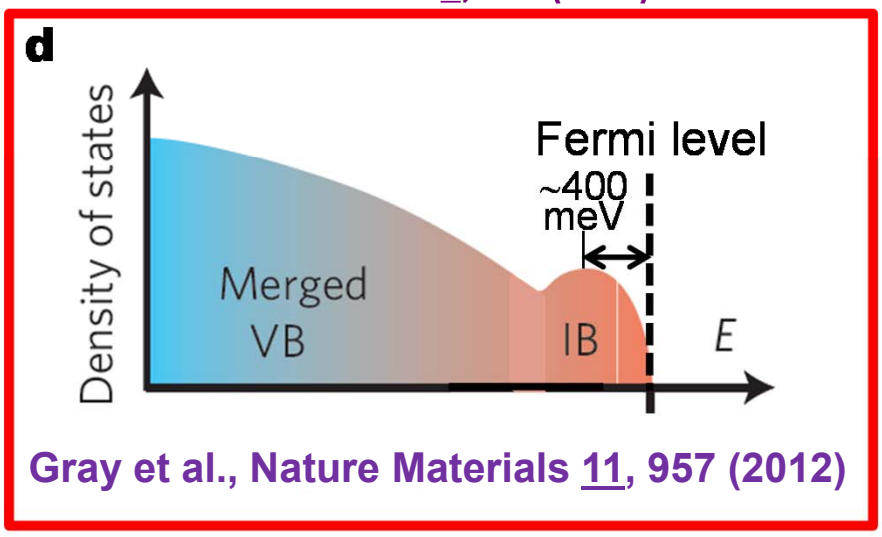

$Ga_{0.975}Mn_{0.025}As$: Resonant soft x-ray ARPES

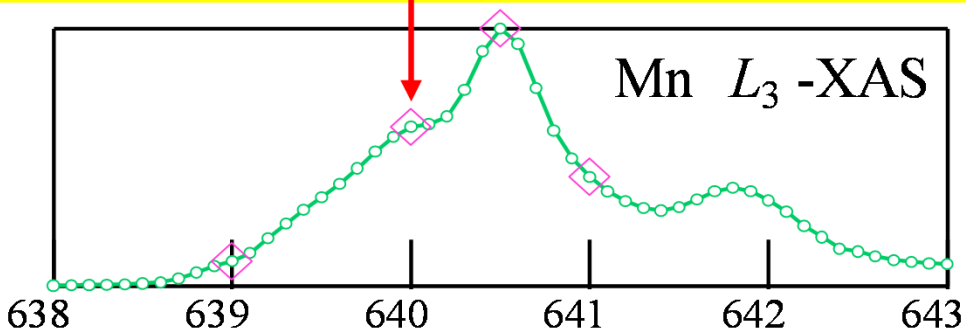

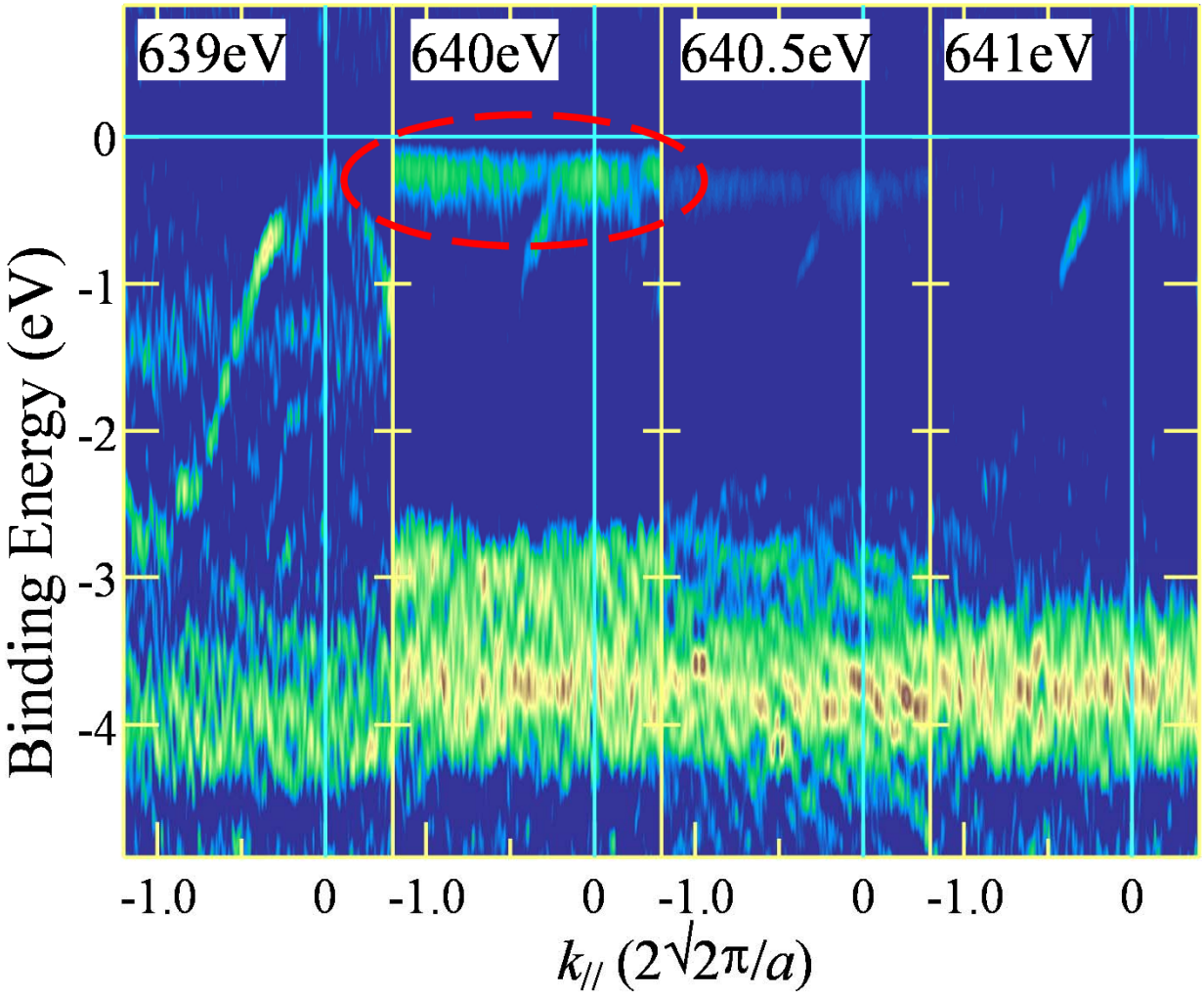

Kobayashi, Strocov, et al.,
Phys Rev B 89, 205204 (2014)

Band structure in core levels!—C 1s from graphene

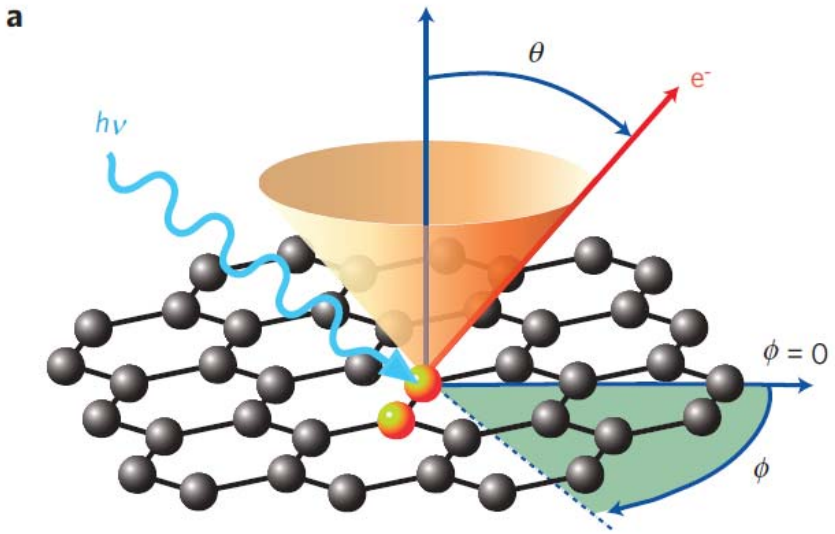

Experiment

C 1s XPD

C 1s $E_{binding}$ vs $k_{||}$

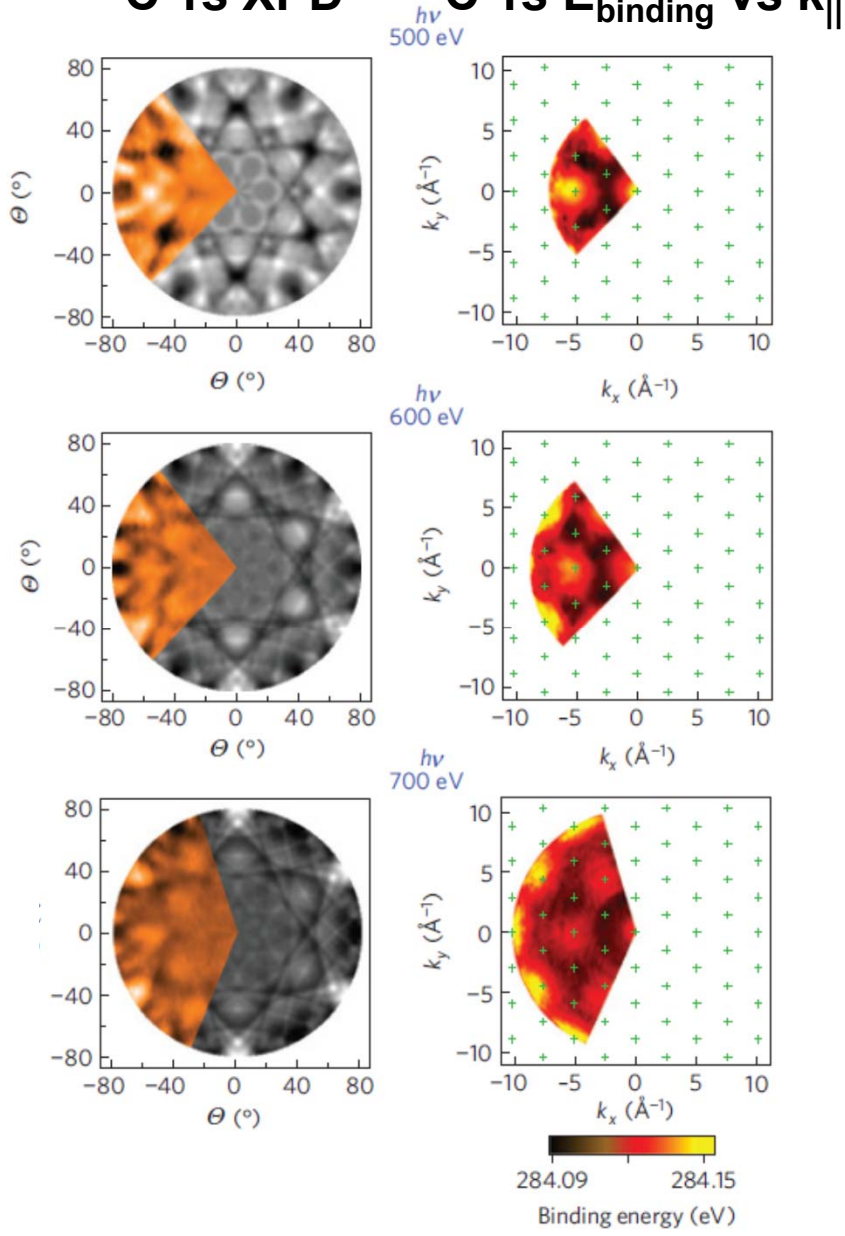

Theory

Tight-binding

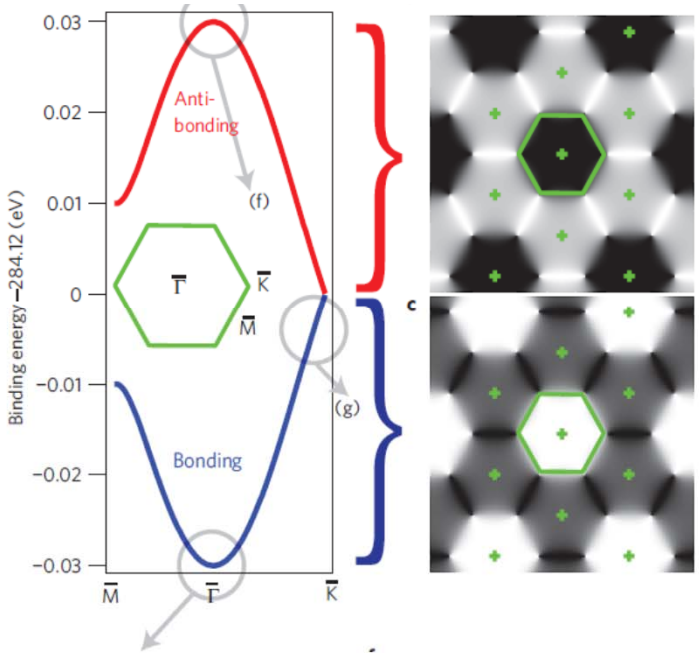

All-electron

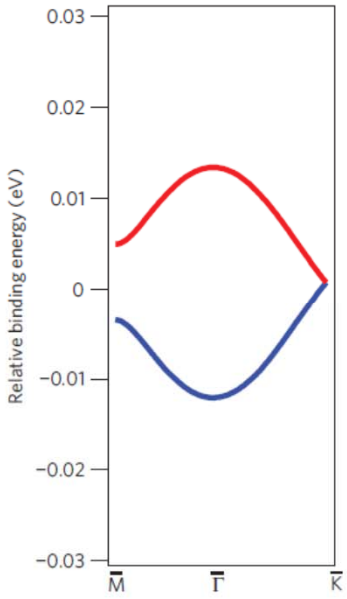

Lizzit et al., Nature Physics 6 , 345 (2010)

Basic Concepts:

A Little Electronic Structure
The X-Ray-Based Experiments
X-Ray Sources, Synchrotron Radiation, Free Electron Lasers

Core-Level Photoemission

Intensities and Quantitative Analysis, the 3-Step Model
Varying Surface and Bulk Sensitivity
Chemical Shifts
Multiplet Splittings
Electron Screening and Satellite Structure
Magnetic and Non-Magnetic Dichroism
Resonant Photoemission
Photoelectron Diffraction and Holography

Valence-Level Photoemission

Band-Mapping in the Ultraviolet Photoemission Limit
Densities of States in the X-Ray Photoemission Limit-Covered already

Some New Directions

Photoemission with Hard X-Rays (throughout lectures)
Photoemission with Standing Wave Excitation-See seminar
Photoemission with: Higher Pressures→multi-Torr→Atmosphere?
Spatial Resolution-Photoelectron Microscopy
Temporal Resolution

Basic Concepts:

A Little Electronic Structure
The X-Ray-Based Experiments
X-Ray Sources, Synchrotron Radiation, Free Electron Lasers

Core-Level Photoemission

Intensities and Quantitative Analysis, the 3-Step Model
Varying Surface and Bulk Sensitivity
Chemical Shifts
Multiplet Splittings
Electron Screening and Satellite Structure
Magnetic and Non-Magnetic Dichroism
Resonant Photoemission
Photoelectron Diffraction and Holography

Valence-Level Photoemission

Band-Mapping in the Ultraviolet Photoemission Limit
Densities of States in the X-Ray Photoemission Limit-Covered already

Some New Directions

Photoemission with Hard X-Rays (throughout lectures)
Photoemission with Standing Wave Excitation-See seminar
Photoemission with: Higher Pressures→multi-Torr→Atmosphere?
Spatial Resolution-Photoelectron Microscopy
Temporal Resolution

Ambient Pressure XPS-Bridging the Pressure Gap: CState- and Time- Resolved Oxidation of Si at Multi-Torr Pressures

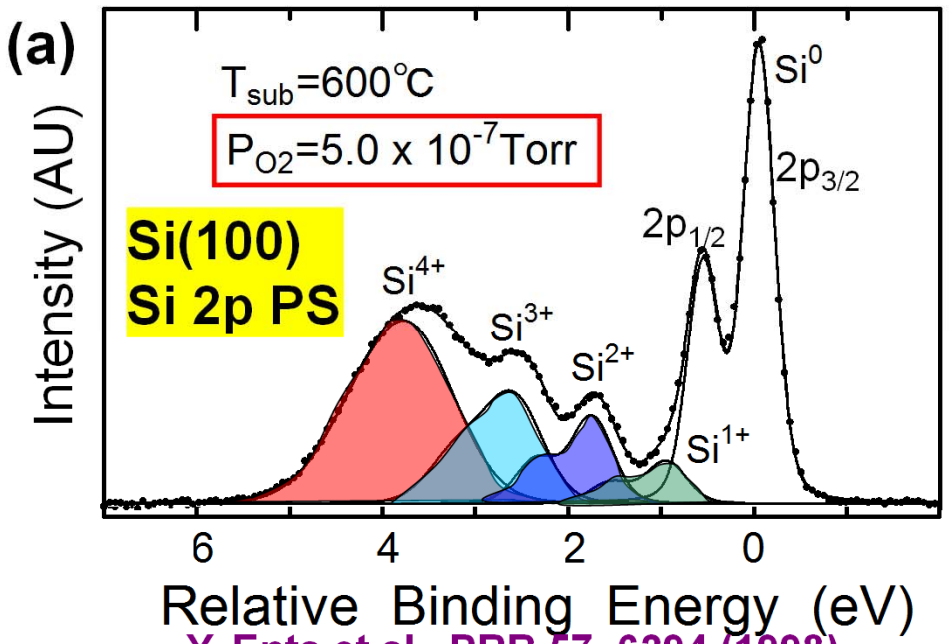

Y. Enta et al., PRB 57, 6294 (1998)

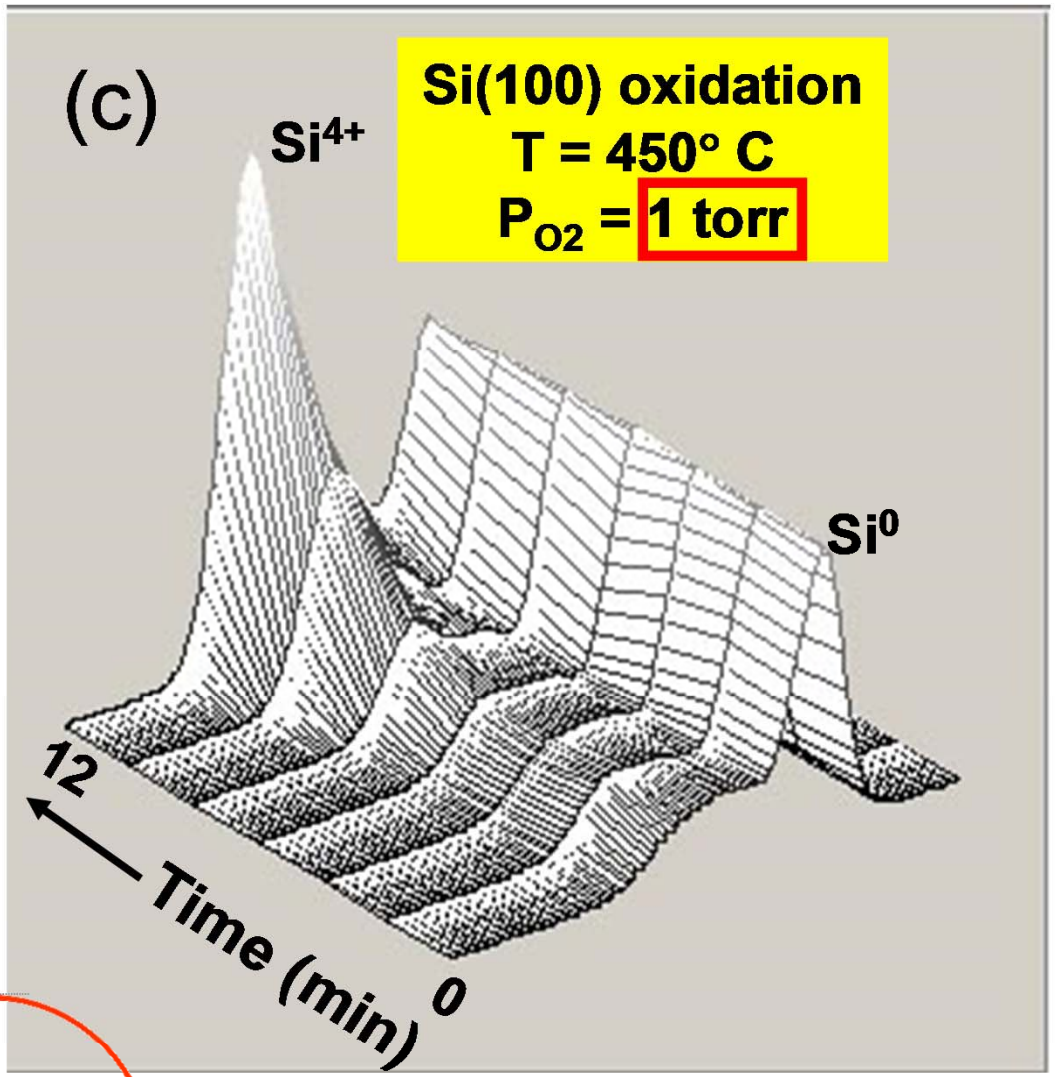

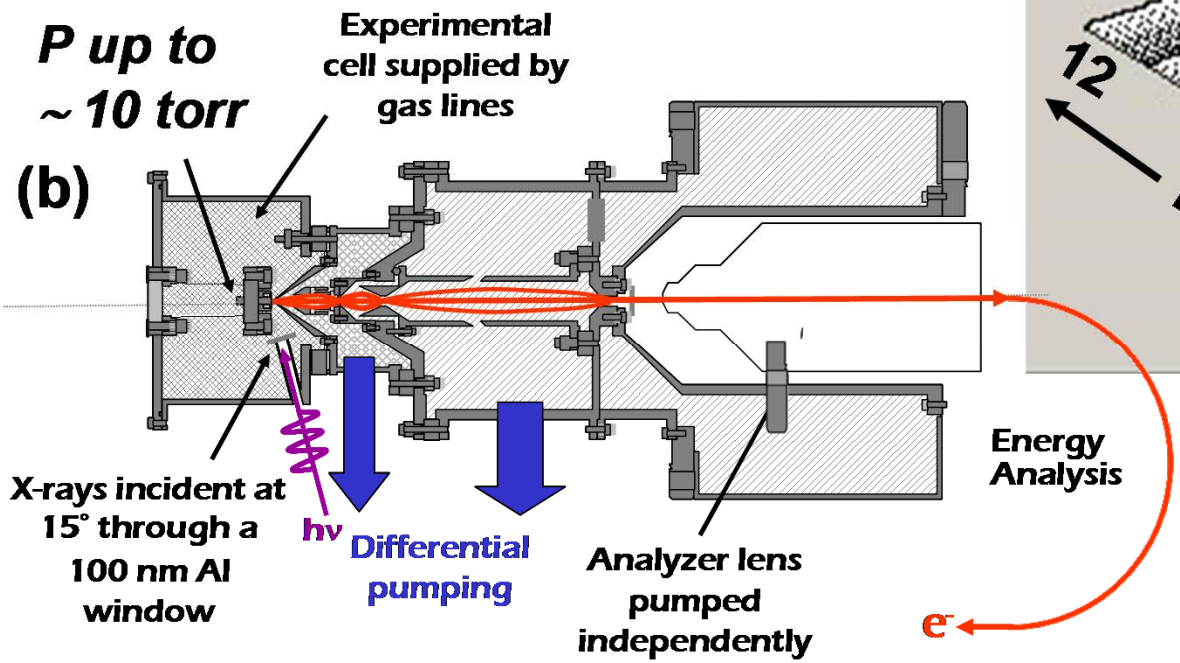

P ≈ 10^{-7} torr or better

Ogletree et al., Rev. Sci. Inst. 73, 3872 (2002)—SR, ALS
Bluhm, Salmeron, Schlögl—ALS, BESSY
Enta, Mun et al., Appl. Phys. Lett. 92, 012110 (2008); J. Appl. Phys. 103, 044104(2008)

Watching the oxide grow in real time: constant P, variable T

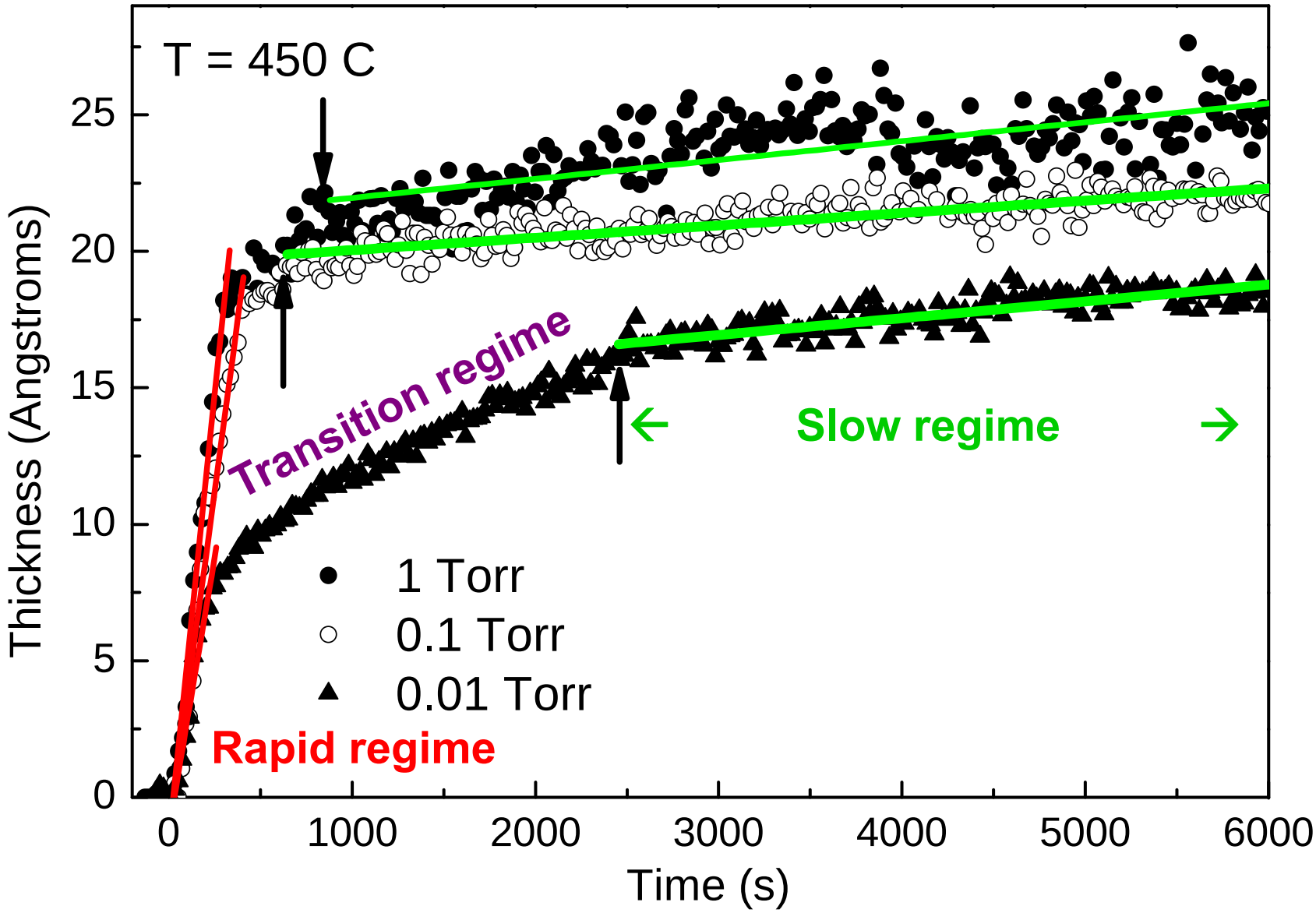

Enta, Mun et al., Appl. Phys. Lett. 92, 012110 (2008)

Measuring the concentration profile of ions near an aqueous surface

KBr (001)

hν = 200 eV

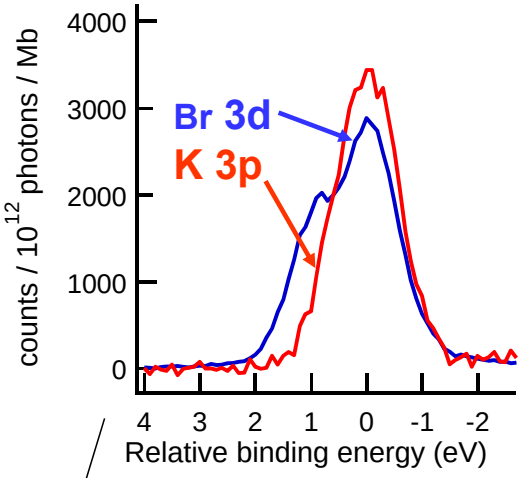

At deliquescence→
droplet formation

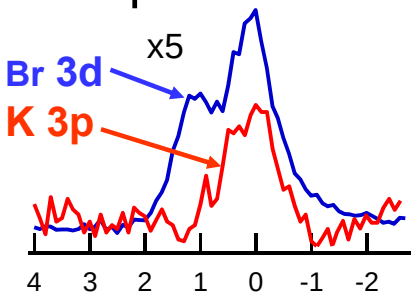

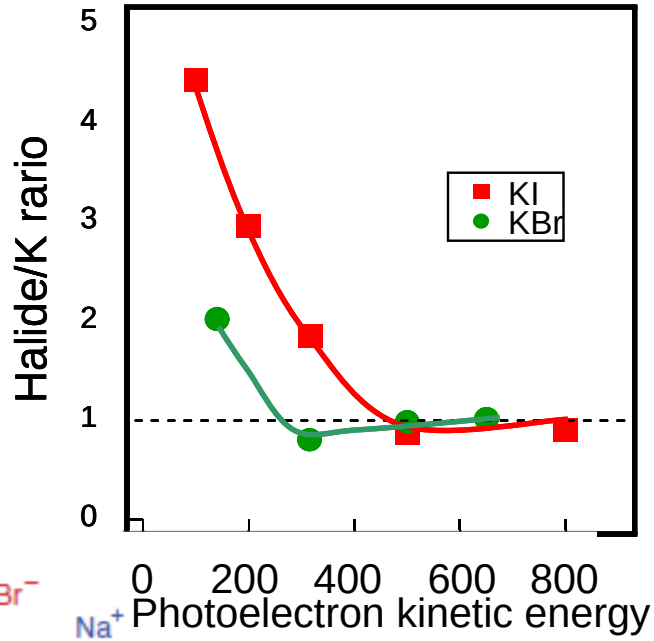

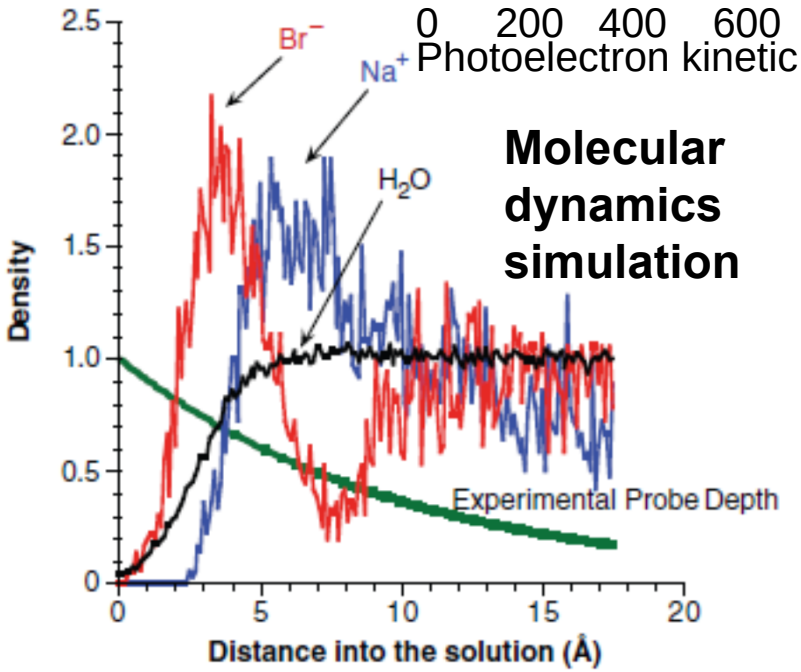

Molecular dynamics simulation

→ More halide near surface—marked change

S. Ghosal, J.C. Hemminger, et al., Science 307, 5709 (2005)

THE ELECTRONS IN CARBON MONOXIDE:

Atomic orbital makeup

$$\varphi_j^{MO}(\vec{r}) = \sum_{\substack{\text{Atoms } A \\ \text{Orbitals } i}} c_{Ai,j}\varphi_{Ai}^{AO}(\vec{r})$$

15. Carbon Monoxide

Symmetry: $C_{\infty v}$

— = φ_i: NEG.
··· = φ_i: POS.
ISOCONTOURS OF $|\varphi_i|^2$

(10)

60 ε = 0.2755

ANTI-BONDING 2π (8,9)

2π ε = 0.1268

2π ε = 0.1268

ε_k = + NO.

UNBOUND + UNOCCUPIED

BOUND + OCCUPIED

BONDING 5σ (7)

50 ε = −0.5544

BONDING 1π (×2) (5,6)

1π ε = −0.6395

1π ε = −0.6395

ε_k = − NO.

$[B.E.]_k \equiv E_b(k) = -\varepsilon_k + \delta E_{relax} + \ldots$

Koopmans' Theo.

NON/WEAKLY BONDING 4σ (4)

40 ε = −0.8038

BONDING 3σ (3)

30 ε = −1.5210

CO: $(O1s)^2(C1s)^2 3\sigma^2 4\sigma^2 1\pi^4 5\sigma^2$

$1\pi_x^2\ 1\pi_y^2$

6$\bar{e}$ 8$\bar{e}$ — 14$\bar{e}$

C 1s CORE (2)

2σ ε = −10.88

O 1s CORE (1)

1σ ε = −20.00 a.u. (1 a.u. = 27.2 eV)

5σ

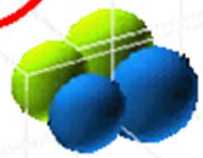

1π_y

1π_x

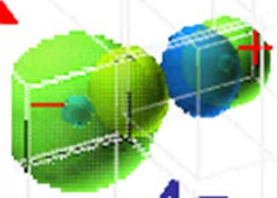

4σ

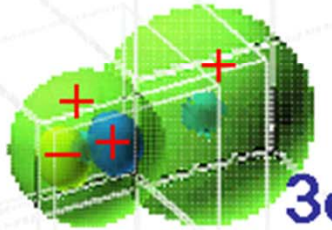

3σ

Seeing both bands and molecular states in ambient pressure XPS: CO above graphite

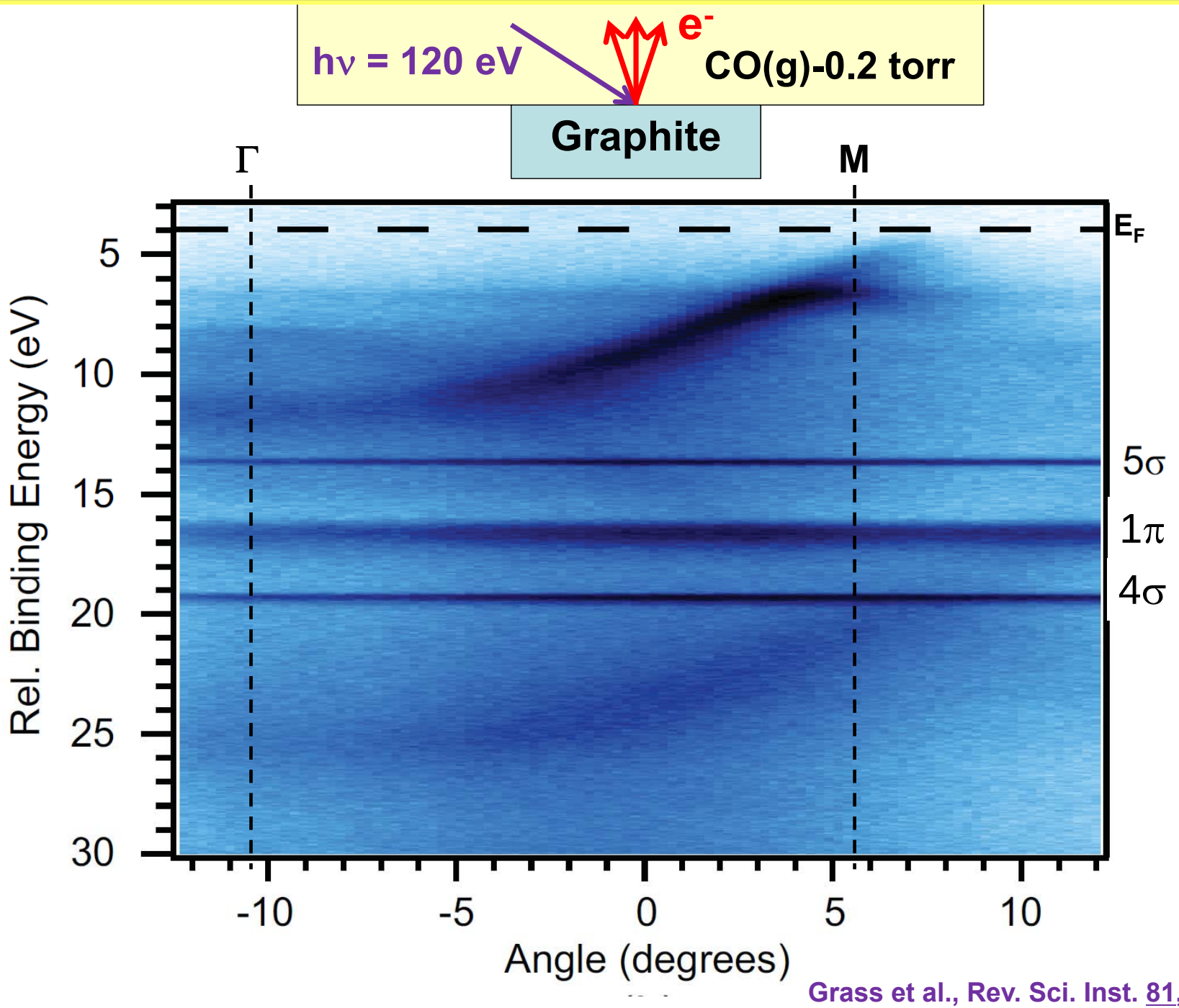

Grass et al., Rev. Sci. Inst. 81, 053106 (2010)

Basic Concepts:

A Little Electronic Structure
The X-Ray-Based Experiments
X-Ray Sources, Synchrotron Radiation, Free Electron Lasers

Core-Level Photoemission

Intensities and Quantitative Analysis, the 3-Step Model
Varying Surface and Bulk Sensitivity
Chemical Shifts
Multiplet Splittings
Electron Screening and Satellite Structure
Magnetic and Non-Magnetic Dichroism
Resonant Photoemission
Photoelectron Diffraction and Holography

Valence-Level Photoemission

Band-Mapping in the Ultraviolet Photoemission Limit
Densities of States in the X-Ray Photoemission Limit-Covered already

Some New Directions

Photoemission with Hard X-Rays (throughout lectures)
Photoemission with Standing Wave Excitation-See seminar
Photoemission with: Higher Pressures→multi-Torr→Atmosphere?

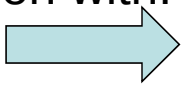

Spatial Resolution-Photoelectron Microscopy
Temporal Resolution

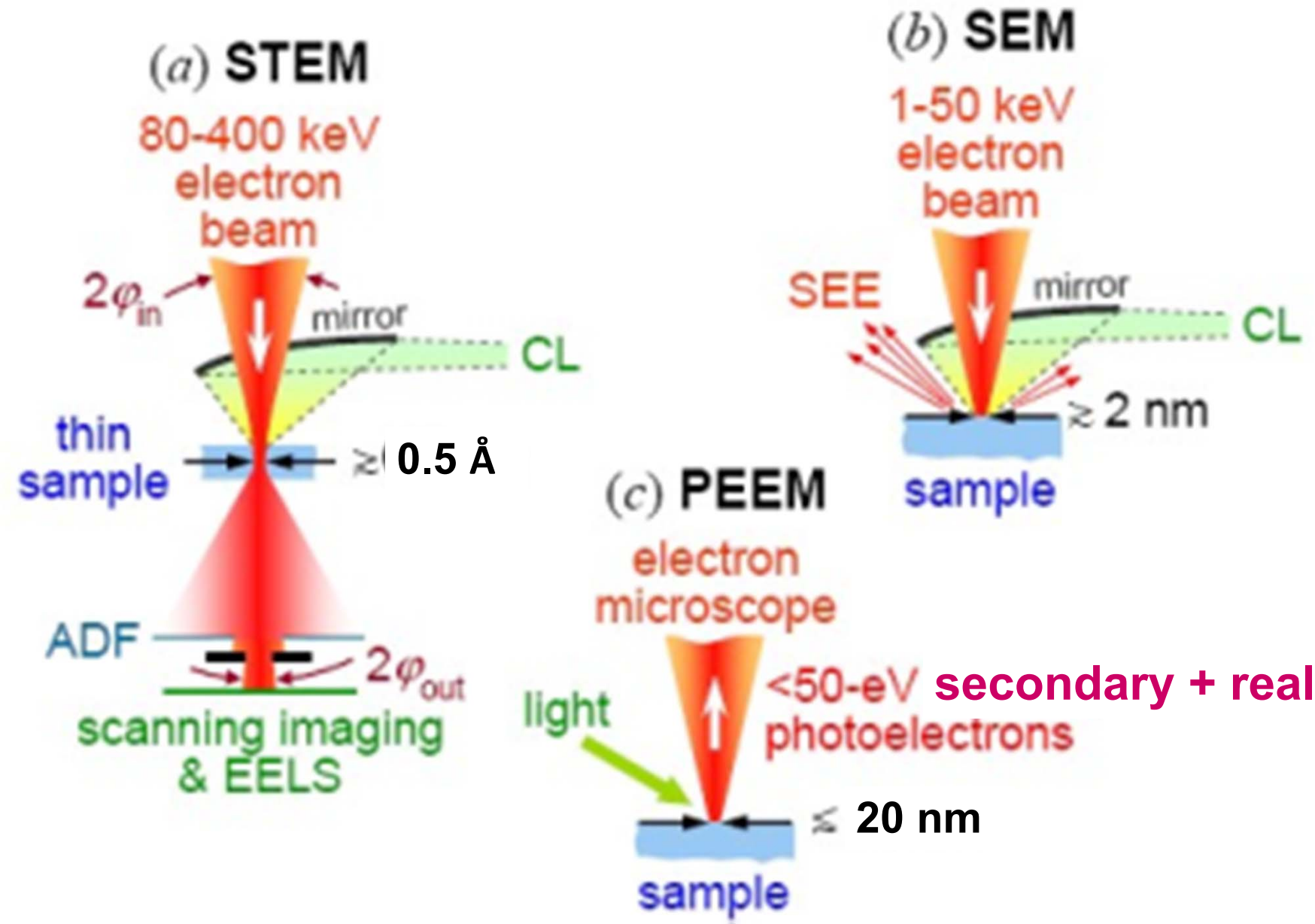
(a) STEM
80-400 keV electron beam
2φin
mirror
CL
thin sample
≳ 0.5 Å
ADF
2φout
scanning imaging & EELS
(b) SEM
1-50 keV electron beam
SEE
mirror
CL
≳ 2 nm
sample
(c) PEEM
electron microscope
light
<50-eV secondary + real photoelectrons
≲ 20 nm
sample

Fresnel Zone Plate Lens for Diffractive Focusing of Spatially Coherent X-rays

Constructive interference of waves from all rings:

$$\sqrt{D^2 + r_{n+1}^2} - \sqrt{D^2 + r_n^2} = n\lambda, \text{ with n = 1, 2, 3, ...}$$

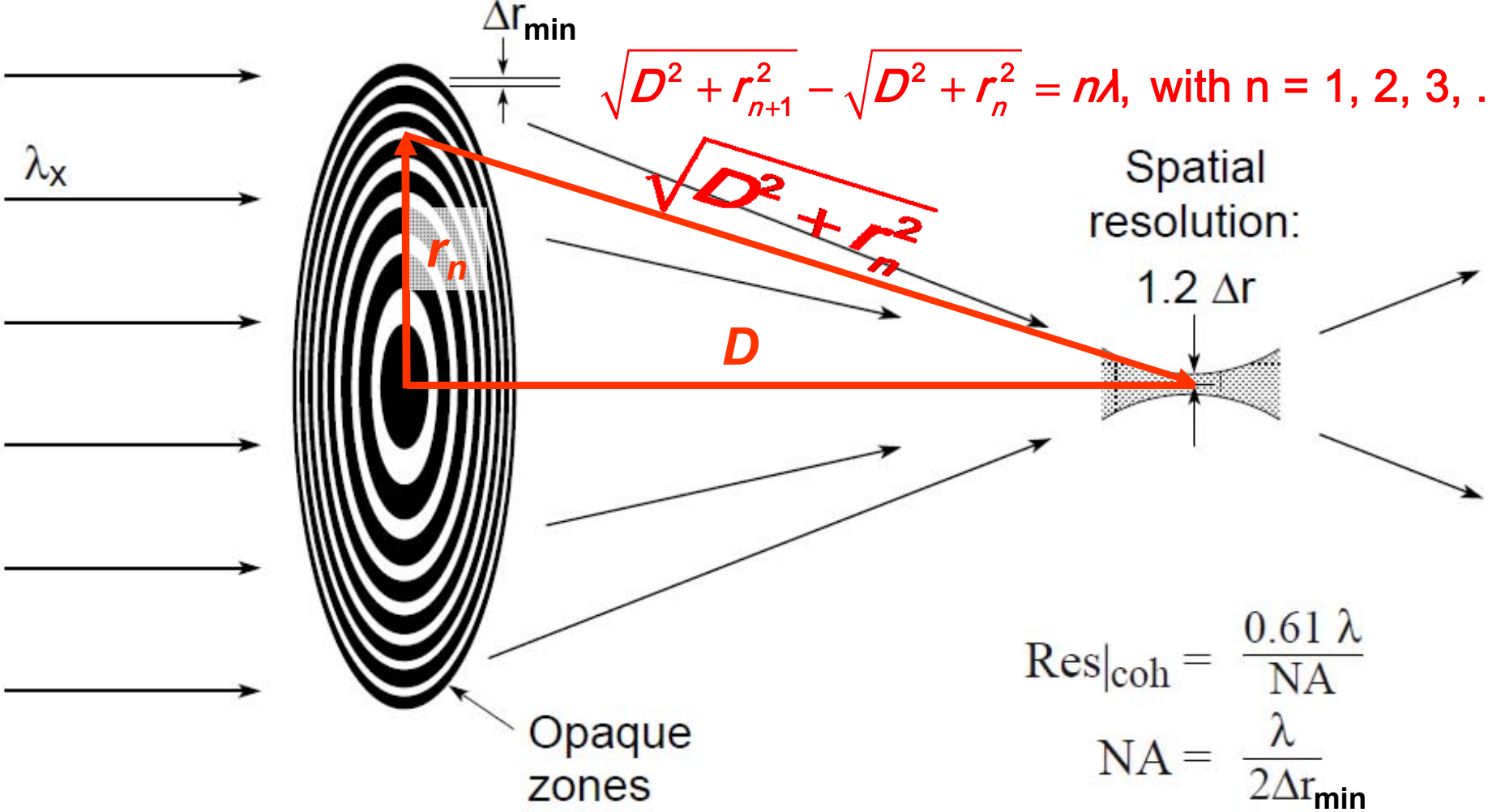

$$\text{Res}|_{coh} = \frac{0.61\,\lambda}{\text{NA}}$$

$$\text{NA} = \frac{\lambda}{2\Delta r_{min}}$$

$$\therefore \text{Res}|_{coh} = 1.22\,\Delta r_{min}$$

Imaging with soft x-ray microscopes—three types

1. Scanning X-ray Microscopy

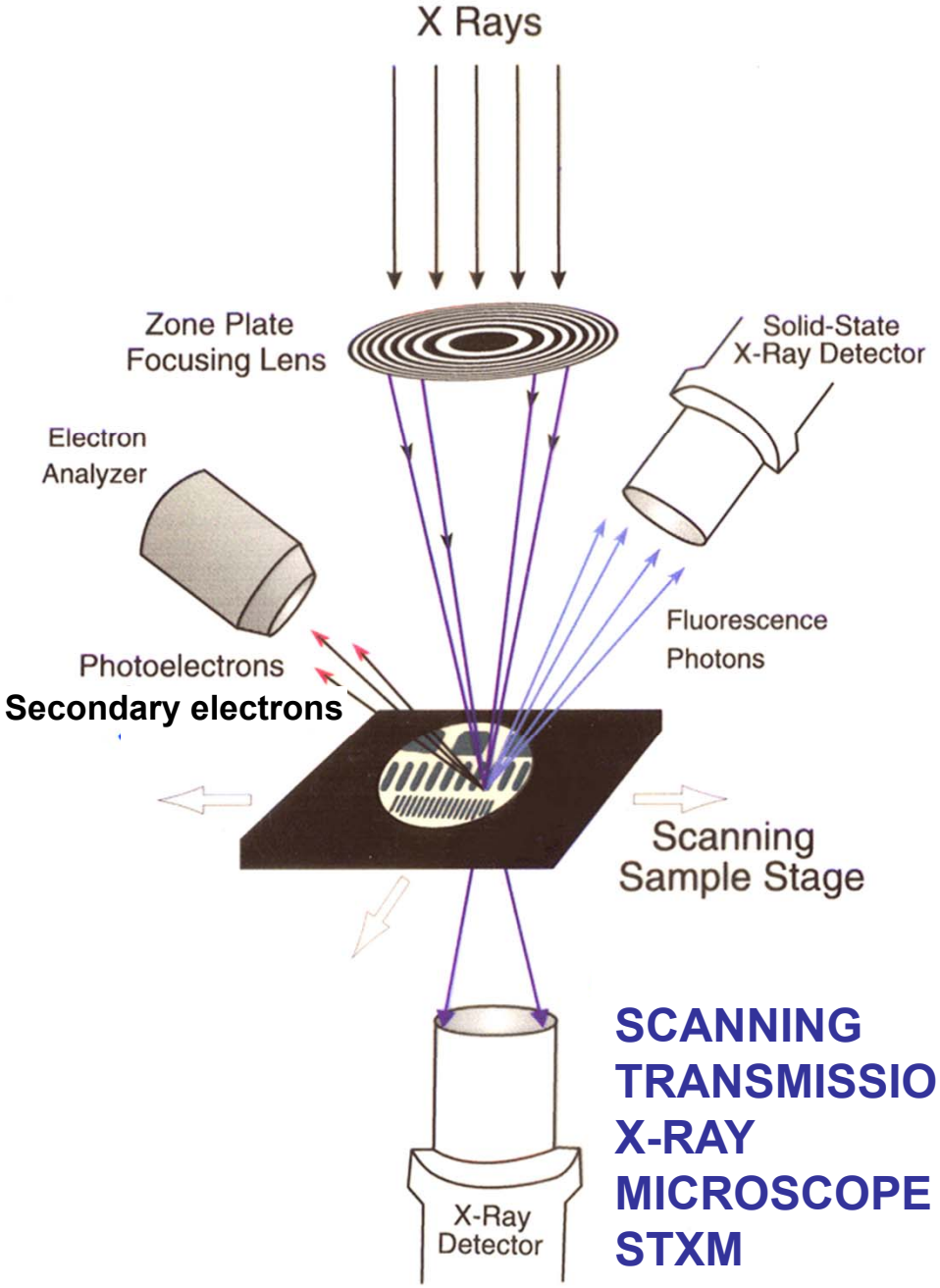

SCANNING TRANSMISSION X-RAY MICROSCOPE = STXM

2. X-Ray Photoelectron Microscopy

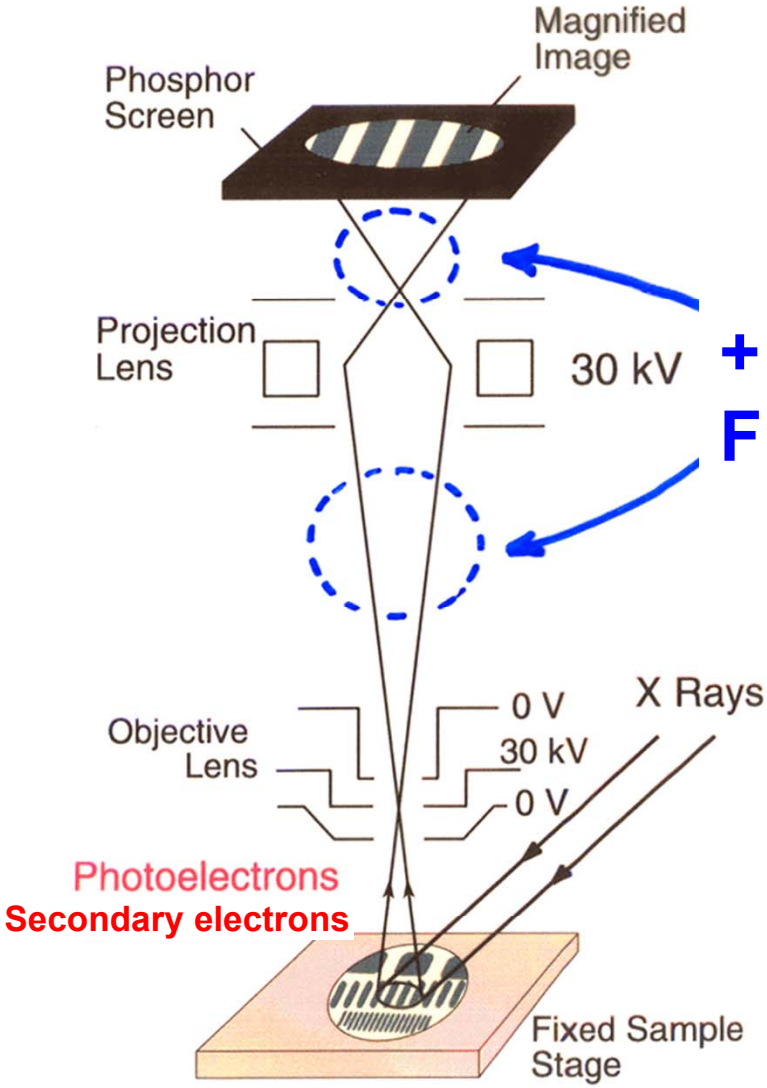

+ Energy Filter?

PHOTOELECTRON EMISSION MICROSCOPE = PEEM

SCANNING TRANSMISSION X-RAY MICROSCOPY OF POLYMER BLEND

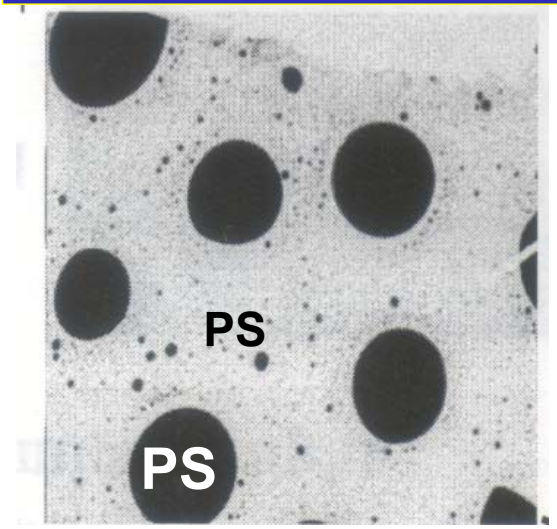

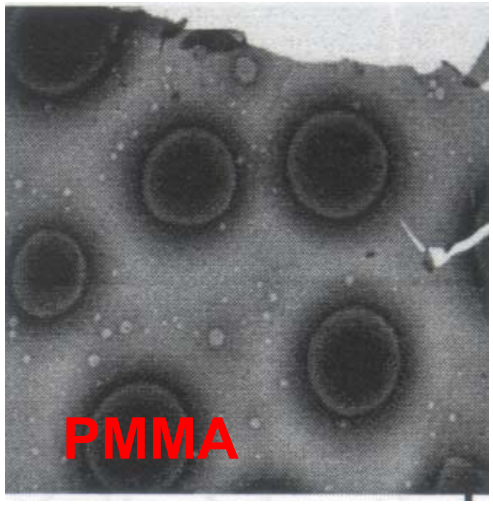

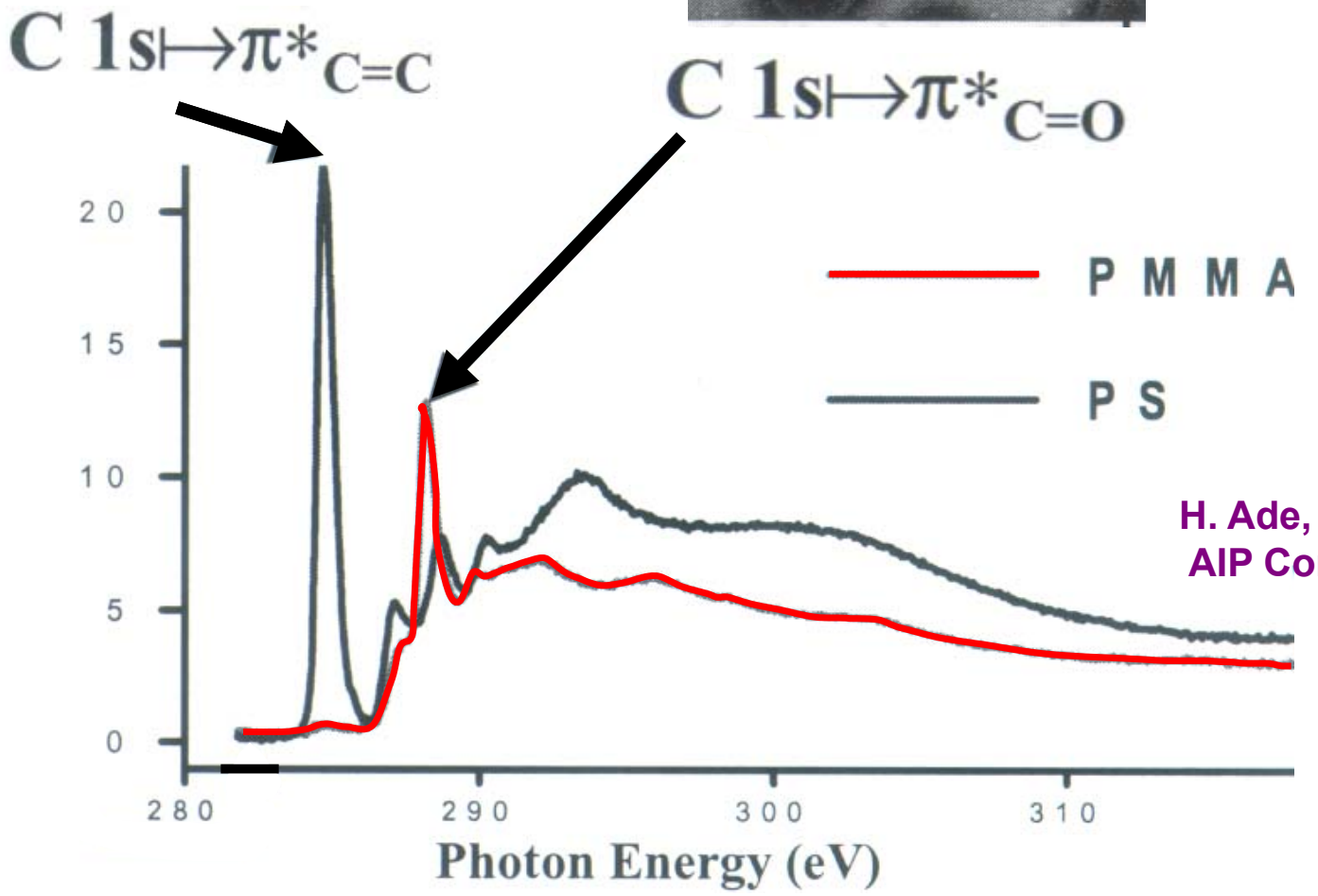

H. Ade, X-ray Microscopy 99, AIP Conf. Proc. 507, p.197

PHOTOELECTRON EMISSION MICROSCOPE (PEEM) USING PHOTOELECTRONS

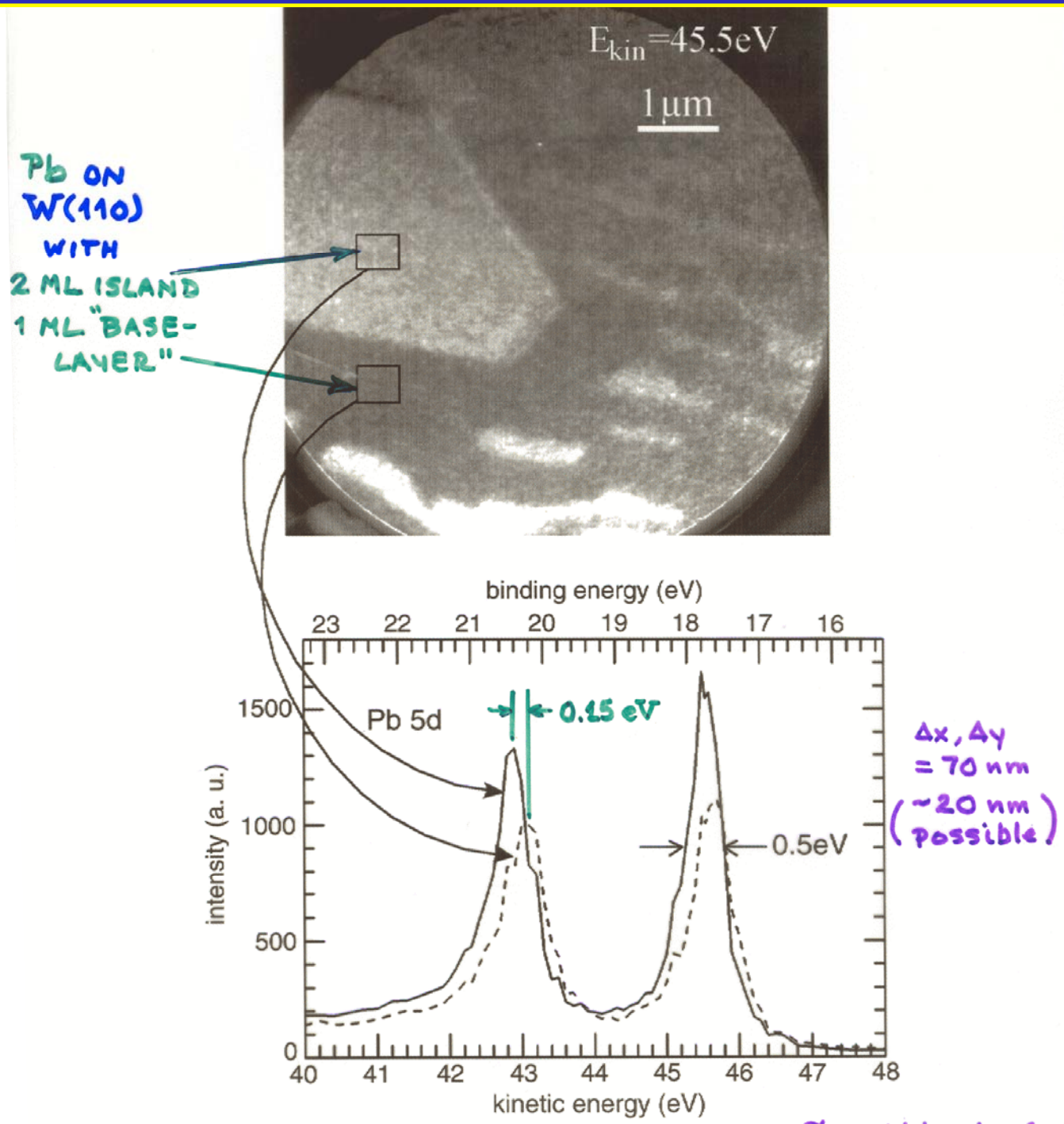

Sixth Int. Conf. On X-Ray Microscopy, (AIP Melville, New York, 2000) pp. 27-32.

PHOTOELECTRON EMISSION MICROSCOPE (PEEM) USING SECONDARY ELECTRONS

Antiferromagnetic $LaFeO_3$ layer XMLD Fe L_3

Ferromagnetic Co layer XMCD Co L_3/L_2

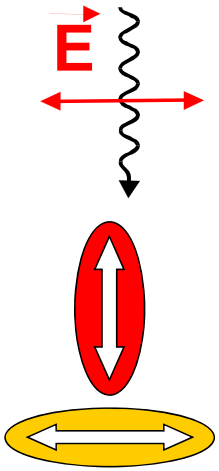

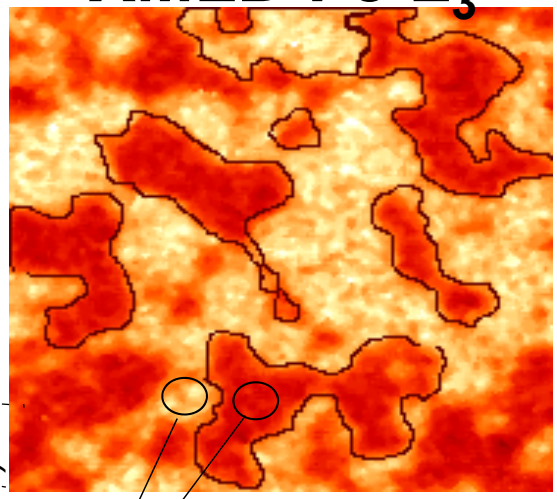

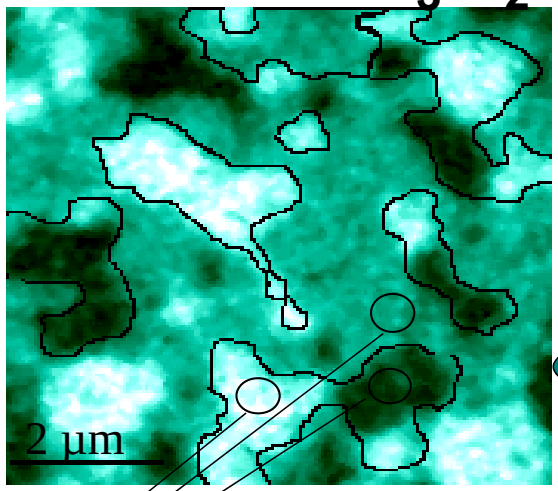

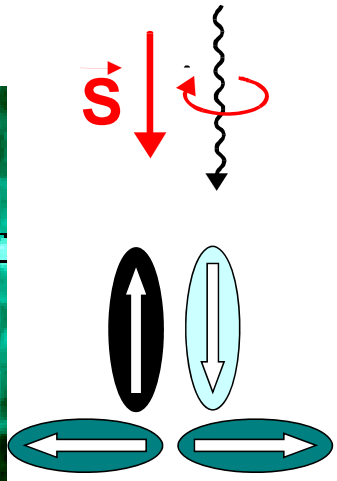

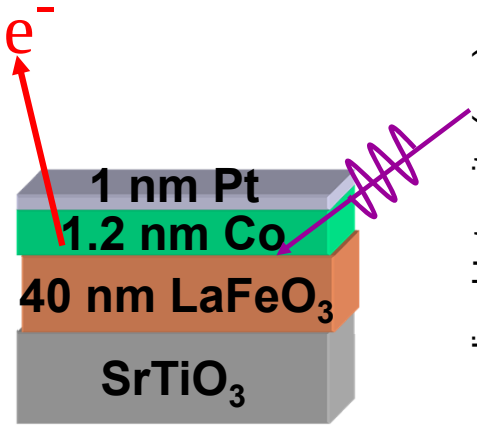

As grown:
bias not set

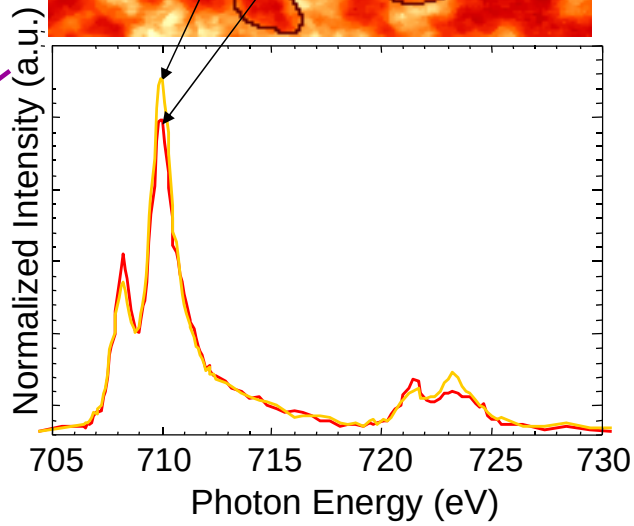

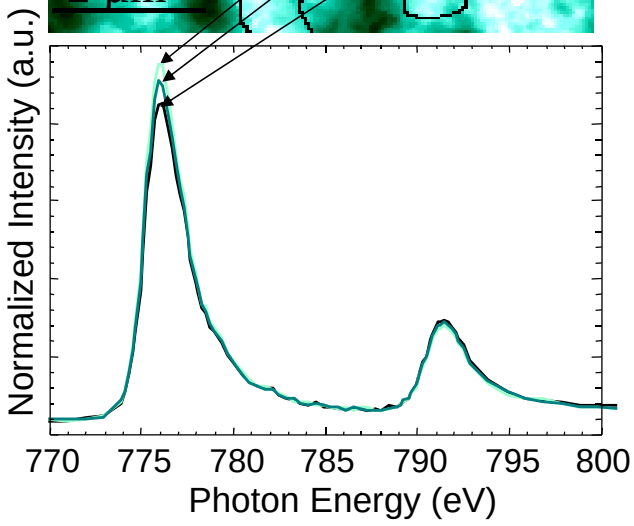

1:1 correlation of domain structure

F. Nolting et al, Nature, 405, 767 (2000)

Third type: Imaging Zone-Plate X-ray microscope: XM-1 @ ALS

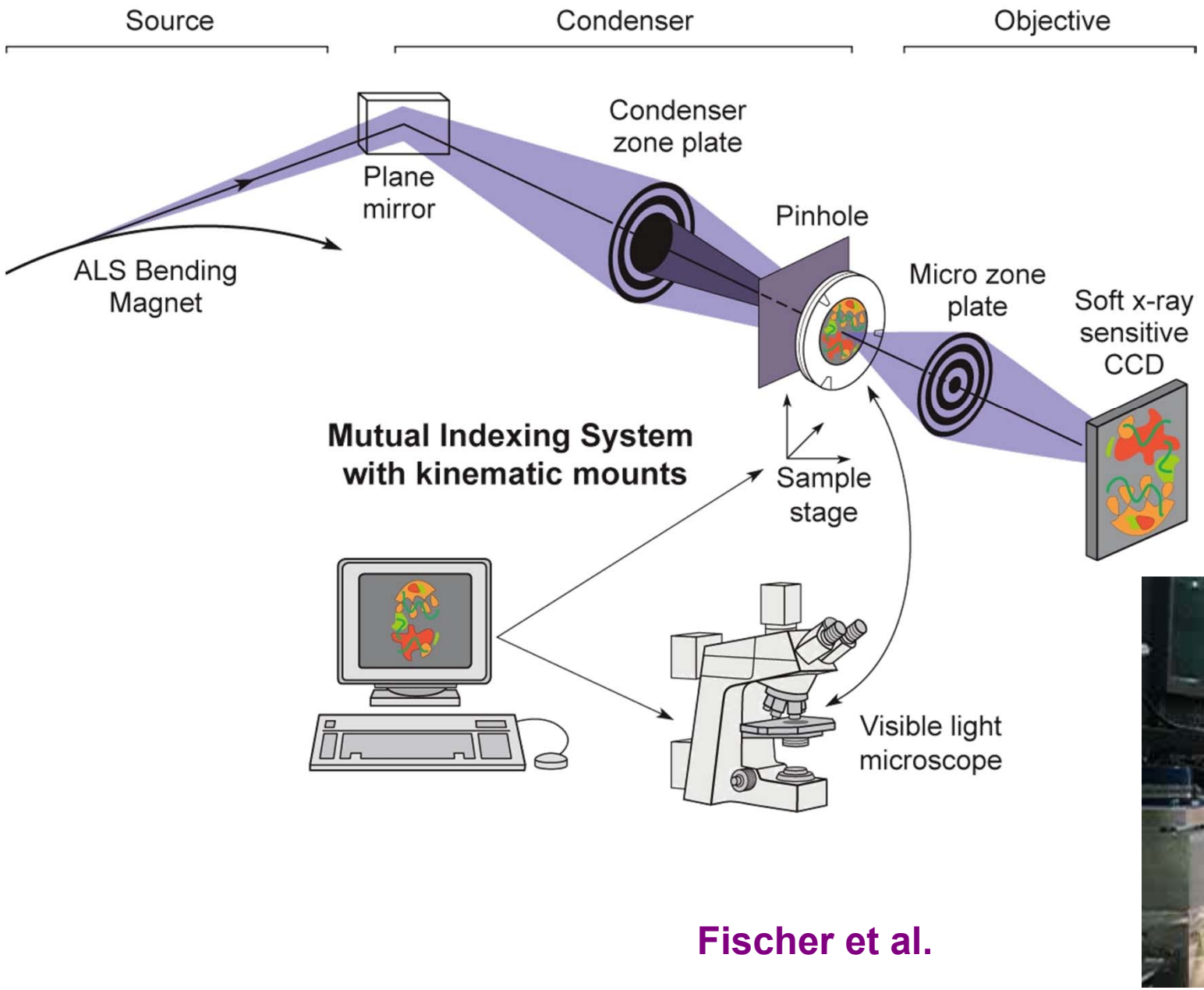

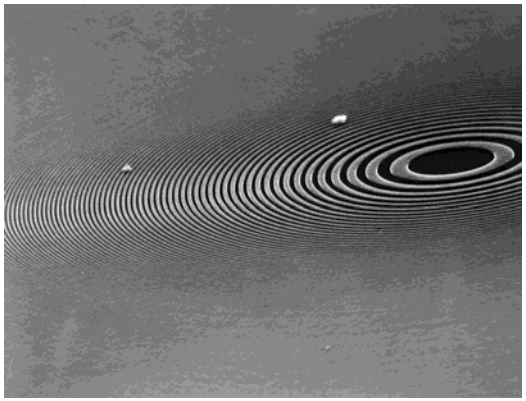

X-ray lens = zone plate
Outer rings 100 atoms apart

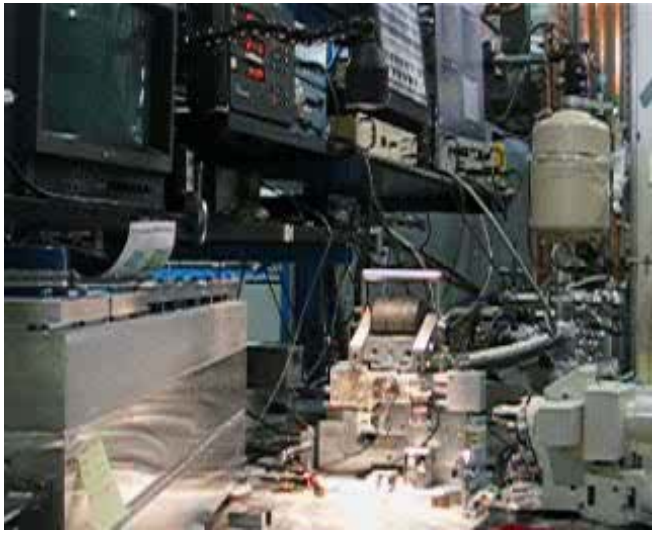

Fischer et al.

Imaging Iron Magnetic Domains with Circular-Polarized Light

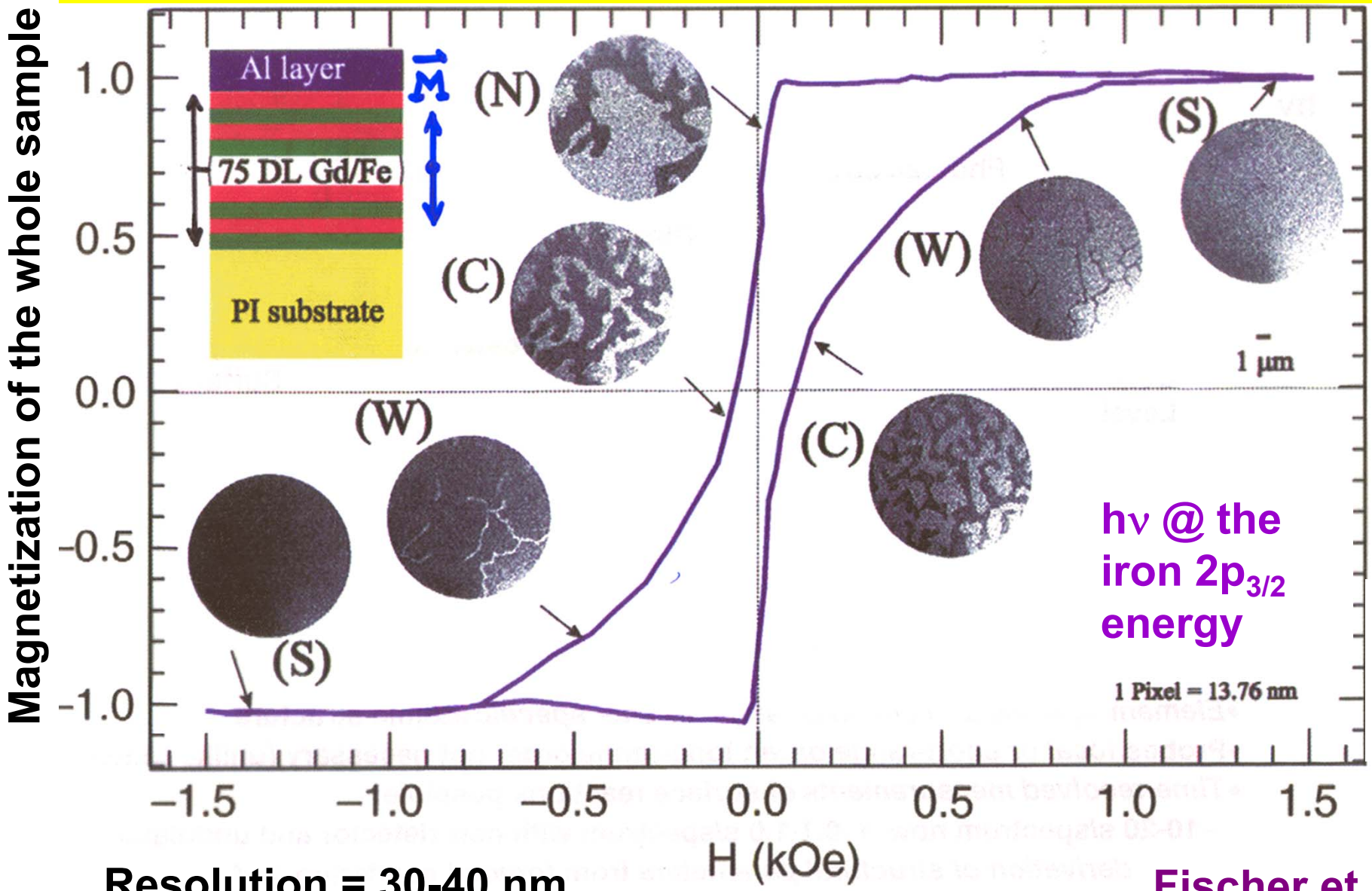

Resolution = 30-40 nm
Now 15 nm→10 nm

Fischer et al.

Nanometer-Scale Angle-Resolved Photoemission

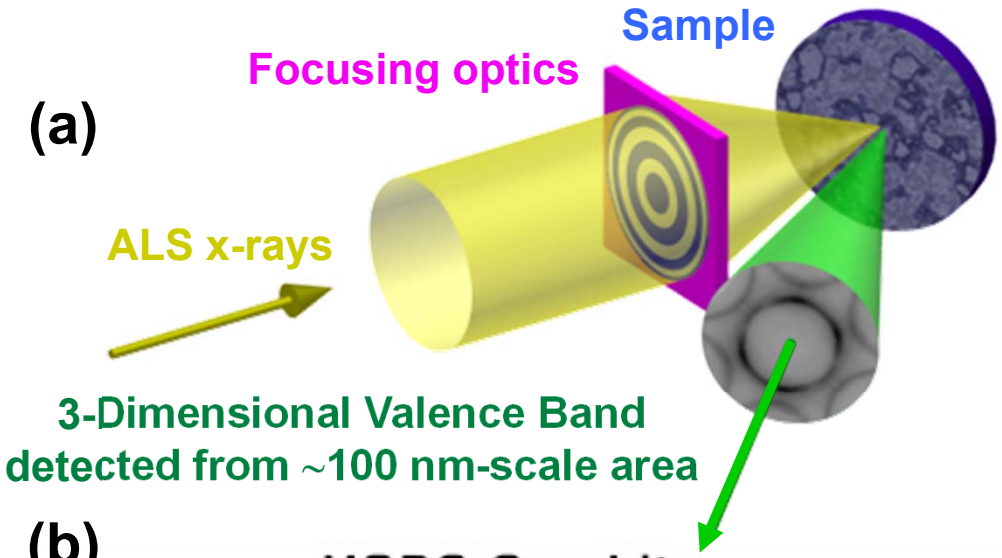

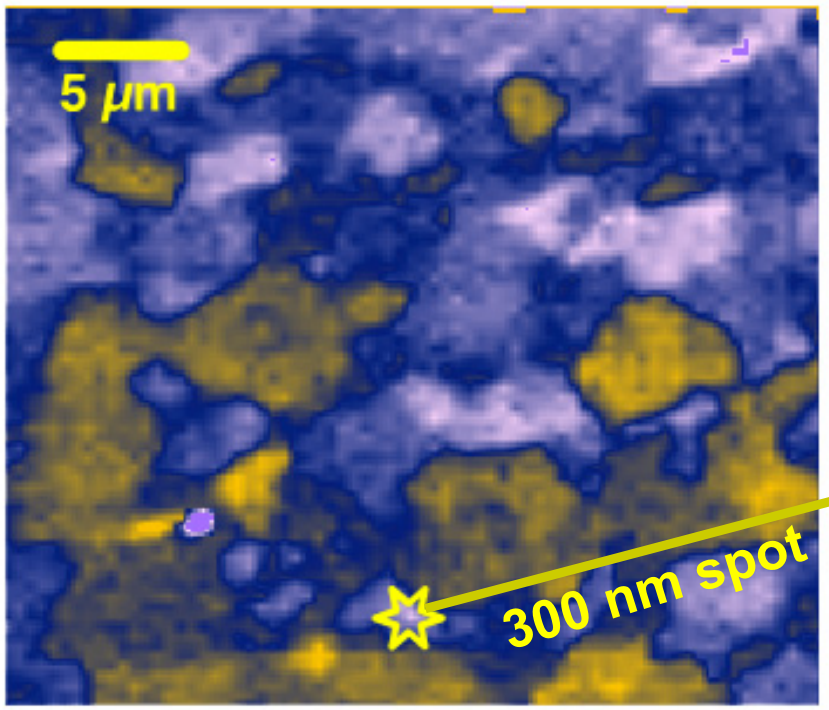

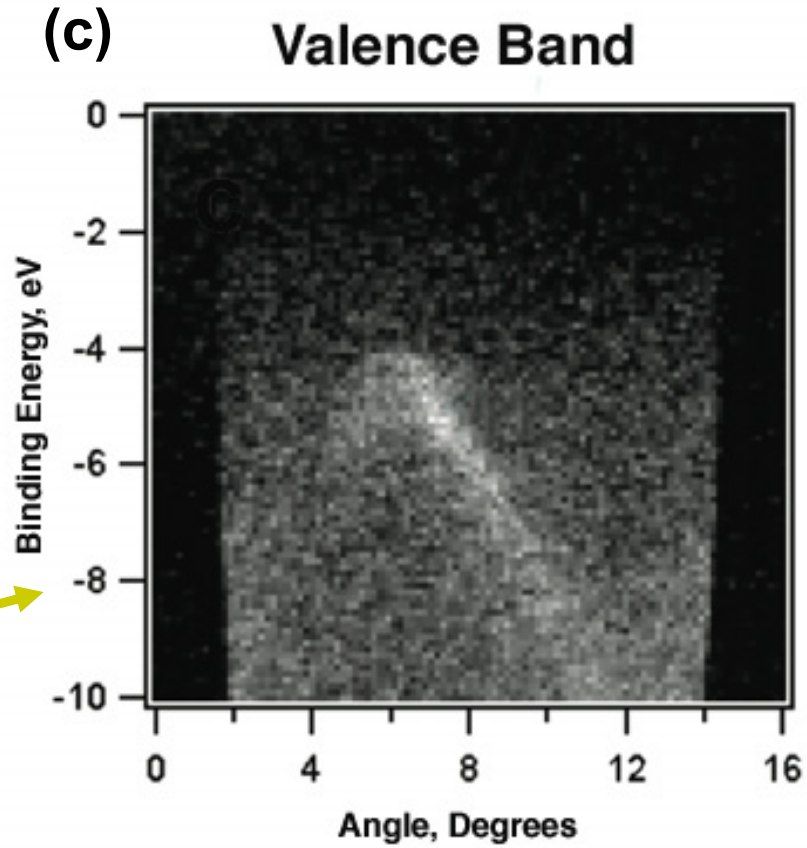

Rotenberg, Bostwick, ALS-LBNL

Basic Concepts:

A Little Electronic Structure
The X-Ray-Based Experiments
X-Ray Sources, Synchrotron Radiation, Free Electron Lasers

Core-Level Photoemission

Intensities and Quantitative Analysis, the 3-Step Model
Varying Surface and Bulk Sensitivity
Chemical Shifts
Multiplet Splittings
Electron Screening and Satellite Structure
Magnetic and Non-Magnetic Dichroism
Resonant Photoemission
Photoelectron Diffraction and Holography

Valence-Level Photoemission

Band-Mapping in the Ultraviolet Photoemission Limit
Densities of States in the X-Ray Photoemission Limit-Covered already

Some New Directions

Photoemission with Hard X-Rays (throughout lectures)
Photoemission with Standing Wave Excitation-See seminar
Photoemission with: Higher Pressures→multi-Torr→Atmosphere?
Spatial Resolution-Photoelectron Microscopy
Temporal Resolution

Time-resolved core-level XPS as a monitor of a charge density wave in Mott insulator 1T-TaS_2

Probe: 156 eV, 700 fs, FLASH FEL

Ta 4f

Pump: 1.55 eV, 120 fs, laser

Graphite

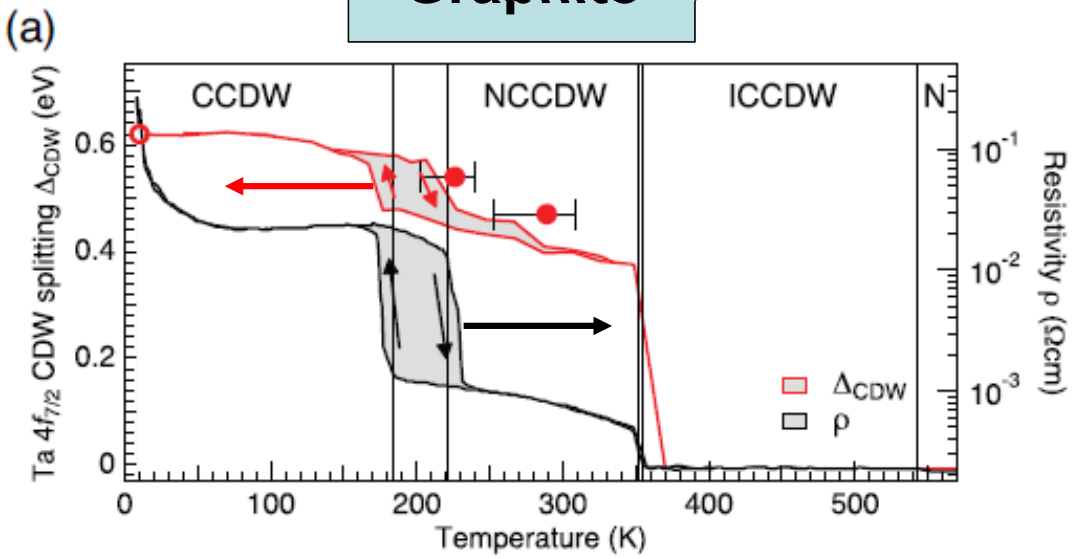

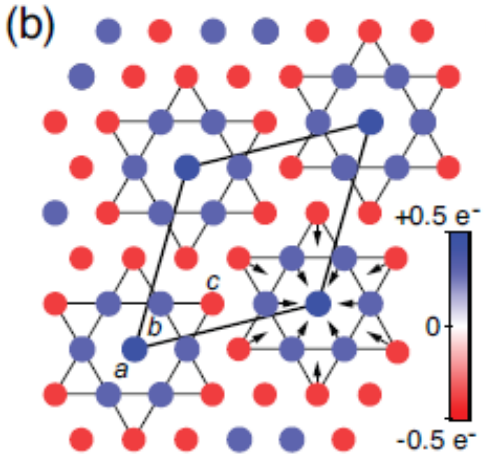

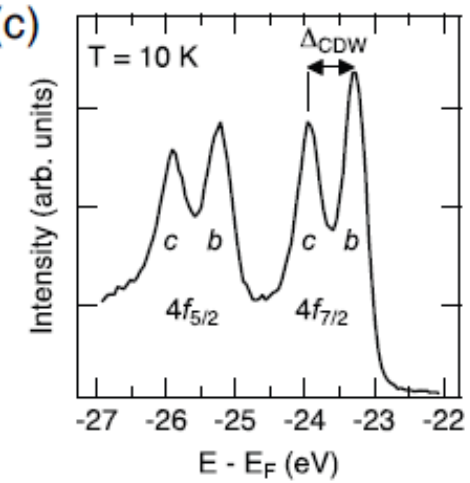

~~a~~:b:c = ~~1~~:6:6

Hellman et al., PRL 105, 187401 (2010)

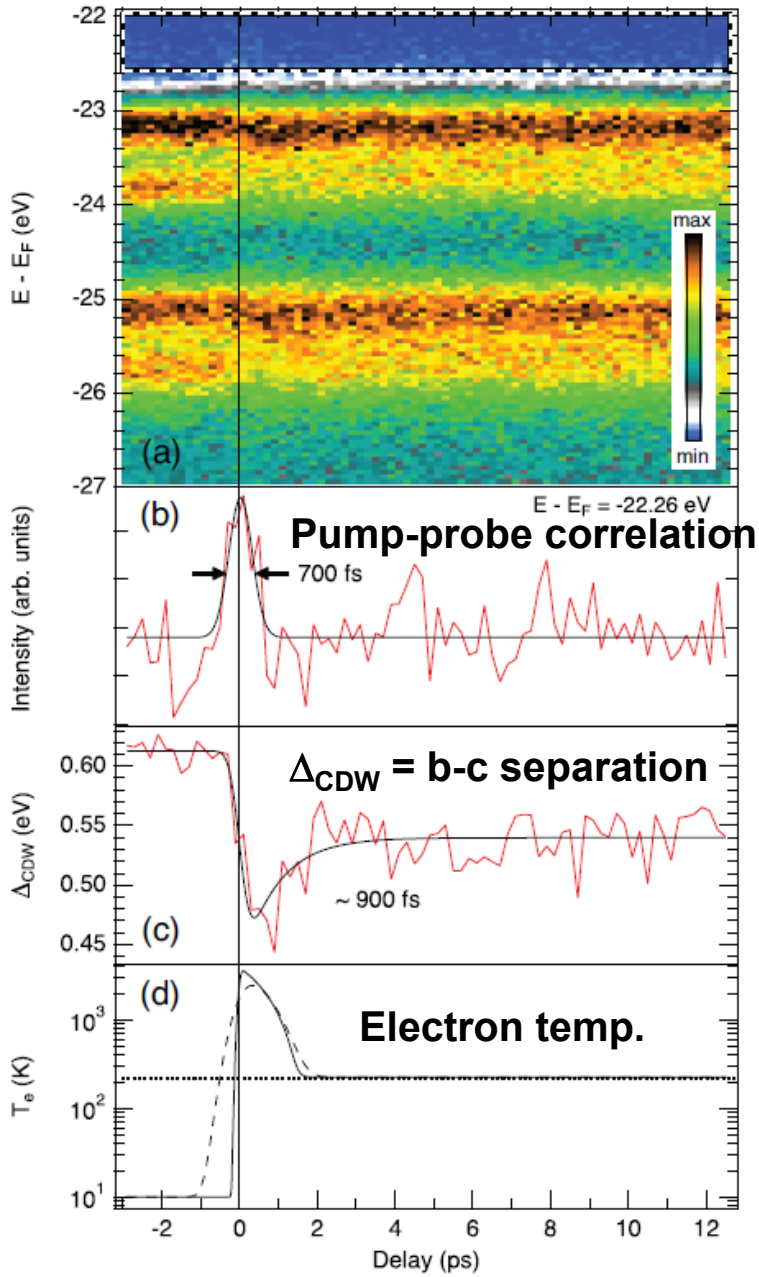

Basic Concepts:

A Little Electronic Structure
The X-Ray-Based Experiments
X-Ray Sources, Synchrotron Radiation, Free Electron Lasers

Core-Level Photoemission

Intensities and Quantitative Analysis, the 3-Step Model
Varying Surface and Bulk Sensitivity
Chemical Shifts
Multiplet Splittings
Electron Screening and Satellite Structure
Magnetic and Non-Magnetic Dichroism
Resonant Photoemission
Photoelectron Diffraction and Holography

Valence-Level Photoemission

Band-Mapping in the Ultraviolet Photoemission Limit
Densities of States in the X-Ray Photoemission Limit

Some New Directions

Photoemission with Hard X-Rays (throughout lectures)
Photoemission with Standing Wave Excitation-See seminar
Photoemission with: Higher Pressures→multi-Torr→Atmosphere?
Spatial Resolution-Photoelectron Microscopy
Temporal Resolution

Typical experimental geometry for energy- and angle-resolved photoemission measurements

Ferromagnet

Tailoring the photon field:
Polarization, Standing wave

Photon

Up to 10-20 keV
Down to 5 eV (Lasers, UV lamps)

θ_{inc}

θ

Ultrahigh Vacuum

Multi-torr at sample

ϕ

Space & Time resolution (Lasers, Free e⁻ lasers)

Measuring spin

Sample

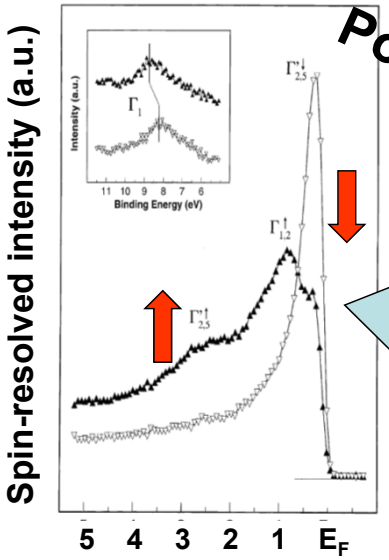

Surf. Sci. 478, 193 ('01)

$\vec{k}$ $\vec{s}$

e-

y
x
z

Irradiated Area

Core-level $I(\theta,\phi)$

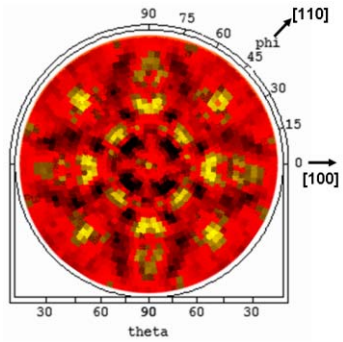

Photoe⁻ diff./holog.

Analyzer Slit

Angle

Energy

Imaging Detector

Kinetic Energy →

No. e⁻

Valence-levels

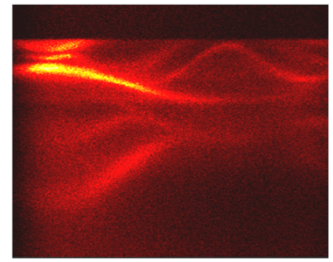

Binding Energy →

Emission angle→ $\vec{k}_x$